TIП

Investigation of a protective gas atmosphere in polymer-based packaging and the development of optical, non-destructive detection methods

Jasmin Dold, M.Sc.

"Errors are notoriously hard to kill, but an error that ascribes to a man what was actually the work of a woman has more lives than a cat."

Hertha Ayrton, 1854-1923

Acknowledgements

I would like to take this opportunity to thank some of my companions who provided me with significant support before and during my PhD.

First and foremost, I would like to thank my supervisor Prof. Dr. Horst-Christian Langowski. In addition to your great professional support, you were always a good listener, cheered me up when I was worried and always gave me help when I needed it. I would also like to thank you for your down-to-earth and friendly manner, which always made it possible to work positively at the chair, and that fun has never been missed out.

I would also like to thank Prof. Dr. Thomas Becker. Thanks for your initiative to involve our working group into your chair, I was not only able to continue my research work within the necessary framework, but also to broaden my horizons beyond food packaging technology, from which I still benefit today.

This work would not have been possible without the help of my students. In particular, I would like to thank Melanie Eichin, Clarissa Hollmann and Caroline Kehr, you have made a valuable contribution to my research.

I would also like to thank Prof. Dr. Rudi Vogel and Dr. Sandra Kolbeck for your support within the project, both from a professional point of view and for the opportunity to carry out experiments at your chair. I would also like to thank the Fraunhofer IVV, especially Dr. Cornelia Stramm, Zuzana Scheuerer and Christopher Schmidt for the same support.

Working at a chair would only be half as nice without great colleagues, which is why I would like to thank my entire working group and other residents at the Weihenstephaner Steig 22, namely Raik Bär, Günther Gaßner, Kai Hartwig, Manuela Horn, Simone Kefer, Benedikt Marschall, Christoph Nophut, Daniel Ochsenkühn, Thaddäus Rapp, Romy Ries, Simon Scheibenzuber, Matthias Staiger, Nikolai Striffler, Dr. Tobias Voigt and Prof. Dr. Heinrich Vogelpohl. Many thanks for unforgettable chair excursions and "Weißwurst Frühstück" moments.

I would also like to take this opportunity to thank "The Legendary Food Packers" for many great jam sessions and gigs: Kai Büchner, Dominik Geier, Sönke Kienitz, Thaddäus Rapp and Dr. Tobias Voigt.

Another thank you goes to my closest and longest friends: Felicitas Flechtmann, Sarah Holzer and Janina Wojtenek. Thank you for your constant support.

I would also like to thank my family, my aunt Ursula Dold, without whose help my studies would not have been possible, and my parents Peter Dold and Ute Wölfle, as well as my sister Vanessa Spitz, you always believed in me without any doubts.

Finally, I would like to thank my partner Philip Schmid. You supported me both professionally and emotionally throughout my whole PhD, which was certainly not always easy. Thank you for your patience and your calmness.

Content

Scientific Contributions

Jasmin Dold, M. Sc.

The results/experiments and publications of this thesis were developed at the Technical University of Munich, Chair of Food Packaging Technology / Chair of Brewing and Beverage Technology from January 2019 to March 2022, with further publications of the gained results in 2023.

Full Papers

The following peer-reviewed publications were generated in the period of this work and are related to the topic of the thesis.

The doctoral candidate is the main author of the four publications presented in this thesis and shares in the fundamental and major part of the conceptualization, methodology, formal analysis, investigation, data curation, writing, visualization, validation, and project administration. The writing of the original drafts of the manuscripts is exclusively her product.

1. **Dold, Jasmin** & Langowski, Horst-Christian (2022). **Optical measurement systems in the food packaging sector and research for the non-destructive evaluation of product quality.** Food Packaging and Shelf Life, 31, 100814. https://doi.org/10.1016/j.fpsl.2022.100814 (Impact Factor: 8).

2. **Dold, Jasmin**, Eichin, Melanie & Langowski, Horst-Christian (2023). **Integration of fluorophore-based sensor spots into food packaging systems for the non-destructive real-time determination of oxygen**. Food Packaging and Shelf Life, 36, 101047. https://doi.org/10.1016/j.fpsl.2023.101047 (Impact Factor: 8).

3. **Dold, Jasmin**, Götzendörfer Lukas, Hollmann Clarissa, Langowski Horst-Christian (2024). **A non-destructive measuring device in the mid-infrared range for measuring the CO_2 concentration in the headspace of food packaging**. Journal of Food Engineering, 375, 112063 . https://doi.org/10.1016/j.jfoodeng.2024.112063. (Impact Factor: 5.5)

4. **Dold, Jasmin**, Kehr, Caroline, Hollmann, Clarissa & Langowski, Horst-Christian (2022). **Non-Destructive Measuring Systems for the Evaluation of High Oxygen Stored Poultry: Development of Headspace Gas Composition, Sensory and Microbiological Spoilage.** Foods, 11(4), 592. https://doi.org/10.3390/foods11040592 (Impact Factor: 5.5).

Thesis related conferences, conference papers and presentations with the first authorship

1. **Optical methods to determine the gas atmosphere in various modified atmosphere packages: applications and correlation in meat spoilage**. The 2nd International Electronic Conference on Foods - "Future Foods and Food Technologies for a Sustainable World." Session 8: Food Packaging and Preservation. Online: 15 - 30 October 2021. Conference paper: https://doi.org/10.3390/Foods2021-11098

2. **Optische Methoden zur nicht invasiven Bestimmung der Gasatmosphäre in Schutzgasverpackungen: Anwendungen und Korrelation beim Fleischverderb.** FREISINGER TAGE: Erhalt der Lebensmittelqualität. Online: 17.03.2022

Presentations with first authorship non-related to the thesis

3. **Tethered Caps: Challenges und innovative Lösungsansätze zur Umsetzung der neuen EU Richtlinie**. 27. Flaschenkellerseminar Weihenstephan. Freising: 11.05.2022

4. **Tethered caps: consequences and solutions for the implementation of the single use plastics directive.** 2nd VLB Packaging Conference Online. Online: 31.08.2022

Abbreviations

CFU	Colony Forming Units
CIE	Commission Internationale de l'Eclairage
CO_2	Carbon dioxide
DeoxyMbFe(II)	Deoxymyoglobin
DGHM	Deutsche Gesellschaft für Hygiene und Mikrobiologie
DFB Laser	Distributed Feedback Laser
DSC	Differential Scanning Calorimetry
EVA	Ethylene Vinyl Acetate
EVOH	Ethylene Vinyl Alcohol
FAO	Food and Agricultural Organization of the United Nations
FIR	Far Infrared
FFI	Food Freshness Indicator
FT-IR	Fourier-Transform Infrared Spectrometers
IR	Infrared
HSI	Hyperspectral Imaging
LAB	Lactic Acid Bacteria
LED	Light Emitting Diode
MAP	Modified Atmosphere Packaging
Mb	Myoglobin
MbNO	Nitrosomyoglobin
MEMS	Micro-Electro-Mechanical-System
MetMbFe(III)	Metmyoglobin
MIR	Mid Infrared
NIR	Near Infrared
N_2	Nitrogen
OxyMbFe (II)	Oxymyoglobin
O_2	Oxygen
O_3	Ozone
PA	Polyamide
PE-HD	Polyethylene High-Density
PE-LD	Polyethylene Low-Density
PET	Polyethylene Terephthalate
PLA	Polylactic Acid
PP	Polypropylene
PS	Polystyrene
PVC	Polyvinyl Chloride

STP	Standard Temperature and Pressure
TDLAS	Tunable Diode Laser Absorption Spectroscopy
TVC	Total Viable Count
UV	Ultraviolet
VCSEL	Vertical Cavity Surface Emitting Lasers
VIS	Visible Spectrum
VOCs	Volatile Organic Compounds
VP	Vacuum Packaging
WVTR	Water Vapor Transmission Rate

List of formula symbols and units

Name	Symbol	Unit
Absorbance	A	%
Film Area	A_{Film}	m^2
Water Activity	a_w	
Concentration	c	mol L^{-1}
Heat Capacity	c_p	J K^{-1}
Film Thickness	d	m
Diffusion Coefficient	D	$m^2\,s^{-1}$
Fluorescence Intensity	F	%
Permeation Rate	F_P	mol m^{-2} s $^{-1}$
Specific Enthalpy	ΔH	J g^{-1}
Transmitted/Incident Intensity of Light	I/I_0	%
Flux Density	J	mol s^{-1}
Bimolecular Quenching Constant	k_q	L mol^{-1} s^{-1}
Path Length	l	m
Partial Pressure	p	Pa
Permeation Coefficient	P	mol m^{-1} s $^{-1}$ Pa^{-1}
Permeability	Q	mol m^{-2} s $^{-1}$ Pa^{-1}
		= $1.936*10^{14}$ cm^3 (STP) m^{-2} d^{-1} bar^{-1}
Heat Flow	$\dot{Q}$	kg m^2 s^{-3}
Quencher Concentration	$[Q]$	mol L^{-1}
Sorption Coefficient	S	mol m^{-3} Pa^{-1}
Transmittance	T	%
Temperature	T	°C
Glass Transition Temperature	T_g	°C
Crystallite Melting Temperature	T_m	°C
Molecular Absorption Coefficient	ε	L mol^{-1} cm^{-1}
Density	ρ	kg·m^{-3}
Stefan-Boltzmann Constant	σ	5.670374419 …10^{-8} W m^{-2} K^{-4}
Luminescence Lifetime	τ	s^{-1}
Modulation Frequency	ω	s^{-1}
Heating Rate	v	K s^{-1}
Length	x	m
Phase Shift	ϕ	°

*Q of an ideal gas with a standard molar volume of $V_{m,0}$=22.414 l/mol at standard temperature (273.17 K) and pressure (1.013 bar)

Summary

The reduction of wasted food is a global issue that has been brought to the attention of the food industry, especially by a report published by the Food and Agricultural Organization of the United Nations (FAO) about 10 years ago. The reasons for and timing of losses along the value chain are manifold and highly dependent on the surrounding infrastructure. In developing countries, for example, the causes are often inefficient production, for example due to lack of cooling equipment. In developed regions, on the other hand, more than half of the waste occurs at retail and at the end consumer. Meat and meat products account for around 20% of discarded food. This is probably often caused when the labeled "best before" or "use by" dates expire. However, after the dates have been expired, food is often still consumable from a microbiological point of view, as the producer is guided by products with a lower quality when setting the dates. Furthermore, past studies have shown that meat products packaged under a high oxygen atmosphere experience a change in the gas atmosphere in the headspace of the package, while the population of aerobic microorganisms on the packaged food increases. More specifically, the O_2 content decreases while the CO_2 content increases *vice versa*. Fresh meat is considered microbially spoiled once a microbial limit of 10^7 colony forming units per gram of sample has been reached. Nowadays, the headspace gas atmosphere in packaging is mostly measured with invasive measurement methods. Non-destructive, optical measurement methods are a promising alternative to invasive measurement methods. They have the advantage that a package is still intact after the determination of the gas atmosphere and product quality would therefore still be suitable for placing on the market, for example in retail.

Three research questions could be derived for the present work from these fundamentals. First, a review article answered the question, which promising optical, non-destructive measurement methods for the quality analysis of already packaged food – in particular meat and meat products – are already available or a subject of current research. Next, in the practical part of the work, two optical measurement methods were developed that are suitable for the non-destructive determination of the O_2 and CO_2 gas composition in the headspace of packaging for meat and meat products. Last, the applicability of the methods for assigning an individual "use by" or "best before" date was validated using non-destructive measurement of the headspace gas atmosphere of packaged meat and meat products. An extensive literature search showed that promising approaches are available in research for non-destructive quality analysis of already packaged food. Six measurement methods emerged as suitable for the focused optical range between 200 nm (UV) and 50 μm (FIR): Fluorescence spectroscopy, hyperspectral imaging (HSI), infrared spectroscopy, Raman spectroscopy, simple color measurements in the CIE L*a*b* color space, and the Tunable Diode Laser Absorption Spectroscopy (TDLAS), which is a measurement method usually operating in the NIR or MIR

that uses tunable laser diodes to measure absorption at a specific wavelength. The research also distinguished between measurements on the packaged product itself (*direct*), and measurements of the surrounding gas atmosphere (*indirect*). For all these measurement methods there were approaches that would be suitable for measuring the quality of packaged meat and meat products, but many approaches were not very practical (e.g., due to the implementation of complex chemometric correlation methods), which could complicate their application, e.g., in retail to determine an individual shelf-life date. A broad field of application to different packaging forms and types, as well as cost factors, also plays a role for commercial application. In direct measurements on the product surface, the quality parameters to be determined are often mixed with other attributes, which can also make correlation difficult. Therefore, indirect measurement of the headspace gas atmosphere was chosen as a feasible approach for the next steps in the work. For O_2 determination the fluorescence quenching approach was chosen; for CO_2 determination an absorption measurement in the MIR was chosen.

For O_2 determination a packaging system with integrated fluorescence sensor material was developed. For the integration of the sensor material, e.g., in the lid film of the packaging, a heat-sealing method was chosen, which could protect both the sensor material towards the product side from contamination with the packaged food and the food from potential migration of fluorescence material. It was demonstrated that the heat-sealing process had no negative influence on the sensor material and that a high measurement precision was given for all tested packaging materials. The focus of the work was also on the question of whether the developed packaging system allows real-time measurement of the O_2 atmosphere. The practical simulation of different permeation and diffusion processes showed that the developed method is limited in this respect. If a change in the O_2 headspace gas atmosphere is induced by a microbiological process, measurement in real time is possible. If a change in the O_2 atmosphere takes place due to diffusion processes, for example due to a leakage in the cover film, measurement in real time is not possible because the reaction of the embedded sensor showed to be too slow due to slow permeation processes through the covering of the sensor material.

For non-destructive determination of the CO_2 gas concentration of the headspace gas atmosphere, a novel measurement device was developed which operates in the MIR range (4.26, 4.27 and 4.45 µm), as this is where the main CO_2 absorption band (antisymmetric stretch) is located. In addition, a reference beam at 3.95 µm was selected to minimize the influence due to packaging-specific properties such as pigmentation, shape and defects. In the final configuration, a rapidly modulated thermal IR emitter was used, which has an emission characteristic close to blackbody radiation. The beam path of the thermal IR emitter was selected so that it passes through the corner of the tray at a 45° angle. On the one hand, this

prevents the measurement path from being disturbed by the filling material. It also ensures that the measurement path always remains the same. A multi-channel system with preceding broadband bandpass filters for the selected wavelengths was used as detector. The work was able to show that the developed measuring device delivers precise real-time results, regardless of the packaging pigmentation or film imprint (except for the pigment "Carbon Black") or the packaging shape. Surface defects or structural changes of the polymer can influence an accurate measurement.

Both measurement systems developed were used to answer the question of whether an individual "use by" or "best before" date for meat and meat products can be determined on the basis of the headspace gas atmosphere. For this purpose, different meat and sausage products (minced meat, boiled sausage, beef steak and poultry cutlets) were stored at different modified gas atmospheres and temperatures and, in addition to determining the O_2 and CO_2 gas concentrations (using both the developed non-destructive measurement methods and an invasive reference method), other quality parameters such as color, sensory characteristics and total plate count were determined. However, an individual shelf life could not be reliably determined for any of the measured samples, as a significant change in the gas atmosphere occurred either simultaneously with the achievement of the microbiological limit value or significantly after the limit value was reached. For red muscle meat, however, a prediction could not be completely ruled out. On the other hand, premature spoilage, e.g., due to incorrect storage, could also well be determined with the measurement methods.

Zusammenfassung

Die Reduktion an verschwendeten Lebensmitteln ist eine globale Problemstellung, die ins besonders durch einen vor rund 10 Jahren veröffentlichten Bericht der *Food and Agricultural Organization* der Vereinten Nationen (FAO) stark in den Fokus der Lebensmittelbranche gerückt wurde. Die Ursachen und Zeitpunkte der Verluste entlang der Wertschöpfungskette sind hierbei vielfältig und stark abhängig von der umgebenden Infrastruktur. In Entwicklungsländern beispielsweise liegen die Ursachen häufig in einer ineffizienten Produktion, beispielsweise durch nicht vorhandene Kühlbedingungen. In entwickelten Regionen fallen hingegen mehr als die Hälfte der Abfälle im Einzelhandel und beim Endverbraucher statt. Fleisch und Fleischprodukte machen hierbei rund 20 % der verworfenen Lebensmittel aus. Ursächlich sind hierfür vermutlich häufig ein Überschreiten des etikettierten Mindesthaltbarkeitsdatums bzw. Verbrauchsdatums. Nach Überschreiten der Daten sind Lebensmittel allerdings häufig aus mikrobiologischer Sicht immer noch verzehrsfähig, da sich der Produzent bei der Festlegung der Daten an Produkten mit einer geringeren Qualität orientiert. Des Weiteren konnten Studien in der Vergangenheit zeigen, dass bei Fleischprodukten, die unter einer hohen Sauerstoffatmosphäre abgepackt wurden, eine Veränderung der Gasatmosphäre im Kopfraum der Verpackung stattfindet, während die Population von aeroben Mikroorganismen auf dem verpackten Lebensmittel steigt. Konkreter gesagt, nahm der O_2 Gehalt ab, während der CO_2 Gehalt *vice versa* zunahm. Frischfleisch wird als mikrobiell verdorben angesehen, sobald eine mikrobielle Grenze von 10^7 koloniebildende Einheiten pro Gramm Probe erreicht wurde. Die Messung der Kopfraum-Gasatmosphäre in der Verpackung findet heutzutage meistens mit invasiven Messmethoden statt. Zerstörungsfreie, optische Messmethoden stellen hierbei eine vielversprechende Alternative zu invasiven Messmethoden dar. Sie haben den Vorteil, dass eine Verpackung nach der Bestimmung der Zusammensetzung der Gasatmosphäre – oder Produktqualität – noch intakt und somit beispielsweise im Einzelhandel noch zur Inverkehrbringung geeignet wäre.

Aus den geschilderten Grundlagen konnten für die vorliegende Arbeit drei Forschungsfragen abgeleitet werden. Zuerst wurde in einer Literaturarbeit die Fragestellung beantwortet, welche vielversprechenden optischen, zerstörungsfreien Messmethoden zur Qualitätsanalyse von bereits verpackten Lebensmitteln – insbesondere von Fleisch und Fleischprodukten – bereits vorhanden oder Gegenstand der aktuellen Forschung sind. Als nächstes wurden im praktischen Teil der Arbeit zwei optische Messmethoden entwickelt, die zur zerstörungsfreien Bestimmung der O_2 und CO_2 Gasatmosphäre im Kopfraum von Verpackungen für Fleisch und Fleischprodukte geeignet sind. Als letztes wurde die Anwendbarkeit der Methoden zur Erstellung eines individuellen „Verbrauchsdatums" oder „Mindesthaltbarkeitsdatums" anhand

der zerstörungsfreien Messung der Kopfraum-Gasatmosphäre von verpacktem Fleisch und Fleischprodukten validiert.

Bei der umfänglichen Literaturrecherche konnte gezeigt werden, dass bereits vielversprechende Ansätze in der Forschung zur zerstörungsfreien Qualitätsanalyse von bereits verpackten Lebensmitteln vorhanden sind. Sechs Messmethoden haben sich für den fokussierten optischen Bereich zwischen 200 nm (UV) und 50 µm (FIR) als geeignete Messmethoden herauskristallisiert: Fluoreszenz-Spektroskopie, Hyperspectral imaging (HSI), Infrarot-Spektroskopie, Raman-Spektroskopie, einfache Farbmessungen im CIE L*a*b* Farbraum, sowie die Tunable Diode Laser Absorption Spectroscopy (TDLAS), welches eine meist im NIR oder MIR agierende Messmethode ist, die mittels durchstimmbarer Laserdioden die Absorption bei einer spezifischen Wellenlänge misst. Bei der Recherche wurde ebenfalls zwischen Messungen auf das verpackte Produkt selbst (*direkt*), sowie die Messung der umgebenen Gasatmosphäre (*indirekt*) unterschieden. Für alle genannten Messmethoden gab es Ansätze, die für eine Messung der Qualität von verpacktem Fleisch und Fleischprodukten geeignet wären, allerdings waren viele Ansätze wenig praktikabel (z.B. durch die Implementierung von komplexen chemometrischen Korrelationsmethoden), was die Anwendung z.B. im Einzelhandel zur Festlegung eines individuellen Haltbarkeitsdatums erschweren könnte. Auch ein breites Anwendungsfeld auf unterschiedliche Verpackungsformen und – arten, sowie Kostenfaktoren spielen für eine kommerzielle Anwendung eine Rolle. Bei direkten Messungen auf der Produktoberfläche werden die zu bestimmenden Qualitätsparameter oftmals mit anderen Attributen vermischt, was eine Korrelation ebenfalls erschweren kann. Als praktikabler Ansatz wurde daher für das weitere Vorgehen der Arbeit eine indirekte Messung der Kopfraum-Gasatmosphäre gewählt. Für die O_2 Bestimmung wurde der Ansatz der Fluoreszenzlöschung (Quenching) gewählt, zur CO_2 Bestimmung wurde eine Messung im MIR Bereich ausgewählt.

Zur O_2 Bestimmung wurde ein Verpackungssystem mit integriertem, Fluoreszenz-Sensormaterial entwickelt. Zur Integration des Sensormaterials – z.B. in die Deckfolie der Verpackung – wurde eine Heißsiegelmethode gewählt, die sowohl das Sensormaterial zur Produktseite hin vor einer Kontamination mit dem verpackten Lebensmittel als auch das Lebensmittel vor einer potenziellen Migration von Fluoreszenzmaterial schützen konnte. Es konnte demonstriert werden, dass der Heißsiegelprozess keinen negativen Einfluss auf das Sensormaterial hat und eine hohe Messpräzision bei allen getesteten Verpackungsmaterialien gegeben war. Hauptfokus der Arbeit lag zudem in der Fragestellung, ob das entwickelte Verpackungssystem eine Messung der O_2-Atmosphäre in Echtzeit erlaubt. Die praktische Simulierung von unterschiedlichen Permeations- und Diffusionsvorgängen konnte zeigen, dass hier eine Limitierung der entwickelten Methode vorliegt. Wird eine Veränderung der O_2 Kopfraum-Gasatmosphäre durch einen mikrobiologischen Prozess induziert, ist eine Messung

in Echtzeit möglich. Findet jedoch eine Veränderung der O_2 Atmosphäre durch Diffusionsvorgänge beispielsweise durch eine Leckage in der Deckfolie statt, ist keine Messung in Echtzeit möglich, weil sich die Reaktion des eingebetteten Sensors aufgrund langsamer Permeationsprozesse durch die Sensormaterialabdeckung als zu langsam erwies. Zur zerstörungsfreien CO_2 Bestimmung der Kopfraum-Gasatmosphäre wurde ein neuartiges Messgerät entwickelt, welches im MIR Bereich (4,26, 4,27 und 4,45 µm) arbeitet, da hier die Haupt-CO_2 Absorptionsbande (asymmetrische Streckschwingung) liegt. Zudem wurde ein Referenzstrahl bei 3,95 µm ausgewählt, um den Einfluss durch verpackungsspezifische Eigenschaften wie Farbe, Form und Defekte zu minimieren. In der endgültigen Konfiguration wurde ein schnell modulierbarer thermischer IR-Strahler verwendet, der eine Emissionscharakteristik nahe der Schwarzkörperstrahlung aufweist. Der Strahlengang des thermischen IR-Emitters wurde so gewählt, dass er im 45 ° Winkel durch die Ecke des Trays verläuft. So wird zum einen verhindert, dass der Messpfad durch das Füllgut gestört wird. Zudem wird ein immer gleich-bleibender Messpfad gewährleistet. Als Detektor wurde ein Multi-Channel System mit vorangesetzten Breitband Bandpassfiltern für die ausgewählten Wellenlängen gewählt. Die Arbeit konnte zeigen, dass das entwickelte Messgerät präzise Echtzeitergebnisse liefert, unabhängig von der Verpackungspigmentierung oder Folienaufdruck (mit Ausnahme des Pigments „Carbon Black") oder der Verpackungsform. Oberflächendefekte oder strukturelle Veränderungen des Polymers können dagegen eine präzise Messung beeinflussen.

Beide entwickelten Messsysteme wurden zur Beantwortung der Fragestellung eingesetzt, ob ein individuelles „Verbrauchsdatum" oder „Mindesthaltbarkeitsdatum" für Fleisch und Fleischprodukte durch die Bestimmung der Kopfraum-Gasatmosphäre festgelegt werden kann. Hierfür wurden unterschiedliche Fleisch und Wurstwaren (Hackfleisch, Brühwurst, Rindersteak und Hähnchengeschnetzeltes) bei unterschiedlichen modifizierten Gasatmosphären und Temperaturen gelagert und neben der Bestimmung der O_2 und CO_2 Gaskonzentrationen (sowohl mit den entwickelten zerstörungsfreien Messmethoden, als auch mit einer invasiven Referenzmethode), weitere Qualitätsparameter wie Farbe, Sensorik und die Gesamtkeimzahl bestimmt. Ein individuelles Haltbarkeitsdatum konnte allerdings für keine der gemessenen Proben sicher bestimmt werden, da eine signifikante Veränderung der Gasatmosphäre entweder gleichzeitig mit dem Erreichen des mikrobiologischen Grenzwertes oder erst deutlich nach Erreichen des Grenzwertes stattgefunden hat. Für rotes Muskelfleisch allerdings konnte eine Vorhersage nicht komplett ausgeschlossen werden. Ein vorzeitiger Verderb bspw. durch eine inkorrekte Lagerung könnte jedoch mit den Messmethoden bestimmt werden.

1   Introduction

1.1   Polymer-based food packaging

Although there is nowadays a lot of criticism in the society regarding the packaging of food with plastics, it is undeniable that polymer-based packaging is, along with paper board, the most important packaging type for retaining the quality of food worldwide (Piergiovanni & Limbo, 2016). Since the first use of polyethylene in the 1930's for the packaging of food (Coles et al., 2003), the development and research on improved packaging types – tailor made for the packaged good – are still ongoing.

Plastic packaging consists of around 70–99% polymers (depending on the amount of additives such as plasticizers, antioxidants, pigments, etc.), which is why the nomenclature "polymers" and "plastics" is often used as synonym (Piergiovanni & Limbo, 2016).

Plastics can be categorized at various levels. Firstly, a distinction can be made regarding the raw material: If it is produced from natural raw materials or synthetically. Secondly, polymer-based materials are classified based on the method of production regarding the polymerization reaction, namely a condensation or addition reaction. Thirdly, they are classified according to the physical properties of the polymers as thermoplastics, elastomers, and thermosets. The group most used for food packaging are thermoplastics. Thermoplastics are linear or branched polymers with either an amorphous or semi-crystalline structure (Brandsch & Piringer, 2008). They have the advantage that they can be melted and thus shaped using temperature and pressure. Figure 1 shows a schematic illustration of amorphous and semi-crystalline structures.
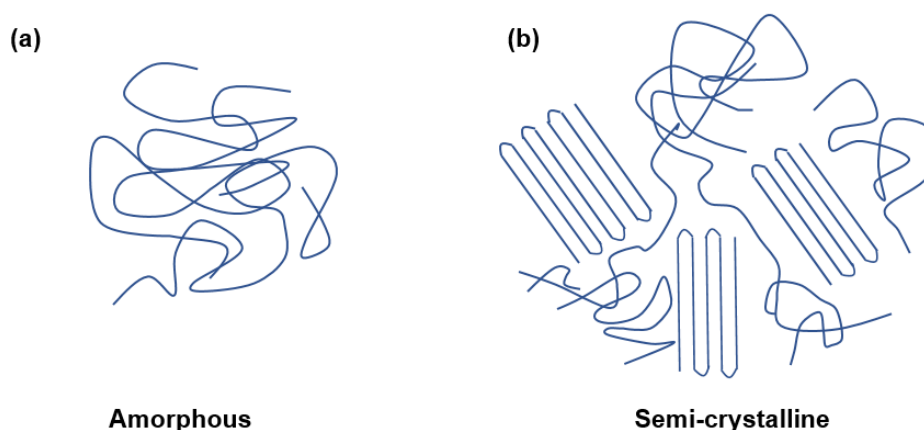

Figure 1: Morphology of thermoplastics: Schematic representation of (a) amorphous and (b) semi-crystalline structures of synthetic polymers (own illustration, according to (Piergiovanni & Limbo, 2016))

The ratio of the amorphous and semi-crystalline parts of a plastic is relevant for its properties, as amorphous and semi-crystalline structures are completely different in their behavior. The following Table 1 shows the main differences:

Table 1: Comparison of the properties of amorphous and semi-crystalline polymers (adapted to (Horvath et al., 2017; D. S. Lee et al., 2008))

Property	Amorphous polymers	Semi-crystalline polymers
Transmission (VIS)	higher transparency	higher opacity
Melting	no distinct melting point	crystallites are melting at a specific temperature
Hardness	generally, relatively weak and flexible	for most polymers hard and brittle, low impact resistance
Gas barrier	moderate to poor	moderate to good
Chemical resistance	moderate	good

However, for the semi-crystalline polymers it must added that their properties can be highly influenced by the cooling rate or orientation, while amorphous polymers are less affected by these factors (D. S. Lee et al., 2008).

There are several important polymers used within the food packaging industry. The most important are shown in Table 3. Polyethylene (PE) is the most-used polymer—in either its low-density (PE-LD) or high-density (PE-HD) form. In the case of PE, for example, so-called chain growth polymerization with ethylene takes place, in which the monomers are covalently linked (by double bonds). Another polymerization would be condensation polymerization which is, for example, the method of choice to produce polyethylene terephthalate (PET). In this process, the molecules pairwise bond by releasing water (Piergiovanni & Limbo, 2016).

1.1.1 Thermal properties of polymers

To gain the desired form of the polymer for use as food packaging, the thermal properties —the behavior of the material when experiencing energy input in form of heat—are of great interest. From that knowledge, the defined temperatures, e.g., during film production (extrusion), form production (blow molding, injection molding or a thermoforming line) or heat-sealing can be chosen. Thermal properties can for example be investigated using so-called differential scanning calorimetry (DSC). The measurement is based on the change in the internal energy of a polymer at constant heat flow $\dot{Q}$ and partial pressure p. The change in internal energy is the enthalpy change ΔH. By comparing the heat flow of the measured sample to the reference sample with no enthalpy changes (baseline), the amount of ΔH can be calculated, using the heat flow difference. Endothermic processes, such as melting, evaporation or glass transition, lead to an increase in enthalpy or decrease in heat flux. Exothermic transformations, such as crystallization, hardening and decomposition, lead to a corresponding decrease in enthalpy or

increase in the measured heat flow. The heat flow $\dot{Q}$ is the amount of heat per time and mass, which is proportional to the specific heat capacity c_p with the proportionality factor of the heating rate v (Ehrenstein et al., 2003). A typical curve for a DSC measurement of a (semi-crystalline) polymer is shown in Figure 2.

The glass transition, which is a shift of the base line due to the transition from the glass-elastic to the rubber-elastic state, is related to the amorphous parts of a polymer. Due to the glass transition, no real phase transition, but a relaxation transition takes place. Above the glass transition temperature, which is defined as the temperature at which half of the change in specific heat capacity has already been converted, the polymer has a more liquid-like behavior ("rubbery state") than a solid-like behavior ("glassy state"). For semi-crystalline polymers, the glass transition is often more difficult to measure via DSC, as its appearance is highly dependent on the degree of initial crystallinity (Frick & Stern, 2011).
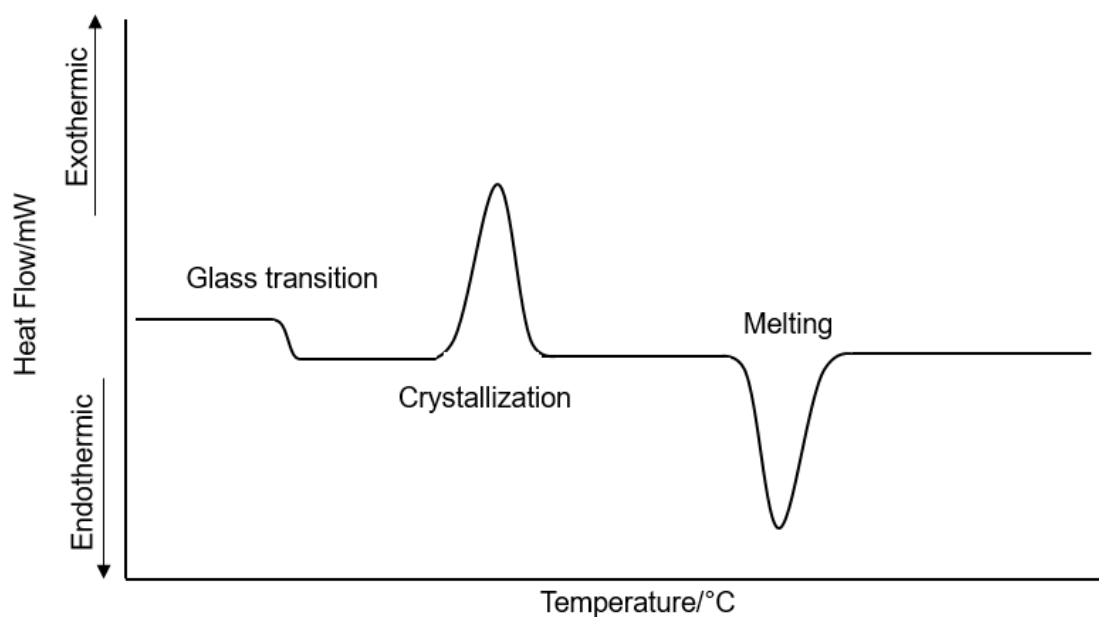

Figure 2: Schematic illustration of a DSC curve for semi-crystalline polymers (own illustration)

Crystallization typically happens during cooling and is the reaction opposite to melting. Melting and crystallization correspond to the crystalline part of a polymer, which is why semi-crystalline polymers have a melting and crystallization peak, whereas amorphous polymers only have a value in glass transition. For some polymers such as PET, it is also quite regular that during the heating process an exothermic peak appears, which is known as the re-crystallization of amorphous structures (Frick & Stern, 2011). The thermal behavior of important food packaging polymers is also shown in Table 3.

1.1.2 Permeation properties of polymers

Among the most important polymer properties, when it comes to the packaging of food products, are their gas barrier properties. They are decisive as to whether a food is protected from gases or water long enough for optimum shelf life. In general, the permeance and water vapor transmission (WVTR) rates are therefore most significant. Figure 3 shows the oxygen permeability and WVTR values for several polymers. Table 3 also gives an overview of typical values for oxygen permeability. The values mentioned are for orientation purposes and should not be understood as fixed values, since large differences in the measured values can be found within the published literature (Buchner, 1999).
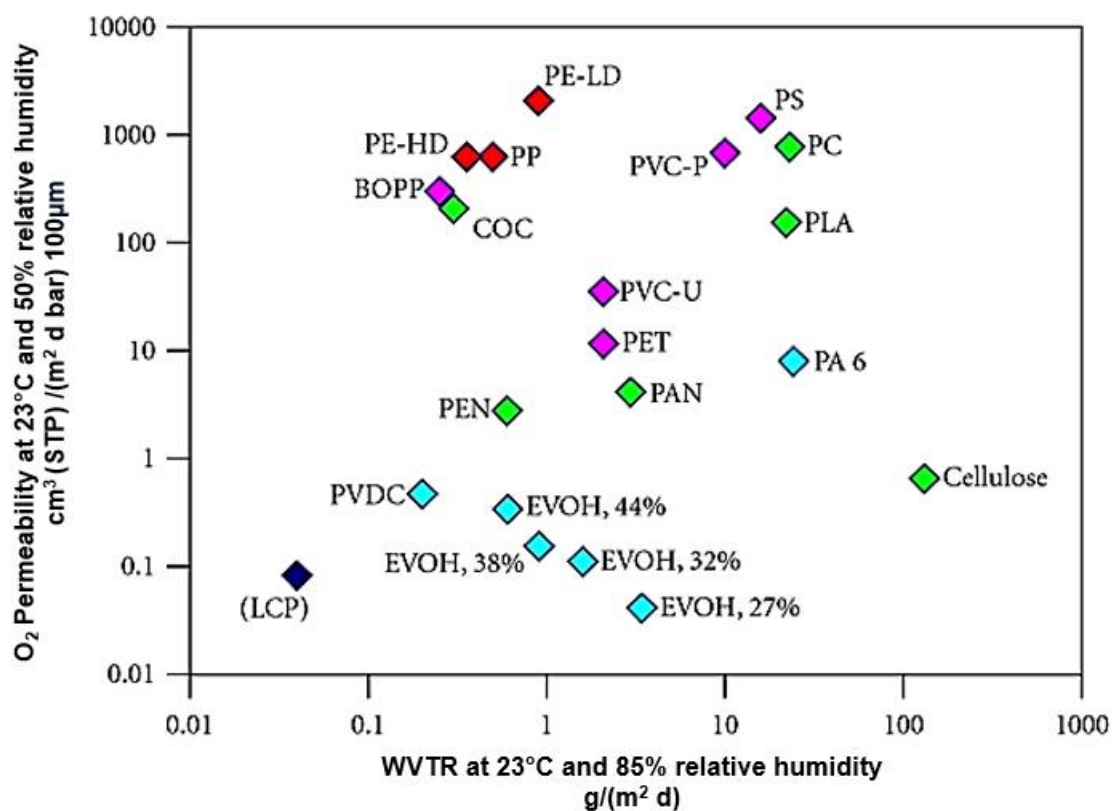

Figure 3: Comparison of oxygen permeability and water vapor transmission rates at 23°C of some polymers commonly used in the packaging industry normalized to a thickness of 100 µm (adapted to (Schmid et al., 2012))

For better comparability, the values are often normalized to a film thickness of 100 µm and standard conditions (273.15 K, 1013 mbar), using the ideal gas law (compare equation 1.8). Even if the standardization of the unit of the O_2 permeability and WVTR would make sense, it is unfortunately often apparent from the literature that there is no uniform designation (Buntinx et al., 2014; Gonzalez et al., 2008; Kim et al., 2005).

The figure shows clearly that there can be large differences in barrier properties depending on the polymer, which has indeed a significant influence on product quality (Baur et al., 2013).

The permeation of gases is, after reaching the stationary state (= equilibrium state of the permeating substance in the to be entered film sample has been reached (Langowski, 2017)), linear over time (Buchner, 1999) and is based on three sub steps: adsorption, diffusion and desorption. First, gas molecules are adsorbed onto the film surface on both sides of the packaging material. This occurs in a concentration dependent on the partial pressure present on the respective side. After adsorption, the molecules initially dissolve near the film surface. Due to the different concentrations on the surfaces, the molecules diffuse through the film in the direction of the lower concentration. As a result, the concentration on the side with the lower partial pressure increases. As a result, there is an imbalance between the concentration and the partial pressure prevailing in the environment. In order to regain the equilibrium, the last step is the desorption of the molecules from the side in contact with the volume of lower substance concentration of the film surface (Langowski, 2008; D. S. Lee et al., 2008). The measurement of gas permeation is accomplished by the measurement of the increase in the gas concentration, e.g., with optical sensors (DIN Standards Committee Packaging, 2014).

<u>Theoretical background of the one-dimensional permeation process</u>:
The calculation of the one-dimensional permeation process, in which the gas permeates through a homogenous film, is based on the combination of Henry's law (1.1) and Fick's first (1.2) and, if the time dependency is relevant, e.g., for the non-steady state, Fick's second law (1.3) (Langowski, 2008, 2017):
In the case of constant solubility, Henry's law applies with the concentration c on the respective side, the partial pressure p of the substance on the respective side, and the sorption coefficient S. Fick's first law describes the diffusion of the substance, whereas J describes the diffusion flux (also abbreviated with F in the literature), because of the diffusion coefficient D, as a function of the concentration of the substance c and the length x. The second law in addition considers the time dependency t.

Henry's law $$c = S * p \tag{1.1}$$

Fick's first law: $$J = -D \frac{\partial c}{\partial x} \tag{1.2}$$

Fick's second law: $$\frac{\partial c}{\partial t} = D \frac{\partial^2 c}{\partial x^2} \tag{1.3}$$

It is often assumed that, for a given polymer and gas, the sorption coefficient remains independent of the concentration (Langowski, 2008). In the following, c_1 stands for the concentration of the substance on the side of the film with the higher partial pressure and c_2

for the concentration on the side with the lower partial pressure. After steady state is reached, a constant or stationary flux density J is reached ($J = \frac{\partial c}{\partial t} = const$). At this point, $\partial c/\partial x$ is also constant, resulting in a linear increase in the permeated mass through the film with a thickness d. The permeation occurs from the side with the higher partial pressure c_1 to the side with the lower partial pressure c_2 and can be described by inserting these values into 1.2:

$$J = D\, \frac{c_1 - c_2}{d} \tag{1.4}$$

By combining this law with the Henry's law, it follows:

$$J = D * S\, \frac{p_1 - p_2}{d} = P\, \frac{p_1 - p_2}{d} \tag{1.5}$$

The permeation coefficient P is defined as the product of the diffusion coefficient D and the sorption coefficient S.

The permeation rate or flux F_P through a film is defined as the product of the flux density with the area A_{Film} of the film through which the gas can permeate (Langowski, 2008):

$$F_P = J * A_{Film} = P * A_{Film}\, \frac{p_1 - p_2}{d} \tag{1.6}$$

The permeability Q is given by (Langowski, 2008):

$$Q = \frac{P}{d} = \frac{F_P}{A_{Film}(p_1 - p_2)} \tag{1.7}$$

To have standardized results, the values have to be adapted, using the ideal gas law:

$$\frac{p_1 V_1}{T_1} = \frac{p_2 V_2}{T_2} \tag{1.8}$$

In the case of permeation through a multilayer film, the individual permeabilities can be reciprocally summed up and calculated with *i* layers as follows (Buchner, 1999; Langowski, 2008):

$$\frac{1}{Q} = \sum_i \frac{1}{Q_i} = \sum_i \frac{d}{P_i} \tag{1.9}$$

1.1.3 Modified atmosphere packaging and vacuum packaging

Modified atmosphere packaging (MAP) involves the replacement or changing of the ambient gas atmosphere within a packaging system to enhance or preserving food quality (Church & Parsons, 1995). The modification and the gases used depend on which food is to be packaged and which (quality) parameter is to be influenced. In many cases, the goal is to enhance the shelf life of a food product. The gases used for the modification are called protective gases. The gas mixtures used for MAP consist mainly of the gases nitrogen (N_2), carbon dioxide (CO_2) and oxygen (O_2). N_2 serves most commonly as an inert filling gas, without any direct influence on the food itself, but to obtain the desired concentration ratio of O_2 and CO_2 (D. S. Lee et al., 2008). CO_2 acts as a bacteriostatic. Its use as a protective gas for a food product was first documented in 1883 by Hermann Kolbe, who placed beef in a CO_2 gas-atmosphere to analyze its antiseptic effect (Kolbe, 1883). The gas influences both the lag phase and the growth rate of microorganisms (Gill & Tan, 1980). O_2 is reduced or removed for MAP in most cases, since many microbiological and enzymatic processes responsible for spoilage require O_2. However, for some products the presence of O_2, such as fresh fruits and vegetables for cellular respiration or red meat for color, is advantageous (D. S. Lee et al., 2008).

When setting the MAP in a package, it must always be taken into account that the gas atmosphere does not remain static. Figure 4 shows the most influential factors responsible for gas changes within a MAP food system: Gases solubilization in the food product (Chaix et al., 2015) can decrease the gas concentration in the headspace. In addition, permeation through the packaging induced by the different partial pressures inside the packaging and of the ambient air – as described in 1.1 – will also affect the protective gas atmosphere during storage (Buchner, 1999).
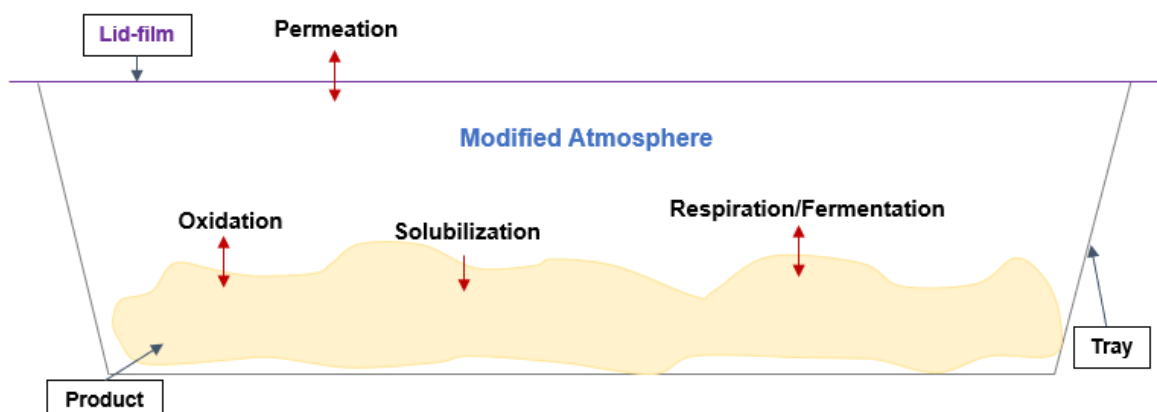

Figure 4: Different processes affecting the modified atmosphere within a packaged food system. The red arrows demonstrate gas exchange and the direction of interaction between tray, lid film, food and headspace (adapted to (Chaix et al., 2015)).

For packaging with, e.g. ,80% (v/v) O_2 and 20% (v/v) CO_2 MAP, both the O_2 and the CO_2 will permeate out of the packaging, as the ambient air has lower O_2 (20.9% (v/v)) and CO_2 (0.041%

(v/v)) concentrations, which can then lead to the collapse of the packaging as a consequence. But the product itself can also change the headspace atmosphere, for example, due to chemical processes such as oxidation or (micro)biological activity such as fermentation or respiration processes (e.g., uptake of O_2 and release of CO_2) (Buchner, 1999; Chaix et al., 2015; Meredith et al., 2014).

Another common way to change the headspace air within packaging is the (almost) complete removal of the air. This method is called vacuum packaging (VP). VP is often used for O_2-sensitive products (which are not negatively influenced by the vacuum), as the almost complete removement of O_2 leads to much lower oxidation activity by simultaneous enhancement of the shelf life by the inhibition of microorganisms. Compared to MAP, VP is more cost and space efficient (Embleni, 2013). For some meat and meat products, vacuum skin packaging is therefore the method of choice. With this VP method, a heated and softened lid film covers the product, which was pre-placed on the lower tray in a vacuum chamber directly (like a second skin of the product) (Yamaguchi, 1990).

1.1.4 Packaging of meat and meat products

Since unpreserved meat and meat products generally have a short shelf life (see section 1.2), suitable packaging plays an important role in maintaining quality so that the product can be stored for an adequate period of time after being placed on the market before being consumed by the end consumer. For meat and meat products, either a modified atmosphere or vacuum packaging is the method of choice. Table 2 gives an overview for typical gas compositions (MAP or vacuum) for meat and meat products mentioned in the literature and their (positive and negative) impact on the quality of the packaged food product:

Table 2: Some typical modified atmospheres for packaged meat and meat products and the impact of gas composition on food product quality.

Meat or Meat-product	Atmosphere	Quality impact		Reference
		positive	negative	
Beef (fresh)	80% (v/v) O_2 20% (v/v) CO_2	• Maintaining of OxyMbFe(II) • Inhibition of anaerobes	• Lipid oxidation • Protein oxidation	(Church & Parsons, 1995)
	Vacuum	• Inhibition of aerobes • Inhibition of oxidation	• DeoxyMbFe(II) formation	(Boles & Pegg, 2010) (Kameník et al., 2014)
Chicken (fresh)	70-80% (v/v) O_2 20-30% (v/v) CO_2	• Inhibition of anaerobes	• Promotion of aerobes • Lipid oxidation • Protein oxidation	(Chmiel et al., 2018) (Herbert et al., 2015) (Höll et al., 2016)
	65% (v/v) N_2 35% (v/v) CO_2	• Inhibition of aerobes	• Potential grow for anaerobic pathogens	(Höll et al., 2016)
Cured boiled sausages	0.5% (v/v) O_2 99.5% (v/v) N_2	• Inhibition of aerobes • Inhibition of lipid oxidation • Inhibition of nitrosomyoglobin oxidation	• Potential grow for anaerobic pathogens	(Böhner & Rieblinger, 2016; Gibis & Rieblinger, 2013)
	70% (v/v) N_2 30% (v/v) CO_2			(Kameník et al., 2015)
Dry fermented sausages	20% (v/v) N_2 80% (v/v) CO_2	• Inhibition of nitrosomyoglobin oxidation		(Walz et al., 2017)
Minced beef	70-80% (v/v) O_2 20-30% (v/v) CO_2	• Maintaining of OxyMbFe(II) • Inhibition of anaerobes	• Fat oxidation	(Church & Parsons, 1995) (Hilgarth et al., 2019)
Pork (fresh)	70% (v/v) O_2 30% (v/v) CO_2	• Inhibition of anaerobes • Color stability	• Lipid and protein oxidation • Lower juiciness	(Cayuela et al., 2004) (Peng et al., 2019) (Lund et al., 2007)
	Vacuum	• Inhibition of aerobes • Inhibition of oxidation	• (Water holding capacity)	(Cayuela et al., 2004) (Kameník et al., 2014)

Maintaining MbFe(II):

This quality aspect is mainly interesting for the packaging of red muscle beef, as it ensures a stable, red coloring attractive the consumer (Corlett et al., 2021).

Myoglobin (Mb) is the heme protein which is, from a physiological point of view, primarily responsible for the temporary storage of O_2 in the erythrocytes (red blood cells). Mb appears red, but, depending on Mb oxidation or reduction state, its color differs (Livingston & Brown, 1981). Figure 5 shows different possibilities for the redox reactions and gives also an indication of the resulting colorization.
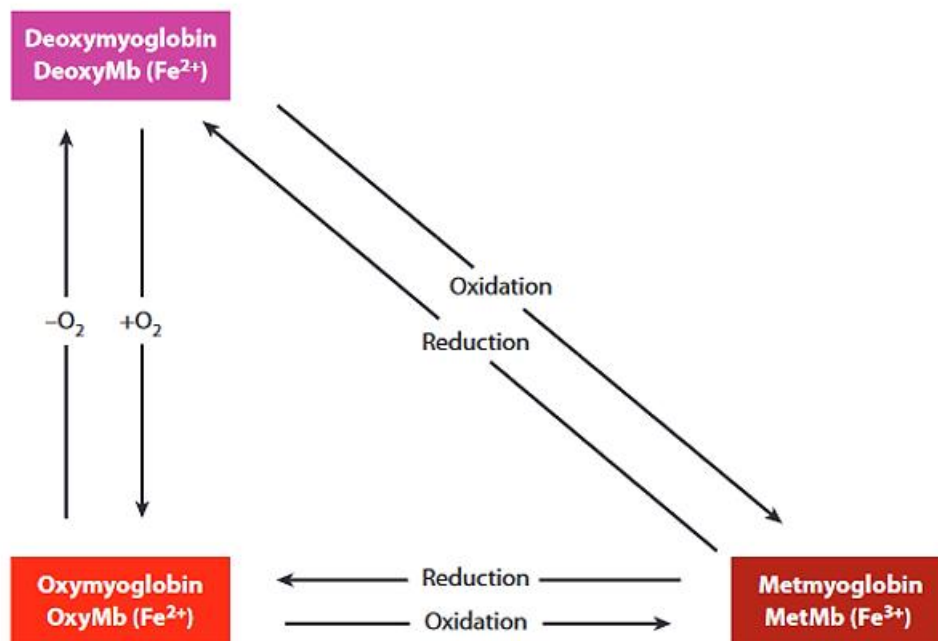

Figure 5: Colorization of myoglobin in red muscle beef as a function of the oxidation or reduction state (adapted to (Suman & Joseph, 2013)).

Oxymyoglobin (OxyMbFe(II)) is the most desired redox variety, as it leads to a bright, red color of the meat and is the reason why red muscle beef is packaged in a high O_2 atmosphere in general. The oxidation to metmyoglobin (MetMbFe(III)) is in contrast the most unwanted state, as it changes the color to grey-brown. That effect occurs at low O_2 partial pressure values. Forrest et al. showed in 1975 that the formation of MetMbFe(III) starts at a O_2 partial pressure of 100 hPa and reaches its maximum at 5 hPa (Forrest et al., 1975; Hood & Riordan, 1973). Vacuum packaging results in contrast in a more purple color, induced by deoxymyoglobin (DeoxyMbFe(II)), which is formed at O_2 partial pressures below 20 hPa, reaching a maximum at O_2 partial pressure values <5hPa (Forrest et al., 1975; Suman & Joseph, 2013). Other meat sources like pork or poultry also experience this transformation. However, due to their significantly lower amounts of MbFe(II), the color change is not that apparent for them (Ginger et al., 1954).

<u>Nitrosomyoglobin oxidation</u>:

Nitrosomyoglobin (or nitrosylmyoglobin, MbNO) arises during the cooking and curing of meat in the presence of nitrites, e.g., in preparing sausages, and results in a pink colorization (Cassens, 1997). Due to exposure to light at a certain wavelength between 300 and 600 nm, the bound NO dissociates. If O_2 is present, it can absorb the energy and thereby be converted into the excited singlet state. This excited state is highly reactive and leads to the oxidation of the food coloring (Fe(II) $\rightarrow$ Fe (III)), which in turn is reflected in a gray-brownish color. That process is called photooxidation and is the reason why sausages are packaged in the absence of O_2, using N_2 and CO_2 as protective gas or under vacuum conditions (Møller et al., 2002; Suman & Joseph, 2013).

<u>Lipid and protein oxidation</u>:

Lipid and protein oxidation processes are especially undesirable in meat and meat products in terms of sensory perception, as oxidation can lead, for example, to the formation of volatile organic compounds (VOC's) (Casaburi et al., 2015). For lipids, oxidation either occurs at stored triglycerides or tissue phospholipids (Love & Pearson, 1971). The oxidation of fat often leads to rancid off-flavors. Due to the oxidation of protein and free amino-acids, off-flavors such as ammonia can be formed. But the structure of the meat and the meat product can also be affected, as oxidation leads to a crosslinking of proteins and, as a result, to a loss of water retention capacity causing the texture to be less juicy and tender (Lund et al., 2011; Lund et al., 2007).

<u>Water retention capacity</u>:

The water retention capacity of meat can be influenced by many process steps along the meat production value chain, and many factors are not totally clarified yet (Hertog-Meischke et al., 1997). However, it is an important quality factor for meat. From an economical point of view, the loss of water before the packaging or production step is unfavorable, as less product can be produced, which means a loss of money. From a consumer point of view, a lower water retention capacity leads to quality changes and unappealing retail aesthetics (Forrest et al., 2000; Pettersen et al., 2021). Many publications have tried to find a correlation between packaging type and drip loss. However, many contrary statements—even within one animal group—are represented here (Cayuela et al., 2004; Doherty et al., 1996; Łopacka et al., 2016; Sørheim et al., 1996). Water retention capacity appears to be largely influenced by early postmortem events that affect meat quality, making it difficult to establish a packaging-effects relationship (Huff-Lonergan & Lonergan, 2005).

Influence on anaerobes and aerobes:

The influence of the surrounding headspace gas atmosphere of packaged meat and meat products on the development of the microbiome on the filling good is significant, since either aerobic or anaerobic microorganisms are inhibited or promoted, respectively. The absence of O_2, for example, can inhibit obligate aerobic microorganisms, since they require O_2 for respiration. Conversely, this promotes microaerophilic or obligate anaerobic microorganisms. If a product is packaged with a high O_2 atmosphere, the effect is reversed (Krämer, 2010). Therefore, it is important to choose a protective gas atmosphere that ensures the best possible product quality.

1.1.5   Optical properties of polymers

For the optical measurement systems investigated in this work, one polymer property was most decisive: Transmittance (T) of light within the electromagnetic spectrum—especially for the visible spectrum (VIS) (300 nm – 800 nm) and the infrared (IR) (800 nm – 500.000 nm). Basically, this property can be described as the ratio of transmitted intensity (I) to the incident intensity (I_0) at a certain frequency:

$$T = \frac{I}{I_0} \tag{1.10}$$

It is known that I is dependent on the length of the path l to be penetrated, as well as the molecular concentration c of the substance or material and the molecular absorption coefficient ε. These relations can be described with the Lambert Beer's law:

$$I = I_0 10^{-\varepsilon c l} \tag{1.11}$$

The molecular absorption coefficient increases with the absorption. A is calculated as a simplification of Lambert Beer's law as follows:

$$A = -log T = \varepsilon * c * l \tag{1.12}$$

The Lambert Beer's law describes transmission and is used in many spectroscopic applications (Atkins et al., 2022).

Polymers can be identified by their transmission behaviors and their characteristic absorption peaks. These properties are in general detected via Fourier-Transform Infrared Spectrometers (FT-IR)—in either transmission or reflectance mode working in the IR spectral range (Böcker, 2014). For non-destructive gas analytics, the absorption and emission properties of which are described in more detail in sections 1.3.1 and 1.3.2, it is indispensable that polymer absorption does not overlap with gas absorption or emission. In addition, colorants or pigments used for packaging may also influence the results, especially in the VIS area. Table 3 shows the absorption properties of common polymers within the IR range.

Table 3: Overview of the most important polymers used for food packaging and their properties. (T_g: Glass transition temperature, T_m: Crystallite melting temperature) (Agroui et al., 2012; Baur et al., 2013; Buchner, 1999; Ciurana et al., 2013; Demarteau et al., 2018; Frick & Stern, 2011; Kamarudin et al., 2018; Lai et al., 2012; D. S. Lee et al., 2008; Piringer & Baner, 2008; Smith, 2021a, 2021b, 2023; Xu et al., 2018)

Polymer	Thermal Characteristic		Oxygen (O_2) Barrier/	Density/	Infrared Absorption Bands and Related Molecular	
	T_g/°C	T_m/°C	cm^3 (STP)/(m^2dbar)100 µm	g/cm^3	Vibrations/cm^{-1}	
Ethylene vinyl alcohol (EVOH) (32% Ethylene)	57–69	183	0.1	1.14–1.21	3300	O-H stretch
					2925	CH_2 asymmetric C-H stretch
					2851	CH_2 symmetric -C-H stretch
					1550	C=O stretch
					1450, 1327	C-H bend
Polyamide (PA)	PA-6: 78 PA-66: 90	220–230 250–265	<10	1.12–1.14	3301	N-H stretch
					3081	Overtone of N-H bend
					1641	C=O stretch
					1542	In-plane N-H bend
					1274	C-N stretch
					691	Out-of-plane N-H bend
Polyethylene high density (PE-HD)	< -100	125–135	800–1000	0.95–0.96	2919	CH_2 asymmetric C-H stretch
					2850	CH_2 symmetric -C-H stretch
					730, 720	Split CH_2 rock
Polyethylene low density (PE-LD)	< -100	105–120	1000–2000	0.92–0.94	2917	CH_2 asymmetric C-H stretch
					2852	CH_2 symmetric -C-H stretch
					1377	CH_3 umbrella mode
					718	Split CH_2 rock
Polyethylene terephthalate (PET)	98–125	250–265	10	1.37–1.41	1721, 1730	Aromatic ester C=O stretch
					1245, 1286	Aromatic ester C-C-O stretch
					1100, 1118	Aromatic O-C-C stretch
Polylactic acid (PLA)	45–65	150–160	100–200	1.24	2939	C-H stretch
					1748	C=O stretch
					1450, 1360	C-H bend

					1184, 1079	C-O stretch
Polypropylene (PP)	0–20	160–170	300–800	0.90–0.91	2956, 2875	CH_2 asymmetric and symmetric C-H stretch
					2921, 2840	CH_2 asymmetric and symmetric C-H stretch
					1377	CH_3 umbrella mode
Polystyrene (PS)	80–110	-	1000–1200	1.04–1.12	3081, 3059, 3025	Aromatic C-H stretches
					2923, 2850	CH_2 asymmetric and symmetric stretches
					1600, 1492	Aromatic ring modes
					756	Aromatic out-of-plane C-H bend
					698	Aromatic ring bend
Polyvinyl chloride (PVC)	81–99	-	800	1.39–1.43	2965	CHCl asymmetric stretch
					2910, 2816	CH_2 asymmetric and symmetric stretches
					2851	CHCl symmetric stretch
					1434	CH_2 amorphous band
					1425	CH_2 crystalline band

1.2 Meat spoilage

Meat is very sensitive to microbiological spoilage, which makes this is a limiting factor for storage. Meat—red muscle meat as well as white meat—has a water activity(a_w) (actively available water) of 0.98–0.99 and an almost neutral pH, which are perfect conditions for the growth of microorganisms (Krämer, 2010; Torres et al., 1994). From the origin, the microbiological milieu of both meat types is similar, but the composition may vary due to the slaughtering process: The carcasses of red meats are first split and then skinned before evisceration. For white (poultry) meat, a purely mechanical process takes place, with neither skinning nor splitting. Slaughtering poultry also requires significantly more water because they are immersed in warm water (52–59°C) before the feathers are removed. Cattle, for example, are skinned without water, and the contamination of the meat by skins and gut contents must be avoided. The microbiological contaminations for both meat types are therefore mainly found on the surface or skin and not in the deeper muscle tissue (Mead, 2006). After slaughtering, the meat is further processed and packaged, and these production steps are most decisive for the spoilage bacteria to be found on the meat product. There are several typical meat spoilers known, such as *Brochothrix thermosphacta,* lactic acid bacteria (LAB) (e.g., *Carnobacterium* ssp*., Leuconostoc* ssp*., Lactobacillus* ssp.), *Pseudomonas* ssp., *Enterobacteriaceae* (e.g. *Serratia* or *Yersinia*) or *Micrococcus* (Alessandroni et al., 2022; Borch et al., 1996; Franke et al., 2017; Höll et al., 2016; Mead, 2006). Recent studies also show that photobacteria, which were originally associated with fish spoilage, also play a crucial role in meat spoilage. Hilgarth et al. showed in 2018 that *Photobacterium carnosum* was predominant in MAP packed beef and chicken meat, while *Photobacterium iliopiscarium* was found on pork (Hilgarth et al., 2018). In thinking about the right choice for preservation of meat and meat products, not only are the predominant microorganisms, but also those that can be present in a minor concentration on the product but are highly pathogenic, are decisive. One of these pathogens may be, for example, *Campylobacter jejuni*. This microorganism can enter the meat via smear infections and fecal contamination and can lead to gut infections and acute diarrhea. *C. jejuni* is microaerophilic (Keweloh, 2019; Krämer, 2010), which means that a high oxygen presence, e.g., adjusted due to a high oxygen atmosphere via MAP, can prevent the growth of this pathogen and thus avoid hazardous meat product. However, the choice of the optimal packaging method to prevent the growth of microorganisms is practically not given, as different microorganisms have different growth characteristics, which in turn entail different consequences for meat quality. In Table 4, some common microorganisms found on meat and meat products are shown and categorized in terms of their respiration, pathogenicity, and impact on quality.

Table 4: Overview of common microorganisms found on meat and meat products within the known literature and their main possible quality impacts.

Bacteria	Respiration	Quality impact	Reference
B. thermosphacta	aerobic	• formation of VOC's	(Nychas & Drosinos, 1999)
C. jejuni	microaerophilic	• highly pathogenic	(D'Agostino & Cook, 2016)
Enterobacteriaceae *Escherichia coli* *Hafnia* ssp. *Serratia* ssp. *Yersinia* ssp.	facultative anaerobic	• potentially pathogenic • formation of VOC's	(Krämer, 2010) (Pennacchia et al., 2011)
Lactic acid bacteria (LAB) *Carnobacterium* ssp. *Lactobacillus* ssp. *Lactococcus* ssp. *Leuconostoc* ssp.	facultative anaerobic	• formation of VOC's • pH decrease	(Alessandroni et al., 2022) (Mead, 2006) (Höll et al., 2020)
Photobacetrium ssp.	facultative anaerobic	• formation of VOC's	(Nieminen et al., 2016)
Pseudomonas ssp.	facultative anaerobic	• discoloration (green) and VOC's	(Casaburi et al., 2015) (Rossaint et al., 2015)

Nychas and Drosinos name many more microorganisms that can be found on meat and meat products (Nychas & Drosinos, 1999), but the microorganisms listed in the table are, to the best of the authors' knowledge, the most frequently mentioned in the literature. Most of the common species are not pathogenic; they are in general more an issue regarding the sensory spoilage of meat and meat products, as most of them are responsible for the formation of VOC's, which are catabolized by the degradation of sugars, proteins, free amino acids and lactic acid to organic acids, ethyl esters, fatty acids, sulfur compounds of ammonia, alcohols and so on (Casaburi et al., 2015; Nychas & Drosinos, 1999), as was already mentioned in section 1.1.4. The number of formed odor-active volatile substances that can be found on a spoiled meat or meat product is enormous (Casaburi et al., 2015), but there are compounds that particularly contribute to odor change, such as 2,3-butanedione (diacetyl), sulfur compounds, lactic or acetic acid or isovaleric acid, resulting in olfactory perceptions such as buttery, (rotten) egg-like, pungent or cheesy (Casaburi et al., 2015; Kadota & Ishida, 1972; Kakouri & Nychas, 1994; Keupp et al., 2015; Nassos et al., 1983). Another process during spoilage that leads to a sensory change is the degradation of muscle tissue, mainly recognizable at a total viable count (TVC) of 10^8 CFU/g (colony forming units per gram), which leads to slime formation on the meat surface (Charles et al., 2006)

The influence of the spoilage of meat and meat products on human sensory perception is described in more detail in the results section of this work.

A TVC of 10^7 CFU/g is defined as a critical value for the microbiological spoilage of fresh meat, (Baumgart et al., 2016). However, for some pathogenic microorganisms such as *Escherichia coli*, coagulase-positive staphylococci, *Bacillus cereus*, *Salmonella* or *Listeria monocytogenes* lower limits are defined—or in case of *Salmonella* its presence is not allowed at all. In Germany, these values are defined by the „Deutsche Gesellschaft für Hygiene und Mikrobiologie (DGHM)".

The respiration of the microorganisms (compare Table 4) is decisive for the adjusted packaging atmosphere. The top priority is usually to inhibit pathogenic microorganisms. As many of them are facultative anaerobic – which means they prefer to grow under aerobic conditions but are also able to grow without the presence of O_2. A minimum level of 20% (v/v) CO_2 is used for the packaging of fresh meat in general, as 20% (v/v) CO_2 is known to be the minimum level to reach the bacteriostatic effect (Stiles, 1995). As a typical MAP condition for poultry for example, 70% (v/v) O_2 and 30% (v/v) CO_2 are named in the literature (Rossaint et al., 2015).

1.3 Optical measurement methods for determining gas composition

There are several methods to determine gases via optics. The methods may be absorption photometers based on Lambert-Beer's law, operating mainly in the ultraviolet (UV), VIS or IR range. The emission of light can also be used for gas detection, e.g., chemical or UV-VIS fluorescence (Wiegleb, 2016). Methods can also be based on Raman spectroscopy (Stoicheff, 1957) or hyperspectral imaging (Kuflik & Rotman, 2012). However, as the two measurement systems developed in this work are based on infrared spectroscopy and fluorescence quenching, they are described in more detail in the following sections. The theoretical background of the other mentioned optical methods is further described in section 2.1.

1.3.1 Infrared Spectroscopy

The IR is located next to the VIS spectra and can be divided into NIR (near infrared) with a spectral range at 800–2500 nm (12500–4000 cm^{-1}), MIR (mid infrared) at 2500 – 50.000 nm (4000–200 cm^{-1}) and FIR (far infrared) at 50,000–500,000 nm (200–20 cm^{-1}). In the NIR and MIR, the principle of IR spectroscopy is since molecules develop mechanical vibrations by absorbing light. In the FIR, on the other hand, rotations develop (Böcker, 2014). However, this phenomenon occurs only if a variable or inducible dipole moment, which makes an interaction between radiation and molecule possible, is present in the molecule. If this does not occur, one speaks of IR-inactive or forbidden transitions (Atkins et al., 2022).

Typical vibrational wavenumbers are shown in Table 5.

Table 5: Typical vibrational types and the respective wavenumbers (Atkins et al., 2022)

Vibration type	Wavenumber $\tilde{v}$/cm^{-1}
C-H stretch	2850–2960
C-H bend	1340–1465
C-C stretch, bend	700–1250
C=C stretch	1620–1680

These vibration types are important, e.g., for the identification of gases in unknown mixtures, because the composition of a molecules leads to a specific vibrational and absorption spectrum which is characteristic for a certain gas. For CO_2, for example, wavenumbers of 1388 cm^{-1} (v_1) (symmetric stretch), 2349 cm^{-1} (v_3) (antisymmetric stretch), and 667 cm^{-1} (v_2) (perpendicular bending motions) are vibrations in the normal mode (Atkins et al., 2022).

For IR measurements – FTIR as well as dispersive spectrometers – broadband radiation sources are common, as a whole spectral range can be considered. Thermal emitters are frequently used radiation sources. The principle of a thermal emitter is that a metal (e.g., tungsten) filament is heated to very high temperatures in order to obtain an emission in the desired wavelength range. The higher the temperature, the shorter the wavelength of the emitted light. Tungsten-halogen lamps, for example, are heated up to 2600°C to generate light in the NIR range. In the MIR range, temperatures <1000°C are sufficient. For the MIR area, silicon-carbide sources (Globar) are very common, nowadays in general manufactured as micro-electro-mechanical-system (MEMS) (Das & Das, 2010; Hsu, 1997; Wang et al., 2022). The output of a thermal emitter is mainly dependent on the temperature T of the radiating body. The emissivity ε is 1 for an ideal blackbody emitter, which means that all electromagnetic radiation is completely absorbed and emitted, i.e., the highest physically possible thermal radiant power is emitted. A blackbody is idealized and is therefore used as a reference for real emitters ($\varepsilon < 1$). The product of ε and the fourth power of the temperature T together with the Stefan-Boltzmann constant σ and the area of the body A result in the Stefan-Boltzmann law:

$$P = \varepsilon \, \sigma \, A \, T^4 \qquad (1.13)$$

Emitters that are energy-efficient and at the same time have a high radiant intensity are particularly suitable for applications that need to be transportable. The aim in the development of thermal emitters is always to achieve a near-blackbody characteristic (high emissivity independent of the wavelength). This has the advantage, for example, that the process is more energy efficient. Optimized emissivity can be achieved, for example, by using a special alloy for the wire. By using a nanostructured nickel-chrome (NiCr) layer, an emitter developed by Infrasolid GmbH was able to achieve an emissivity in the NIR and MIR range close to

blackbody (>0.9). The wire was arranged in a spiral shape (compare Figure 6), which made it possible to achieve a homogeneous temperature distribution (up to 1180 K) and minimal energy consumption. Compared to other thin-film emitters, this emitter was able to achieve a higher temperature with the same power consumption (Schossig et al., 2015).

Figure 6: Thermal IR emitter with a spiral shape radiation element (2.8 mm^2) with an NiCr nanostructured layer, operating with a near-blackbody characteristic (Schossig et al., 2015)

Also phosphor-converted NIR light emitting diodes (LED) are the subject of current research as a light source, as they are more durable and therefore more sustainable compared to halogen lamps (H. Lee et al., 2023).

To achieve the absorption characteristics within the desired infrared range, a monochromator – for an FTIR in most cases a Michelson interferometer – is placed in front of the detector (Hsu, 1997). Another possibility is the use of an optical filter (e.g., optical bandpass filters) that separates two or more parts of the IR spectrum. That set-up makes sense when different wavelengths are of interest. The different filters are placed directly in front of the detector segments, which is then called a multi-channel detector. This means that only the wavelengths with the desired absorption characteristics are guided into the detector, as the frequency ranges below and above the passband are blocked or significantly attenuated by the filter (Levin & Bhargava, 2005).

Thermal radiation can be achieved by measuring the heating of a sensor surface. For sensors or detectors used for IR spectroscopy, two types are commonly distinguished. One measures the heating induced by the incident radiation directly; such detectors are called "thermopiles." The other group uses the pyroelectric effect. The change in temperature (the rise in

temperature of the sensor material due to the incident radiation) and the temperature of the sensor or the crystal it contains, e.g., lithium tantalate, leads to the formation of the electrical signal. These are then "pyroelectric sensors" (Feng & Xu, 1999; Fraden, 2016).

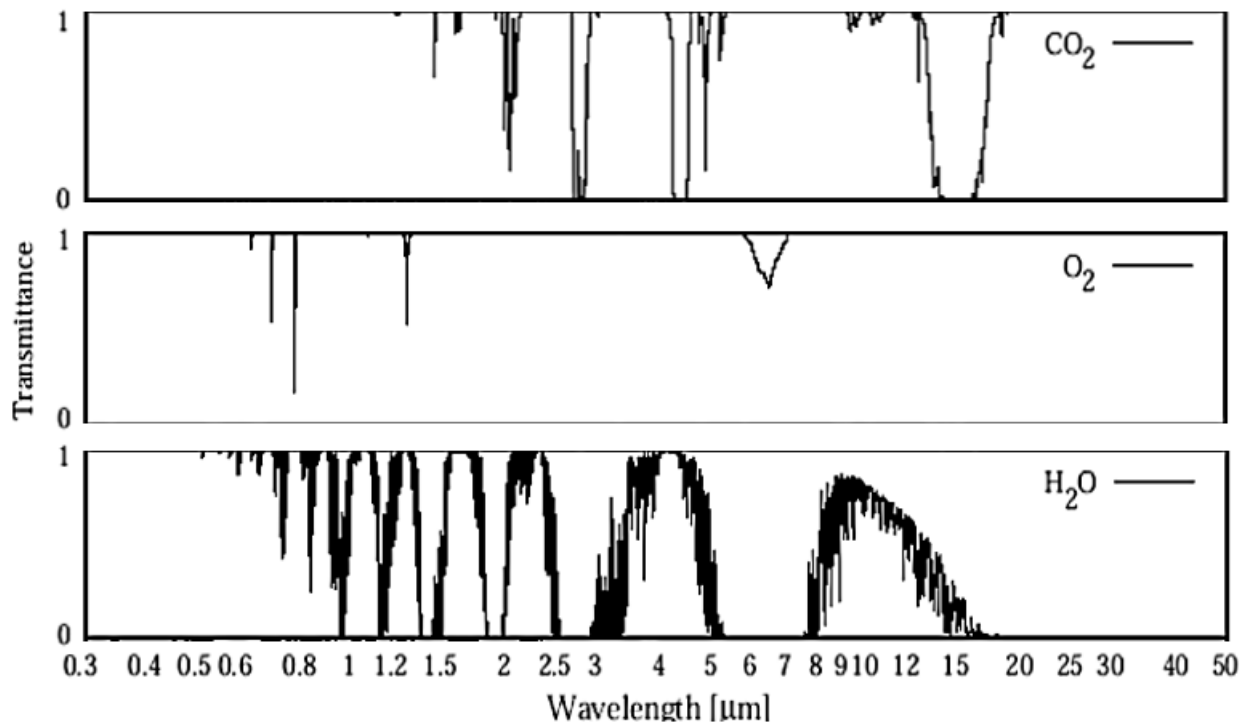Figure 7 shows the transmittance of O_2, CO_2 and water (H_2O) in the UV, VIS, NIR and MIR ranges.

Figure 7: Transmittance in the UV, VIS and IR (NIR and MIR) ranges of O_2, CO_2 and H_2O (adapted to (Sokolik, 2009)).

H_2O shows the most striking absorption bands along the spectral range. CO_2 has also some very strong absorption bands in the NIR and MIR areas, which is why infrared absorption spectroscopy is a common measurement system for the identification and quantification of CO_2 (Wong & Anderson, 2012; Guangjun Zhang & Wu, 2004). However, in the VIS area no CO_2 absorption occurs. The detection of O_2 via infrared spectroscopy is more difficult, as the absorption bands are narrowed or weak. O_2 has its strongest absorption in the VIS area at 760 nm, the so-called A-band. This occurs during the electronic transition of the unexcited triplet state to one of the excited singlet states ($^3\sum_g - \rightarrow^1 \sum_g +$). The singlet state of the A-band is at a higher level compared to the ground state, but has a much shorter lifetime with $<10^{-9}$ s compared to the $^1\Delta_g$ singlet state, which is responsible for the weak absorption bands in the NIR (1269 nm and 1908 nm) (Baier, 2005). A schematic illustration can be seen in the first publication of this work (see section 2.1).

In this case, optical measuring systems that can provide precise results even with a weak signal must be used. One of these measuring systems is tunable diode laser absorption

spectroscopy (TDLAS). In contrast to the FT-IR spectrometers currently in general use (Atkins et al., 2022), the TDLAS does not detect absorption over the whole spectrum, but from one defined absorption line characteristic for medium to be analyzed. As the monochromatic laser is tunable, it can be adjusted to that specific absorption line in the first step. In addition, the current or temperature can also be varied, which leads to a variation of emission frequency ("wavelength scanning interval") with a subsequent change in signal strength. The absorption peak occurs then as a result of the ratio of the signal levels of the detector and the laser, even if the signal is comparable low – as is the case for O_2 detection at 760 nm (L. Cocola et al., 2016; Lackner, 2007).

Typical diode lasers for TDLAS systems are Fabry-Pérot, distributed-feedback (DFB) and vertical cavity surface emitting lasers (VCSEL) (Lewander, 2010). For measurement in the MIR, Quantum Cascade DFB lasers, Interband Cascade DFB lasers and MIR VCSEL lasers, for example, can be used. One advantage of the use of diode lasers is that the operating temperature is room temperature (Du et al., 2019). Photodiodes are broadly used as detectors; they use the photoelectric effect, at which light exposure leads to current flow or voltage build-up (Lewander, 2010). In between, many different set-ups are possible. To generate different wavelengths, e.g., to measure different gas types or have a calibration beam, beam splitters (e.g., based on zinc selenide) can be used (Durry et al., 2010; Guoyong Zhang et al., 2018). To increase the measurement path, set-ups containing spherical mirrors which reflect the laser light several times are also possible. This is called a multi-pass cell (Lewander, 2010). The implementation of a gas cell requires, of course, that the gas is passed through a body for determination, which is not possible, for example, in the application for non-destructive detection of gases in food packaging.

Another possibility to measure O_2 gas concentration is an emission-based method, e.g., based on fluorescence quenching, which is further described in the following.

1.3.2 Fluorescence quenching

Fluorescence is the spontaneous emission of light from an appropriate molecule, called a fluorophore, previously excited at a specific wavelength. Emission usually takes place at a lower energy, i.e. longer wavelength, than does the absorption (excitation) (Lakowicz, 2006). This phenomenon was first described by G.G. Stokes in 1852 and is therefore called the "Stokes Shift" (Stokes, 1852). The electronic states are in general described by the Jablonski diagram (Figure 8). It shows that, after the excitation of a fluorophore from its ground state (S_0), the change to reach a higher vibrational level (S_1 or S_2) occurs. Subsequently, most molecules relax to the lowest energy level of S_1, which is called *internal conversion* or *thermalization* and consequently results in emission at a lower energy level than absorption. When the photon returns to one of the ground states S_0, energy is released in the form of fluorescence (Lakowicz, 2006).
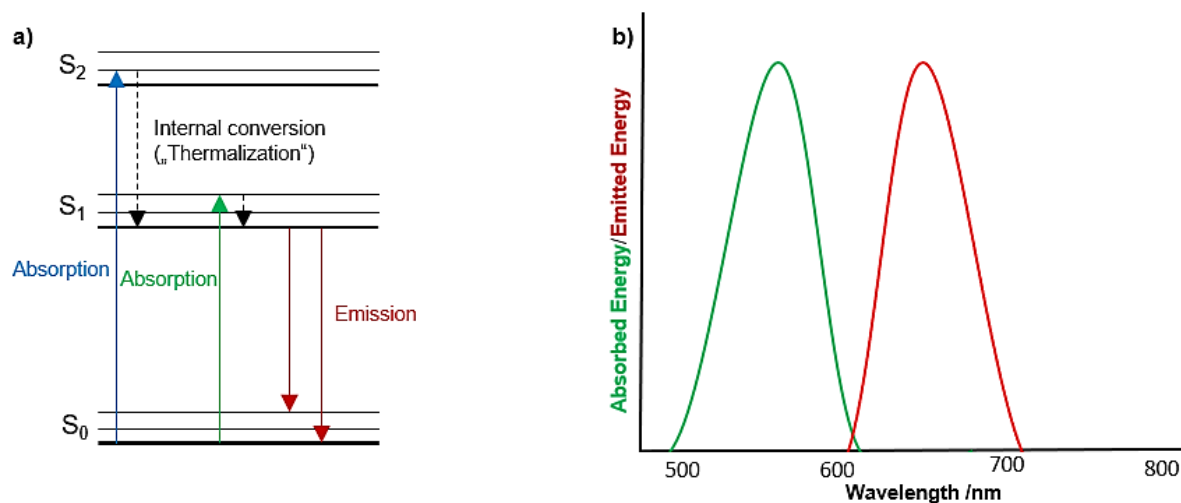
Figure 8: a) Schematic illustration of a) the ground and electronically excited states during fluorescence according to Jablonski and b) excitation (green) and emission (red) during fluorescence ("Stokes Shift") (adapted to (Lakowicz, 2006))

There are some molecules that are able to work as a quencher for the fluorescence process, for example O_2. It is not completely known which process is responsible for quenching in terms of O_2, but the most commonly held theory is that the O_2 forces the fluorophore to go into the triplet state. As consequence, the luminescence lifetime is shortened. There are two types of quenching: dynamic or collisional quenching and static quenching. The latter is caused by a phenomenon in which a complex is formed between the fluorophore and the quencher, and in some cases this complex absorbs light, which means the direct return of the fluorophore to the ground state without any photon emission. In the case of O_2 quenching, the process is dynamic, which can be described via the Stern-Volmer equation:

$$\frac{F_0}{F} = \frac{\tau_0}{\tau} = 1 + k_q\tau_0[Q] \tag{1.14}$$

The term F or F_0 stands in this case for *fluorescence intensity* and τ or τ_0 for the *luminescence lifetime* with and without the presence of O_2, respectively. k_q is the *bimolecular quenching constant*, which in turn expresses the probability that a quencher and a fluorophore collide and that this collision triggers a quenching process. $[Q]$ is the *concentration of the quencher*, in the case of O_2, the O_2 concentration in the measured gas or liquid (Lakowicz, 2006).

One common way to determine the quencher concentration is a frequency-domained measurement, using a sinus-wave modulated light for the excitation. In this case, emission also occurs with the same modulation frequency, but, due to the luminescence lifetime, this emission is delayed relative to excitation, which ends up in intensity curves, modulated by the

modulation frequency. The shift between emission and excitation is called *phase shift* ϕ, which can be used to determine the luminescence lifetime at the given *modulation frequency* ω, using the following formula (Lakowicz, 2006):

$$\tan \phi = \omega\tau_{\phi} \tag{1.15}$$

Using phase shift and the luminescence lifetime as parameters has the advantage that it is independent of turbidity properties in the environment to be measured, in contrast to measurements of fluorescence intensity, e.g., using pulse fluorimetry (Huber, 2008; Lakowicz, 2006).

Most fluorophores absorb and emit light in the VIS spectral range (Banerjee et al., 2016). In general light emitting diodes (LED) or laser diodes are therefore used nowadays as light sources (Herman et al., 2001; Lakowicz, 2006; Xiong et al., 2016). To gain a modulated signal, a modulator with the defined modulation frequency can be used. If an LED or other light sources are polychromatic, the use of a monochromator or optical filter for the defined wavelengths is useful. Via an optical glass-fiber, the light can then be guided to the sample – in general the fluorophore dye. The emitted light and its shifted frequency are then measured via a photodiode or a photomultiplier tube after passing through the optical fiber and an optical filter, again (Jorge et al., 2004; Lakowicz, 2006; Xiong et al., 2016).

1.4 Motivation and objective

Food waste is a worldwide issue. Although value chains are being constantly optimized, one-third – or more than 1.3 billion tons – of globally produced food is wasted per year along the whole supply chain. For meat and meat products, around 20 % is lost or wasted. The reasons – and therefore the kind of waste – are different, depending on the production region. In developing countries, the loss occurs mainly during slaughtering, processing or distribution, as maintaining cooling chains or hygienic conditions is more difficult (Gustavsson et al., 2011). But in Europe, too, more than 88 million tons of food are wasted each year (European Parliament, 2017). However, in industrialized countries more than 50 % of food waste occurs during distribution within the retail sector or purchasing households, probably often because the "best before" or "use by" date is passed (Gustavsson et al., 2011; Lipinski et al., 2013). However, it is also known that these dates are not necessarily an indication for a significant loss of food product quality or even microbiological spoilage, as the estimation of a "best before" or "use by" date is in general oriented to a product with a lower quality and, in addition, especially in terms of microbiological perishable food, a safety margin is applied. That raises the question if there are possibilities to overcome these issues, e.g., a real-time quality analysis of a food product, to set an individual "best before" or "use by" date, or, on the other hand, to detect a shortened shelf life due to improper handling such as failure to maintain the cooling chain.

Several studies were done in the past to develop so called Food Freshness Indicators (FFIs). The idea of an FFI is to integrate – in most cases a pH sensitive color dye – into the packaging to give consumers the chance to monitor product freshness by themselves, as the dye changes its color, e.g., due to the reaction with formed volatile organic compounds (VOC's), which are produced, for example, during fat or protein oxidation. In the case of protein degradation, for example, ammonia is produced (Casaburi et al., 2015; Franke & Beauchamp, 2017; Luo et al., 2022; Morsy et al., 2016). However, that type of shelf-life indication has some limitations. The methods and the related dye color changes are highly dependent on the formation of the responsible VOC's. More concretely, some VOC's can lead to a decrease in pH (e.g., acetic acid or lactic acid) and some can increase the pH (e.g., various amines), which can have a neutralizing effect (Casaburi et al., 2015). As a consequence, the color change is not reliable, which can lead in the worst case to a false negative results and hence the consumption of a product containing pathogens such as *Campylobacter jejuni* (Kerry et al., 2006).

Optical methods are promising tools as a non-destructive measurement alternative to FFIs, as they are highly sensitive analytical systems offering a wide range of measuring points – directly on the product itself or indirectly, e.g., the surrounding gas atmosphere (Grau et al., 2011; Lundin, 2014; O'Mahony et al., 2006; Sowoidnich et al., 2010). That results in the first research question to be answered within this work:

Which optical measurement systems are promising tools to evaluate the quality of already packaged meat and meat products?

It is known that there can be a link between a change in the protective gas atmosphere in packaged food products as a consequence of a quality change. The concentration of O_2 for example can decrease due to chemical processes such as oxidation (C. A. Kelly et al., 2020), and due to O_2 respirating microorganisms such as *Brochothrix thermosphacta* (Kolbeck et al., 2019). In contrast, the concentration of CO_2 can increase as the product of respiration, e.g., by the activity of yeasts and lactic acid bacteria (LABs) (Danilovic et al., 2016). The opposite evolutions of the concentrations of O_2 and CO_2 in the spoilage process were further investigated by (Höll et al., 2016). They measured the headspace gas atmosphere of high O_2 packaged poultry (MAP: 80 % O_2/ 20 % CO_2) stored at 10 °C and 4 °C using an invasive gas concentration measurement device that did not leave the packages intact. These invasive measurement devices are the current state of the art. In addition, they examined the growth of microorganisms. They were able to find a correlation between the significant changes in the O_2 and CO_2 headspace gas concentrations and the attainment of the critical total viable count (TVC) of 10^7 CFU/g, especially for the samples stored at 10 °C. The samples constantly stored at 4 °C showed a slower, but also visible change in headspace gas concentration (Höll et al., 2016). These findings in turn again raise the question, if an individual "best before" or "use by" date might be possible for some meat or meat-products, as different storage, or cooling chain conditions, as well as initial microbiological load might influence the date of attainment of the critical TVC of 10^7 CFU/g and if a reproduceable correlation with the change in head space gas concentration can be established. In this case, however, the properties of gas permeation through and solving in the packaging material and those of the product itself must also be considered. In an application perspective, the measurement of the gas concentration using a non-destructive device might be meaningful because, for a later application, for example in retail, an invasive measurement would not be possible if the product is still to be sold afterwards. Thinking in terms of application, the packaging integrity could also be monitored using a non-destructive measurement device for gas concentration analytics, and hence the device could be used as an inspection tool during packaging or for incoming product inspection in retail. Against this background another research question becomes clear and must be answered in this work:

Is it possible to develop a convenient method for the non-destructive evaluation of the O_2 / CO_2 gas concentration in meat packages?

Here, two different methods—one for the O_2 and one for the CO_2 gas concentration measurement are the focus. For the O_2 measurement, a method based on fluorescence quenching is the core of the work. For CO_2 measurement in the mid-infrared range (MIR) seems to be the most promising option. Here, the choice of a suitable CO_2 absorption band is

crucial: one that shows a strong signal on one side but does not overlap with the packaging absorption properties on the other side.

The third research question to be answered is the proof-of-concept of the developed methods and is defined as:

Can individual "use by" or "best before" dates be established for meat and meat products by the measurement of the headspace gas concentration?

Here, the above-mentioned hypothesis that the growth of microorganisms can be determined by monitoring the change in the O_2 and CO_2 composition of the headspace atmosphere by using the methods developed should be reviewed. This part of the research must also involve the change in the head-space gas concentration of empty packaging systems to distinguish between "product effects" such as spoilage, oxidation and dissolving in the product and "permeation effects" of the gases permeating the polymer itself. A comparison with state-of-the-art proven invasive measurement systems also had to be made to validate measurement accuracy. In addition, not only the relationship between the gas atmosphere and the microbiological spoilage of the meat and meat products, but also other quality aspects such as color changes and sensory evaluation were to be considered.

Figure 9 shows the defined research questions to be answered in the following work.
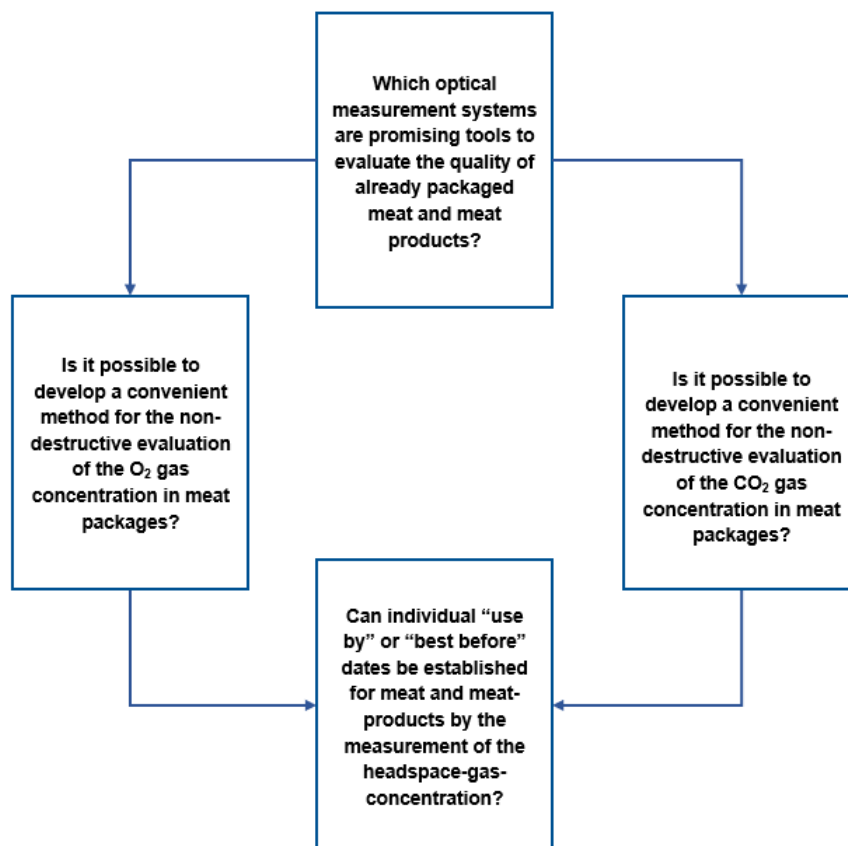

Figure 9: Defined research questions of the work.

2 Results – Thesis Publications

The summaries of the published results are shown in the following sections. The copyright licenses are shown in chapter 5, the full printed publications are shown in chapter 7.

2.1 Publication I

Dold, Jasmin & Langowski, Horst-Christian (2022). **Optical measurement systems in the food packaging sector and research for the non-destructive evaluation of product quality.** Food Packaging and Shelf Life, 31, 100814.

https://doi.org/10.1016/j.fpsl.2022.100814

A great deal of research has been done in the past years to investigate diverse quality parameters of already packaged food using non-destructive measurement systems. The quality parameters of interest are as diverse as the measurement set-ups and tools used, e.g., as adulteration, freshness or ripeness, oxidation, microbiological spoilage, packaging integrity or moisture content. Also, a broad range of product groups has been the subject of research. To achieve a more structured overview of the current state-of-the art, a detailed literature search was done in this review paper, covering the spectral range between UV and MIR radiation. As a further distinction, the *direct* measurement of product quality, which means the measurement of product properties, and the *indirect* measurement of product quality, which means the measurement of the surrounding gas atmosphere, were considered. Fluorescence spectroscopy, hyperspectral imaging (HSI), infrared spectroscopy, Raman spectroscopy, simple color measurements (using the Commission Internationale de l'Eclairage (CIE) L*a*b* color space) and tunable diode laser absorption spectroscopy (TDLAS) were therefore described as basic principles and evaluated for their suitability for the different applications. For the *direct* application, fluorescence spectral analysis, Hyperspectral Imaging (HSI), simple color measurement, IR and Raman spectroscopy were the methods of choice in the current literature, although the fluorescent and CIE based systems were less present. To evaluate the surrounding headspace gas atmosphere (*indirect*), TDLAS and the insertion of fluorophores into the packaging for the quenching-based method were methods mentioned in the published literature so far. If the measured parameter is a degradation product related to a quality change, which factors might influence these results must be carefully considered. Methods containing complex chemometric conversion systems might be more suitable for research applications and less for practical applications, e.g., in retail or for the consumer. IR- and Raman-based systems offer the broadest application spectra and would also be suitable for indirect measurement applications.

Contributions of the doctoral candidate (CRediT):

Conceptualization; Investigation; Writing - Original Draft; Visualization; Project administration

2.2 Publication II

O_2 determination by fluorescence quenching is a valid and proven measurement method for the non-destructive evaluation of gas concentration, which is already described in several studies as well as patent applications. However, the current literature does not consider the fixed integration of the fluorophores into the packaging itself, or the packages were prepared in such a way that a precise measurement can only be made immediately after the packaging process, or no research regarding food safety was done. In the presented research paper, all mentioned aspects are included: First, a method for the tight and safe integration of the sensor-material via heat-sealing into the lid film of a packaging was developed. This method was applied on different film combinations, and their suitability for a precise and fast determination of changes of the headspace O_2 concentration was determined. To assess the potential for a food safe integration, tests for potential migration of constituents of the sensor material were done. To evaluate the developed method from a more practical point of view, three different meat and meat products were packed into packaging containing the integrated fluorescence material. Beside the continuous O_2 headspace gas concentration determination, further quality aspects such as surface color and microbiological growth (TVC) were monitored during a storage of 7 and 13 days at 4 °C. The tight and safe integration of fluorophores into a food packaging system, using common films such as PP, PE-LD, PA and EVOH for a non-destructive real-time determination of headspace O_2 gas concentration was possible with the developed method, without a decrease of the measurement precision. Also, first results showed that the integration does not lead to the migration of critical substances. The applicability of the system shows some limitations, as the response time after the sealing process is 2−3 days, which is rather impractical for e.g., a leaking-test after the MAP packaging in a packaging machine. However, slow and continuous gas-changes resulting from a microbiological spoilage process could be determined in real-time. Especially for the high O_2 packaged minced beef, a correlation of the oxygen concentration with the determined quality parameters could be established. For the vacuum packaged samples (sausage "Lyoner" type and beef steak), the results were less clear.

Contributions of the doctoral candidate (CRediT):

Conceptualization, Methodology, Validation, Formal analysis, Investigation, Data Curation, Writing - Original Draft, Visualization, Project administration

2.3   Publication III

Dold, Jasmin, Götzendörfer Lukas, Hollmann Clarissa, Langowski Horst-Christian. **A non-destructive measuring device in the mid-infrared range for measuring the CO₂ concentration in the headspace of food packaging** (2024). Journal of Food Engineering, 375, 112063. https://doi.org/10.1016/j.jfoodeng.2024.112063

The objective of the following publication was the construction and application of a measuring device capable of the non-destructive measurement of the headspace gas concentration of CO_2 in common polymer trays and lid films used for food packaging. As light source, a thermal broadband IR emitter and a multi-channel detector as sensor were used. Four different measuring channels were selected: 4.26 µm (2347 cm^{-1}) and 4.27 µm (2342 cm^{-1}) located directly on the band of the antisymmetric stretching vibration of CO_2 as well as 4.45 µm (2247 cm^{-1}) which is located at the edge on the CO_2 absorption band and 3.95 µm (2532 cm^{-1}) as a reference measurement outside the absorption band. The housing of the device was designed in such a way that a constant measuring path and angle of incidence of the IR emitter could be guaranteed. For this purpose, light guiding through the corner of the packaging tray at a 45° angle was considered as optimal, since the measurement path is relatively short and remains unchanged regardless of the tray size. In addition, there is usually no food product in this area of the package, which might disrupt the measurement. The device was then examined for various influencing factors as was their effect on measurement precision. Hereby, the influence of the angle at which the IR radiation enters the tray corner, pigmentation and printings of the tray and the lid film, optical polymer irregularities and product residues (meat juice and water) were the subject of the assessment. Finally, the suitability of the device for a range of commercially available packaging found in the retail was verified. For this purpose, different calibration standards were created and the measured CO_2 concentration in the headspace of the packaging was compared with results obtained via an invasive measurement device.

The shape of the tray corner had no influence on measurement precision, nor did the use of the pigments or printings (except for carbon black). Optical irregular polymer structures seem to have a major influence, especially if irregular polymer structures are formed due to an unsteady cooling process during thermoforming. Food residues or water condensation had a measurable but tolerable influence on the measurement result. The applicability of the device to a wide range of commercially available polymer forms and types was also demonstrated.

Contributions of the doctoral candidate (CRediT):

Conceptualization, Methodology, Validation, Formal analysis, Investigation, Data Curation, Writing - Original Draft, Visualization, Project administration

2.4 Publication IV

Dold, Jasmin, Kehr, Caroline, Hollmann, Clarissa & Langowski, Horst-Christian (2022). **Non-Destructive Measuring Systems for the Evaluation of High Oxygen Stored Poultry: Development of Headspace Gas Composition, Sensory and Microbiological Spoilage**. Foods, 11, 592. https://doi.org/10.3390/foods11040592

The aim of this study was to use both developed measurement principles for the non-destructive determination of O_2 (fluorescence quenching) and CO_2 (IR spectroscopy) gas concentration in the headspace of high-oxygen-packed poultry, to make a statement on the development of the gas compositions and its correlation to the sensory and microbiological spoilage. The meat was stored under two different initial modified atmospheres (70% (v/v) O_2 / 30% (v/v) CO_2 and 80% (v/v) O_2 / 20% (v/v) CO_2) and two different storage temperatures (4 °C and 10 °C) over a period of 15 days. A previously trained sensory panel did a visual and olfactory assessment of the stored samples. Parallel, the microbiological growth (TVC) was examined as well as an invasive headspace gas detection, to compare the real-time results to the non-destructive devices. To include permeation and dissolving effects on change of the gas composition, empty trays filled with the same initial modified atmospheres were stored and monitored under the same storage conditions during the 15 days.

We were able to demonstrate again that the non-destructive methods are quite comparable to the invasive methods in terms of measurement precision in real-time, when it comes to a microbiologically induced change of the head-space gas concentration. Our results allowed some correlations, in terms of the tested quality parameters: Both storage conditions showed a good correlation of the sensory attribute *slime*, while reaching the critical microbiological value of 10^7 $CFUg^{-1}$. For the samples stored at 10°C, the significant change of the gas atmosphere (compared to the empty trays) correlated with most of the sensory spoilage attributes. The defined parameter "cross-over," which describes the intersection of the curve of the respective gas concentration in the filled trays with that of the empty trays, also correlated with reaching of the critical microbiological value for the irregularly stored samples (10 °C). For the regularly stored samples (4 °C) the indication of the change of the gas atmosphere only correlated with the sensory attributes days after the critical TVC was already reached, leading us to the assumption that the non-destructive measurement systems are not useful to define an individual "use-by" day for regular high-oxygen stored poultry.

Contributions of the doctoral candidate (CRediT):

Conceptualization, Methodology, Validation, Formal analysis, Investigation, Data Curation, Writing - Original Draft, Visualization, Project administration

3 Discussion

The overall aim of this thesis was to develop or implement optical measurement systems to determine the composition of the protective gas atmosphere in polymer-based food packaging. The idea was to develop measurement tools that work non-destructively, which means that the packaging remains intact after the measurement of the gas atmosphere inside. Nowadays, measurement with invasive methods, which means that a needle must be inserted into the headspace of the packaging through the lid film to extract small aliquots of the gas, is state-of-the-art. However, these methods have the disadvantage of limited applicability. For some fields of application, e.g., monitoring of outgoing goods in production or incoming goods in supermarkets, an invasive method is not suitable. For this reason, the current state of the art in the literature for non-destructively working optical methods was screened, and the focus was placed on the detection of food quality parameters. Here especially the applicability of a method or possible sources of measurement errors were identified and critically reviewed. The differentiation between *indirect* measurements, which means the measurement of the surrounding gas atmosphere, and *direct* measurements on the product itself, were also core of the research.

For packaged meat and meat products, only a few suitable and applicable optical methods for the non-destructive evaluation of quality aspects were found in the literature, which is why this product group was the focus of development in this work. Here, O_2 and CO_2 are typical filling gases, which is why the development of measurement methods for both gases were targeted. For the respective gases, the appropriate measurement methods were first evaluated and then the specific requirements and implementation options were determined. Different measurement and integration methods were selected for both gases and investigated for their individual advantages and limitations, such as real-time detection of gases, food-safe integration, and polymer specific limitations.

Moreover, the main application focus in this work was on gaining information on the microbiological growth and therefore the spoilage of the filling product by monitoring the protective gas atmosphere, as the growth of microorganisms leads to changes of it. During microbiological spoilage, CO_2 is often a respiration product of O_2. Through the correlation of the change in the head-space gas atmosphere with microbiological growth and other quality parameters such as discoloration or sensory evaluation, the possibility of setting an individual best-before or use-by date was investigated.

Figure 9 in section 1.4 shows the defined research questions, also mirroring the structure of the work and the resulting publications, which was shown in the previous section. In the following, the research questions and the results shown in the publications are critically discussed.

3.1 Which optical measurement systems are promising tools to evaluate the quality of already packaged meat and meat products?

As already mentioned in section 1.4, the interest of non-destructive measurement devices to make a statement about the quality of food is highly given, especially in terms of food waste reduction. Measurement systems based on optics are able to provide fast and precise results and have already been implemented in many cases in the food sector, e.g., for the in-line analysis of nutritional values. However, most of the methods here refer to foods that are not yet packaged. As explained in section 1.1.5, packaging materials also have optical properties and absorb light at certain wavelengths (Table 3), which is why the application of already implemented optical measurement methods to already packaged foods must be carefully examined.

In Publication I, an extensive literature review of the past five years was conducted on the development of optical non-destructive quality analysis of already packaged food products. To narrow down the field of "optics," only the wavelength range between 200 nm and 50 µm (UV−FIR) was considered, including the following optical measurement systems: fluorescence spectral analysis, fluorescence quenching, hyperspectral imaging (HSI), infrared spectroscopy (IR), Raman spectroscopy, simple color measurements and tunable diode laser absorption spectroscopy (TDLAS).

Most of the research articles found dealt with *direct* quality analysis of the filling product, which means the measurement was carried out through the packaging directly on the product itself to analyze special quality parameters. These parameters are, for example, the adulteration of vacuum packaged (PE-HD/PA film) meat, analyzed via NIR spectroscopy working at a spectral range between 1.6 and 1.8 µm (6250–5556 cm^{-1}) (Schmutzler et al., 2015, 2016), the freshness of packaged salad leaves, analyzed by using a simple color measurement (CIE L*a*b* color space) (Cavallo et al., 2018) or the growth of microorganisms on vacuum packaged smoked salmon, analyzed by the detection of VOC's through a film on the salmon surface, using HSI (illumination in the VIS-NIR range of 400−1000 nm) (Ivorra et al., 2016). However, there are some issues relating to a set-up aiming the light-source directly on the product surface to gain quality parameters:

The surface of packaged food – especially meat and meat products – is very complex, consisting of fats, proteins, carbohydrates, water, diverse degradation products, etc. Furthermore, the shape of the product surface may vary widely, even for the same product type. These effects can influence the absorption and/or backscattering signal, leading to a misinterpretation or miscorrelation.

If the measurement of the optical system pertained to the surrounding atmosphere in the headspace of packaging, it was categorized in Publication I as *indirect* measurement. The monitored quality attributes found in the current literature were much more limited than those

33

in *direct* measurement. While eight different quality attributes were detected non-destructively for *direct* measurement, only four different attributes were available in the literature for *indirect* measurement. The measured variables were either the degradation effect in the headspace of the surrounding gas atmosphere (e.g., O_2 decrease in the headspace of packaged meat induced by oxidative changes (C. A. Kelly et al., 2020; C. Kelly et al., 2020; Sikorska et al., 2019)) or due to microbiological spoilage (Escobedo Araque et al., 2018) measured via fluorescence quenching; or the increase of CO_2 in the headspace of packaged dairy beverages and yoghurt induced by microbiological spoilage, using a TDLAS set-up (Danilović et al., 2018). Another focus was the determination of the composition of the remaining or protective gas atmosphere, e.g., to implement a process control ("in-line") (e.g., the measurement of the absence of O_2 in flow bags, using a TDLAS-based system working at 760 nm, which is the O_2 absorption band (Lorenzo Cocola et al., 2018)). If an optical system is used to determine a degradation product, it must be considered that, for an exact correlation with the target quality parameter (e.g., oxidation or growth of microorganisms), the primary reaction must also be determined cleanly in order to be able to make a reasonable correlation. In addition, other processes such as solubility or permeation of gases or the formation of the measured gas by other metabolic processes should be included in the correlation. This aspect has been completely neglected in the given literature shown in Publication I.

The review showed that there are several scientifically well-studied possibilities for the non-destructive evaluation of the product quality of already packaged food. However, some of them are probably not convenient methods for practical applications. To decrease the amount of food waste, measurement tools which are implementable in retail or even at the consumer would be necessary, as a major part of products are wasted during that part of the value chain in developed countries (Gustavsson et al., 2011; Lipinski et al., 2013). Three important aspects, which were compared in Publication I must therefore be considered as well: complexity, usability, and total costs. In terms of complexity, fluorescence spectral analysis, IR spectroscopy, Raman spectroscopy and the simple color measurement were considered to have the lowest complexity (application and set-up). The handling of and applicability for different products and packaging materials ("usability") was rated as medium for most of the measurement systems considered; for HSI, applicability to different products and materials is probably the highest; more limitations were identified for Raman spectroscopy. In terms of costs, fluorescence spectral analysis, IR spectroscopy and the color measurement are probably the most economical.

As a result of the literature research, it can be said that in general all methods under consideration would be suitable for the quality detection of already packed meat and meat products. However, especially for the question posed by (Höll et al., 2016) whether the spoilage

state of meat and meat products can be identified by detecting the change in the gas atmosphere in the headspace of meat packed under a modified atmosphere, the tools presented for *indirect* measurement are preferred (fluorescence quenching and TDLAS). In addition, the use of a device working with a thermal IR emitter would be useful as well, particularly in terms of low complexity, usability, and probably low costs, even if the latter is not mentioned in the current literature.

3.2 Is it possible to develop a convenient method for the non-destructive evaluation of the O_2/CO_2 gas concentration in meat packages?

The review successfully demonstrated that there are already good approaches to measure the O_2 and CO_2 gas atmosphere non-destructively for already packed meat and meat products, using an *indirect measurement* system. However, there is a need for further research, especially regarding the applicability and interpretation of the results for the generation of suitable correlations, which are therefore addressed in the present thesis and will be discussed in the following.

3.2.1 Oxygen

In Publication II, the successful integration of fluorescence material into a food packaging system for meat and meat products was demonstrated. In contrast to the existing literature, several aspects necessary for a practical application were combined in this work. On the one hand, an integration process using heat sealing with a covering thin film was selected, which not only protects the food from potential contamination with the fluorescent material, but also prevents contamination of the sensor spot, e.g., with meat juice, as this can also lead to a loss of measurement quality (Lakowicz, 2006). In selecting the polymers for the cover film, it was found that all common food packaging films – if they transmit light in the VIS range – are suitable for measurement. The insertion of sensor spots with the developed ring-shaped sealing tool was also successfully carried out, resulting in a tight sealing seam without the measurement precision being affected by the heat-sealing process.

In addition to the actual integration process, however, several aspects must be taken into account in order to be able to make a statement as to whether the measurement method is suitable for the intended purpose or not. In terms of food safety, the results shown in Publication II pointed out that no critical migration of components occurred, which makes food law conformity very likely.

An important aspect for production scale is how and when to apply the sensor material to the lid film. Although it was shown that the integrated sensor material can be stored without a loss of measurement precision over a period of a minimum of one year (stored at 6 °C), the application would be probably more reasonable directly during the food packaging process. As

the spot-covering creates bumps, the winding of the lid film is much more complicated. The setup of the integration process on a production scale still needs to be clarified.

The major aspect for the applicability of a method is whether it can measure O_2 partial pressure values in real time or if the covering of the sensor spot leads to a delayed response due to permeation of the gas and the polymer. A review of the results in Publication II and IV shows clearly that this point seems to be the most limiting for a practical application. Three different set-ups were evaluated for this purpose within this thesis:

First, the response time in a closed system (standardized measuring chamber, DIN 53380-5, (DIN Standards Committee Packaging, 2014)); second, the response time in a real packaging system with simulated packaging defects and simulated microbiological O_2 respiration; and third, the application with packaged meat and meat products (Publication II and IV).

The results for the closed system without product and for the application with packed meat and meat products make it evident that the response time for the sensor material incorporated into the lid film after subsequent exposure to a gas atmosphere (either by flooding the measurement chamber with test gas or by admitting the modified atmosphere in the semi-automatic tray sealer) can vary from 2.58 h (for a PE-LD$_{50\mu m}$ lidding at 21 °C, cf. Publication II) to more than 48 h (for a PP cover at 4 °C, cf. Publication IV). That excludes, for example, the possibility of using the method directly after packaging, e.g., for leak detection or proper MAP monitoring for outgoing inspection. Therefore, spectroscopy-based methods such as TDLAS would be more suitable for this specific purpose, as demonstrated by Cocola et al. in several studies (L. Cocola et al., 2016; L. Cocola et al., 2015).

For the time regime after attainment of the equilibrium in both compartments (gas composition in the headspace = gas composition in the encapsulation of the sensor spot), two different scenarios were analyzed:

In the first scenario, a relatively fast change in the O_2 gas concentration within the headspace is induced by a leak in the packaging. In this case, the response time of the encapsulated sensor spot is not fast enough, and the actual O_2 gas concentration present in the headspace was indicated by the sensor only after 48 h at the earliest in the experiments shown in Publication II. As is the case with outgoing inspection, the detection of packaging leaks would not be practically useful with the currently developed method.

If, as in the second scenario, the change of the gas atmosphere is induced by microbiological processes, the response time of the encapsulated sensor spot is fast enough. This was proven on the simulated set-up in Publication II, as well as in the application tests with minced beef under a high-oxygen atmosphere (Publication II) and high-oxygen packed poultry (Publication IV).

The explanation for the different response times lies in the different diffusion and permeation properties of the gases. In the case of a hole in the lid film, the ambient air (containing mainly

N_2 and O_2) diffuses much faster into the headspace of the packaging (N_2 and O_2 have approximately the same diffusion rate). Permeation from the headspace into the area of the lid film occurs much more slowly, as N_2 permeates 4 times more slowly through the film than does O_2. As a consequence, an under-pressure results in the spot area, leading to an even slower O_2 permeation process. The change in the gas concentrations induced by microorganisms is only a change in O_2 and CO_2 gas concentration, resulting in stable permeation between the area of the sensor spot and the headspace of the packaging. Thus, the applicability of the method for monitoring gas changes during the storage of an intact package, e.g., to create an individual "use by" or "best before" date for meat and meat-products is given.

Two different types of packaging were tested for the method developed herein: the integration into the lid film of PP or PE-LD trays to set a protective gas atmosphere (Publication II and IV) and the integration into PE-LD pouches for vacuum packaging (Publication II). The integration of the sensor spot for vacuum packaging is much more complex, as the under-pressure in the packaging after removing the air is influenced by the remaining water vapor and O_2, which are slowly released during storage, in the packaging and the product itself. This makes it rather difficult to determine the ambient partial pressure in the spot area, which has an effect on the measurement accuracy, especially if the aim of the investigation is not a relative deviation, as shown in Publication II, but the quantification of the O_2 partial pressures plays a decisive role. In summary it can be said that the measuring method developed has still some open research and application points, especially when it comes to production scale. Furthermore, food-safe integration in form of the covering of the sensor material has some limitations that cannot be denied. Due to permeation processes, the response time is in some cases too slow to give reliable values. For monitoring of the O_2 gas concentration during the storage of meat and meat products to evaluate changes due to microbiological respiration, the method gives precise results compared to an invasive method, after equilibrium is reached (gas composition in the headspace = gas composition in the encapsulation of the sensor spot, 1-3 days after the sealing process depending on permeation conditions mainly influenced in these trials by the polymer used and the ambient temperature).

3.2.2 Carbon dioxide

For the non-destructive measurement of the CO_2 gas concentration in food packaging, especially for meat and meat products, a convenient, fast, and precise measuring device was the goal of this work. The device ("Demonstrator") offers several advantages that are not offered by any comparable device, yet.

Comparing the IR absorption properties of the common polymers (see Table 3 in section 1.1.5) with the adjusted channels of the detector (Channel 1: 4.26 µm/2347 cm^{-1}, Channel 2: 4.45 µm/2247 cm^{-1}, Channel 3: 4.27 µm/2342 cm^{-1} and Channel 4: 3.95 µm /2532 cm^{-1}) makes it

obvious that none overlaps with the absorption properties of the polymers under study. The measurement range of the detector is located – except for the reference Channel 4 – directly on the main CO_2 absorption band located at 2230–2400 cm^{-1}, belonging to the antisymmetric stretch vibration of the CO_2 molecule (Atkins et al., 2022).

The theoretical assumption that the function of the constructed measurement device is therefore not affected by common polymer types was further confirmed in Publication III. The FT-IR analysis of the different trays and polymer films did not reveal any polymer-related absorption within the measuring range of the four channels. However, the FT-IR measurements showed that a reduction in transmission may occur due to different pigmentation and printing. To eliminate such effects, – as well as haze effects due to contamination by product residues or different tray shapes – the reference wavelength was used. It is located outside the CO_2 absorption band and can therefore be used to compensate for non-CO_2-related optical effects.

Another advantage of the measurement device is the chosen angle for the measurement path. The 45° angle through the corner of the packaging allows measurement without any disruption of the results by the filling good. The current literature describing IR- or TDLAS-based measurement systems for the detection of the filling gas in meat packages either works in a reflectance/backscattering mode, where the light is guided onto the food and the backscattering signal is detected, or in transmission mode, where the light is guided either vertically from the top to the bottom of the tray or horizontally through the side walls of the tray (L. Cocola et al., 2017; Czerwiński et al., 2021).

The decisive factor for the suitability of a measuring device is the generation of precise and reproducible measurement results. Based on the screening of eight different, real packaging systems with different tray shapes, sizes and colors in Publication III and measurement during the storage test with MAP-packed poultry in Publication IV, it has been found that the measurement of the CO_2 gas concentration in the headspace of the packages with the non-destructive device in most cases does not show any significant deviation compared to an invasive gas analyzer. However, only the results generated between the measurement range of 2296 – 2398 cm^{-1} (compare Figure 3, Publication III) were used to calculate the mean values, as they turned out to be the most reliable ones. Also, advantageous – especially in comparison to the measurement system based on fluorescence quenching for the detection of the O_2 gas concentration – is the ability of the device to gain results in short response time. It enables broad possibilities for application, for example for leak detection or proper MAP monitoring for outgoing inspection at food production facilities, as well as incoming inspection and the monitoring of the CO_2 gas atmosphere during storage in retail.

Nevertheless, limiting effects that might have an influence on the convenient application of the Demonstrator were identified in Publication III as well:

Due to the integration of a reference channel/beam, pigmentations and printings of the trays and the lid films were no issue, in general. However, if a tray contained carbon black as pigment for coloration, the whole MIR light was absorbed by the pigment and no measurement was possible in that case. If the measurement was performed through a labeled part of the lid film, there was a statistically significant deviation in the measured CO_2 gas concentration for almost all samples compared to non-destructive measurement through the transparent part of the lid film, as well as to the invasive measurement device. A further phenomenon, which could not be clarified in total within this thesis, was the effect of an inhomogeneous inner polymer structure or an optical irregular polymer structure on the measurement accuracy of the constructed device. For some trays, a polymer with a stronger scattering structure was present, resulting in a high statistical deviation ($p < 0.001$, alpha-level 0.05) for the non-destructive measurement of the CO_2 gas-concentration. The first assumption that these structures are the result of a higher degree in crystallization could be disproven, as the signal of the CO_2 measurement was higher than expected (and crystalline structures have a lower light transmittance) and the DSC measurement also showed no difference in enthalpy between the reference and the irregular tray. It is therefore reasonable to assume that this is due to an altered polymer structure, which can be caused, for example, by irregular cooling during the thermoforming processes (Cho et al., 1999). Furthermore, the formation of water condensate in the measurement area has also led to a reduction in measurement precision, which is why a punctual heating unit should be integrated in the further development of the demonstrator to keep the measurement area free of condensate.

In Publication IV, a modified version of the device described in Publication III was used for the study. Instead of a system with a thermal IR emitter, a TDLAS based system was used. The three wavelengths located directly on (4.26 µm, 4.27 µm) and at the edge (4.45 µm) of the CO_2 absorption band, the reference beam outside the absorption band (3.95 µm, not mentioned in Publication IV), and the 45° angle for the measurement path stayed the same. However, in terms of a later industrial use, costs, and robustness, the preferred set-up would be as described in Publication III.

In summary it can be said that the development of a novel, non-destructive and convenient measurement device for the analysis of the CO_2 gas atmosphere for meat packages was successfully demonstrated within this thesis. The advantages compared to the system developed for the determination of the O_2 gas concentration in this thesis, as well as to existing systems offer a broad field of application. The identified limitations are mostly avoidable through proper handling, except for the measurement of trays with carbon black pigmentation. The device is well suited for the most tray shapes and sizes, but it would be not suitable for

the measurement of flat packages such as for sliced sausages. Also, meat products packed in tubular bags (e.g., minced beef) cannot be evaluated with the current set-up.

3.3 Can individual "use by" or "best before" dates be established for meat and meat products by the measurement of the headspace gas concentration?

In the present work, four different meat and meat products were examined using the developed non-destructive measurement methods and evaluated for the possibility of correlating the determined and changing O_2 and/or CO_2 gas concentration in the packaging with various quality parameters. As parameter in terms of microbiological spoilage, 10^7 colony forming units per gram (CFU/g) was set as critical value for fresh meat. Fresh meat was used in Publication II, where, on one hand, minced beef was packaged under a high-oxygen gas atmosphere, and beef steak was vacuum packed on the other hand. In Publication IV, fresh poultry was also packaged under a high-oxygen gas atmosphere. No critical value is defined for sliced, boiled sausages, which were tested in Publication II as the Lyoner sausage, also vacuum packed. However, the DGHM defines for these category a guideline value of $5*10^6$ CFU/g (DGHM, 2018).

Other quality aspects were color changes, examined using a simple color measurement (CIE L*a*b* color space) in Publication II and an extensive investigation of visual and olfactory sensory changes determined by a previously trained panel.

To set an individual "use by" or "best before" date for meat or meat products it would be useful to see a change in the O_2 or CO_2 gas concentration at least one day before the critical microbiological value is reached, so that it can be labeled accordingly in when sold in stores, as it was, for example, the case in the study of (Höll et al., 2016). The results obtained during this work led to different assumptions and insights:

The high oxygen packed minced beef (stored at 4°C) (Publication II), for example, showed an immediate decrease in the O_2 headspace gas concentration, but the microbiological load was already at the critical number of 10^7 CFU/g on day zero. For meat with a high amount of heme, the respiration of O_2 to CO_2 by meat spoilers is significantly more pronounced, especially for the spoiler *Brochothrix thermosphacta* (Kolbeck et al., 2019). These findings would also fit by comparing these results to the ones with 4°C and high oxygen stored poultry (same initial gas atmosphere) (Publication IV), which showed the first decrease in O_2 gas concentration on day 10 – while the critical TVC was reached on day 6 for that sample. Poultry is a white muscle meat, with less heme. However, to be able to make a statement as to whether an individual best-before date for high-oxygen packed red meat is possible, further tests with lower initial microbiological quantities would be necessary. Nevertheless, as a tool to detect samples which are microbiologically spoiled before the labelled shelf life expires, non-destructive methods are likely useful for red muscle beef packed at a high-oxygen gas atmosphere. For high-oxygen

packed poultry, this use case would be possible only if spoilage was accelerated due to improper product storage conditions. Publication IV showed the potential for this, as the samples stored at 10°C showed a correlation with the first noticeable increase of CO_2, which was defined as the "cross-over" point (intersection of the curve of the respective gas concentration in the filled trays with that of the empty trays). These findings are further underlined by the literature, where a similar trial occurred using invasive devices to detect O_2 and the CO_2 gas concentrations (Herbert et al., 2015).

The vacuum-packed samples showed a quite good correlation between the decrease in the O_2 gas concentration and the increase in the TVC. For the beef steak an already high load of initial microorganisms was present on day zero, so the decrease in O_2 on day one was linked to attainment of the critical TVC. The question whether the decrease would be noticeable at minimum one day before reaching the critical microbiological load is, as for minced beef, still unclear. However, the detection of the premature expiration of shelf life is promising here as well. For the vacuum packaged Lyoner sausage, the cross-over was reached on the same day that the limit of 10^7 CFU/g was reached, which would imply a tool for detecting already expired samples rather than establishing an individual shelf life.

But not only is the change in the gas atmosphere a marker for an exceeding the shelf-life date, the color measurement (Publication II) and attributes characterized by the trained sensory panel (Publication IV) correlated with the microbiological spoilage. A reliable sensory marker was the attribute *slime*—for the proper stored poultry (4°C) as well as for the improper stored poultry (10 °C). The presence of the olfactory attribute *buttery* (diacetyl) was also noticed by the panel when the critical TVC was reached. However, while the formation of VOCs is highly dependent on the meat spoiler species (compare Publication IV), the formation of diacetyl seems not to be a reliable parameter. The formation of *slime* is induced by the breakdown of the meat tissue by microorganisms and occurs at a microbiological load around 10^8 $CFUg^{-1}$ (Charles et al., 2006), which is why it can be a marker only for already spoiled meat. The color change as determined in Publication II was well visible only for minced beef. Here – according to the correlation with the change of the gas atmosphere – no final remark can be made, as the initial microbiological load already reached the critical TVC.

In summary, it can be said that the establishment of an individual "use by" or "best before" date with the help of non-destructive optical methods is not yet possible for any of the samples and storage conditions investigated within this thesis. For high oxygen and vacuum-packed red muscle beef, the possibility cannot be completely ruled out, as promising results were obtained here. For white muscle meat stored under proper conditions, no correlation between a significant change in the gas atmosphere and the attainment of critical microbiological spoilage of 10^7 CFU/g exists. For improper conditions, as well as for the tested vacuum-packed sliced

boiled sausage, attainment of the "cross-over" could be correlated with attainment of the microbiological critical limit and thus could be useful to identify already spoiled samples, e.g., if the shelf life at retail was prematurely exceeded.

4 Final Remarks and Outlook

The present thesis achieved the overall aim of developing optical, non-destructive measurement systems for the investigation of the protective gas atmosphere in polymer-based packaging. Two different measuring systems were considered. For the non-destructive detection of O_2 gas concentration, a packaging system with an integrated sensor material for a measurement based on the principle of fluorescence quenching was developed. For the detection of CO_2 gas concentration, a novel measurement device working in the MIR was constructed and successfully applied. The measurement device to detect the CO_2 gas concentration was therefore able to gain the most precise results, while being more convenient compared to the measurement system for the non-destructive detection of the O_2 gas concentration. The hypothesis to use these tools to set an individual "use by" or "best before" date for meat and meat products, could not be confirmed, not because the devices measured imprecisely, but because the growth rate of the microorganisms in most cases cannot be correlated with the change in the gas atmosphere before the critical microbiological TVC is reached. However, promising results for red muscle beef were obtained in terms of a decrease in O_2 gas concentration, by reaching the critical microbiological figure of 10^7 $CFUg^{-1}$. As the sample material already had a high initial microbiological load, further trials with a lower initial viable count must therefore be done. Furthermore, for boiled cooked sausages, as well as for improper stored poultry, the devices were able to detect a significant change in the headspace gas concentration on the day when they were microbiological spoiled. For poultry stored under regular conditions, the detection of the gas atmosphere is not a reliable method to make a statement in terms of microbiological spoilage. However, the sensory evaluation of the poultry samples clearly showed a correlation between the formation of *slime* when the samples reached their critical microbiological limit. Applying the knowledge gained from the review article, it might be also an idea to find markers for the formation of *slime* before it becomes visible for the human eye, e.g., using HSI technology, to predict spoilage.

The integration of the fluorescent material into the packaging system as shown in this work is difficult industrially and has too few practical fields of application for large-scale implementation. Further research could optimize integration and permeation properties, for example by using thin membranes or direct embedding of the fluorescent material in the polymer itself. However, the benefits and costs are not comparable here. In addition, a number of questions remain unanswered, such as the recyclability of such packaging types.

In contrast the device developed for the measurement of CO_2 gas concentrations offers a broad range of potential applications besides setting an individual "use by" or "best before" date. To gain a deeper understanding of its requirements and limitations, a broad customer study with the prototype would be the next step, including laboratories of food producers for quality analysis (production and outgoing inspection) as well as research facilities. In addition, screening a wide variety of MAP-packed products in supermarkets would also be a sensible next step. The focus here would not have to be exclusively on packaged meat and meat products. Newer products on the market such as vegan alternatives that are often packaged under MAP could also be screened. On the one hand, it could be documented whether the products reach the retail trade with consistent quality (incoming inspection) or whether they were stored improperly during transportation.

In addition, a separate study could be carried out to determine at which improper storage temperatures and times premature spoilage occurs and how reliably this can be measured by achieving the CO_2 "cross-over" marker which was identified within this work.

It would also make sense to develop more flexible designs that work not only for standard polymer trays (as they are used in general for fresh meat), but also for flatter shapes, such as those used for sliced cooked sausage or cheese, or for tubular bags. It would also be feasible to implement an O_2 sensor in addition. However, as absorption at 760 nm is rather weak, the use of a TDLAS-based system would therefore make more sense. A limitation here could be that the O_2 absorption band is located directly at the transition between visible light and the near-infrared range, which is an issue for applicability for printed or pigmented packaging. The integration of a TDLAS system would also make the device unattractive in terms of price for some potential user groups such as the retail trade.

5 Copyright

Publication I and II:

Reprinted with permission of Elsevier, who state in their copyright policy that the author has the right to include the article in a thesis or dissertation (https://www.elsevier.com/about/policies-and-standards/copyright).

Publication III:

© 2024 The Authors. Journal of Food Engineering published by Elsevier. This is an open access article under the terms of Elsevier (https://www.elsevier.com/about/policies-and-standards/copyright), which permits use, distribution and reproduction in any medium, provided the original work is properly cited.

Publication IV:

© The Authors. Licensee MDPI, Basel, Switzerland. This in a open access article distributed under the terms and conditions of the Creative Commons Attribution (CC BY) license (https://www.mdpi.com/authors/rights).

6 References (Chapter 1 & 3)

Agroui, K., Collins, G., & Farenc, J. (2012). Measurement of glass transition temperature of crosslinked EVA encapsulant by thermal analysis for photovoltaic application. *Renewable Energy*, *43*, 218–223. https://doi.org/10.1016/j.renene.2011.11.015

Alessandroni, L., Caprioli, G., Faiella, F., Fiorini, D., Galli, R., Huang, X., Marinelli, G., Nzekoue, F., Ricciutelli, M., Scortichini, S., Silvi, S., Tao, J., Tramontano, A., Turati, D., & Sagratini, G. (2022). A shelf-life study for the evaluation of a new biopackaging to preserve the quality of organic chicken meat. *Food Chemistry*, *371*, 131134. https://doi.org/10.1016/j.foodchem.2021.131134

Atkins, P., Paula, J. de, & Keeler, J. (2022). *Atkins' Physical Chemistry* (Twelfth edition). Oxford University Press.

Baier, J. (2005). *Lumineszenz-Untersuchungen zur Generierung und Relaxation von Singulett-Sauerstoff in zellulärer Umgebung* [Dissertation]. Universität Regensburg, Regensburg.

Banerjee, S., Kelly, C., Kerry, J. P., & Papkovsky, D. B. (2016). High throughput non-destructive assessment of quality and safety of packaged food products using phosphorescent oxygen sensors. *Trends in Food Science & Technology*, *50*, 85–102. https://doi.org/10.1016/j.tifs.2016.01.021

Baumgart, J., Becker, B., & Stephan, R. (Eds.). (2016). *Mikrobiologische Untersuchung von Lebensmitteln: Ein Leitfaden für das Studium* (6th ed.). B.Behr's Verlag GmbH & Co. KG. Hamburg.

Baur, E., Brinkmann, S., Osswald, T., Rudolph, N., & Schmachtenberg, E. (2013). *Saechtling Kunststoff Taschenbuch* (31. Ausgabe). Hanser. München.

Böcker, J. (2014). *Spektroskopie: Instrumentelle Analytik mit Atom- und Molekülspektrometrie* (1st ed.). *LaborPraxis*. Vogel Buchverlag. Würzburg.
https://ebookcentral.proquest.com/lib/gbv/detail.action?docID=1651435

Böhner, N., & Rieblinger, K. (2016). Impact of different visible light spectra on oxygen absorption and surface discoloration of bologna sausage. *Meat Science*, *121*, 207–209. https://doi.org/10.1016/j.meatsci.2016.06.019

Boles, J., & Pegg, R. (2010). *Meat color*. Montana State University and Saskatchewan Food Product Innovation, Program University of Saskatchewan.

Borch, E., Kant-Muermans, M.-L., & Blixt, Y. (1996). Bacterial spoilage of meat products and cured meat. *International Journal of Food Microbiology*, *33*, 103–120.

Brandsch, J., & Piringer, O. G. (2008). Characteristics of Plastic Materials. In O. G. Piringer & A. L. Baner (Eds.), *Plastic Packaging: Interactions with Food and Pharmaceuticals* (2nd ed., Vol. 2, pp. 15–61). WILEY-VCH Verlag GmbH & Co. KGaA. Weinheim.

Buchner, N. (1999). *Verpackung von Lebensmitteln: Lebensmitteltechnologische, verpackungstechnische und mikrobiologische Grundlagen.* Springer-Verlag Berlin Heidelberg GmbH.

Buntinx, M., Willems, G., Knockaert, G., Adons, D., Yperman, J., Carleer, R., & Peeters, R. (2014). Evaluation of the Thickness and Oxygen Transmission Rate before and after Thermoforming Mono- and Multi-layer Sheets into Trays with Variable Depth. *Polymers*, *6*(12), 3019–3043. https://doi.org/10.3390/polym6123019

Casaburi, A., Piombino, P., Nychas, G.-J., Villani, F., & Ercolini, D. (2015). Bacterial populations and the volatilome associated to meat spoilage. *Food Microbiology*, *45, Part A*, 83–102. https://doi.org/10.1016/j.fm.2014.02.002

Cassens, R. G. (1997). Composition and safety of cured meats in the USA. *Food Chemistry*, *59*(4), 561–566. https://doi.org/10.1016/S0308-8146(97)00007-1

Cavallo, D. P., Cefola, M., Pace, B., Logrieco, A. F., & Attolico, G. (2018). Non-destructive automatic quality evaluation of fresh-cut iceberg lettuce through packaging material. *Journal of Food Engineering*, *223*, 46–52. https://doi.org/10.1016/j.jfoodeng.2017.11.042

Cayuela, J., Gil, M., Ban, S., & Garrido, M. (2004). Effect of vacuum and modified atmosphere packaging on the quality of pork loin. *European Food Research and Technology*, *219*(4). https://doi.org/10.1007/s00217-004-0970-x

Chaix, E., Couvert, O., Guillaume, C., Gontard, N., & Guillard, V. (2015). Predictive Microbiology Coupled with Gas (O_2 /CO_2) Transfer in Food/Packaging Systems: How to Develop an Efficient Decision Support Tool for Food Packaging Dimensioning. *Comprehensive Reviews in Food Science and Food Safety*, *14*(1), 1–21. https://doi.org/10.1111/1541-4337.12117

Charles, N., Williams, S. K., & Rodrick, G. E. (2006). Effects of packaging systems on the natural microflora and acceptability of chicken breast meat. *Poultry Science*, *85*(10), 1798–1801. https://doi.org/10.1093/ps/85.10.1798

Chmiel, M., Hać-Szymańczuk, E., Adamczak, L., Pietrzak, D., Florowski, T., & Cegiełka, A. (2018). Quality changes of chicken breast meat packaged in a normal and in a modified atmosphere. *Journal of Applied Poultry Research*, *27*(3), 349–362. https://doi.org/10.3382/japr/pfy004

Cho, K., Li, F., & Choi, J. (1999). Crystallization and melting behavior of polypropylene and maleated polypropylene blends. *Polymer*, *40*(7), 1719–1729. https://doi.org/10.1016/S0032-3861(98)00404-2

Church, I. J., & Parsons, A. L. (1995). Modified Atmosphere Packaging Technology : A Review. *Journal of the Science of Food and Agriculture*, *67*(2), 143–152. https://doi.org/10.1002/jsfa.2740670202

Ciurana, J. de, Serenóa, L., & Vallès, È. (2013). Selecting Process Parameters in RepRap Additive Manufacturing System for PLA Scaffolds Manufacture. *Procedia CIRP*, *5*, 152–157. https://doi.org/10.1016/j.procir.2013.01.031

Cocola, L., Allermann, H., Fedel, M., Sønderby, S., Tondello, G., Bardenstein, A., & Poletto, L. (2016). Validation of an in-line non-destructive headspace oxygen sensor. *Food Packaging and Shelf Life*, *9*, 38–44. https://doi.org/10.1016/j.fpsl.2016.05.007 (Fig 1 reprinted with permission of Elsevier).

Cocola, L., Fedel, M., Poletto, L., & Tondello, G. (2015). Laser spectroscopy for totally non-intrusive detection of oxygen in modified atmosphere food packages. *Applied Physics B: Lasers and Optics*, *119*, 37–44.

Cocola, L., Fedel, M., Tondello, G., & Poletto, L. (2017). A Modular Approach of Different Geometries for Non-invasive Oxygen Measurement inside Moving Food Packages. *Packaging Technology and Science*, *30*(4), 159–170. https://doi.org/10.1002/pts.2292

Cocola, L., Fedel, M., Tondello, G., Frazzi, G., Poletto, L., Bardenshtein, A., Landa, S., & Allermann, H. (2018). Design and evaluation of an in-line system for gas sensing in flow-packed products. *Food Packaging and Shelf Life*, *17*, 91–98. https://doi.org/10.1016/j.fpsl.2018.06.006 (Fig. 9 & 11 reprinted with permission of Elsevier)).

Coles, R., McDowell, D., & Kirwan, M. J. (Eds.). (2003). *Food packaging technology*. Blackwell Publishing. Oxford.

Corlett, M. T., Pethick, D. W., Kelman, K. R., Jacob, R. H., & Gardner, G. E. (2021). Consumer Perceptions of Meat Redness Were Strongly Influenced by Storage and Display Times. *Foods*, *10*(3). https://doi.org/10.3390/foods10030540

Czerwiński, K., Rydzkowski, T., Wróblewska-Krepsztul, J., & Thakur, V. K. (2021). Towards Impact of Modified Atmosphere Packaging (MAP) on Shelf-Life of Polymer-Film-Packed Food Products: Challenges and Sustainable Developments. *Coatings*, *11*(12), 1504. https://doi.org/10.3390/coatings11121504

D'Agostino, M., & Cook, N. (2016). Foodborne Pathogens. In *Encyclopedia of Food and Health* (pp. 83–86). Elsevier. https://doi.org/10.1016/B978-0-12-384947-2.00326-3

Danilovic, B., Cocola, L., Fedel, M., Poletto, L., & Savic, D. (2016). Formation and Cumulation of CO2 in the Bottles of the Fermented Milk Drinks. *IPCBEE*, *95*, 26–31.

Danilović, B., Savić, D., Cocola, L., Fedel, M., & Poletto, L. (2018). Determination of CO2 Content in the Headspace of Spoiled Yogurt Packages. *Journal of Food Quality*, *2018*, 1–6. https://doi.org/10.1155/2018/8121606

Das, I., & Das, S. (2010). Emitters and Infrared Heating System Design. In Z. Pan & G. Atungulu (Eds.), *Contemporary Food Engineering. Infrared Heating for Food and*

Agricultural Processing (Vol. 20104123, pp. 57–88). CRC Press. https://doi.org/10.1201/9781420090994-c4

Demarteau, J., Winter, J. de, Detrembleur, C., & Debuigne, A. (2018). Ethylene/vinyl acetate-based macrocycles via organometallic-mediated radical polymerization and CuAAC 'click' reaction. *Polymer Chemistry*, *9*(3), 273–278. https://doi.org/10.1039/c7py01891f

DGHM. (2018). *Mikrobiologische Richt- und Warnwerte zur Beurteilung von Lebensmitteln: Richt- und Warnwerte für Brühwurst, Kochwurst, Kochpökelwaren sowie Sülzen und Aspikwaren auf Handelsebene.* https://www.dghm.org/wpcontent/uploads/2018/10/Entw%C3%BCrfe_03.18_Ver%C3 %B6ff._NEU.pdf

DIN Standards Committee Packaging. (2014). *DIN 53380-5: Testing of plastics - Determination of gas transmission rate - Part 5: Optical method for plastic films and moulded plastic parts*. Beuth Verlag GmbH.

Doherty, A. M., Sheridan, J. J., Allen, P., McDowell, D. A., & Blair, I. S. (1996). Physical characteristics of lamb primals packaged under vacuum or modified atmospheres. *Meat Science*, *42*(3), 315–324. https://doi.org/10.1016/0309-1740(95)00040-2

Du, Z., Zhang, S., Li, J., Gao, N., & Tong, K. (2019). Mid-Infrared Tunable Laser-Based Broadband Fingerprint Absorption Spectroscopy for Trace Gas Sensing: A Review. *Applied Sciences*, *9*(2), 338. https://doi.org/10.3390/app9020338

Durry, G., Li, J. S., Vinogradov, I., Titov, A., Joly, L., Cousin, J., Decarpenterie, T., Amarouche, N., Liu, X., Parvitte, B., Korablev, O., Gerasimov, M., & Zéninari, V. (2010). Near infrared diode laser spectroscopy of C2H2, H2O, CO2 and their isotopologues and the application to TDLAS, a tunable diode laser spectrometer for the martian PHOBOS-GRUNT space mission. *Applied Physics B*, *99*(1-2), 339–351. https://doi.org/10.1007/s00340-010-3924-y

Ehrenstein, G. W., Riedel, G., & Trawiel, P. (2003). *Praxis der thermischen Analyse von Kunststoffen* (2., völlig überarb. Aufl.). Hanser. München.

Embleni, A. (2013). Modified atmosphere packaging and other active packaging systems for food, beverages and other fast-moving consumer goods. In *Trends in Packaging of Food, Beverages and Other Fast-Moving Consumer Goods (FMCG)* (pp. 22–34). Elsevier. https://doi.org/10.1533/9780857098979.22

Escobedo Araque, P., Perez de Vargas Sansalvador, I. M., Lopez Ruiz, N., Erenas, M. M., Carvajal Rodriguez, M. A., & Martinez Olmos, A. (2018). Non-Invasive Oxygen Determination in Intelligent Packaging Using a Smartphone. *IEEE Sensors Journal*, *18*(11), 4351–4357. https://doi.org/10.1109/JSEN.2018.2824404

European Parliament. (2017). *Food waste: the problem in the EU in numbers.* European Parliament.

https://www.europarl.europa.eu/news/en/headlines/society/20170505STO73528/food
-waste-the-problem-in-the-eu-in-numbers-infographic

Feng, C., & Xu, P. (1999). The detection mechanism of LiTaO3 type II pyroelectric detectors. *Infrared Physics & Technology*, *40*(2), 71–78. https://doi.org/10.1016/S1350-4495(98)00045-0

Forrest, J. C., Aberle, E. D., Hedrick, H. B., Judge, M. D., & Merkel, R. A. (1975). *Principles of Meat Science*. W.H. Freeman and Company. San Francisco.

Forrest, J. C., Morgan, M. T., Borggaard, C., Rasmussen, A. J., Jespersen, B. L., & Andersen, J. R. (2000). Development of technology for the early post mortem prediction of water holding capacity and drip loss in fresh pork. *Meat Science*, *55*(1), 115–122. https://doi.org/10.1016/S0309-1740(99)00133-3

Fraden, J. (2016). *Handbook of modern sensors: Physics, designs, and applications* (Fifth edition). *Springer eBook Collection*. Springer.
https://link.springer.com/book/10.1007/978-3-319-19303-8
https://doi.org/10.1007/978-3-319-19303-8

Franke, C., & Beauchamp, J. (2017). Real-Time Detection of Volatiles Released During Meat Spoilage: a Case Study of Modified Atmosphere-Packaged Chicken Breast Fillets Inoculated with Br. thermosphacta. *Food Analytical Methods*, *10*, 310–319.

Franke, C., Höll, L., Langowski, H.-C., Petermeier, H., & Vogel, R. F. (2017). Sensory evaluation of chicken breast packed in two different modified atmospheres. *Food Packaging and Shelf Life*, *13*, 66–75.

Frick, A., & Stern, C. (2011). *Praktische Kunststoffprüfung*. Hanser. München.

Gibis, D., & Rieblinger, K. (2013). Application of different kinds of packaging to prevent greying of a special type of chilled sausages. *The 59 Th International Congress of Meat Science and Technology (ICOMST)*, Izmir, Turkey.

Gill, C. O., & Tan, K. H. (1980). Effect of carbon dioxide on growth of meat spoilage bacteria. *Applied and Environmental Microbiology*, *39*(2), 317–319.
https://doi.org/10.1128/aem.39.2.317-319.1980

Ginger, I. D., Wilson, G. D., & Schweigert, B. S. (1954). Biochemistry of Myoglobin - Quantitative Determination in Beef and Pork Muscle. *Journal of Agricultural and Food Chemistry*, *2*(20), 1037–1038. https://doi.org/10.1021/jf60040a008

Gonzalez, J., Ferrer, A., Oria, R., & Salvador, M. L. (2008). Determination of O2 and CO2 transmission rates through microperforated films for modified atmosphere packaging of fresh fruits and vegetables. *Journal of Food Engineering*, *86*, 194–201.

Grau, R., Sánchez, A. J., Girón, J., Iborra, E., Fuentes, A., & Barat, J. M. (2011). Nondestructive assessment of freshness in packaged sliced chicken breasts using SW-

NIR spectroscopy. *Food Research International*, *44*(1), 331–337. https://doi.org/10.1016/j.foodres.2010.10.011

Gustavsson, J., Cederberg, C., Sonesson, U., van Otterdijk, O., & Meybeck, A. (2011). *Global food losses and food waste - Extent, causes and prevention*. Food and Agriculture Organization of the United Nations (FAO).

Herbert, U., Albrecht, A., & Kreyenschmidt, J. (2015). Definition of predictor variables for MAP poultry filets stored under different temperature conditions. *Poultry Science*, *94*(3), 424–432. https://doi.org/10.3382/ps/peu002

Herman, P., Maliwal, B. P., Lin, H. J., & Lakowicz, J. R. (2001). Frequency-domain fluorescence microscopy with the LED as a light source. *Journal of Microscopy*, *203, Part 2*, 176–181. https://doi.org/10.1046/j.1365-2818.2001.00943.x

Hertog-Meischke, M. J. den, van Laack, R. J., & Smulders, F. J. (1997). The water-holding capacity of fresh meat. *The Veterinary Quarterly*, *19*(4), 175–181. https://doi.org/10.1080/01652176.1997.9694767

Hilgarth, M., Fuertes-Pèrez, S., Ehrmann, M., & Vogel, R. F. (2018). An adapted isolation procedure reveals Photobacterium spp. As common spoilers on modified atmosphere packaged meats. *Letters in Applied Microbiology*, *66*(4), 262–267. https://doi.org/10.1111/lam.12860

Hilgarth, M., Lehner, E. M., Behr, J., & Vogel, R. F. (2019). Diversity and anaerobic growth of Pseudomonas spp. Isolated from modified atmosphere packaged minced beef. *Journal of Applied Microbiology*, *127*(1), 159–174. https://doi.org/10.1111/jam.14249

Höll, L., Behr, J., & Vogel, R. F. (2016). Identification and growth dynamics of meat spoilage microorganisms in modified atmosphere packaged poultry meat by MALDI-TOF MS. *Food Microbiology*, *60*, 84–91.

Höll, L., Hilgarth, M., Geissler, A. J., Behr, J., & Vogel, R. F. (2020). Metatranscriptomic analysis of modified atmosphere packaged poultry meat enables prediction of Brochothrix thermosphacta and Carnobacterium divergens in situ metabolism. *Archives of Microbiology*, *202*(7), 1945–1955. https://doi.org/10.1007/s00203-020-01914-y

Hood, D. E., & Riordan, E. B. (1973). Discolouration in pre-packaged beef: measurement by reflectance spectrophotometry and shopper discrimination. *International Journal of Food Science and Technology*, *8*, 333–343.

Horvath, L., Min, B., & Kim, Y. T. (2017). Testing of Mechanical Properties for Plastic Packaging Materials. In P. Singh, A. A. Wani, & H.-C. Langowski (Eds.), *Food Packaging Materials* (pp. 103–122). CRC Press. https://doi.org/10.1201/9781315374390-4

Hsu, C.-P. S. (Ed.). (1997). *Infrared spectroscopy: Handbook of instrumental techniques for analytical chemistry.*

Huber, C. (2008). Wie viel kommt durch? Ermittlung der Sauerstoffdurchlässigkeit von PET-Flaschen. *Getränkeindustrie*, *11*, 48–57.

Huff-Lonergan, E., & Lonergan, S. M. (2005). Mechanisms of water-holding capacity of meat: The role of postmortem biochemical and structural changes. *Meat Science, 71*(1), 194–204. https://doi.org/10.1016/j.meatsci.2005.04.022

Ivorra, E., Sánchez, A. J., Verdú, S., Barat, J. M., & Grau, R. (2016). Shelf life prediction of expired vacuum-packed chilled smoked salmon based on a KNN tissue segmentation method using hyperspectral images. *Journal of Food Engineering*, *178*, 110–116. https://doi.org/10.1016/j.jfoodeng.2016.01.008

Jorge, P., Caldas, P., Rosa, C. C., Oliva, A. G., & Santos, J. L. (2004). Optical fiber probes for fluorescence based oxygen sensing. *Sensors and Actuators B: Chemical, 103*(1-2), 290–299. https://doi.org/10.1016/j.snb.2004.04.086

Kadota, H., & Ishida, Y. (1972). Production of volatile sulfur compounds by microorganisms. *Annual Review of Microbiology*, *26*, 127–138. https://doi.org/10.1146/annurev.mi.26.100172.001015

Kakouri, A., & Nychas, G. J. (1994). Storage of poultry meat under modified atmospheres or vacuum packs: Possible role of microbial metabolites as indicator of spoilage. *The Journal of Applied Bacteriology*, *76*(2), 163–172. https://doi.org/10.1111/j.1365-2672.1994.tb01612.x

Kamarudin, S. H., Abdullah, L. C., Aung, M. M., & Ratnam, C. T. (2018). A study of mechanical and morphological properties of PLA based biocomposites prepared with EJO vegetable oil based plasticiser and kenaf fibres. *IOP Conference Series: Materials Science and Engineering*, *368*, 12011. https://doi.org/10.1088/1757-899X/368/1/012011

Kameník, J., Saláková, A., Hulánková, R., & Borilova, G. (2015). The effect of high pressure on the microbiological quality and other characteristics of cooked sausages packed in a modified atmosphere or vacuum. *Food Control*, *57*, 232–237. https://doi.org/10.1016/j.foodcont.2015.04.010

Kameník, J., Saláková, A., Pavlík, Z., Bořilová, G., Hulanková, R., & Steinhauserová, I. (2014). Vacuum skin packaging and its effect on selected properties of beef and pork meat. *European Food Research and Technology*, *239*(3), 395–402. https://doi.org/10.1007/s00217-014-2233-9

Kelly, C. A., Santovito, E., Cruz-Romero, M., Kerry, J. P., & Papkovsky, D. P. (2020). Application of O2 sensor technology to monitor performance of industrial beef samples

packaged on three different vacuum packaging machines. *Sensors and Actuators B: Chemical*, *304*, 127338. https://doi.org/10.1016/j.snb.2019.127338

Kelly, C., Yusufu, D., Okkelman, I., Banerjee, S., Kerry, J. P., Mills, A., & Papkovsky, D. B. (2020). Extruded phosphorescence based oxygen sensors for large-scale packaging applications. *Sensors and Actuators B: Chemical*, *304*, 127357. https://doi.org/10.1016/j.snb.2019.127357

Kerry, J. P., O'Grady, M. N., & Hogan, S. A. (2006). Past, current and potential utilisation of active and intelligent packaging systems for meat and muscle-based products: A review. *Meat Science*, *74*, 113–130.

Keupp, C., Höll, L., Beauchamp, J., & Langowski, H.-C. (2015). Online monitoring of volatile freshness indicators from modified atmosphere packaged chicken meat using PTR-MS. *27th IAPRI Symposium on Packaging. Conference Proceedings*.

Keweloh, H. (2019). *Mikroorganismen in Lebensmitteln: Theorie und Praxis der Lebensmittelhygiene* (7. Auflage). Pfanneberg. Gruiten.

Kim, J. G., Luo, Y., Tao, Y., Saftner, R. A., & Gross, K. C. (2005). Effect of initial oxygen concentration and film oxygen transmission rate on the quality of fresh-cut romaine lettuce. *Journal of the Science of Food and Agriculture*, *85*(10), 1622–1630. https://doi.org/10.1002/jsfa.2158

Kolbe, H. (1883). Antiseptische Eigenschaften der Kohlensäure; Nachtrag. *Journal für praktische Chemie*, *28*(1), 61–62. https://doi.org/10.1002/prac.18830280106

Kolbeck, S., Reetz, L., Hilgarth, M., & Vogel, R. F. (2019). Quantitative Oxygen Consumption and Respiratory Activity of Meat Spoiling Bacteria Upon High Oxygen Modified Atmosphere. *Frontiers in Microbiology*, *10*, 2398.

Krämer, J. (2010). Lebensmittelmikrobiologie. In W. Frede (Ed.), *Handbuch für Lebensmittelchemiker: Lebensmittel, Bedarfsgegenstände, Kosmetika, Futtermittel* (3rd ed., pp. 509–526). Springer-Verlag. Berlin. Heidelberg. New York.

Kuflik, P., & Rotman, S. R. (2012). Band selection for gas detection in hyperspectral images. In *2012 IEEE 27th Convention of Electrical and Electronics Engineers in Israel* (pp. 1–4). IEEE. https://doi.org/10.1109/EEEI.2012.6376973

Lackner, M. (2007). Tunable diode laser absorption spectroscopy (TDLAS) in the process industries– a review. *Reviews in Chemical Engineering*, *23*(2), 65–147.

Lai, H., Wang, Z., Wu, P., Chaudhary, B. I., Sengupta, S. S., Cogen, J. M., & Li, B. (2012). Structure and Diffusion Behavior of Trioctyl Trimellitate (TOTM) in PVC Film Studied by ATR-IR Spectroscopy. *Industrial & Engineering Chemistry Research*, *51*(27), 9365–9375. https://doi.org/10.1021/ie300007m

Lakowicz, J. R. (2006). *Principles of Flourescence Spectroscopy* (3rd ed.). Springer Science+Business Media, LLC.

Langowski, H.-C. (2008). Permeation of Gases and Condensable Substances Through Monolayer and Multilayer Structures. In O. G. Piringer & A. L. Baner (Eds.), *Plastic Packaging: Interactions with Food and Pharmaceuticals* (2nd ed., pp. 297–347). WILEY-VCH Verlag GmbH & Co. KGaA. Weinheim.

Langowski, H.-C. (2017). Shelf Life of Packed Food and Packaging Functionality. In P. Singh, A. A. Wani, & H.-C. Langowski (Eds.), *Food Packaging Materials* (pp. 11–66). CRC Press. https://doi.org/10.4324/9781315374390-2

Lee, D. S., Yam, K. L., & Piergiovanni, L. (2008). *Food Packaging Science and Technology*. CRC Press. https://doi.org/10.1201/9781439894071

Lee, H., Cho, S., Lim, J., Lee, A., Kim, G., Song, D.-J., Chun, S.-W., Kim, M.-J., & Mo, C. (2023). Performance Comparison of Tungsten-Halogen Light and Phosphor-Converted NIR LED in Soluble Solid Content Estimation of Apple. *Sensors*, *23*(4). https://doi.org/10.3390/s23041961

Levin, I., & Bhargava, R. (Eds.). (2005). *Spectrochemical analysis using infrared multichannel detectors*. Blackwell Publishing. Oxford. https://ebookcentral.proquest.com/lib/kxp/detail.action?docID=351450

Lewander, M. (2010). *Laser Absorption Spectroscopy of Gas in Scattering Media* [Doctoral Thesis]. Lund University, Lund.

Lipinski, B., Hanson, C., Lomax, J., Kitinoja, L., Waite, R., & Searchinger, T. (2013). Reducing food loss and waste. *World Resources Institute Working Paper*, 1–40.

Livingston, D. J., & Brown, W. D. (1981). The chemistry of myoglobin and its reactions. *Food Technology*, *35*(5), 244–252.

Łopacka, J., Półtorak, A., & Wierzbicka, A. (2016). Effect of MAP, vacuum skin-pack and combined packaging methods on physicochemical properties of beef steaks stored up to 12 days. *Meat Science*, *119*, 147–153. https://doi.org/10.1016/j.meatsci.2016.04.034

Love, J. D., & Pearson, A. M. (1971). Lipid oxidation in meat and meat products - A review. *Journal of the American Oil Chemists' Society*, *48*(10), 547–549. https://doi.org/10.1007/BF02544559

Lund, M. N., Heinonen, M., Baron, C. P., & Estévez, M. (2011). Protein oxidation in muscle foods: A review. *Molecular Nutrition & Food Research*, *55*(1), 83–95. https://doi.org/10.1002/mnfr.201000453

Lund, M. N., Lametsch, R., Hviid, M. S., Jensen, O. N., & Skibsted, L. H. (2007). High-oxygen packaging atmosphere influences protein oxidation and tenderness of porcine longissimus dorsi during chill storage. *Meat Science*, *77*(3), 295–303. https://doi.org/10.1016/j.meatsci.2007.03.016

Lundin, P. (2014). *Laser Sensing for Quality Control and Classification – Applications for the Food Industry, Ecology and Medicine* [Doctoral Thesis]. Lund University, Lund.

Luo, X., Zaitoon, A., & Lim, L.-T. (2022). A review on colorimetric indicators for monitoring product freshness in intelligent food packaging: Indicator dyes, preparation methods, and applications. *Comprehensive Reviews in Food Science and Food Safety*, *21*(3), 2489–2519. https://doi.org/10.1111/1541-4337.12942

Mead, G. (2006). *Microbiological Analysis of Red Meat, Poultry and Eggs. Woodhead Publishing Series in Food Science, Technology and Nutrition*. Elsevier Science. http://gbv.eblib.com/patron/FullRecord.aspx?p=1666670

Meredith, H., Valdramidis, V., Rotabakk, B. T., Sivertsvik, M., McDowell, D., & Bolton, D. J. (2014). Effect of different modified atmospheric packaging (MAP) gaseous combinations on Campylobacter and the shelf-life of chilled poultry fillets. *Food Microbiology*, *44*, 196–203.

Møller, J. K. S., Bertelsen, G., & Skibsted, L. H. (2002). Photooxidation of nitrosylmyoglobin at low oxygen pressure. Quantum yields and reaction stoechiometries. *Meat Science*, *60*(4), 421–425. https://doi.org/10.1016/S0309-1740(01)00155-3

Morsy, M. K., Zor, K., Kostesha, N., Alstrøm, T. S., Heiskanen, A., El-Tanahi, H., Sharoba, A., Papkovsky, D., Larsen, J., Khalaf, H., Jakobsen, M. H., & Emneus, J. (2016). Development and validation of a colorimetric sensor array for fish spoilage monitoring. *Food Control*, *60*, 346–352.

Nassos, P. S., King, A. D., & Stafford, A. E. (1983). Relationship between lactic acid concentration and bacterial spoilage in ground beef. *Applied and Environmental Microbiology*, *46*(4), 894–900. https://doi.org/10.1128/aem.46.4.894-900.1983

Nieminen, T. T., Dalgaard, P., & Björkroth, J. (2016). Volatile organic compounds and Photobacterium phosphoreum associated with spoilage of modified-atmosphere-packaged raw pork. *International Journal of Food Microbiology*, *218*, 86–95. https://doi.org/10.1016/j.ijfoodmicro.2015.11.003

Nychas, G.-J. E., & Drosinos, E. H. (1999). MEAT AND POULTRY | Spoilage of Meat. In *Encyclopedia of Food Microbiology* (pp. 1253–1260). Elsevier. https://doi.org/10.1006/rwfm.1999.0990

O'Mahony, F. C., O'Riordan, T. C., Papkovskaia, N., Kerry, J. P., & Papkovsky, D. B. (2006). Non-destructive assessment of oxygen levels in industrial modified atmosphere packaged cheddar cheese. *Food Control*, *17*(4), 286–292. https://doi.org/10.1016/j.foodcont.2004.10.013

Peng, Y., Adhiputra, K., Padayachee, A., Channon, H., Ha, M., & Warner, R. D. (2019). High Oxygen Modified Atmosphere Packaging Negatively Influences Consumer Acceptability Traits of Pork. *Foods*, *8*(11). https://doi.org/10.3390/foods8110567

Pennacchia, C., Ercolini, D., & Villani, F. (2011). Spoilage-related microbiota associated with chilled beef stored in air or vacuum pack. *Food Microbiology*, *28*(1), 84–93. https://doi.org/10.1016/j.fm.2010.08.010

Pettersen, M. K., Nilsen-Nygaard, J., Hansen, A. Å., Carlehög, M., & Liland, K. H. (2021). Effect of Liquid Absorbent Pads and Packaging Parameters on Drip Loss and Quality of Chicken Breast Fillets. *Foods*, *10*(6). https://doi.org/10.3390/foods10061340

Piergiovanni, L., & Limbo, S. (2016). Plastic Packaging Materials. In L. Piergiovanni & S. Limbo (Eds.), *SpringerBriefs in Molecular Science. Food Packaging Materials* (pp. 33–49). Springer International Publishing. https://doi.org/10.1007/978-3-319-24732-8_5

Piringer, O. G., & Baner, A. L. (Eds.). (2008). *Plastic Packaging: Interactions with Food and Pharmaceuticals* (2nd ed.) (pp. 523 ff.) WILEY-VCH Verlag GmbH & Co. KGaA. Weinheim.

Rossaint, S., Klausmann, S., & Kreyenschmidt, J. (2015). Effect of high-oxygen and oxygen-free modified atmosphere packaging on the spoilage process of poultry breast fillets. *Poultry Science*, *94*(1), 96–103. https://doi.org/10.3382/ps/peu001

Schmid, M., Dallmann, K., Bugnicourt, E., Cordoni, D., Wild, F., Lazzeri, A., & Noller, K. (2012). Properties of Whey-Protein-Coated Films and Laminates as Novel Recyclable Food Packaging Materials with Excellent Barrier Properties. *International Journal of Polymer Science*, *2012*, 1–7. https://doi.org/10.1155/2012/562381

Schmutzler, M., Beganovic, A., Böhler, G., & Huck, C. W. (2015). Methods for detection of pork adulteration in veal product based on FT-NIR spectroscopy for laboratory, industrial and on-site analysis. *Food Control*, *57*, 258–267. https://doi.org/10.1016/j.foodcont.2015.04.019

Schmutzler, M., Beganovic, A., Böhler, G., & Huck, C. W. (2016). Modern Safety Control for Meat Products: Near Infrared Spectroscopy Utilised for Detection of Contaminations and Adulterations of Premium Veal Products. *NIR News*, *27*(4), 11–13. https://doi.org/10.1255/nirn.1610

Schossig, M., Ott, T., Hüller, S., Norkus, V., & Gerlach, G. (2015). 3.4 - Efficient thermal infrared emitter with high radiant power. In *Proceedings IRS² 2015* (pp. 934–937). AMA Service GmbH, Von-Münchhausen-Str. 49, 31515 Wunstorf, Germany. https://doi.org/10.5162/irs2015/3.4

Sikorska, E., Wójcicki, K., Kozak, W., Gliszczyńska-Świgło, A., Khmelinskii, I., Górecki, T., Caponio, F., Paradiso, V. M., Summo, C., & Pasqualone, A. (2019). Front-Face Fluorescence Spectroscopy and Chemometrics for Quality Control of Cold-Pressed Rapeseed Oil During Storage. *Foods*, *8*(12). https://doi.org/10.3390/foods8120665.

Smith, B. C. (2021a). The Infrared Spectra of Polymers II: Polyethylene. *Spectroscopy*, 24–29. https://doi.org/10.56530/spectroscopy.xp7081p7

Smith, B. C. (2021b). The Infrared Spectra of Polymers III: Hydrocarbon Polymers. *Spectroscopy*, 22–25. https://doi.org/10.56530/spectroscopy.mh7872q7

Smith, B. C. (2023). Infrared Spectroscopy of Polymers, XI: Introduction to Organic Nitrogen Polymers. *Spectroscopy*, 14–18. https://doi.org/10.56530/spectroscopy.vd3180b5

Sokolik, I. (2009). *Absorption by atmospheric gases in the IR, visible and UV spectral regions.*

Sørheim, O., Kropf, D. H., Hunt, M. C., Karwoski, M. T., & Warren, K. E. (1996). Effects of modified gas atmosphere packaging on pork loin colour, display life and drip loss. *Meat Science*, *43*(2), 203–212. https://doi.org/10.1016/0309-1740(96)84592-X

Sowoidnich, K., Schmidt, H., Maiwald, M., Sumpf, B., & Kronfeldt, H.-D. (2010). Application of Diode-Laser Raman Spectroscopy for In situ Investigation of Meat Spoilage. *Food and Bioprocess Technology*, *3*(6), 878–882. https://doi.org/10.1007/s11947-010-0360-2

Stiles, M. E. (1995). Scientific Principles of Controlled/Modified Atmosphere Packaging. In B. Ooraikul & M. E. Stiles (Eds.), *Modified Atmosphere Packaging Of Food* (pp. 18–25). Springer US. https://doi.org/10.1007/978-1-4615-2117-4_2

Stoicheff, B. P. (1957). High Resolution Raman Spectroscopy of Gases: IX. Spectra of H2, HD, and D2. *Canadian Journal of Physics*, *35*(6), 730–741. https://doi.org/10.1139/p57-079

Stokes, G. G. (1852). On the change of refrangibility of light. *Philosophical Transactions of the Royal Society of London*, *142*, 463–562. https://doi.org/10.1098/rstl.1852.0022

Suman, S. P., & Joseph, P. (2013). Myoglobin chemistry and meat color. *Annual Review of Food Science and Technology*, *4*, 79–99. https://doi.org/10.1146/annurev-food-030212-182623

Torres, E. A., Shimokomaki, M., Franco, B. D., Landgraf, M., Carvalho, B. C., & Santos, J. C. (1994). Parameters determining the quality of charqui, an intermediate moisture meat product. *Meat Science*, *38*(2), 229–234. https://doi.org/10.1016/0309-1740(94)90112-0

Walz, F. H., Gibis, M., Herrmann, K., Hinrichs, J., & Weiss, J. (2017). Chemical and optical characterization of white efflorescences on dry fermented sausages under modified atmosphere packaging. *Journal of the Science of Food and Agriculture*, *97*(14), 4872–4879. https://doi.org/10.1002/jsfa.8358

Wang, X., Han, B., Ehrhardt, M., Zhang, F., Wang, J., Wang, P., Monka, P. P., & Sun, S. (2022). Non-damage deep etching of SiC by hybrid laser-high temperature chemical processing. *International Journal of Applied Ceramic Technology*, *19*(4), 2344–2355. https://doi.org/10.1111/ijac.14061

Wiegleb, G. (2016). *Gasmesstechnik in Theorie und Praxis: Messgeräte, Sensoren, Anwendungen.* Springer Vieweg. Wiesbaden.

Wong, J. Y., & Anderson, R. L. (2012). *Non-dispersive infrared gas measurement* (First Edition). Ifsa Publishing. Barcelona.

Xiong, Y., Tan, J., Wang, C., Zhu, Y., Fang, S., wu, J., Wang, Q., & Duan, M. (2016). A miniaturized oxygen sensor integrated on fiber surface based on evanescent-wave induced fluorescence quenching. *Journal of Luminescence*, *179*, 581–587. https://doi.org/10.1016/j.jlumin.2016.08.005

Xu, D., Lu, J., Yan, S., & Xiao, R. (2018). Aminated EVOH nanofiber membranes for Cr(vi) adsorption from aqueous solution. *RSC Advances*, *8*(2), 742–751. https://doi.org/10.1039/C7RA11940B

Yamaguchi, N. (1990). Vacuum Packaging. In *Food Packaging* (pp. 279–292). Elsevier. https://doi.org/10.1016/B978-0-08-092395-6.50020-9

Zhang, G., & Wu, X. (2004). A novel CO2 gas analyzer based on IR absorption. *Optics and Lasers in Engineering*, *42*(2), 219–231 . https://doi.org/10.1016/j.optlaseng.2003.08.001

Zhang, G., Wang, G., Huang, Y., Wang, Y., & Liu, X. (2018). Reconstruction and simulation of temperature and CO2 concentration in an axisymmetric flame based on TDLAS. *Optik*, *170*, 166–177. https://doi.org/10.1016/j.ijleo.2018.05.123

7 Appendix

7.1 Publication I

Optical measurement systems in the food packaging sector and research for the non-destructive evaluation of product quality

Jasmin Dold [a,*], Horst-Christian Langowski [b]

[a] Chair of Brewing and Beverage Technology, Technical University of Munich, Weihenstephaner Steig 20, D-85354 Freising, Germany
[b] TUM School of Life Sciences, Technical University of Munich, Weihenstephaner Steig 22, D-85354 Freising, Germany

ABSTRACT

The quality standards of food products are becoming increasingly important in our society, and have been reinforced by various food scandals in recent years. At the same time, the proportion of packaged products is constantly increasing, as the packaging itself plays a decisive role in maintaining many quality characteristics. In order to examine the quality of packaged foodstuffs, invasive analyses are still often standard. Optical measuring methods offer a possibility to determine quality parameters through the plastic. The following review therefore examines the state of the art in current research in this area and critically examines any possibilities for improvement.

1. Introduction

Optical measurement systems use light at different wavelengths and frequencies to determine physical properties or quantities. The application of optical measuring methods related to the food and packaging sector covers a broad range of the electromagnetic spectrum, from the long-wave infrared (IR) through the visible range to the short-wave ultraviolet (UV). For example, infrared light and visible light are used for the identification and classification of plastics using IR and Raman spectroscopy (Pivokonsky et al., 2018; Schymanski, Goldbeck, Humpf, & Fürst, 2018). In contrast, very short-wave electromagnetic radiation, such as that used in X-ray detection of foreign bodies (Heuft & Polster, 2006) – e.g. glass splinters in bottling plants – or longer-wave terahertz radiation, is no longer referred to as light and the corresponding measuring systems are no longer called optical systems. In order to narrow this field, only the spectral range between ultraviolet (UV) and mid-infrared radiation (MIR) or between 100 nm and 50 μm is considered in this article.

The FAO (Food and Agriculture Organization of the United Nations) estimates that about 1.3 billion tons of the globally produced food gets wasted per year (FAO, 2011). The reasons for food losses can vary along the value chain and depends also on the wealth of a country. In developing countries, a large quantity of the products is wasted during production, storage and distribution because the manufacturing conditions

are not optimized. Richer countries benefit from more modern equipment e.g. refrigeration processes, so most of the products are disposed of in the retail industry or at the consumer's home, often unseen, simply because their nominal best before date has passed (FAO, 2011; Lipinski et al., 2013).

Much research has already been done to integrate intelligent sensors into packaging to provide information about the quality of the product to stakeholders in the value chain and to the consumer. The majority of this research is aimed at so-called Food Freshness Indicators (FFI's). To determine the change in product status, different parameters can be used. Fish and meat, for example, typically emit volatile organic compounds (VOC) upon the growth of microorganisms (e.g. basic volatile amines, which could for example be detected by pH sensitive dyes (Franke & Beauchamp, 2017; Morsy et al., 2016)). Other quality characteristics such as the degree of fruit ripeness can also be determined via FFI's in the packaging (Kuswandi & Murdyaningsih, 2017; Lee et al., 2019). However, there are some problems associated with the use of FFI's. Using a colorimetric system often results in imprecise or not clearly apparent color changes of the indicator, which makes it difficult for the viewer to assess product quality. In the case of microbiological spoilage, a false negative diagnosis could have very negative consequences, since the growth of microorganisms cannot only lead to sensory deficits of the product, but also to food borne diseases caused by pathogens (e.g. *Salmonella* or *Campylobacter jejuni*) (Heiss & Eichner, 1995;

Kerry, O'Grady, & Hogan, 2006), Therefore, any false negative diagnosis has to be avoided. However, in order to reduce food waste, the number of false-positive diagnoses (safe products that appear to be unsafe) must also be low. In many cases, mismeasurements can be caused because the metabolites needed for measurement are rarely produced in the same quantity. This may be due, for example, to different initial bacterial counts or to different microorganism species - both pathogenic and non-pathogenic (Kerry et al., 2006).

There is also a gap for some quality parameters that are not associated with gaseous metabolites and therefore cannot be determined with an FFI. The adulteration or authentication of food remains a major issue here, which has been shaped by several scandals in recent years, particularly in the meat industry (Premanandh, 2013). Other attributes such as moisture or pest infestation are also difficult to measure with such sensors, which is why there is a need for fast and non-destructive methods. Optical methods might be the ideal choice here.

For example, retailers can carry out independent checks on the products supplied without having to remove them from sale. This includes, for example, the individual assessment of the best before date or the detection of food adulteration on the manufacturers' side. The consumer could also benefit from such measurements. In retail establishments, "test stations" where the consumer himself can test a product for certain quality attributes before he purchases it, are conceivable.

Nowadays, the use of optical sensors is standard in many laboratories and productions ("in-line"). The advantage of these systems is that they provide fast results, and at the same time provide comparable accuracies to analytical measuring methods. In the grain industry, for example, IR sensors are used to determine the protein and fat content as well as ash and moisture during the milling process or other grain-specific process steps (e.g. NIR Multi Online Analyzer, Bühler AG, Uzwil, Switzerland) (Hahne, 2015). The milk industry is using near infrared spectroscopy (NIR) as well for decades, for example to evaluate the milk fat, lactose or total protein amount (van de Voort, 1980). In most cases, the unpackaged product is tested.

However, some research was already done in the past to investigate the product quality through the intact packaging via optical measurement systems. A distinction can be made here between a measurement directly on the product or in the liquid phase and an indirect measurement of the gas phase (headspace) – which is also the basic distinction in this publication.

Smiddy et al. for example used sensor spots with embedded fluorophores for the monitoring of the oxygen content in the headspace of packaged meat to correlate the oxygen concentration with the lipid oxidation (measured in a destructive way) (Smiddy, Papkovskaia, Papkovsky, & Kerry, 2002). The same technology was used by O'Mahony et al. in 2006 to measure the amount of oxygen in the headspace of packaged cheddar cheese by taping the sensor material under the

lidding film and monitoring the oxygen content over a period of time (O'Mahony et al., 2006). Other studies chose direct measurements on the product itself, e.g., NIR or Raman spectroscopy, to identify food quality. This could be, for example, the change in the absorption properties of the meat surface during storage of packaged chicken breast (Grau et al., 2011), or the change of the scattering effects induced by microbiological meat spoilage (Sowoidnich, Schmidt, Maiwald, Sumpf, & Kronfeldt, 2010). All studies showed the potential for the investigation of quality attributes via non-destructive optical measurement systems, but they also concluded that there is a need of further research. That is why this review aims to show the most important optical measurement techniques used in the food packaging industry and research in recent years, for the examination and non-destructive quality evaluation of packaged foods.

2. Optical measurement systems in the food packaging sector – basic principles

Optical measurement systems are widely used to determine the quality of food (Nielsen, 2010), but as mentioned before, most of them focus on the quality of the product itself without non-destructive measurements through the packaging material. In the following, the physical principles of optical measurement systems used in research or industry to obtain information about quality parameters through the intact packaging material are presented. Some of them are used for measuring the gas atmosphere in the *headspace of the packaging* (as *indirect* measurement for food quality), others for measuring the optical properties *of the product* itself (=*direct*), some for both.

2.1. Fluorescence Spectroscopy

Fluorescence is defined as the spontaneous emission of light that occurs shortly after the fluorescent molecules have been excited by light absorption (Wedler, 1997). There are two measuring principles, which can be used for the determination of product quality based on fluorescence spectroscopy and they are described in the following.

2.1.1. Dynamic quenching

This method can quantify the concentration of oxygen present in the package, either in the headspace or directly dissolved in the product. In the sequence of the physical steps involved here, oxygen serves as a quencher for excited fluorophore molecules. Fluorophores are embedded in a sensor spot placed in the package. These fluorophores are excited from the outside at a defined wavelength, usually via a fiber optic system. When the molecules return to their ground state, they emit fluorescent light. When a quencher - such as oxygen - collides with an excited fluorophore molecule, its extra energy is absorbed by the oxygen
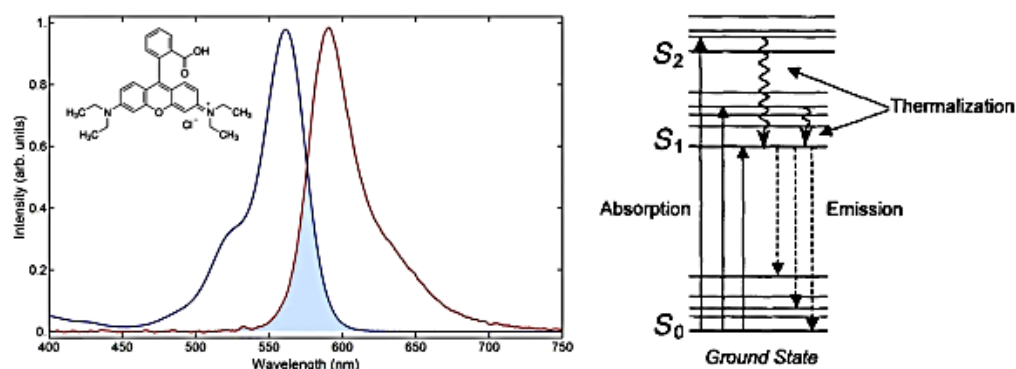

Fig. 1. Absorption (blue) and shifted emission (red) of Rhodamine B (left) (Tomazio et al., 2017) and the schematic illustration according to Jabłoński of the ground and electronically excited states during fluorescence (right) (Jameson, 2003).
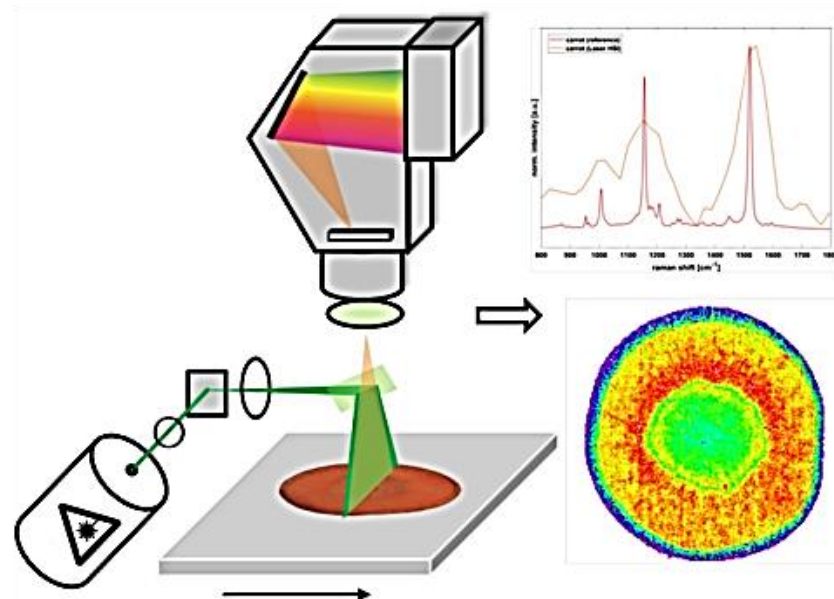
2

Fig. 2. Raman-based HSI of the carotenoid concentration in a carrot slice (Gruber et al., 2019).

molecule before fluorescent light is emitted. Therefore, both the fluorescence intensity and the average luminescence lifetime (the time the molecule stays in the excited state) are reduced as a function of the amount of oxygen present (Huber, 2008; Lakowicz, 2006). Such measuring systems are easy to handle, as the measuring devices are usually hand-held and portable. On the one hand, it can serve as a straight determination of the oxygen content, or the determined partial pressures can be used for correlation with other quality attributes - e.g. microbial spoilage. One possible disadvantage is the need for integration of the sensor spot into the packaging system. Firstly, integration means higher packaging effort. Secondly, an additional covering of the sensor spot is often necessary. For one thing, the sensor material may contain components that are not allowed to have direct contact with the food owing to food contact regulations. However, there are already some suppliers who produce sensor spots that conform to food standards (e.g. PreSens Presicion Sensing GmbH, Germany). In dynamic quenching, however, it is also often necessary for the fluorophores to be protected from the food itself, since the action of macromolecules can immobilize the quencher, reducing its effectiveness and altering the measurement result. (Lakowicz, 2006).

2.1.2. Spectral analysis (fluorimetry)

Another way to use fluorescence to gain information about product quality is to measure changes of the emitted light from the product itself, after its excitation at a defined wavelength. The relevant wavelengths in fluorimetry are in the UV–VIS–NIR range, between 200 and 1000 nm. Due to the Stokes shift – which was discovered in 1852 by G.G. Stokes (Stokes, 1852) – the emitted photons usually have a lower energy than the excited ones and, consequently, a higher wavelength. After excitation to a higher electronic state, the transition to a higher vibrational level of the ground state can occur. Furthermore, initial excitation to a higher electronic state is possible, after which the molecule does not return to the ground state (S_0), but to a lower excited electronic state (S_1). This results in the energy of the emitted photon being lower than that of the previously absorbed photon. The competing process is the non-radiative transition to a lower vibrational state, which increases the temperature of the overall system ("thermalization"). These effects are shown in Fig. 1 (Jameson, 2003; Tomazio, Boni, & Mendonca, 2017).

Different product changes can influence the emission and can possibly be correlated to a quality factor (Sahar, Boubellouta, & Dufour, 2011). This type of spectral analysis is typically used for measurements on the product itself (Henihan, O'Donnell, Esquerre, Murphy, & O'Callaghan, 2018; Ma, Birlouez-Aragon, & Amamcharla, 2019; Mbesse Kongbonga, Ghalila, Majdi, Mbogning Feudjio, & Ben Lakhdar, 2015; Sikorska et al., 2019).

2.2. Hyperspectral imaging

The unique aspect of hyperspectral imaging analysis is that it combines spectroscopy and digital image acquisition (Birngruber et al., 2009). Hyperspectral imaging (HSI) was first named by Goetz, Vane, Solomon, and Rock (1985), who used this technique for the remote sensing of the earth surface. The principle of HSI involves the spectral analysis of individual pixels of an image taken from a sample. In most cases, absorption-based spectral analysis is used, where the spectral ranges can be between UV and MIR, mostly in the visible and near infrared range (Chang, 2003). However, it is also possible to combine and evaluate Raman (see Section 2.4) and fluorescence-based spectra with HSI (Gruber, Grählert, Wollmann, & Kaskel, 2019), giving the method a very wide range of direct measurements of product quality.

Fig. 2 shows an example of a Raman-based HSI investigation of carotenoid in a carrot slice. Because the carotenoid shows a central Raman peak at a frequency of 1521 cm^{-1}, the false color imaging was created at this frequency, and the carotenoid content in the carrot (red = high content, pink = low content) could be visualized (Gruber et al., 2019).

In contrast to purely spectroscopically based measuring methods, it is thus possible to obtain not only a single spectrum for the detection area, but a large number of spectra originating from different positions in the detection area (Chang, 2003). Due to this large amount of information, it is possible to obtain very specific information about the product and product changes. However, this large amount of data also has the disadvantage that very complex chemometric methods are required to identify correlations.
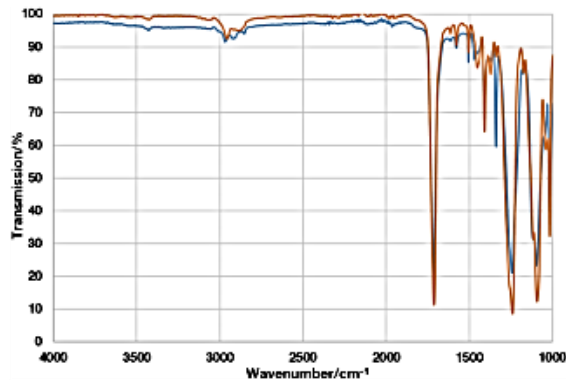
3

60

Fig. 3. Transmission of two PET films in the MIR range (own illustration).

2.3. Infrared spectroscopy

One of the most important optical methods for the spectroscopic characterization of different substances is based on infrared spectroscopy – today predominantly the Fourier-Transform Infrared Spectroscopy (FT-IR) measuring method showing substantial advantages, e.g. measurement speed, sensitivity and precision (Böcker, 2014).

The principle of IR spectroscopy is based on the property of molecules to develop mechanical vibrations detectable in the NIR and MIR range or rotations in the far infrared range (FIR) by the absorption of IR radiation (Böcker, 2014). That is only possible if a variable or inducible dipole moment exists in the molecule that allows the interaction between the radiation and the molecule. Transitions where no changes of the dipole moment will appear, are called IR inactive or "forbidden" transitions (Atkins & Paula, 2013). Here, it is distinguished between the NIR with a spectral range between 800 and 2500 nm or 12500 – 4000 cm^{-1}, the MIR with 2500 – 50.000 nm or 4000 – 200 cm^{-1} and the FIR with 50.000 – 500.000 nm or 200 – 20 cm^{-1} (Böcker, 2014).

IR spectroscopy can be used for both, the detection of a gas phase or the absorption properties of the product itself. Another advantage is that most polymer-based packaging materials are partially transparent in the NIR and short-wave MIR area, what's advantageous regarding non-invasive measurements through the packaging material. An example of the transmission properties of polyethylene terephthalate (PET) is shown in Figs. 3 and 4.

2.4. Raman spectroscopy

Transitions that are not detectable by infrared spectroscopy might be measured via Raman spectroscopy, because they are often Raman active. This is the reason why IR and Raman spectroscopy are often combined in appropriate measurement systems, as is described in the further review. The principle of Raman spectroscopy is based on the Raman Effect or Raman scattering, which is the inelastic scattering of light by molecules. Here, the investigated samples are irradiated with a monochromatic laser (Böcker, 2014). In contrast to other spectroscopic measurement techniques - where absorption and emission are measured directly at the wavelength of the incident light - Raman spectroscopy uses scattered radiation from a sample excited by a laser of defined wavelength and the spectroscopic measurement of this scattered radiation relative to the excitation wavelength.

After impinging the sample, the laser light is scattered. A portion of the scattered light has the same energy as the excitation light, the so-called Raleigh scattering. A smaller fraction of the scattered photons has a lower energy than the excitation light (red shift), the difference having been used to excite molecular vibrations. This is the so-called Stokes Raman scattering. If, on the other hand, the emitted photon acquires additional energy from a molecular vibration, it has a higher energy (blue shift) than the excitation energy. This process, which is even less probable than Stokes Raman scattering, is referred to as anti-Stokes Raman scattering. The difference between the initial energy and the energy of the scattered light is called the Raman shift. The resulting Raman shifts are very specific to different molecular compositions, which is why the Raman spectrum is often referred to as a molecular fingerprint (Wedler, 1997).

Molecular vibrations are IR-active if the existing dipole moment of a molecule changes with the vibration. Raman-active vibrations, on the other hand, do not require a changed dipole moment, but a changed polarizability. Therefore, Raman spectroscopy is complementary to IR spectroscopy. Moreover, Raman shifts can be observed in the VIS region of the spectrum. Both facts allow the measurement of samples not quantifiable via IR. However, it should be noted that Raman spectra are rather weak and therefore affected by other resonant interactions - such as fluorescence (Atkins & Paula, 2013; Böcker, 2014).

One variant of Raman spectroscopy is the so-called spatially offset Raman spectroscopy (SORS) that allows the identification and characterization of samples or gases beneath a surface, by doing one or more further measurements at different points on the sample surface. Although this is a very common method for the identification of explosive material (Loeffen et al., 2011), for example, it also plays an important role in controlling product quality in the food industry, as
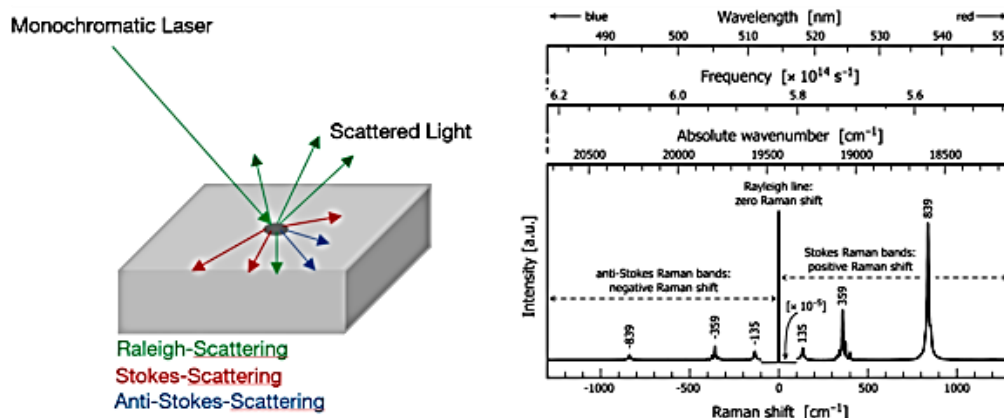

Fig. 4. The principle of Raman scattering (left; own illustration) and the resulting Raman- shifts in the spectra (right (Nasdala, Smith, Kaindl, & Ziemann, 2004)).
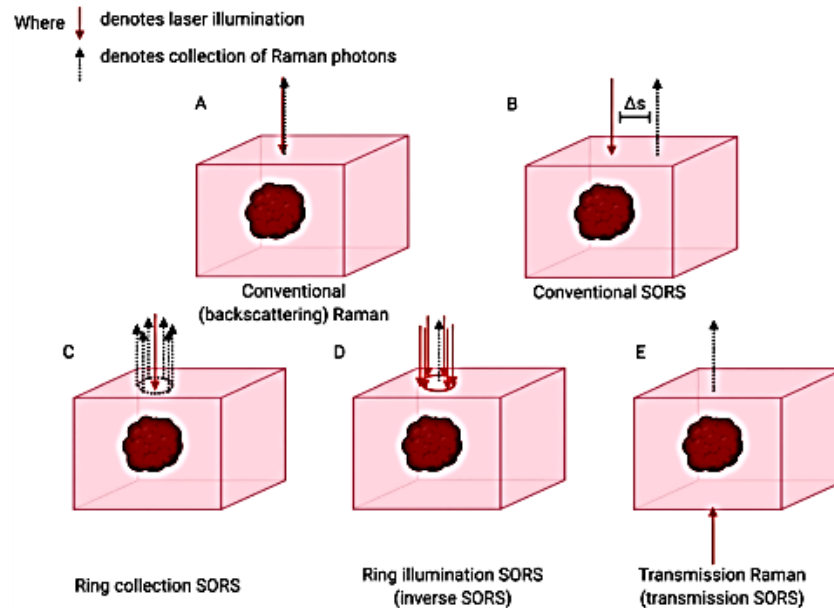
4

Fig. 5. Conventional Raman spectroscopy (A) and different setups of SORS (B)-(E) (Nicolson et al., 2020).
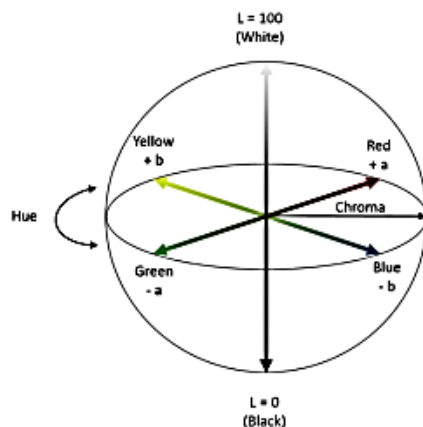

Fig. 6. Schematic illustration of the CIE L*a*b* color space (Ly, Dyer, Feig, Chien, & Del Bino, 2020).

further described in Chapter 3. In contrast to conventional Raman spectroscopy, SORS measures the scattering locally shifted to the excitation zone. This is particularly useful for non-transparent materials, where the monochromatic light is usually scattered. This scattered light also has Raman signals that can be determined using SORS (Nicolson, Kircher, Stone, & Matousek, 2020). Fig. 5 shows the conventional Raman setup, and different SORS setups.

2.5. (Simple) Color measurements

There are different evaluation systems available to quantify visible color changes. All of them are based on the chromaticity diagram defined in the early 20th century by the Commission Internationale de l'Eclairage (CIE) that defines red (R) at 700 nm, green (G) at 546.1 nm and blue (B) at 435.8 nm as primary valences. So all real colors can be represented, three arbitrary, imaginary measures X (red), Y (green) and

Z (blue) were defined on this basis by the CIE in 1931 as primary valences, which serve as the calculation basis for all color measurement systems (Schanda, 2007). One very common method to measure color changes in the food sector is the use of the CIE L*a*b* color space that is an addition to the CIE XYZ color space (Oliveira, de, Leme, Barbosa, Rodarte, & Pereira, 2016; Saldaña et al., 2013). Additionally, the black to white area is defined (brightness = L*) and is perpendicular to the color planes a* (green-red) and b* (blue-yellow) (Schanda, 2007), that are shown in Fig. 6. A defined light source (e.g. D65) is used for the measurement and the camera is calibrated with a specific color chart, prior to the measurement (Matusiak, 2015).

By comparing the hue proportions, color changes can be determined relatively easily, even if they are not yet visible to the human eye.

2.6. Tunable diode laser absorption spectroscopy (TDLAS)

Like most spectroscopic methods, the TDLAS is based on the Lambert-Beer's law, which describes the relation of the initial light intensity and a penetrated light intensity after crossing a specific sample in dependence of substance concentration, pathway and absorption coefficient. TDLAS is used to determine gas concentrations within a gas phase, which is why it is generally used as an indirect measurement method. The advantage of TDLAS is that it is applicable for gases in low concentrations. Absorption bands in the VIS range can be used, which is necessary e.g. for the detection of oxygen (Lackner, 2007), but also in the IR range, e.g. for CO_2 (Lewander, 2010).

The principle of TDLAS is shown in Fig. 7. Since the monochromatic laser can be tuned by changing the current or temperature, the emission frequency ("wavelength scanning interval") can be varied and the signal strength changes. The ratio of the signal level of the detector and the laser results in the absorption peak (Cocola et al., 2016; Lackner, 2007). That makes it possible to adjust the measurement conditions very specifically to the product under study and its surrounding. It is, for example, conceivable to measure at high pressure, or to vary the measurement temperature (Lundin, 2014). The disadvantage of this specificity could be that it can only be used very product-specific due to these settings.

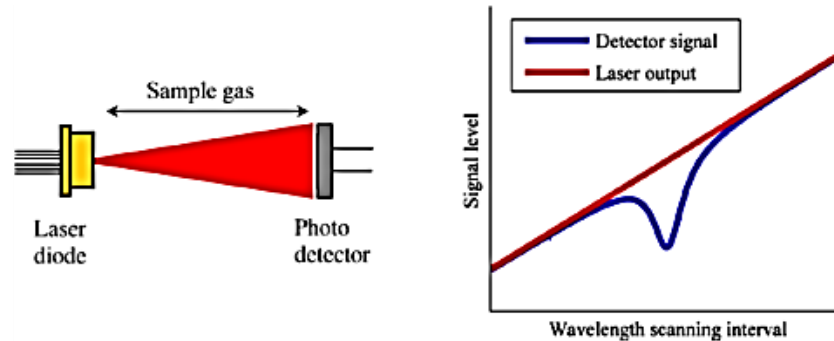The most common band for the oxygen detection is around 760 nm,

J. Dold and H.-C. Langowski

Food Packaging and Shelf Life 31 (2022) 100814

Fig. 7. Principle of tunable diode laser absorption spectroscopy (TDLAS) (Cocola et al., 2016).
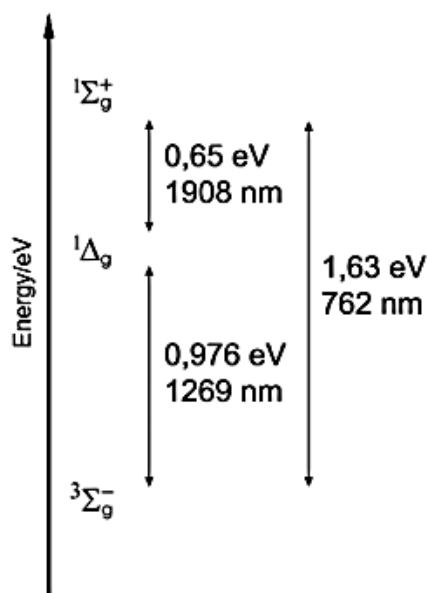

Fig. 8. Triplet and singlet states of oxygen (according to Baier (2005)).

which is also called the A-band. This band is formed by the electronic transition from the unexcited triplet ($^3\Sigma_g^-$) to one of the excited singlet states of oxygen ($^1\Sigma_g^+$). That singlet state is located at a higher level relative to the ground state, but has a significantly shorter lifetime ($<10^{-9}$ s) compared to another singlet state $^1\Delta_g$, which is responsible for the weaker absorption bands at 1269 and 1908 nm (Baier, 2005). The energy differences from the triplet to the described singlet states and the resulting absorption bands are schematically shown in Fig. 8.

The oxygen detection has the disadvantage that the ambient oxygen of around 20.9% could affect the results. To prevent this, some applications include oxygen scavenger in its measuring device (Cocola et al., 2015; Cocola et al., 2017).

3. Optical, non-destructive measurement systems for the determination of filling quality

The quality of packaged food can take many different forms. Filling quality and shelf life are often related to the microbiological spoilage of a product, which is indeed the most important aspect for the consumer and producer, as this is the most likely health risk. But there are other quality aspects as well, such as product adulteration, fat oxidation or ripening processes which are of great interest.

For some of these quality attributes, research has been carried out that allows non-destructive quantification based on optical measurement methods. As already mentioned in the introduction and in Table 1 and Table 2, the distinction in this publication is made between non-destructive measurement of the gas phase in the headspace of a package (=indirect) and on the product through the package (=direct). In

Table 1
Optical measuring methods for the **direct product** evaluation of different quality characteristics in packaged food with reference to the measured variable.

Optical Measurement System	Measured Variable	Quality Attribute	Product Group	Reference
Fluorescence Spectroscopy	Product component	Adulteration	Fats	(Hossain, Canning, & Yu, 2019)
	Degradation product	Oxidative Change	Fats	(Sikorska et al., 2019)
Hyperspectral Imaging	Product component	Freshness	Fish	(Washburn, Stormo, Skjelvareid, & Heia, 2017)
		Ripening	Cheese	(Darnay, Králik, Oros, Koncz, & Firtha, 2017)
	Degradation product	Ripening	Cheese	(Darnay et al., 2017)
		Microbiological Spoilage	Fish	(Ivorra et al., 2016)
IR Spectroscopy	Product component	Adulteration	Meat	(Schmutzler, Beganovic, Böhler, & Huck, 2015; Schmutzler, Beganovic, Böhler, & Huck, 2016)
		Moisture	Herbs	(Mendes Novo, Iriel, & Lagorio, 2016)
Raman Spectroscopy	Product component	Adulteration	Beverages	(Ellis et al., 2017, 2018; Fleming, Chen, Bruce, & Dholakia, 2020; Kiefer & Cromwell, 2017)
			Fats	(Lohumi, Lee, Kim, Qin, & Cho, 2018)
		Identification	Sugar	(Qin et al., 2017)
Simple Color Measurement	Product component	Color Change	Beverages	(Cubeddu, Fava, Pulvirenti, Haghighi, & Licciardello, 2021)
		Freshness	Salad	(Cavallo, Cefola, Pace, Logrieco, & Attolico, 2018)

6

63

Table 2
Optical measuring methods for the **indirect headspace** evaluation of different quality characteristics in packaged food with reference to the measured variable (*) (The literature does not mention a specific product group, but the general determination in packaging systems).

Optical Measurement System	Measured Variable	Quality Attribute	Product Group	Reference
Fluorescence Spectroscopy	Degradation effecting the headspace	Oxidative Change	Fats	(Sikorska et al., 2019)
			Meat	(C.A. Kelly et al., 2020; C. Kelly et al. 2020)
		Microbiological Spoilage	Meat	(Escobedo Araque et al., 2018; C. Kelly et al., 2020)
	Composition of Modified Atmosphere	Packaging Integrity	Cheese	(C.A. Kelly et al., 2020; C. Kelly et al., 2020; O'Callaghan, Papkovsky, & Kerry, 2016)
			Meat	(C.A. Kelly et al., 2020; C. Kelly et al., 2020)
			Not defined*	(Havens et al., 2007; Krottmaier and Ribitsch, 2015; Steffen et al., 2018)
Tunable Diode Laser Spectroscopy	Degradation effect in the headspace	Microbiological Spoilage	Beverages	(Danilovic, Cocola, Fedel, Poletto, & Savic, 2016)
			Milk	(Danilović et al., 2018; Li, Lin, Zhang, Svanberg, & Svanberg, 2017)
	Composition of Modified Atmosphere	Packaging Integrity	Bread	(Li et al., 2017)
			Cheese	(Cocola et al., 2016; Cocola et al., 2018)
			Meat	(Cocola et al., 2015; Cocola et al., 2017)
			Milk	(Li et al., 2017)
			Not defined*	(Forestelli & Frazzi, 2019)
			Pasta	(Cocola et al., 2017)

addition, a distinction is made according to the quality attributes and the measured variable, as categorized in Table 1 and Table 2.

3.1. Fluorescence spectroscopy

Most of the fluorescence-based measurement methods found are indirect methods, as they are often used for the detection of the oxygen amount in the headspace of a packaged product via the previously described quenching method (Escobedo Araque et al., 2018; C. A. Kelly et al., 2020; C. Kelly et al., 2020; Krottmaier & Ribitsch, 2015; O'Callaghan et al., 2016; Sikorska et al., 2019; Steffen et al., 2018). The direct measurement via quenching only occurred in case of liquid products

(Sikorska et al., 2019). However, the investigation of product-specific properties with a fluorescence based spectral analysis might be better suited for direct measurement (Hossain et al., 2019).

3.1.1. Adulteration

Almost every product group in the food industry is affected by this problem. Milk, for example, can be adulterated with plant-based milk (Jaiswal et al., 2015), water or sucrose (Botelho, Reis, Oliveira, & Sena, 2015). Butter is often mixed with margarine (Koca, Kocaoglu-Vurma, Harper, & Rodriguez-Saona, 2010) and the addition of sugar sirup to honey is also a known problem (Rios-Corripio, Rios-Leal, Rojas-López, & Delgado-Macuil, 2011). For the analysis of these unwanted ingredients, different optical measurement systems are available.

Fluorescence spectroscopy is a common method for estimating oil quality (Guzmán, Baeten, Pierna, & García-Mesa, 2015; Kongbonga et al., 2011), but as already mentioned, a sample preparation is often necessary for the measurement. Hossain et al. used a fluorescence-based method for the determination of different oil types and production methods ("extra virgin" or "refined") in 2019, which is able to measure the spectra through a glass bottle. They used an endoscopic smart mobile spectrofluorimeter, which allows the use of a smart phone as evaluation unit. The excitation was carried out at 370 nm, the emission spectra were measured between 300 and 700 nm. With that setup, they were able to identify the differences between different oil types. More specifically, they focused on the peak difference at 452 nm, which is known to increase with the amount of oxidation, and at 670 nm, an indicator for chlorophyll-α that is only present in extra virgin oils (Hossain et al., 2019). Although the test setup was not carried out with the original packaging, an application for packaged goods - for example in the retail trade - can be considered. However, tests with commercial products would have to be carried out for this.

3.1.2. Oxidative change

In most cases, oxygen is not welcome in food packaging because it could lead to negative product properties. Due to its ability to oxidize lipids or phenolic compounds, for example, the product can get rancid or change its color (Belitz, Grosch, & Schieberle, 2008; Church & Parsons, 1995).

The oxygen uptake during the storage of oil can lead to unwanted oxidation processes, which might be strengthened by photosensitized effects. The oxygen amount in the bottle headspace decreases significantly during storage time but the effect is distinctly slower for bottles stored in darkness. This oxygen decrease can be measured in the headspace, using bottles equipped with a ruthenium chloride complex sensor dot that works with the already described quenching method. A second dot can be inserted into the lower part of the bottle to measure the oxygen dissolved in the product. Such a combination of non-destructive oxygen measurement allows the quantitative determination of solution and oxidation processes. The use of other measurements for which sample preparation is necessary – e.g. the measurement of the fluorescence spectra with a spectrofluorometer – can confirm these process presumptions (Sikorska et al., 2019).

Kelly et al. also concluded during their storage trial, which is more described in detail in the next chapter, that the decrease of the headspace oxygen might be due to oxidation processes of the packaged meat (C. A. Kelly et al., 2020), which could be an appropriate assumption, but further trials would be necessary to proof it, as oxygen consumption can also be the result of microbiological activity.

Both examples show that the use of non-destructive fluorescence-based measurement systems is useful to quantify oxygen development in packaged products, but it is not possible to correlate this effect to oxidation processes without the use of invasive analytical methods yet.

3.1.3. Packaging integrity

Modified atmosphere packaging (MAP) is a common method to maintain the quality of food and to enhance its shelf life. The product

7

group ranges from fruits and vegetables to fish, fresh meat, baked products, cheese, snacks, pasta and ready-to-eat meals (Gibis, Sängerlaub, & Müller, 2015). The gas combination used depends on the respective product, as product-specific factors such as respiration, enzymatic browning and microbial spoilage can vary (Buchner, 1999). One of the best-known examples for the importance of a well-adjusted packaging atmosphere is the MAP packaging of beef. At low oxygen amounts, oxymyoglobin (MbFe(II)) is oxidized to metmyoglobin (MbFe (III)), which leads to an undesired color change from red to brown. By adding high oxygen amounts, the red muscle pigment that is a freshness indicator for product remains (Hood & Riordan, 1973). Other foodstuffs, by contrast, are very oxygen sensitive and the absence of oxygen is crucial for maintaining product quality (Buchner, 1999). Due to the importance of a well-adjusted gas atmosphere, the control during or immediately after the production process is of great interest and extensive research has been done in this field. To control the amount – or for most cases the absence – of oxygen in a packaging, the fluorescence-based quenching method is highly suitable. To this end, there have been a number of patent applications from the industry on the one hand (Havens et al., 2007; Krottmaier & Ribitsch, 2015; Steffen et al., 2018) and extensive application-related research on the other (C. A. Kelly et al., 2020; C. Kelly et al., 2020; O'Callaghan et al., 2016).

As mentioned before, the absence of oxygen is often important for shelf life and other quality attributes, which is the reason for vacuum packaging or the adjustment of a nitrogen/carbon dioxide atmosphere (Church & Parsons, 1995). To make sure that the packaging process went well, it is possible to integrate a layer of fluorophores into the packaging – for example into the lid film – and to measure the presence of oxygen right after the sealing process by illuminating the sensor spot at a defined wavelength (Havens et al., 2007; Krottmaier & Ribitsch, 2015; Steffen et al., 2018). For example, in 2007 Havens et al. tried to patent the measurement as well as the measuring device for the detection of oxygen in a container by illuminating different fluorophores (e.g. ruthenium-based components) at a defined wavelength and to measure the luminescence lifetime τ in dependence of temperature – which is the previous described quenching measurement (Havens et al., 2007). Since this is a generally applicable and widely known measurement method, patentability is questionable. Up to this point, no patent has been granted either. Thus, two further patent applications dealing with the same topic have not been granted to date as well. Both focus on the measuring based on fluorescence quenching and the measuring device inside a packaging machine to remove non-sealed packages by detecting oxygen immediately after the packaging process (Krottmaier & Ribitsch, 2015; Steffen et al., 2018).

Kelly et al. used that principle for two different studies in 2020. In the first study, optical sensor dots (OpTech™O$_2$ Platinum; MOCON, United States) were placed inside beef packaging before the packaging process to investigate the accuracy of three different vacuum-packaging machines and the beef quality or the oxygen change during the storage time. Neither the sensor material nor the excitation or absorption wavelength was described in more detail in this paper, but Banerjee et al., 2016b mentioned for this sensor type a PtBP (Pt(II)-benzoporphyrin) based dye, which is excitable around 600 nm and shows an emission around 750 nm (Banerjee, Arzhakova, Dolgova, & Papkovsky, 2016). They concluded that none of the tested machines reached a total vacuum, with residual oxygen amounts between 0.5% and 1%, which is a highly expected result. The publication confirmed, that an implementation of such a sensor system into a vacuum packaging machine is useful for controlling the product immediately after the packaging process, as it is already applied in the industry (GEA OxyCheck, GEA Group AG, Germany (GEA Group Aktiengesellschaft, 2021)).

On the other hand, they focused on the development of a polymer-based sensor spot using a multi-stage extrusion process for the preparation of polymer-based sensor-materials. The aim of the study was to create food safe and heat-sealable films, which are also able to provide information about the oxygen change in a packaging system. The sensor

material was therefore a powder, consisting of 7 µm polystyrene/divinylbenzene particles, stained with a phosphorescent O$_2$-sensitive PtBP dye. The film laminates were made from polylactic acid (PLA) and low-density polyethylene (PE-LD). For the film preparation, 5% sensor powder was added to PLA or PE-LD pellets. For the integration into a packaging system, the PE films were afterwards sandwich laminated between PA/PE and PE-HD films (with the PE side placed on top of each other) to fulfill food contact regulations. The produced sensor films were afterwards fixed onto the inner side of a conventional lid film, thus allowing the oxygen concentration in the headspace to be monitored under the modified atmosphere packaged cheese and beef. During a storage time of 32 (cheese) and 7 (beef) days, the extruded sensor materials achieved similar results to a conventional sensor spot (C. Kelly et al., 2020). The study shows a new way of producing fluorescence-based sensor spots that could be suitable for the integration into food packaging. However, this requires more concrete application possibilities and verification of food suitability (e.g. migration tests).

However, not only the packaging process can lead to an insufficient seal, even the distribution chain can result in leakage. The use of fluorophore-based sensor spots for O$_2$ detection integrated into the packaging system would be suitable to trace leaks in the distribution chain. In the study of O' Callaghan et al. the oxygen increase over storage time could be detected and assigned to the formation of leakages due to poor distribution conditions. This study shows that the application of a fluorescence-based sensor spot would also be useful in retail to check the products for leaks upon delivery and, if necessary, to return leaking packaging to the supplier.

3.1.4. Microbiological spoilage

Meat is very spoilage sensitive as it has a high a$_w$ value, a moderate pH and its nutrients provide optimum growing conditions (Krämer, 2010). Without the determination of the total bacteria count, it is not easy to get information about the spoiling status. An interesting approach for a possible control of meat quality was done by Escobedo et al. in 2018. They invented a measuring system which allowed to detect the oxygen amount in a pork packaging using the flashlight of a smartphone as excitation source for a platinum-based fluorophore sensor membrane PtOEP (platinum octaethylporphyrin) that was put on the inside of the tray before closing it at ambient air conditions. To act as a source of excitation, a light filter has to be applied onto the smartphone, as the unfiltered flashlight emits too many different wavelengths, which would lead to interferences. Based on a previous study (López-Ruiz et al., 2012), the filter was set around 530 nm. A photo could only be taken with the installed app if a defined distance to the spot was reached. The emission of the fluorescent light occurs in the red spectrum (645 nm) (López-Ruiz et al., 2012), so in view of the processed images the decrease of the red color can be converted into the oxygen content using a calibration curve. During the storage of the pork, they were able to detect a decrease of oxygen content and therefore concluded that the ambient air was metabolized due to microbiological activity (Escobedo Araque et al., 2018).

However, this measuring system shows some weaknesses. Simply using the emitted fluorescent light as a metric for oxygen concentration is susceptible to different optical transmission of films. For known differences in film transmission, adapted calibration curves might be used. But sometimes – especially in the food sector – non-predictable opacities may occur e.g. grease stains or marinade. This is why it is more common to use the luminescence lifetime for the calculation, which is independent of turbidity effects (Huber, 2008). Another issue is that they assumed to observe microbiological activity as the oxygen amount changed, but no correlation between bacterial growth was done in that study. It is also quite possible that the oxygen consumption was an effect of the myoglobin induced oxidation processes. However, the observation of atmosphere change due to microorganisms in packaged meat has already been done (Höll, Behr, & Vogel, 2016), but it is a process that must be evaluated for every combination of packaging system and

8

product. Otherwise, the risk to produce either an unsafe food product or to discard a still safe one would be too high.

Kelly et al. also tried to use the change in oxygen content as an indicator for microbiological growth in their study. They found a different O_2 profile when the sensor spot was placed on the product itself (decreasing oxygen) and on the inside of the packaging (no oxygen change) (C. Kelly et al., 2020). However, their finding has not been confirmed with microbiological analyses. Oxidation processes would probably be more likely in this case, since the oxygen content in the headspace would also decrease with the microbiological growth.

3.2. Hyperspectral imaging

As described in 2.2, HSI enables the analysis of images made with all described optical measurement principles – fluorescence, VIS, Infrared and Raman spectra, which allows an extremely wide range of applications. In general, the packaged product itself is analyzed (Darnay et al., 2017; Ivorra et al., 2016; Washburn et al., 2017).

3.2.1. Freshness

To enable producers and distributors to control the freeze-thaw history of fish, Washburn et al. (2017) tried to characterize this in 2017 via HSI, working with a spectral analysis in the VIS-NIR range and analyzed the whole spectrum between 430 and 1000 nm with specific focus on a blood specific region (450–600 nm) and a water specific region (900–990 nm). The samples were variously frozen and thawed after vacuum packing in PA/PE pouches, and imaged at the different states. Unfortunately, they were not able to correlate all tested variations, but they were e.g. able to distinguish between fresh, once and twice frozen samples.

3.2.2. Ripening

As general practice, the products are visually controlled during the ripening process to detect possible maturation deficiencies. Chemical, physical and microbiological parameters, such as pH or moisture content, are tested on a random basis. Sensory tastings are also carried out during storage. However, these random evaluations do not allow for an individual evaluation of each sample, as they are destructive and therefore cannot be carried out on all samples (Guamis et al., 1997; Kammerlehner, 2015).

For the control of food in transparent packaging, the hyperspectral imaging analysis is suitable if the desired substances show significant differences in their absorption properties. For example, it is possible to obtain information of the fat content or enzyme activity during the ripening of cheese, since both the fat content (1190 and 1234 nm) and the enzyme activity (1387 nm) respond to different wavelengths. To get useful information out of the measurements, it is necessary to cluster the results, e.g. with a partial least squares analysis (PLS). These results can be compared with previously collected chemical and physical properties - for example texture - and any correlations determined (Darnay et al., 2017). But these measurements are very specific, as different components or product properties might affect the spectral range and complex chemometric methods are required to get usable results.

3.2.3. Microbiological spoilage

During the spoiling process, most of the microorganisms form VOCs (for example, volatile basic nitrogen), which can be analyzed and quantified off-line e.g. with proton-transfer-reaction mass spectroscopy (Franke & Beauchamp, 2017) or steam distillation with subsequent titration (Malle & Tao, 1987) and thus constitute the base for packaging with integrated FFI's as mentioned before. Assuming that these compounds differ due to their absorption behaviors, Ivorra et al. postulated that it should be possible to correlate the changes of the spectra measured via hyperspectral imaging with invasive measurements of VOC and microbiological growth. Therefore, smoked salmon was stored vacuum packed at 4 °C for 60 days (packaging material not mentioned).

To obtain a hyperspectral imaging, the samples were illuminated at a spectral range of 400 – 1000 nm and an image was recorded in diffuse reflectance at a resolution of 1312 × 1060 pixels. Indeed, they were able to correlate the non-invasive and the destructive measurements. More precisely, the amount of unsaturated carbo chains (~500 nm) increased, which was interpreted as a result of fat oxidation and rearrangement by microorganisms. The validation of the test model was able to confirm the model (Ivorra et al., 2016). But as mentioned before and also reported in the discussed paper, as the results were highly dependent from the fat content – the wavelengths often overlap with other attributes – e. g. fat oxidation, this complicated the quantification of the VOC amount. Only if the storage conditions and product parameters do not differ from the primary measurement series and, in addition, the same measurement setup and the same correlation model are used, it is possible to make statements about the respective product. In addition, the correlation model often appears very unclear to outsiders. This method is rather unsuitable for making an individual prediction about the shelf life of the product, as too many parameters can influence the measurement result.

3.3. Infrared spectroscopy

Theoretically, IR spectroscopy is suitable for both direct and indirect determination of quality attributes, since a spectrum can be derived from the product surface or the surrounding gas atmosphere through the packaging. However, only direct measurements were found for this review (Mendes Novo et al., 2016; Schmutzler et al., 2015, 2016).

3.3.1. Adulteration

An experimental setup which includes real conditions for optical "through the packaging" measurements for the identification of food adulteration was used as an example by Schmutzler et al. in 2015. They chose NIR setups in reflectance mode for the identification of meat and fat adulterations in veal sausage. In their study, measurements were made on the unpackaged and the packaged product. The unpackaged samples were examined with three different measuring systems which were named as follows: laboratory setup, industrial setup and a portable hand-held spectrometer. The samples packaged under vacuum in HD-PE/PA film were evaluated exclusively with the industrial setup and the hand-held spectrometer, since the lab setup only allowed destructive measurements. For this reason, only the results for these two devices are shown below.

The spectral range for the evaluation was chosen between 1.6 and 1.8 μm, as peak changes due to the adulteration – which could not be further identified at the molecular level – were observed in this range. On the one hand, the veal sausage samples were prepared with different ratios of pork and veal (with constant fat content), and on the other hand, different amounts of veal fat were replaced by pork fat in the sausage samples with constant total meat content. For both types, the non-adulterated sample was compared to 10%, 20%, 30%, 40% and 50% adulteration, once in unpackaged and subsequently in packaged form.

Comparing these results by clustering them via PCA, they concluded that the industrial setup would be able to detect the adulterated samples for all measured concentrations and both, the meat and fat adulteration, even for the measurement through the plastic package. For the hand-held measuring system, an inferior detection limit was observed. It was only able to identify all adulterated samples in the case of unpackaged veal sausage. In the plastic packaged samples, veal meat adulterations could only be identified from 20% upwards. The results were even less precise for adulteration with pork fat. While in this case an adulteration from 20% upwards was identified for the unpackaged sample, only 40% fat adulteration and higher could be detected in the packaged sample (Schmutzler et al., 2015). Thus, the best "through the packaging" results were obtained with the industrial setup. The measurement with the inexpensive handheld spectrometer - which would be
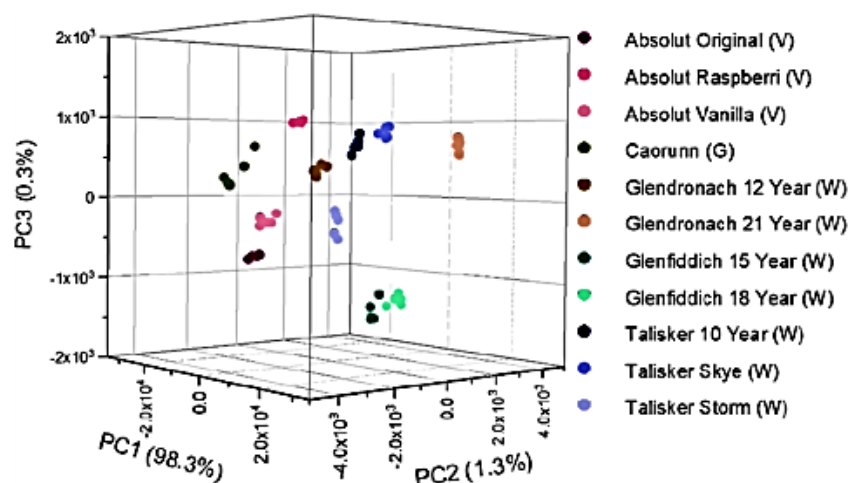
9

Fig. 9. Principal component analysis of different spirits, measured with an axicon-based Raman measurement setup (G=gin, V=vodka, W=whisky) (Fleming et al., 2020).

most useful for an application e.g. in the retail trade, was significantly less precise. The investigation of adulterations below 10% was not carried out, which would have been important to provide information about the detection limits. Therefore, for this application, further research must be conducted to improve the statistical basis, especially because the measurement quality and reproducibility are subject to many natural variations, such as the homogeneity of the matrix, the age of the meat, the feeding conditions or the nutrient composition (Schmutzler et al., 2016).

3.3.2. Moisture

There are different analytical methods to determine food moisture. One very common method is the sea sand method (Matissek, Steiner, & Fischer, 2010). Much faster are moisture analyzers, with an integrated heating and weighing device (Melcher, Pertsch, Spannagel, & Oldendorf, 1991). However, there is also the obvious disadvantage that the sample must be unpackaged and ground before the measurement. Non-destructive measurement systems in the VIS and IR range for the determination of moisture in food or food packaging are not common yet.

Novo et al. tried to implement a non-destructive measurement method in 2016 by using NIR to investigate the moisture of oregano. To make sure that the packaging did not affect the measurement, unpackaged and subsequently packaged oregano leaves as well as the empty packaging material was measured, using both, a diffuse transmittance and reflectance mode. As the moist leaves showed peaks at 1440 and 1920 nm in contrast to the dry ones, these were defined as "water" peaks – what agrees well with the literature that mentions absorptions for water in that area (Curcio & Petty, 1951). The measurement of the two-layer packaging film (polyethylene terephthalate 12 µm and polyethylene 90 µm) showed transmission of about 90% at the corresponding wavelengths, which is why only minor deviations have been detected compared to the unpackaged samples (Mendes Novo et al., 2016). That study shows that a non-destructive optical measurement system might be useful for the determination of moisture in packaged food, but more research has to be done, as the absorption wavelength might differ between products or absorption by other ingredients may overlap the signal. A simple approach e.g. would be the indirect measurement of the headspace atmosphere, as the water vapor partial pressure can be correlated with the water content of the packaged product via its sorption isotherm.

3.4. Raman spectroscopy

Comparable to IR spectroscopy, Raman is mostly used for the direct identification of product attributes (Ellis et al., 2018; Fleming et al., 2020; Kiefer & Cromwell, 2017; Qin et al., 2017), but an indirect identification of the headspace atmosphere through the packaging would be possible as well.

3.4.1. Adulteration

Food adulteration in already packaged products can also be examined via Raman spectroscopy, for example for the detection of fake spirits (Ellis et al., 2017, 2018; Fleming et al., 2020; Lohumi et al., 2018) or butter adulteration (Lohumi et al., 2018). Spirits are, for example, often adulterated with methanol, which can be a health risk for the consumer (Aylott, 2013). Several earlier studies chose among others 785 nm as excitation wavelength for the detection of ethanol or methanol in alcoholic beverages (Cleveland et al., 2007; Nordon et al., 2005; Xu, Ye, Cai, & Qu, 2010), but the use of a wavelength in the VIS-NIR transition range has the disadvantage that the transilluminated glass bottles may exhibit intrinsic fluorescence, leading to disturbance of the Raman signal. One way to solve this problem is to use a wavelength which has a low or no fluorescence contribution (Ellis et al., 2018), or to choose a measuring and evaluation set up, which reduces the unwanted effects to a minimum (Ellis et al., 2017; Fleming et al., 2020). Ellis et al. tried both. A hand-held SORS Raman spectrometer with an excitation wavelength at 830 nm on one side (Ellis et al., 2017) was used. On the other side, they tested a conventional hand-held Raman spectrometer that works at 1064 nm and scanning a spectral range of $400 – 2300$ cm^{-1} (Ellis et al., 2018). With both methods, they were able to cluster commercial glass bottled spirits, after spiking them with methanol amounts between 0% and 3 (Ellis et al., 2017) resp. 5% (Ellis et al., 2018) using a PCA (principal component analysis) plot. For the SORS-based method however, it became clear that colored bottles (green and brown), led to very high interference of the relevant peaks, due to their self-fluorescence, despite the SORS setup (Ellis et al., 2017). The conventional Raman spectrometer with the higher wavelength was a bit more successful, as only the brown bottled samples were difficult to be evaluated. They absorbed a part of the laser light, which significantly disturbed the Raman signal (Ellis et al., 2018). Methanol bands were detected at 1023 (Ellis et al., 2017) or 1030 cm^{-1} (Ellis et al., 2018). They were used for the model creation. Another way to minimize the backscattering signal was employed by Fleming et al. in 2020. They

10

decided to use a very complex measuring setup to measure ethanol concentrations in spirits, in which - similar to the SORS method - the excitation laser beam is focused with an axicon lens to an inner zone of the sample in a ring shape and not to a single point on its surface. The advantage that the researchers expected from this setup is that the origin of the detected signal can be fixed to an area within the container and is less disturbed by the scattering effects of the container glass. The wavelength of the excitation source was set to the above-mentioned 785 nm and the Raman spectra were obtained at shifts between 800 and 1800 cm^{-1}, as the ethanol peak is visible at 881 and the glass peak at 1370 cm^{-1}. This setup was additionally compared with a SORS system using the same wavelength. The axicon-based system showed a significant lower glass-induced offset compared to the SORS method. Additionally, a PCA cluster with eleven different spirits measured with the axicon-based setup was done, comparing the spectral features with the highest variance. Thus, they were able to create a cluster that sorts aromatic components, spirit types and aging into different groups, as seen in Fig. 9.

Using this cluster, a contamination of these sorts e.g. with foreign spirits or methanol could be identified very probably (Fleming et al., 2020). On the contrary, Kiefer & Cromwell tried to analyze single malt whisky on 2017, but without an optimized Raman measurement as described above. They chose 785 nm as excitation source and worked with a commercial Raman spectrometer. All samples were measured in their original glass bottles, except for those in green bottles, which had to be filled into transparent bottles because the green bottles led to fluorescence interference. They were able to determine the correct alcohol content due to the known ethanol peak at 879 cm^{-1}, and also the differentiation of age and color due to the Raman-specific fingerprint using PCA was possible (Kiefer & Cromwell, 2017). However, sorting by different attributes like distillery or cask-type showed inferior results in the performed PCA plot, which may be due to the non-optimized measurement conditions.

SORS is also suitable for the determination of the adulteration of butter, which is often packaged in partially or completely non-transparent films. For the partially transparent films, this method was successfully used by Lohumi et al. in 2018 (Lohumi et al., 2018). As excitation source, a 785 nm laser was used. By measuring pure butter and margarine, they found different main peaks. Two of them were visible in both samples, at 1442 and 1300 cm^{-1}, and were concluded to be induced by the δ (C–H) scissoring vibration and the C–H twisting vibration of the –CH_2 group of the fatty acids. Margarine showed additionally a clear peak at 1268 cm^{-1} associated with the δ (C–H) bending vibration at the *cis* double bond in R–HC=CH–R, which is more present in that fat. For the calibration of the measurement setup, they mixed butter with different concentrations of margarine and covered the samples with commercial butter packaging-films. Afterwards, a screening of commercial butter and margarine was made. It was shown that the measuring setup was able to identify the butter-margarine-concentration very accurately, if the butter was packaged in plastic packaging. One issue for the measuring system is that butter is often packaged in aluminum foil where no optical access is possible.

3.4.2. Identification

Qin et al. combined the SORS technology with a line scan spectral analysis, for the identification of cane sugar beneath a colored plastic container. For the experiment, a 1 mm thick square plastic sheet (polymer not mentioned) was cut from the original cane sugar container and placed on top of the nickel container filled with cane sugar to simulate a "through the pack" application. For the excitation, they used a monochromatic laser at 785 nm, and the Raman shift was investigated between 0 and 2815 cm^{-1}. As they identified a main peak at 531 cm^{-1} for the pure cane sugar and a peak at 1438 cm^{-1} for the pure plastic, they were well able to distinguish the resulting peaks in the combined SORS setup (Qin et al., 2017). However, a strong noise was present between

the two main peaks, which made it possibly difficult to distinguish a third component – e.g. in case of adulteration. In addition, the sample was strongly adapted to the measurement setup, as the sample was filled into a nickel container, which is characterized by low Raman and fluorescence signals on one hand, and the plastic sheet was plane instead of rounded on the other hand, what may affect the results as well for a real application.

3.5. Simple color measurement

A simple way to characterize product changes is the measurement of the visible product color. Here, changes can be induced e.g. due to enzyme activity, oxidation processes, fouling or even microbiological spoilage (Belitz et al., 2008). However, not much research has been done regarding non-destructive measurements in already packaged foods. One reason therefore might be, that the packaging material tends to reflect during image acquisition and could falsify the results (Cavallo et al., 2018).

3.5.1. Color change induced by enzyme activity

In a recent study, Cubeddu et al. tried to evaluate the color change of Apple Juice pre-treated with high pressure over a storage time of 28 days, bottled in PLA and PET. To obtain information about the color change, they measured the L*a*b* values with a portable colorimeter during this time through the plastic. Indeed, the brightness increased significantly during storage, as well as the overall color variation ΔE in a similar way for both packaging types. The authors concluded that the high-pressure procedure did not inactivate those enzymes responsible for the color change (e.g. polyphenol oxidase) strongly enough (Cubeddu et al., 2021).

3.5.2. Freshness

In 2018, Cavallo et al. used the CIE L*a*b* color space, combined with a machine learning program based on convolutional neural networks for the freshness evaluation of salad leaves. For this purpose, images via a computer vision system (CVS) and a digital camera were taken. In addition, a color correction with a standardized color chart was done. The computer learning program was trained to distinguish between packaging, artifact (e.g. reflection) of the packaging and product. They also defined various quality characteristics, depending on the degree of freshness or rottenness, which was additionally correlated with the measured ammonia content. For the quality level characterization, relevant pixels from the image of the product) were converted into the CIE L*a*b* color space, whereas L* was excluded due to its sensitivity to reflections, a* and b* were used for a histogram, that was correlated with the ammonia contents and therefore the defined quality levels. Actually, the network was able to classify the products to the defined quality stage in 83% of cases for the packaged and 86% for the unpackaged samples (Cavallo et al., 2018).

3.6. Tunable diode laser spectroscopy (TDLAS)

As already mentioned in 2.6, these kinds of systems are used for measuring gas concentrations, and are therefore indirect measurement systems.

3.6.1. Packaging integrity

For the measurement, either the transmitted or scattered light can be used, depending on the sample or measuring set up. A research team led by Cocola et al. did extensive research in this field, resulting in several publications and a patent application in recent years (Cocola et al., 2015, 2016, 2017, 2018; Forestelli & Frazzi, 2019):

In 2015, they tested a measurement setup, in which the laser was led through the lid film of a food tray, and either the scattered light of the tray bottom or the hit food was measured. For the oxygen determination, the wavelength at 761 nm was chosen.
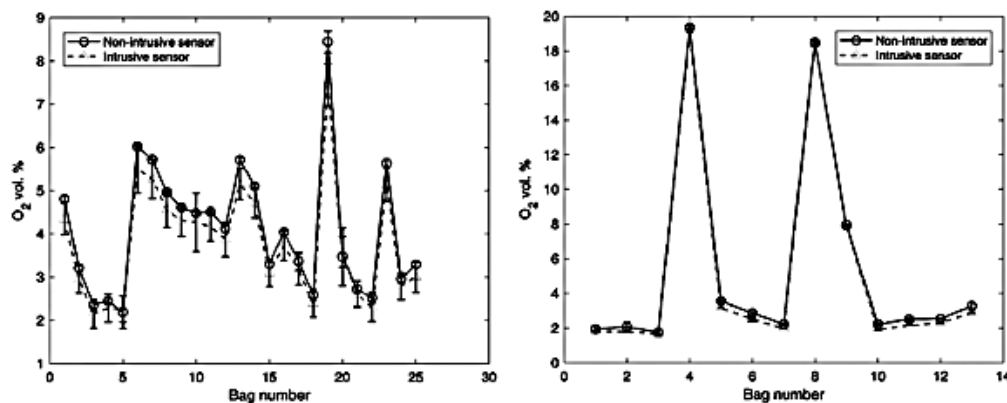
Fig. 10. Comparison of oxygen concentrations in flow-bags after the packaging process measured with an invasive and a non-invasive TDLAS sensor (offline sensor: left; online sensor: right) (Cocola et al., 2018).

The quality of the measurement results was highly dependent on the chosen measuring point. The accuracy was lower when the measurement point was selected directly on the product itself. Here, e.g. roughness or glossy effects (e.g. in case of strong humidity) led to more inaccurate results. The measurement on the tray bottom led to better results in this case. With a measuring accuracy between 0.2% and 0.6% at low oxygen amounts (~0–5%), it would be a good and uncomplicated measuring device for the control of nitrogen or carbon dioxide flushed samples, but measuring higher oxygen amounts is also thinkable (Cocola et al., 2015). The potential of the backscattering mode was again confirmed in another publication, but the measuring quality was once again highly dependent on the product surface (Cocola et al., 2017).

In the following publications, they also focused on applications in the transmission mode. Special attention was paid to an "in line" application, for determining the oxygen content in white semi-transparent flow bags filled with pre-cut mozzarella. Since the oxygen content ($\leq 10\%$ (v/v)) was the parameter to be measured, an approx. wavelength of 760 nm was again selected. In this specific setup, the bag was placed in a sample holder, and the measurement point was on the upper side of the bag, where there was no product. The sensor and detector were placed opposite each other while the sample was pressed between them. They compared the two measuring setups against each other. The offline measuring setup consisted exclusively of the measuring unit. The samples were inserted manually so that no slippage was possible. These measurement results served to validate the online setup. Basically, the online setup was an extension in which the measuring unit was integrated into the flow-bag packaging system immediately after the packaging step. A trap door mechanism was installed for the removal of non-conforming bags. For both, the online and the offline setup, several bags were packed and the oxygen amount was measured, first with the non-destructive and afterwards with an intrusive measurement system that works with an electrochemical zirconium dioxide sensor (CheckMate 9900). It became clear that the oxygen amounts in the various bags showed no significant difference between the destructive and the non-destructive systems (Cocola et al., 2016, 2018). Fig. 10 illustrates these results exemplarily. The big deviations of the oxygen content between the individual packages were presumably product-related, since both measuring methods were able to record similar oxygen values here as well (Cocola et al., 2018).

Beside this application, they also tested the measuring principle with other packaging types: transparent flow bag (PA/PE), PA/PE-based flow bag with one transparent and one colored side, a transparent PET tray and colored PP yoghurt packages. For the flow-bags, good accuracies comparable to the invasive measurements were achieved (deviation: 0.2 vol% O_2), the others were negatively influenced by their round

geometry. Here, an adaptation of the measurement technique would have to take place (Cocola et al., 2016, 2017).

Therefore, they concluded that the method is well suited for detecting oxygen non-destructively in closed packages, even for packaging with reduced light transmission, e.g. from translucent packaging.

3.6.2. Spoilage

A more reliable way to determine spoilage or microbial growth is to measure the metabolic products. As microorganisms respirate e.g. oxygen to carbon dioxide, the change of the gas atmosphere in the head space of a sample might be a good way to provide information about the degree of spoilage (Höll et al., 2016; Kolbeck, Reetz, Hilgarth, & Vogel, 2019). As described in Chapter 2.6, the TDLAS measurement is suitable for oxygen measurement in semi-transparent packaging systems. In 2017, Li et al. tried to apply the method to measure oxygen at 760 nm in milk cartons consisting of a translucent polymer-paper-polymer laminate. As the packaging leads to strong laser scattering, they used a special application of the TDLAS method, namely the so-called GASMAS method. This variant does not directly apply the Lambert-Beer's law, but rather an equation, which includes a so-called equivalent mean path length (L_{eq}), that expresses the path length of the light through a medium and/or packaging. There are different ways to measure or calculate that path length (Lewander, 2010; Zhang, Huang, Li, Svanberg, & Svanberg, 2015), but they are not further described in the paper (Li et al., 2017). However, for the calculation, they perforated some packages to obtain the L_{eq} at 20% oxygen. This allowed them to relate the path length at unknown and known (20%) O_2 concentration at constant absorbance and thus calculate the oxygen content. Hence, they were able to measure the development of the oxygen amount in the headspace of the milk packaging under different storage conditions. Their results show that the oxygen amount of the samples stored at room temperature decreased significantly (Li et al., 2017), which could be a sign for microbiological activity. However, it is unclear how precise the measuring method is, as no control measurement with a destructive measurement system took place. It is certainly conceivable that the scattering effects lead to high imprecision. Using a transparent or semi-transparent material for the detection is certainly more sensible from a technical measurement point of view. Furthermore, more correlation factors – e.g. microbiological growth – should be determined. To make a statement about the yeast induced spoilage in milk-based beverages and yoghurts by monitoring the gas atmosphere through a packaging was the basis for two studies done by Danilovic et al. in 2016 and 2018. For the CO_2 determination, the absorption band around 2 μm was used (Danilović et al., 2018). They were indeed able to determine for both, yeast inoculated milk-based beverages (Danilovic et al., 2016)

12

69

and yoghurts, (Danilović et al., 2018) an increase of CO$_2$ with the simultaneous yeast increase. More specifically, the CO$_2$ amount in the headspace of the samples increased from $\leq$ 5% to $\geq$ 20%, while reaching yeast amounts of 10^6 CFU/mL (start: $\leq$ 10^2 CFU/mL) (Danilovic et al., 2016; Danilović et al., 2018).

4. Conclusions

There are promising approaches for the non-destructive quality control of filling goods through the packaging material in the field of food and packaging research. All presented methods have advantages and disadvantages, which are also highly product specific.

A distinction was made between *direct* determination on the product surface or in liquids and *indirect* determination via the headspace of the packaging.

The **fluorescence-based** measurement systems (spectral analysis and quenching) are useful in both ways, the direct and indirect quality determination. For the *direct* determination, the spectral analysis with a fluorometer or the insertion of sensor material on the bottle wall of liquid products are possible. Using a fluorometer to gain an emission spectrum is not so broadly represented – only one publication for the period of the last six years was found (Hossain et al., 2019). Probably, spectroscopic measurements using IR or Raman are more suitable here. This could be related to the intrinsic fluorescence of packaging, for example.

The insertion of fluorophores into the packaging with direct food contact for the quenching- based method also needs specific migration tests to ensure food safety, which could be a reason for the likewise low application in this area. Here, too, there was only one publication (Sikorska et al., 2019). This is also a point that must be considered when integrating sensor material for *indirect* determination in the headspace. However, there is considerably more literature on this. All the literature found used oxygen as a quencher for quality determination. However, the decrease of oxygen content as a measure for a primarily preceding reaction - e.g. photoinduced oxidation processes - can only be determined in connection and correlation with other measuring methods. If this is done product-specifically, the oxygen content could be used as a simple and fast measurement. In the case of packaging quality, for example, after the packaging process under modified atmosphere, no further correlation is necessary and the method is well suitable.

Hyperspectral imaging has the big advantage that it can use different spectral analytical techniques – fluorescence, IR, Raman and VIS-based. To the best of our knowledge, only *direct* product evaluation was done through the packaging yet a wide range of quality characteristics could be assessed (cf. Table 1). HSI is usually associated with a very complex and partially obscure evaluation procedure and very often, the results are strongly product- specific and have to be correlated with the searched quality attribute. That might be problematic, especially when it comes to changes in the measurement conditions or product-specific, natural variations. From an authors' point of view, HSI has a high potential for the non-invasive quality characterization of packaged food, but it would be helpful to include factors that are easy to apply so that a transfer to other product groups or measurement setups are possible.

Infrared- and Raman-based spectroscopic measurements have a broad applicability, as they are able to identify substances, on the one hand, and to quantify them on the other hand. Both systems have so far only been used for *direct* determination on the product surface, even though they would work for both. Therefore, they could be taken together for the quantification of almost all quality characteristics. One issue here might be the overlap of peaks for different substances (Qin et al., 2017) or the limitations due to absorption, scattering or reflectance effects. That is especially an issue for glass bottles (Ellis et al., 2017, 2018). A possible way to avoid this problem is the use of a SORS (Ellis et al., 2017) or SORS–based application (Fleming et al., 2020), that measures the scattered light locally shifted to the excitation zone. Compared to the methods described so far, a less complex evaluation is

Table 3

Comparison of optical measurement systems in terms for complexity of application or setup, usability and equipment or application costs.

Measurement System	Complexity	Usability	Total costs
Fluorescence Spectral Analysis	+	++	+
Fluorescence Quenching	++	++	++
Hyperspectral Imaging	+++	+	++
Infrared Spectroscopy	+	++	+
Raman Spectroscopy	+	+++	++
Color Measurements	+	++	+
TDLAS	++	++	++

usually necessary.

Simple color measurements - which, of course, can only be measured *directly* on the product - have so far played a rather minor role in non-destructive quality evaluation of packaged food. However, publications such as the one by Cavallo et al. (2018) show that there is a very high potential here, especially in combination with machine learning programs. Though it must be said at this point that only a limited type of quality impairments, such as rot, could be determined with this. Nevertheless, there is also the risk that complex conversion methods (e. g. convolutional neural networks) are used for the evaluation, which could result in problems similar to those already discussed for the HSI method.

TDLAS enables the *indirect* measurement of absorption bands, which are usually very weak (e.g. the oxygen band at 760 nm), and therefore offers a good complement to the other spectroscopic methods. Especially the oxygen headspace determination in different packages is already well studied (e.g. Cocola et al., 2015, 2018). However, a problem similar to the oxygen determination by quenching exists here, as the gas concentration has to be correlated with a quality attribute – unless the packaging integrity is the investigated parameter.

Table 3 shows a tentative qualitative comparison of the different measurement methods in terms of their complexity in application or setup, handling and applicability for different products and packaging materials ("usability"), and assumed cost of equipment and/or application ("total costs"). But here, too, a generally valid statement is not possible, since there is inhomogeneity in complexity, usability and costs even within the same measurement principle, as shown, for example, in the study of Schmutzler et al. (2016).

In summary, it can be said that there is no "method of choice" for every product or quality attribute. It has to be carefully considered which quality aspect should be determined and what kind of application should take place. In particular, the measurement of a degradation product often has the disadvantage that the result has to be correlated with the investigated quality attribute. From a consumer or retail point of view, a fast and easy way to handle measuring method would be preferable. Complex chemometric conversions might be difficult here, as a deviation from the defined standards are difficult to interpret. For quality control during production or research, more complex and expensive measurement systems are conceivable.

Acknowledgment

Declaration of Competing Interest

The authors declare no conflict of interest.

13

70

References

Atkins, P.W. , & Paula, D.J. (2013), 63, 568, 6. Physikalische Chemie (5th ed.). WILEY-VCH Verlag GmbH & Co. KGaA.

Aylott, R. (2013). Analytical strategies supporting protected designations of origin for alcoholic beverages. In *Comprehensive analytical chemistry. food protected designation of origin - methodologies and applications* (Vol. 60, pp. 409–438). Elsevier. https://doi.org/10.1016/B978-0-444-59562-1.00016-5

Baier, J. (2005). Lumineszenz-Untersuchungen zur Generierung und Relaxation von Singulett-Sauerstoff in zellulärer Umgebung [Dissertation]. Universität Regensburg, Regensburg.

Banerjee, S., Arzhakova, O. V., Dolgova, A. A., & Papkovsky, D. B. (2016). Phosphorescent oxygen sensors produced from polyolefin fibres by solvent-crazing method. *Sensors and Actuators B: Chemical, 230*, 434–441. https://doi.org/10.1016/j.snb.2016.02.062

Belitz, H.-D., Grosch, W., & Schieberle, P. (2008). *Lehrbuch der Lebensmittelchemie* (6th ed.). Springer-Verlag Berlin Heidelberg GmbH.

Birngruber, C., Ramsthaler, F., Heidorn, F., & Verhoff, M. A. (2009). Spectral imaging. *Rechtsmedizin, 19*(3), 157–161. https://doi.org/10.1007/s00194-009-0592-5

Böcker, J. (2014). Spektroskopie: Instrumentelle Analytik mit Atom- und Molekülspektrometrie (1st ed.). LaborPraxis. Vogel Buchverlag. (https://ebookcentral.proquest.com/lib/gbv/detail.action?docID=1651435).

Botelho, B. G., Reis, N., Oliveira, L. S., & Sena, M. M. (2015). Development and analytical validation of a screening method for simultaneous detection of five adulterants in raw milk using mid-infrared spectroscopy and PLS-DA. *Food Chemistry, 181*, 31–37. https://doi.org/10.1016/j.foodchem.2015.02.077

Buchner, N. (1999). *Verpackung von Lebensmitteln: Lebensmitteltechnologische, verpackungstechnische und mikrobiologische Grundlagen.* Springer-Verlag Berlin Heidelberg GmbH.

Cavallo, D. P., Cefola, M., Pace, B., Logrieco, A. F., & Attolico, G. (2018). Non-destructive automatic quality evaluation of fresh-cut iceberg lettuce through packaging material. *Journal of Food Engineering, 223*, 46–52. https://doi.org/10.1016/j.jfoodeng.2017.11.042

Chang, C.-I. (2003). Hyperspectral imaging: Techniques for spectral detection and classification.

Church, I. J., & Parsons, A. L. (1995). Modified atmosphere packaging technology: A review. *Journal of the Science of Food and Agriculture, 67*, 143–152.

Cleveland, D., Carlson, M., Hudspeth, E. D., Quattrochi, L. E., Batchler, K. L., Balram, S. A., … Michel, R. G. (2007). Raman spectroscopy for the undergraduate teaching laboratory: Quantification of ethanol concentration in consumer alcoholic beverages and qualitative identification of marine diesels using a miniature Raman spectrometer. *Spectroscopy Letters, 40*(6), 903–924. https://doi.org/10.1080/00387010701525638

Cocola, L., Allermann, H., Fedel, M., Sønderby, S., Tondello, G., Bardenstein, A., & Poletto, L. (2016). Validation of an in-line non-destructive headspace oxygen sensor. *Food Packaging and Shelf Life, 9*, 38–44. https://doi.org/10.1016/j.fpsl.2016.05.007 (Fig. 1 reprinted with permission of Elsevier).

Cocola, L., Fedel, M., Poletto, L., & Tondello, G. (2015). Laser spectroscopy for totally non-intrusive detection of oxygen in modified atmosphere food packages. *Applied Physics B: Lasers and Optics, 119*, 37–44.

Cocola, L., Fedel, M., Tondello, G., & Poletto, L. (2017). A modular approach of different geometries for non-invasive oxygen measurement inside moving food packages. *Packaging Technology and Science, 30*(4), 159–170. https://doi.org/10.1002/pts.2292

Cocola, L., Fedel, M., Tondello, G., Frazzi, G., Poletto, L., Bardenshtein, A., … Landa, S., & Allermann, H. (2018). Design and evaluation of an in-line system for gas sensing in flow-packed products. *Food Packaging and Shelf Life, 17*, 91–98. https://doi.org/10.1016/j.fpsl.2018.06.006 (Fig. 9 & 11 reprinted with permission of Elsevier)).

Cubeddu, A., Fava, P., Pulvirenti, A., Haghighi, H., & Licciardello, F. (2021). Suitability assessment of PLA bottles for high-pressure processing of apple juice. *Foods.* https://doi.org/10.3390/foods10020295

Curcio, J. A., & Petty, C. C. (1951). The near infrared absorption spectrum of liquid water. *Journal of the Optical Society of America, 41*(5), 302. https://doi.org/10.1364/josa.41.000302

Danilovic, B., Cocola, L., Fedel, M., Poletto, L., & Savic, D. (2016). Formation and Cumulation of CO2 in the Bottles of the Fermented Milk Drinks. IPCBEE, 95, 26–31.

Danilović, B., Savić, D., Cocola, L., Fedel, M., & Poletto, L. (2018). Determination of CO 2 content in the headspace of spoiled yogurt packages. *Journal of Food Quality, 2018*, 1–6. https://doi.org/10.1155/2018/8121606

Darnay, L., Králik, F., Oros, G., Koncz, Á., & Firtha, F. (2017). Monitoring the effect of transglutaminase in semi-hard cheese during ripening by hyperspectral imaging. *Journal of Food Engineering. 196*, 123–129. https://doi.org/10.1016/j.jfoodeng.2016.10.020

Ellis, D. I., Muhamadali, H., Xu, Y., Eccles, R., Goodall, I., & Goodacre, R. (2018). Rapid through-container detection of fake spirits and methanol quantification with handheld Raman spectroscopy. *The Analyst, 144*(1), 324–330. https://doi.org/10.1039/c8an01702f

Ellis, D. I., Eccles, R., Xu, Y., Griffen, J., Muhamadali, H., Matousek, P., … Goodacre, R. (2017). Through-container, extremely low concentration detection of multiple chemical markers of counterfeit alcohol using a handheld SORS device. *Scientific Reports, 7*(1), 12082. https://doi.org/10.1038/s41598-017-12263-0

Escobedo Araque, P., Perez de Vargas Sansalvador, I. M., Lopez Ruiz, N., Erenas, M. M., Carvajal Rodriguez, M. A., & Martinez Olmos, A. (2018). Non-invasive oxygen determination in intelligent packaging using a smartphone. *IEEE Sensors Journal, 18* (11), 4351–4357. https://doi.org/10.1109/JSEN.2018.2824404

FAO. (2011). *Global food losses and food waste - Extent, causes and prevention.*

Fleming, H., Chen, M., Bruce, G.D., & Dholakia, K. (2020, May 27). Through-Bottle Whisky Sensing and Classification using Raman Spectroscopy in an Axicon-Based Backscattering Configuration. Permission rights: (https://creativecommons.org/licenses/by/3.0/. http://arxiv.org/pdf/2005.13538v1).

Forestelli, F., & Frazzi, G. (2019). Non-destructive measurement unit of the gas concentration in sealed flexible containers and automatic filling and/or packaging line using such a unit(US2019/0113465).

Franke, C., & Beauchamp, J. (2017). Real-time detection of volatiles released during meat spoilage: a case study of modified atmosphere-packaged chicken breast fillets inoculated with Br. thermosphacta. *Food Analytical Methods, 10*, 310–319.

GEA Group Aktiengesellschaft. (2021). GEA LeakCheck & OxyCheck [Fully integrated monitoring of oxygen content and leakage]. (https://www.gea.com/de/products/filling-packaging/thermoforming/gea-leakcheck-oxycheck.jsp).

Gibis, D., Sängerlaub, S., & Müller, K. (2015). Modified atmosphere packaging: Potential cost savings for plastic food packaging. *Kunststoffe International, 8*, 18–22.

Goetz, A. F., Vane, G., Solomon, J. E., & Rock, B. N. (1985). Imaging spectrometry for Earth remote sensing. *Science, 228*(4704), 1147–1153. https://doi.org/10.1126/science.228.4704.1147

Grau, R., Sánchez, A. J., Girón, J., Iborra, E., Fuentes, A., & Barat, J. M. (2011). Nondestructive assessment of freshness in packaged sliced chicken breasts using SW-NIR spectroscopy. *Food Research International, 44*(1), 331–337. https://doi.org/10.1016/j.foodres.2010.10.011

Gruber, F., Grählert, W., Wollmann, P., & Kaskel, S. (2019). Classification of black plastics waste using fluorescence imaging and machine learning. *Recycling, 4*(4), 40. https://doi.org/10.3390/recycling4040040 (Permission rights: (http://creativecommons.org/licenses/by/4.0/)).

Guamis, B., Trujillo, A. J., Ferragut, V., Chiralt, A., Andres, A., & Fito, P. (1997). Ripening control of Manchego type cheese salted by brine vacuum impregnation. *International Dairy Journal, 7*(2–3), 185–192. https://doi.org/10.1016/S0958-6946(97)00002-2

Guzmán, E., Baeten, V., Pierna, J. A. F., & García-Mesa, J. A. (2015). Evaluation of the overall quality of olive oil using fluorescence spectroscopy. *Food Chemistry, 173*, 927–934. https://doi.org/10.1016/j.foodchem.2014.10.041

Hahne, J. (2015, May 2). Multi Online NIR in Oil Seed Extraction. World Congress on Oils & Fats.

Havens, M.R., Austin, D.C., & Paul, D.J. (2007). Method and Apparatus for Measuring Oxygen Concentration(WO2007/106776 A1).

Heiss, R., & Eichner, K. (1995). Haltbarmachen von Lebensmitteln: Chemische, physikalische und mikrobiologische Grundlagen der Verfahren (Dritte, überarbeitete und erweiterte Auflage). Springer Berlin Heidelberg. (https://doi.org/10.1007/978-3-662-07664-4).

Henihan, L. E., O'Donnell, C. P., Esquerre, C., Murphy, E. G., & O'Callaghan, D. J. (2018). Quality assurance of model infant milk formula using a front-face fluorescence process analytical tool. *Food and Bioprocess Technology, 11*(7), 1402–1411. https://doi.org/10.1007/s11947-018-2112-7

Heuft, B., & Polster, W. (2006). Device for Examining Filled Containers by Means of X-Rays and use of this Device(US007106827).

Höll, L., Behr, J., & Vogel, R. F. (2016). Identification and growth dynamics of meat spoilage microorganisms in modified atmosphere packaged poultry meat by MALDI-TOF MS. *Food Microbiology, 60*, 84–91.

Hood, D. E., & Riordan, E. B. (1973). Discolouration in pre-packaged beef: Measurement by reflectance spectrophotometry and shopper discrimination. *International Journal of Food Science and Technology, 8*, 333–343.

Hossain, M.A., Canning, J., & Yu, Z. (2019). Fluorescence-based determination of olive oil quality using an endoscopic smart mobile spectrofluorimeter. *IEEE Sensors Journal.*

Huber, C. (2008). Wie viel kommt durch? Ermittlung der Sauerstoffdurchlässigkeit von PET-Flaschen. *Getränkeindustrie, 11*, 48–57.

Ivorra, E., Sánchez, A. J., Verdú, S., Barat, J. M., José, M., & Grau, R. (2016). Shelf life prediction of expired vacuum-packed chilled smoked salmon based on a KNN tissue segmentation method using hyperspectral images. *Journal of Food Engineering, 178*, 110–116. https://doi.org/10.1016/j.jfoodeng.2016.01.008

Jaiswal, P., Jha, S. N., Borah, A., Gautam, A., Grewal, M. K., & Jindal, G. (2015). Detection and quantification of soymilk in cow-buffalo milk using Attenuated Total Reflectance Fourier Transform Infrared spectroscopy (ATR-FTIR). *Food Chemistry, 168*, 41–47. https://doi.org/10.1016/j.foodchem.2014.07.010

Jameson, D.M. (Ed.). (2003). Methods in Enzymology. Biophotonics, Part A. Fig. 3 reprinted with permission of Elsevier. Elsevier.

Kammerlehner, J. (2015). Käsetechnologie (3., überarb. u. erw. Aufl.). Kammerlehner.

Kelly, C. A., Santovito, E., Cruz-Romero, M., Kerry, J. P., & Papkovsky, D. P. (2020). Application of O2 sensor technology to monitor performance of industrial beef samples packaged on three different vacuum packaging machines. *Sensors and Actuators B: Chemical, 304*, Article 127338. https://doi.org/10.1016/j.snb.2019.127338

Kelly, C., Yusufu, D., Okkelman, I., Banerjee, S., Kerry, J. P., Mills, A., & Papkovsky, D. B. (2020). Extruded phosphorescence based oxygen sensors for large-scale packaging applications. *Sensors and Actuators B: Chemical, 304*, Article 127357. https://doi.org/10.1016/j.snb.2019.127357

Kerry, J. P., O'Grady, M. N., & Hogan, S. A. (2006). Past, current and potential utilisation of active and intelligent packaging systems for meat and muscle-based products: A review. *Meat Science, 74*, 113–130.

Kiefer, J., & Cromwell, A. L. (2017). Analysis of single malt Scotch whisky using Raman spectroscopy. *Analytical Methods, 9*(3), 511–518. https://doi.org/10.1039/c6ay02907h

Koca, N., Kocaoglu-Vurma, N. A., Harper, W. J., & Rodriguez-Saona, L. E. (2010). Application of temperature-controlled attenuated total reflectance-mid-infrared

(ATR-MIR) spectroscopy for rapid estimation of butter adulteration. *Food Chemistry, 121*(3), 778–782. https://doi.org/10.1016/j.foodchem.2009.12.083

Kolbeck, S., Reetz, L., Hilgarth, M., & Vogel, R. F. (2019). Quantitative oxygen consumption and respiratory activity of meat spoiling bacteria upon high oxygen modified atmosphere. *Frontiers in Microbiology, 10*, 2398.

Kongbonga, Y. G. M., Ghalila, H., Onana, M. B., Majdi, Y., Lakhdar, Z. B., Mezlini, H., & Sevestre-Ghalila, S. (2011). Characterization of vegetable oils by fluorescence spectroscopy. *Food and Nutrition Sciences, 02*(07), 692–699. https://doi.org/10.4236/fns.2011.27095

Krämer, J. (2010). Lebensmittelmikrobiologie. In W. Frede (Ed.), *Handbuch für Lebensmittelchemiker: Lebensmittel, Bedarfsgegenstände, Kosmetika, Futtermittel* (3rd ed., pp. 509–526). Springer-Verlag.

Krottmaier, J., & Ribitsch, V. (2015). Measurement of the Fluorescence of an Idicator in a Gas-Tight Packaging, which Contains Products Having Limited Storage Time (WO2015/172166 A1).

Kuswandi, B., & Murdyaningsih, E. A. (2017). Simple on package indicator label for monitoring of grape ripening process using colorimetric pH sensor. *Journal of Food Measurement and Characterization, 11*, 2180–2194.

Lackner, M. (2007). Tunable diode laser absorption spectroscopy (TDLAS) in the process industries– a review. *Reviews in Chemical Engineering, 23*(2), 65–147.

Lakowicz, J.R. (2006). Principles of Flourescence Spectroscopy (3rd ed.). Springer Science+Business Media, LLC.

Lee, K., Park, H., Baek, S., Han, S., Kim, D., Chung, S., … Seo, J. (2019). Colorimetric array freshness indicator and digital color processing for monitoring the freshness of packaged chicken breast. *Food Packaging and Shelf Life, 22*, Article 100408 (Article).

Lewander, M. (2010). Laser Absorption Spectroscopy of Gas in Scattering Media [Doctoral Thesis]. Lund University, Lund.

Li, T., Lin, H., Zhang, H., Svanberg, K., & Svanberg, S. (2017). Application of tunable diode laser spectroscopy for the assessment of food quality. *Applied Spectroscopy, 71*(5), 929–938. https://doi.org/10.1177/0003702816667515

Lipinski, B., Hanson, C., Lomax, J., Kitinoja, L., Waite, R., & Searchinger, T. (2013). Reducing food loss and waste. *World Resources Institute Working*, 1–40.

Loeffen, P. W., Maskall, G., Bonthron, S., Bloomfield, M., Tombling, C., & Matousek, P. (2011). Chemical and explosives point detection through opaque containers using spatially offset Raman spectroscopy (SORS). *SPIE Proceedings, Chemical, Biological, Radiological, Nuclear, and Explosives (CBRNE) Sensing XII (80181E)*. SPIE. https://doi.org/10.1117/12.882126

Lohumi, S., Lee, H., Kim, M. S., Qin, J., & Cho, B.-K. (2018). Through-packaging analysis of butter adulteration using line-scan spatially offset Raman spectroscopy. *Analytical and Bioanalytical Chemistry, 410*(22), 5663–5673. https://doi.org/10.1007/s00216-018-1189-1

López-Ruiz, N., Martínez-Olmos, A., Pérez de Vargas-Sansalvador, I. M., Fernández-Ramos, M. D., Carvajal, M. A., Capitan-Vallvey, L. F., & Palma, A. J. (2012). Determination of O2 using colour sensing from image processing with mobile devices. *Sensors and Actuators B: Chemical, 171–172*, 938–945. https://doi.org/10.1016/j.snb.2012.06.007

Lundin, P. (2014). Laser Sensing for Quality Control and Classification – Applications for the Food Industry, Ecology and Medicine [Doctoral Thesis]. Lund University, Lund.

Ly, B. C. K., Dyer, E. B., Feig, J. L., Chien, A. L., & Del Bino, S. (2020). Research techniques made simple: cutaneous colorimetry: A reliable technique for objective skin color measurement. *The Journal of Investigative Dermatology, 140*(1), 3–12.e1. https://doi.org/10.1016/j.jid.2019.11.003 (Fig. 1 reprinted with permission of Elsevier).

Ma, Y. B., Birlouez-Aragon, I., & Amamcharla, J. K. (2019). Development and validation of a front-face fluorescence spectroscopy-based method to determine casein in raw milk. *International Dairy Journal, 93*, 81–84. https://doi.org/10.1016/j.idairyj.2019.02.004

Malle, P., & Tao, S. H. (1987). Rapid quantitative determination of trimethylamine using steam distillation. *Journal of Food Protection, 50*(9), 756–760. https://doi.org/10.4315/0362-028X-50.9.756

Matissek, R., Steiner, G., & Fischer, M. (2010). Lebensmittelanalytik (4th ed.). Springer-Verlag.

Matusiak, M. (2015). Digieye application in cotton colour measurement. *Autex Research Journal, 15*(2), 77–86. https://doi.org/10.2478/aut-2014-0036

Mbesse Kongbonga, Y., Ghalila, H., Majdi, Y., Mbogning Feudjio, W., & Ben Lakhdar, Z. (2015). Investigation of heat-induced degradation of virgin olive oil using front face fluorescence spectroscopy and chemometric analysis. *Journal of the American Oil Chemists' Society, 92*(10), 1399–1404. https://doi.org/10.1007/s11746-015-2704-6

Melcher, F.-J., Pertsch, T., Spannagel, W., & Oldendorf, C. (1991). Device for the Determination of Dry Substance(US5064009).

Mendes Novo, J., Iriel, A., & Lagorio, M. G. (2016). Rapid spectroscopic method to assess moisture content in free and packaged oregano (Origanum vulgare L.). *Journal of Applied Research on Medicinal and Aromatic Plants, 3*(4), 211–214. https://doi.org/10.1016/j.jarmap.2016.08.004

Morsy, M. K., Zor, K., Kostesha, N., Alstrøm, T. S., Heiskanen, A., El-Tanahi, H., … Emneus, J. (2016). Development and validation of a colorimetric sensor array for fish spoilage monitoring. *Food Control, 60*, 346–352.

Nasdala, L., Smith, D.C., Kaindl, R., & Ziemann, M.A. (2004). Raman spectroscopy. In G. Papp, T.G. Weiszburg, A. Beran, & E. Libowitzky (Eds.), Spectroscopic methods in mineralogy (pp. 281–343). Mineralogical Society of Great Britain and Ireland. (https://doi.org/10.1180/EMU-notes.6.7) (Fig. 3 reprinted with permission of EMU).

Nicolson, F., Kircher, M. F., Stone, N., & Matousek, P. (2020). Spatially offset Raman spectroscopy for biomedical applications. *Chemical Society Reviews*. https://doi.org/10.1039/d0cs00855a. Permission rights (https://creativecommons.org/licenses/by/3.0/de/)).

Nielsen, S. S. (2010). *Food analysis*. US: Springer. https://doi.org/10.1007/978-1-4419-1478-1

Nordon, A., Mills, A., Burn, R. T., Cusick, F. M., & Littlejohn, D. (2005). Comparison of non-invasive NIR and Raman spectrometries for determination of alcohol content of spirits. *Analytica Chimica Acta, 548*(1–2), 148–158. https://doi.org/10.1016/j.aca.2005.05.067

O'Callaghan, K. A. M., Papkovsky, D. B., & Kerry, J. P. (2016). An assessment of the influence of the industry distribution chain on the oxygen levels in commercial modified atmosphere packaged cheddar cheese using non-destructive oxygen sensor technology. *Sensors*. https://doi.org/10.3390/s16060916

O'Mahony, F. C., O'Riordan, T. C., Papkovskaia, N., [Natalia], Kerry, J. P., Joe, P., & Papkovsky, D. B. (2006). Non-destructive assessment of oxygen levels in industrial modified atmosphere packaged cheddar cheese. *Food Control, 17*(4), 286–292. https://doi.org/10.1016/j.foodcont.2004.10.013

Oliveira, E. M., de, Leme, D. S., Barbosa, B. H. G., Rodarte, M. P., & Pereira, R. G. F. A. (2016). A computer vision system for coffee beans classification based on computational intelligence techniques. *Journal of Food Engineering, 171*, 22–27. https://doi.org/10.1016/j.jfoodeng.2015.10.009

Pivokonsky, M., Cermakova, L., Novotna, K., Peer, P., Cajthaml, T., & Janda, V. (2018). Occurrence of microplastics in raw and treated drinking water. *The Science of the Total Environment, 643*, 1644–1651. https://doi.org/10.1016/j.scitotenv.2018.08.102

Premanandh, J. (2013). Horse meat scandal – A wake-up call for regulatory authorities. *Food Control, 34*(2), 568–569. https://doi.org/10.1016/j.foodcont.2013.05.033

Qin, J., Kim, M. S., Chao, K., Schmidt, W. F., Dhakal, S., Cho, B.-K., … Huang, M. (2017). Subsurface inspection of food safety and quality using line-scan spatially offset Raman spectroscopy technique. *Food Control, 75*, 246–254. https://doi.org/10.1016/j.foodcont.2016.12.012

Rios-Corripio, M. A., Rios-Leal, E., Rojas-López, M., & Delgado-Macuil, R. (2011). FTIR characterization of Mexican honey and its adulteration with sugar syrups by using chemometric methods. *Journal of Physics: Conference Series, 274*, 12098. https://doi.org/10.1088/1742-6596/274/1/012098

Sahar, A., Boubellouta, T., & Dufour, É. (2011). Synchronous front-face fluorescence spectroscopy as a promising tool for the rapid determination of spoilage bacteria on chicken breast fillet. *Food Research International, 44*(1), 471–480. https://doi.org/10.1016/j.foodres.2010.09.006

Saldaña, E., Siche, R., Huamán, R., Luján, M., Castro, W., & Quevedo, R. (2013). Computer vision system in real-time for color determination on flat surface food. *Scientia Agropecuaria*, 55–63. https://doi.org/10.17268/sci.agropecu.2013.01.06

Schanda, J. (Ed.). (2007). *Colorimetry: Understanding th CIE system*. Wiley. (http://www.loc.gov/catdir/enhancements/fy0739/2007026256-d.html).

Schmutzler, M., Beganovic, A., Böhler, G., & Huck, C. W. (2015). Methods for detection of pork adulteration in veal product based on FT-NIR spectroscopy for laboratory, industrial and on-site analysis. *Food Control, 57*, 258–267. https://doi.org/10.1016/j.foodcont.2015.04.019

Schmutzler, M., Beganovic, A., Böhler, G., & Huck, C. W. (2016). Modern safety control for meat products: Near infrared spectroscopy utilised for detection of contaminations and adulterations of premium veal products. *NIR News, 27*(4), 11–13. https://doi.org/10.1255/nirn.1610

Schymanski, D., Goldbeck, C., Humpf, H.-U., & Fürst, P. (2018). Analysis of microplastics in water by micro-Raman spectroscopy: Release of plastic particles from different packaging into mineral water. *Water Research, 129*, 154–162. https://doi.org/10.1016/j.watres.2017.11.011

Sikorska, E., Wójcicki, K., Kozak, W., Gliszczyńska-Świgło, A., Khmelinskii, I., Górecki, T., … Pasqualone, A. (2019). Front-face fluorescence spectroscopy and chemometrics for quality control of cold-pressed rapeseed oil during storage. *Foods*. https://doi.org/10.3390/foods8120665

Smiddy, M., Papkovskaia, N., Papkovsky, D. B., & Kerry, J. P. (2002). Use of oxygen sensors for the non-destructive measurement of the oxygen content in modified atmosphere and vacuum packs of cooked chicken patties; impact of oxygen content on lipid oxidation. *Food Research International, 35*(6), 577–584. https://doi.org/10.1016/S0963-9969(01)00160-0

Sowoidnich, K., Schmidt, H., Maiwald, M., Sumpf, B., & Kronfeldt, H.-D. (2010). Application of diode-laser raman spectroscopy for in situ investigation of meat spoilage. *Food and Bioprocess Technology, 3*(6), 878–882. https://doi.org/10.1007/s11947-010-0360-2

Steffen, A., Jaindl, R., & Krottmaier, J. (2018). Gas Concentration Measurement with Temperature Compensation(WO2018/202784 A1).

Stokes, G. G. (1852). XXX. On the change of refrangibility of light. *Philosophical Transactions of the Royal Society of London, 142*, 463–562. https://doi.org/10.1098/rstl.1852.0022

Tomazio, N. B., Boni, L. de, & Mendonca, C. R. (2017). Low threshold Rhodamine-doped whispering gallery mode microlasers fabricated by direct laser writing. *Scientific Reports, 7*(1), 8559. https://doi.org/10.1038/s41598-017-09293-z. Permission rights (https://creativecommons.org/licenses/by/4.0/)).

van de Voort, F. R. (1980). Evaluation of milkoscan 104 infrared milk analyzer. *Journal of AOAC International, 63*(5), 973–980. https://doi.org/10.1093/jaoac/63.5.973

Washburn, K. E., Stormo, S. K., Skjelvareid, M. H., & Heia, K. (2017). Non-invasive assessment of packaged cod freeze-thaw history by hyperspectral imaging. *Journal of Food Engineering, 205*, 64–73. https://doi.org/10.1016/j.jfoodeng.2017.02.025

15

Wedler, G. (1997). Lehrbuch der physikalischen Chemie (4., völlig überarb. und erw. Aufl.). Wiley-VCH.

Xu, Q., Ye, Q., Cai, H., & Qu, R. (2010). Determination of methanol ratio in methanol-doped biogasoline by a fiber Raman sensing system. *Sensors and Actuators B: Chemical, 146*(1), 75–78. https://doi.org/10.1016/j.snb.2010.01.041

Zhang, H., Huang, J., Li, T., Svanberg, S., & Svanberg, K. (2015). Optical detection of middle ear infection using spectroscopic techniques: Phantom experiments. *Journal of Biomedical Optics, 20*(5), 57001. https://doi.org/10.1117/1.JBO.20.5.057001

7.2 Publication II

Integration of fluorophore-based sensor spots into food packaging systems for the non-destructive real-time determination of oxygen

Jasmin Dold [a,*], Melanie Eichin [a], Horst-Christian Langowski [b,c]

[a] Chair of Brewing and Beverage Technology, Technical University of Munich, Weihenstephaner Steig 20, D-85354 Freising, Germany
[b] TUM School of Life Sciences, Technical University of Munich, Weihenstephaner Steig 22, D-85354 Freising, Germany
[c] Fraunhofer Institute for Process Engineering and Packaging, Giggenhauser Str. 35, D-85354 Freising, Germany

ARTICLE INFO

ABSTRACT

Oxygen is an important filling gas for modified atmosphere food packaging. To measure the oxygen amount non-destructively in the headspace, the integration of fluorescence material into the packaging system is a meaningful method, as oxygen serves as quencher for dynamic fluorescence. In this study, the integration of fluorescencent material into packaging films using a heat-sealing process was successfully demonstrated. Real-time determination of changes in oxygen partial pressure was also possible, with some limitations. The use of the technology for the determination of food quality changes (microbiological growth and color changes) were evaluated with high-oxygen stored minced beef (7 d, 4 °C), vacuum-packed sausage "Lyoner" type and beef steak (13 d, 4 °C). The increase in total viable count to the critical value of 10^7 CFU/g and the change of the surface color was well in common with the oxygen decrease for the high-oxygen packed minced beef. The vacuum packaged samples also showed correlations between reaching the critical microbiological value and a significant decrease of oxygen. However, no color changes were visible in that case.

1. Introduction

Modified atmosphere packaging (MAP) is the removal of ambient air from a packaging environment and the subsequent injection of a defined gas mixture (Robertson, 1993). Typically, three different gases are used: oxygen (O_2), carbon dioxide (CO_2) and nitrogen (N_2). N_2 serves thereby as inert filling gas for the replacement of O_2 (Church & Parsons, 1995) while CO_2 is mainly added to inhibit bacterial growth. O_2 is mostly removed or reduced from the packaging, as many microbiological or enzymatic processes responsible for spoilage respire O_2. However, in some cases, the presence of O_2 is advantageous, e.g. in packed fresh fruits or vegetables for their cellular respiration or the maintenance of the red color in packed beef (Lee et al., 2019). In contrast to earlier suggestions, also white muscle beef like poultry is packed under a high O_2 atmosphere, as the pathogen *Campylobacter jejuni* is inhibited by O_2 (Höll et al., 2016).

There is a high interest in the food packaging industry for the non-invasive measurement of the gas composition in the headspace for different reasons. On the one hand, the food industry can monitor goods immediately after the packaging process ("in-line") and thus ensure greater product safety. In addition, random sample analyses can be carried out without unnecessary product waste due to the destruction of the packaging. In quality assurance, the non-invasive control could reduce the amount of retention samples. In retail, the technology would allow the control of delivered products.

But there is also the potential to control the quality or shelf-life, by monitoring the gas atmosphere of already packaged foods. Höll et al. showed a correlation of the rapid decrease of the O_2 partial pressure and the reaching of the typical limit of the total viable count (TVC) of 10^7 CFU/g in high oxygen packed poultry (Höll et al., 2016). However, this effect could not be confirmed in total by other studies (Herbert et al., 2015). Kolbeck et al. were able to build a correlation between oxygen respiration and the presence of heme (Kolbeck et al., 2019; Kolbeck et al., 2021).

One method for non-destructive monitoring of O_2 could be the integration of fluorophore based sensor spots into the packaging system and to measure the O_2 partial pressure based on the principle of fluorescence quenching. Fluorescence quenching is the overall term for a process in which the fluorescence intensity or lifetime of the excited state of a specific dye is reduced. The embedded fluorophores can be excited, using a modulated light source – often in the green visible range. The fluorophores in the excited state are returning into their ground

---

state by emitting light – often in the red visible range. The delay of emission time relative to the excitation can be measured as a phase shift, which is preferable as the peak-to-peak height of the modulated sinus wave may differ. That phase shift builds the basis for the calculation of the luminescence lifetime (Lakowicz, 2006). For the non-invasive measurement of O_2, usually the dynamic or collisional quenching plays a role (Huber, 2008). In this process, O_2 serves as a so called quencher, absorbing energy of the excited fluorophores, when O_2 molecules collide with the fluorophore. Therefore, the luminescence lifetime and intensity is reduced. Dynamic quenching can be described by the Stern-Volmer equation and shows that the quenching process efficiency has a linear relationship to the O_2 partial pressure. The equation allows the calculation with both, the decrease of the fluorescence intensity or the fluorescence lifetime (Lakowicz, 2006). Nevertheless, for the application in food packaging, the use of the fluorescence lifetime is more suitable, as it is not affected by opacities e.g. of the packaging itself or generated by product residues (Huber, 2008).

The insertion of fluorophores into a packaging system for the non-invasive determination of O_2 has been described in several studies (Escobedo Araque et al., 2018; Kelly et al., 2020; Callaghan et al., 2016; Santovito et al., 2021) and patent applications (Havens et al., 2007; Krottmaier & Ribitsch, 2015; Steffen et al., 2018). However, most of them did either not directly integrate the sensor material into the packaging or the application was intended for a very short time to determine a sufficient MAP packaging or leakages or no testing for the food safety was done. For the precise examination of the amount of O_2 according to the principle of fluorescence quenching, it is not only important to protect the food from possible contact with the sensor material, but also to protect the fluorophores from contamination with food, since contamination can lead to inaccurate results, as the O_2 has to diffuse to the fluorophores first (Banerjee et al., 2016; Lakowicz, 2006). For that reason, we designed the set-up of a large study that combines a safe fluorophore integration (for a safe food-product on one hand, and for a precise measurement on the other hand), the determination of the influence on the measurement precision, the evaluation of the migration behaviour and the different application possibilities and their ability to gain fast results of the time behavior of the oxygen gas concentration in the headspace of a packaging:

In this publication, the non-invasive detection of the O_2 gas concentration via a fluorescence quenching device integrated into a food packaging is determined. For this purpose, the tight and safe integration of a sensor material via heat-sealing into a food packaging builds the basis of the research. The sensor material was covered with a plastic film to prevent the contact of sensor material with food and vice versa, for the above mentioned reasons. After integration, the suitability of different film combinations for the precise and fast determination of changes of the O_2 gas composition in the headspace was examined. Also, the potential for food safety was determined. Furthermore, the application in different food packaging systems was investigated. More precise, three different meat and meat products were used for this purpose. During a storage time between 7 and 13 days, the O_2 gas concentration, surface color and microbiological growth was monitored and possible correlations verified. The goal here was to develop a package that allows the non-destructive measurement of the O_2 content in real time, so that in a later application it might be possible to detect quality changes - e.g. microbiological spoilage - during the storage time of a food product.

2. Material and methods

2.1. Materials

The oxygen sensor spots (Ø 5 mm, total thickness: 550 μm) with embedded Platinum(II)– 5,10,15,20-tetrakis-(2,3,4,5,6-penta-fluorphenyl)-porphyrin fluorophores (SP-PSt3-NAU) as well as the Fibox 4 LCD trace oxygen meter with an integrated light source were provided by PreSens Precision Sensing GmbH, Regensburg, Germany. The O_2

sensitive coating is immobilized on 125 μm flexible transparent polyester film and additional covered with a black silicone film. The light source used for excitation is a light emitting diode connected with an optical polymer fiber, irradiating the sensor spot with light of a modulated intensity at a frequency of 4.5 kHz at 505 nm. The light emitted by the sensor spot at 650 nm is collected and guided by the fiber to a photodiode. The maxima of the sinus wave of the emission are retarded relative to the modulated excitation, resulting in a phase shift between the exciting versus the emitted light. That phase shift is measured with the device, and builds the basis for the luminescence lifetime and oxygen partial pressure calculation.

2.2. Validation of the measuring quality

2.2.1. Calibration of the sensor spots

In the following, all gas concentrations measured with the device are expressed as partial pressure (hPa). The mixing ratios of the used test gases are to be understood as percent by volume (% (v/v)).

Usually, the sensor spots are calibrated batchwise before use by a two-point calibration at zero and at one elevated oxygen partial pressure (recommendation of the company in the operating manual). To obtain an optimum accuracy in the relevant region of the oxygen partial pressure between 400 and 700 hPa, we first performed calibrations at different partial pressures and then examined the accuracy of a subsequent measurement at four different partial pressures.

To find the calibration conditions resulting in the highest measuring quality within the relevant measuring range between 400 and 700 hPa O_2, some calibration trials were carried out. Three different two-point calibrations (0 and 200.6 hPa, 0 and 576.0 hPa and 0 and 672.0 hPa O_2) were performed at first. Afterwards, the measuring quality at 384, 480, 576 and 672 O_2 was validated and the calibration condition with the lowest deviation was chosen for further trials in this study. Prior to the calibrations and measurements, the current air pressure was measured with a digital barometer (GHM Messtechnik GmbH, Regenstauf, Germany) and adjusted in the device settings of the instrument. Since the quenching process is highly dependent on temperature, the temperature was monitored directly at the surface adjacent to the respective sensor spot with a surface temperature sensor (Testo SE & Co. KGaA, Titisee-Neustadt, Germany) and manually adjusted in the device settings. For the calibration and further measurements, a measuring cell as seen in Fig. 1 was used. The spots were applied to a quartz glass cover plate with vacuum grease in such a way that the emitting side was directed to the glass plate. The quartz glass plate was fixed to the stainless steel body of the cell with vacuum grease and a O-ring between the glass plate and the measuring cell and a Plexiglas ring and six screws on top.

For the two-point calibration, the measuring cell was flooded with 100% N_2 (Linde GmbH, Pullach, Germany) for 20 min at ambient air pressure and the phase angle of each sensor spot for the oxygen-free atmosphere was measured by placing the light fiber centered to the respective spot on the glass plate. For the 200.6 hPa O_2 atmosphere, ambient air was brought into the measuring cell, leaving it open for at
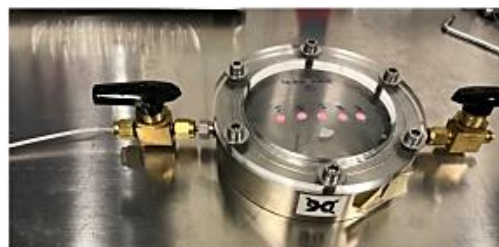

Fig. 1. Measuring cell for sensor spot calibration and measurement.

least 1 h after the nitrogen measurement before measuring again the phase angle. For the other O_2 amounts, test gases (60% O_2/40% CO_2 and 70% O_2/30%CO_2, both Linde GmbH, Pullach, Germany) were used, and the measuring cell was flooded again for 20 min at ambient air pressure prior to phase angle measurement. The calibration data was investigated for seven different sensor spots, to allow a multiple determination. The respective calibration data were saved in the instrument and are described below as K20 (calibration at 200.6 hPa O_2), K60 (calibration at 576.0 hPa O_2) and K70 (calibration at 672.0 hPa O_2).

To determine the calibration with the highest measurement precision, the verification of the calibration was subsequently done as follows: The measuring cell with the sensor spots was flooded again with several test gases (40%O_2/60%CO_2, 50%O_2/50%CO_2, 60%O_2/40%CO_2 and 70%O_2/30%CO_2, all Linde GmbH, Pullach, Germany) for at least 20 min at ambient air pressure, respectively. Afterwards, the values for the measured O_2 partial pressure were recorded for each calibration routine (K20, K60 and K70) and for each test gas.

2.2.2. Comparison of different polymer films

The sensor spots are used in this study for the integration into a food packaging as it is described in more detail in 2.3. To ensure that the measuring principle is not affected by absorption or reflectance properties of packaging materials, a comparison of different films was done.

For this purpose, the following polymer films were investigated in the indicated thicknesses: cellulose hydrate, 22 µm (Innovia Films, Wigton, UK), ethylene vinyl alcohol copolymer (EVOH), 58 µm (Infiana Germany GmbH & Co. KG, Forchheim, Germany), polyamide/polypropylene/polyamide/polypropylene multilayer film (PA/PP/PA/PP), 100 µm (allvac Folien GmbH, Waltenhofen, Germany), polyamide/polyethylene (PA/PE), 70 µm (allvac Folien GmbH, Waltenhofen, Germany), polyethylene low density (PE-LD), 50 µm (Infiana Germany GmbH & Co.KG, Forchheim, Germany), polyethylene/polyamide/EVOH/polyamide/polypropylene$_{peel}$ (PE/PA/EVOH/PA/PP$_{peel}$, 56 µm (Südpack Verpackungen GmbH & Co. KG, Ochsenhausen, Germany), PE-LD based plastic wrap, 15 µm (Cedo Folien und Haushaltsprodukte GmbH, Mönchengladbach, Germany), polypropylene (PP), 56 µm (Huhtamaki Flexible Packaging Germany GmbH & Co. KG, Ronsberg, Germany), polystyrene (PS), 50 µm (INEOS Styrolution Group GmbH, Frankfurt a.M., Germany) and polyvinyl chloride (PVC), 150 µm (INEOS, London, UK). For the measurement, two round pieces (d = 10.4 cm) were cut out of each of the films for the measuring cell. Five spots calibrated with K20 were attached to the different films and the quartz glass as reference, respectively, as described in 2.2.1, and the measured value for the atmospheric O_2 composition was recorded.

The actual O_2 content in the air-conditioned measurement room (calculated reference value) was calculated from mean values (n = 7) of relative humidity φ = 51.1%, temperature ϑ = 23.6 °C and air pressure p_{Air} = 967 mbar, using the O_2 content in dry air (20.94%) (Mortimer & Müller, 2020) and the saturation water vapor pressure of 28.977 mbar at 23.6 °C (Haar et al., 1988).

2.2.3. Influence of storage conditions to long-term stability of the calibration values

In the context of a potential application, it is not only important to know how the calibration of the sensor material should occur, but also when it should be done and as a consequence, at which point in the process the attachment to the packaging would be most useful. The sensor spots produced are currently calibrated per batch during production, i.e. representative data is given for an entire batch. For this reason, a storage trial of sensor spots packed in polyethylene pouches at different storage conditions was done. The tested storage conditions with varying temperature ϑ and relative humidity φ were as follows: ϑ = 6 °C / φ = 70%; ϑ = 23 °C / φ = 27%; ϑ = 23 °C / φ = 50% and ϑ = 40 °C / φ = 50%. Three spots for each storage condition were calibrated with 100% N_2 and 60% CO_2 as already described. The change of the measured O_2 partial pressure after flooding the measuring cell with

60% O_2 was monitored for 112 (ϑ = 23 °C / φ = 27%; ϑ = 23 °C / φ = 5% and ϑ = 40 °C / φ = 50%) and 353 days (ϑ = 6 °C / φ = 70%). To ensure that the results were not affected by UV light, the spots were stored in the dark.

2.3. Integration into a packaging system via heat-sealing

Fig. 2 shows a scheme for the experimental integration of the sensor spot into the packaging system, by sealing it onto the lid-film and covering it with a film towards the food side.

For the integration of the sensor spots into the lid film, a special heat-sealing jaw was designed (see Fig. 3). This consists of an annular sealing surface, with an inner diameter of 17 mm and an outer diameter of 21 mm, so that the sealing seam has a width of 2 mm.

The sealing tool is compatible with a heat-sealing machine (HSG-CC, Brugger Feinmechanik GmbH, Munich, Germany), with which sealing temperature, time and pressure are adjustable. The used films for the integration are shown in Table 1.

2.3.1. Heat-sealing with annular sealing seam

Once the knowledge of the exact melting points was obtained, the sealing tool could be tested for different film combinations. Therefore, different film-, temperature-, and time-combinations were chosen, as shown in Table 2.

For sealing, two pieces of film, each 5 × 5 cm, were cut out and placed with the side to be sealed on top of each other between the sealing jaws and sealed for the appropriate time. The sensor spot was attached with vacuum grease in such a way that the emitting side was directed to the lid-film. To control the sealing, first a visual observation occurred.

### 2.3.2. Dye penetration testing of the integrity of the seal of the cover film

The samples with visually good seals were additionally checked for small leaks with a dye penetration test in reference to the ASTM standard method (American Society for Testing and Materials, 2004), with modifications in the following way:

For this purpose, circularly cut-out blotter sheets (absorbency 135 g/m^2, Baier & Schneider GmbH & Co. KG, Heilbronn, Germany) with a diameter of 14 mm were placed between the films and sealed in at the appropriate conditions. In addition to the samples with the visually good results, one uncovered paper and one sample with a bad sealing was chosen. Afterwards, the samples were submerged in a 0.5% rhodamine B (Sigma Aldrich, Merck KGaA, Darmstadt, Germany) in isopropanol solution for at least 15 min and dried afterwards for at least 2 h at room temperature. Then, the blotting paper was taken out of the package and compared to the control sample. The use of an alcoholic rhodamine solution as penetration test for the leak detection in packaging is a well-known and often used test in packaging technology and thus it is possible to make leakages ≥ 20 µm visible (Arndt, 1995; Hurme & Ahvenainen, 1998).

2.3.3. Influence of the heat-sealing process to the measuring quality of the oxygen partial pressure

A very important question to answer for the application is how strong the heat sealing process affects the measuring quality, as the presence of high temperatures could lead to an altering of the fluorophores (Lakowicz, 2006) and therefore a deviation of the previous calibration is possible. For the investigation, 12 sensor spots were calibrated with 100% N_2 and 60% O_2/40% CO_2 (K60), as described before. After calibration, the phase angle of each spot and the measured O_2 amount at a O_2 partial pressure of 582 hPa was determined. The sensor spots were then placed between two films as described in the previous chapter and sealed-in with the sealing tool.

To screen the whole temperature spectrum, film combinations of PP-PP at 160 °C, PA/PP/PA/PP-PP at 155 °C, PA/PE - PE-LD$_{15\,µm}$ at 120 °C and PA/PE-PE-LD$_{50\,µm}$ at 115 °C were used for this purpose (comp.
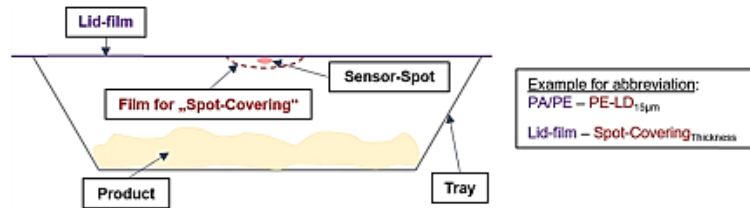
Fig. 2. Scheme of the sensor spot integration into the packaging. The example for abbreviation shows the used description of the lid-film and spot-covering combinations in the further trials.

Fig. 3. Sealing jaw for the annular heat-sealing with a Teflon-coated sealing surface.

Tables 1 and 2). First, the uncovered sensor spots were calibrated, using K60 calibration conditions. After the sealing with the sealing jaw, the sealed-in spots were placed again into the measuring-cell, using tape to fix them onto the quartz glass. After flooding the measuring cell with 60% O_2/40% CO_2, the phase angle as well as the measured O_2 partial pressure for each spot was taken, after conditioning for at least 48 h to ensure complete permeation of the gas into the spot interior. Then the sealed-in sensor spots were taped under a 30×45cm PA/PP/PA/PP or PA/PE lid-film and placed with the polypropylene or polyethylene side on a PP (205×160×50mm, transparent, ES-Plastic GmbH, Hutthurm, Germany) or PP/EVOH/PE (205×160×37mm, white, ES-Plastic GmbH, Hutthurm, Germany) tray.

The sealing of the lid-film onto the trays occurred at 160 °C for the

PP and 120 °C for the PE samples, with a sealing time of 4 s in a semi-automatic Traysealer (T250, Multivac GmbH & Co. KG, Wolfertschwenden, Germany). Afterwards, a circular part of the lid-film was cut out again, together with the sensor spots without destroying the annular sealing, and placed into the measuring-cell, using tape to fix them onto the quartz glass. The measuring cell was flooded again with the 60%O_2/40%CO_2 test gas, and the phase angle and the O_2 partial pressure was measured, after conditioning the samples for at least 48 h. The process is further shown in Fig. 4.

2.4. Screening analyses of a sensor spot for organic and inorganic components

To further make a statement for a potential food compatibility, the integrated sensor spots were screened for migratable organic and inorganic components. Therefore, sensor spots were sealed between a PA/PE lid-film and PE-LD$_{50 \mu m}$ cover film. The PE cover film was therefore the food contact material. The investigations were carried out with the sealed material including sensor spots and the sealed material without sensor spots as a reference in order to characterize the specific substances of the sensor spots and their migration potential through the cover film. In addition, the uncovered sensor spots were analyzed for organic compounds using a dipping method. Table 3 shows the testing conditions in more detail. All tests are further described in the standards that are also named in Table 3 (German Institute for Standardization, 2004, 2017). The GC-FID analysis was performed as already described in

Table 1
Overview of the flexible polymer films used in the publication, the related melting properties analyzed via Differential scanning calorimetry (Tm) and the role (lid-film or spot-covering to the food-side) during the different trials: Cellulose hydrate: brown, EVOH: blue, PA/PE: light-green, PA/PP/PA/PP: grey, PE-LD50μm: dark-green, PE-LD15μm: orange, PE/PA/EVOH/PA/PPpeel: yellow, PP: red, PS: light-brown and PVC: pink. The coloration indicates whether the flexible films were used and for which trials. A non-coloring means that the film was not used in these tests.

Polymer	Tm properties	2.2.2	2.3.1	2.3.2	2.3.3	2.4	2.5.1	2.5.2	2.6
Cellulose hydrate 22 μm	-								
EVOH 58 μm	178 °C								
PA/PE 70 μm	106 °C (PE) 217 °C (PA)		←———————————————————— Lid-film ————————————————————→						
PA/PP/PA/PP 100 μm	149°C (PP) 222°C (PA)		←————— Lid-film —————→				←————— Lid-film —————→		
PE-LD 50 μm	109°C		←Lid-film and Spot-Covering→	←— Spot-Covering —→			Lid-film and Spot-Covering	←—— Spot-Covering ——→	
PE-LD 15 μm	118°C		←————— Spot-Covering —————→				Spot-Covering		
PE/PA/EVOH/PA/PPpeel 56 μm	118°C (PE) 166°C (PP)* 219°C (PA) 260°C (PA)		←—— Lid-film ——→				Lid-film		
PP 56 μm	164°C		←———— Lid-film and Spot-Covering ————→				Lid-film and Spot-Covering	←—— Spot-Covering ——→	
PS 50 μm	-								
PVC 150 μm	-								

4

Table 2

Film combinations and tested sealing temperatures based on the previous DSC analysis. A constant contact pressure of 0.5 bar was chosen for all combinations. The time was varied for each film combination with 10, 5 and 2 s.

Film Combinations	PA/PP/PA/ PP – PP	PE/PA/EVOH/PA/ PP$_{peel}$ – PP	PP – PP
Sealing Temperatures/°C	145 150 155	155 160 170	155 160 170
Film Combinations	PA/PE – PE-LD$_{50\,\mu m}$	PA/PE – PE-LD$_{15\,\mu m}$	PE-LD$_{50\,\mu m}$ – PE-LD$_{50\,\mu m}$
Sealing Temperatures/°C	110 115 120	100 120 130	110 115 120

Franz et al. (2016).

For the screening of organic compounds, the aliquots of the extraction solutions were spiked with 50 μl of the internal standards tert-butylhydroxyanisole (BHA) (Sigma-Aldrich, Merck KGaA, Darmstadt, Germany) and Tinuvin 234 (Ciba Specialty Chemicals, BASF SE, Ludwigshafen, Germany) (each 1000 μg/L) prior to GC-FID analysis.

2.5. Real-time determination of oxygen gas concentration with sealed-in sensor spots

2.5.1. Determination of O$_2$ response-time in a closed system

The six film combinations (see Table 2) with sealed-in calibrated sensor spots were used to make a prediction about the measurement capacity in real time. For this purpose, both the gas *permeability* Q and the *permeation coefficient* P were determined and compared with the manufacturer values. For the measurement a measuring chamber was used, which is described in more detail in DIN 53380–5 (DIN Standards Committee Packaging, 2014). The films were taped into the measuring cell so that the side of the sensor surface was located on the quartz glass of the upper measuring chamber, and the optical fiber could thus be placed for continuous O$_2$ measurement. The O$_2$ concentration was measured in hPa.

For preparation, the measuring chamber was first flooded with 100% N$_2$ and conditioned for at least 48 h so that the measurement could start at an O$_2$ partial pressure of virtually 0 hPa. Then, the measurement occurred in three steps: First, the chamber was flooded with a 80% O$_2$ / 20% CO$_2$ test gas mixture (Linde GmbH, Pullach, Germany). The device recorded a value every 5 min until the O$_2$ partial pressure reached to the current ambient pressure, was reached. The next two steps used

subsequently lowered O$_2$. For this purpose, the measuring cell was flooded with 60% O$_2$/40% CO$_2$ in the second step and, after the measurement reached a stable value, with 20% O$_2$/80% CO$_2$ in the third step (calibrated gas mixtures supplied by Linde GmbH, Pullach, Germany). To verify the reproducibility of the method, the measurements were performed in triplicate.

With the cascade-shaped curve, the *permeability* Q and the *permeation coefficient* P could then be calculated. The calculation was based on the steady-state increase or decrease of O$_2$ within a defined time period. The calculation is further described in DIN 53380–5 (DIN Standards Committee Packaging, 2014). To make a statement regarding the real-time determination of the O$_2$ change with the sealed-in spots, we defined a characteristic response-time, which means the necessary time period at which 90% of the difference to the previous partial pressure is measurable.

2.5.2. Determination of O$_2$ gas concentration in real packaging systems

To further evaluate the ability for an O$_2$ determination in real-time, two types of kinetics for changes in the internal gas composition were simulated, after integrating the sensor spots into real-packaging systems. Therefore, PA/PP/PA/PP and PA/PE lid films were prepared as

Table 3

Extraction and analysis conditions to test potential migration properties of the sealed sensor spots.

	Organic compounds	Inorganic compounds
Reference & Sealed-in spots (food contact side)	one-side contact extraction (Directive (EU) No. 10/2011) extraction agent: 95% ethanol (Chemsolute, Th. Geyer GmbH & Co. KG, Renningen, Germany) contact time and -temperature: 3d / 60 °C Analysis: GC-FID	European standard DIN EN 13130–1:2004–08: simulant: 3% Acetic acid (Chemsolute, Th. Geyer GmbH & Co. KG, Renningen, Germany) contact time and -temperature: 10d / 40 °C Analysis: ICP-MS (DIN EN ISO 17294–2:2017–01)
Uncovered sensor spots	Extraction by dipping method: dichloromethane (DCM) (Chemsolute, Th. Geyer GmbH & Co. KG, Renningen, Germany): 3d / 40 °C or 95% ethanol: 3d / 60 °C. Analysis: GC-FID	
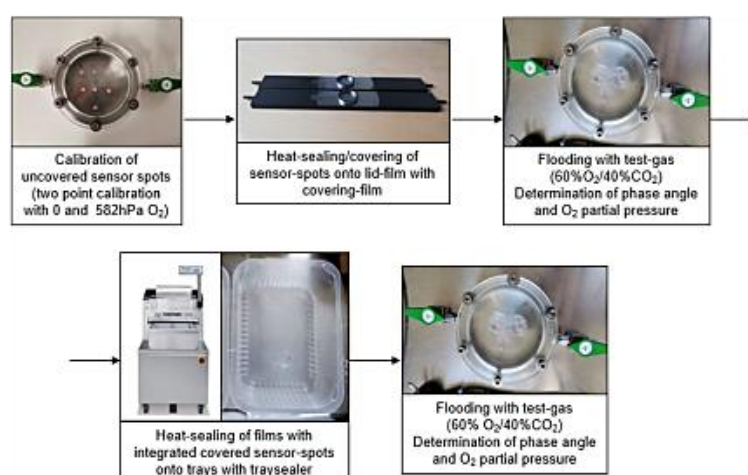
Fig. 4. Scheme of the successive calibration, sealing and testing steps to determine the influence of the integration to the measuring quality.

5

described in 2.3, by integrating and covering the sensor spots with PP or PE-LD$_{50\,\mu m}$ films and sealed onto empty PP or PP/EVOH/PE trays with the semi-automatic Traysealer, with a gas atmosphere of 70% O$_2$ and 30% CO$_2$ set with a gas mixer (WITT-GASETECHNIK GmbH & Co KG, Witten, Germany) connected to it. Afterwards, the trays with the integrated sensor spots (PP trays with PA/PP/PA/PP-PP lid-film and spot-covering and PP/EVOH/PE trays with PA/PE-PE-LD$_{50\,\mu m}$ lid-film and spot-covering) were conditioned for at least 48 h.Two different set-ups where afterwards chosen for each packaging type, to simulate two different scenarios:

The first set-up served for the simulation of a packaging defect. For this purpose, the lid film was perforated with a needle ($\varnothing=1$ mm; n = 1). Over a period of 96 h (PP/EVOH/PE trays with PA/PE-PE-LD$_{50\,\mu m}$ lid-film and spot-covering) and 120 h (PP trays with PA/PP/PA/PP-PP lid-film and spot-covering), the O$_2$ content was measured regularly with the non-destructive device and a destructive gas analyzer in parallel (see 2.6.4) for O$_2$, CO$_2$ and N$_2$ detection.

The second set-up served for the simulation of a microbiological O$_2$ respiration during spoilage as described in the introduction, which is characterized by a decrease of O$_2$ and a simultaneous increase of CO$_2$. Therefore, the closed and gas-filled trays (70% O$_2$/30% CO$_2$) were put into a larger tray (PP, 227×178×90 mm, transparent, ES-Plastic GmbH, Hutthurm, Germany), which was sealed with the PA/PP/PA/PP lid film. Then, the outer tray was flooded with a testgas mixture with a higher CO2 and a lower O2 content in relation to the inner tray (80% CO$_2$ / 20% O$_2$, Linde GmbH, Pullach, Germany). At time 0, the gas concentration inside the inner tray with the integrated sensor-material was determined with the destructive measurement method (see 2.6.4) by inserting the needle, thus causing a perforation ($\varnothing=1$ mm) at the same time, which allowed gas exchange between the outer and inner trays. The entry of ambient air into the outer tray was prevented by using a septum attached to the lid-film. The gas concentration of the inner tray was monitored over a period of 72 h, for both, the PP/EVOH/PE and the PP trays. All samples were stored at 4 °C.

The principle is also described in Fig. 5.

2.6. Application in various food / packaging combinations (MAP and vacuum packaging)

2.6.1. Sample preparation

Minced beef, "Lyoner" type sausage and beef steaks were purchased from a local butcher.

512 g of minced beef was weighed into transparent PP trays and sealed with the semiautomatic traysealer in a modified gas atmosphere of 80% O$_2$ / 20% CO$_2$. Three packages were sealed with a PA/PP/PA/PP lid film, with integrated sensor material, prepared with a PP covering, as described in 2.3. 14 samples of the same type were prepared without the integration of fluorophores. The samples were stored for 7 days, as this is the average shelf-life for fresh meat in modified atmosphere at 4 °C.

50 g of sliced type "Lyoner" sausage and beef steaks were weighed into transparent vacuum bags (PA/PE, 150 ×260 mm, 96 µm, packpack. de GmbH, Jever, Germany), respectively, and sealed with a free-standing chamber machine (C 300, Multivac GmbH & Co. KG, Wolfertschwenden, Germany). Beef steaks were vacuum packed, adjusting the final pressure of the chamber machine to 1 hPa, while type "Lyoner" sausage was packed, adjusting the final pressure to 100 hPa. For the sausage, a higher partial pressure was possible, as the processed product is much more color stable, than the fresh beef even at "higher" oxygen amounts. Three vacuum bags of each product were prepared with an integrated sensor spot, covered-up with PE, as previously described. For each food product, 14 samples without integrated sensor material were prepared. In addition, three empty bags for "total" vacuum (1 hPa), and three empty bags with 100 mbar with integrated sensor material were prepared. The samples were stored for 13 days at 4 °C. All integrated sensor spots were calibrated with the "K60″ calibration routine prior to the integration process, as described in 2.2.

2.6.2. Microbiological analysis

The samples were evaluated regarding their total viable count (TVC) as already described in Höll et al. (2016) with slight modifications: about 70 g sample was weighed into a sample bag, (VWR International, Darmstadt, Germany) by using sterile wood toothpicks and homogenized for 120 s with 50 ml Ringer's solution (Merck KGaA, Darmstadt, Germany) in a stomacher (LabBlender400, Gemini BV, APE-LDoorn,
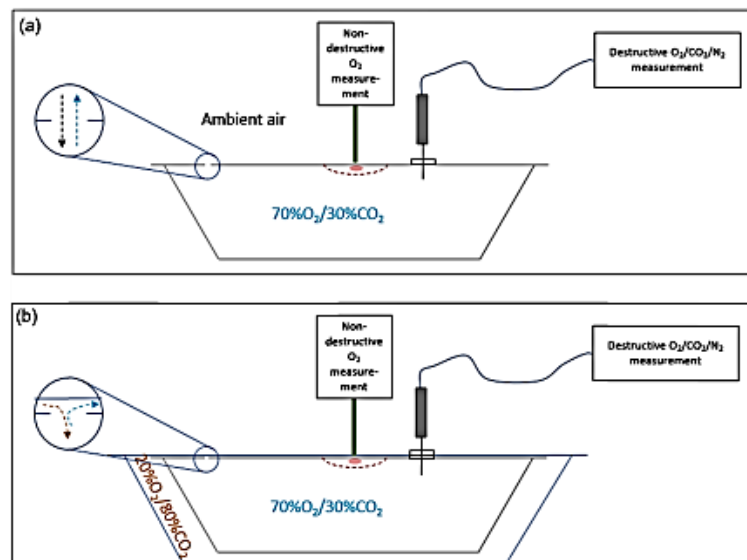
Fig. 5. Test setup for gaining an artificial kinetic of a packaging with initial 70%O$_2$/30%CO$_2$ MAP and (a) a packaging perforation (diffusing gas into packaging: ambient air) and (b) a microbiological respiration process (diffusing gas into packaging: 20%O$_2$/80% CO$_2$).

6

Netherlands). Each sample was prepared in duplicate. A tenfold dilution series of sample homogenate was prepared with Ringer's solution. 100 µl of each dilutions were later spread onto the brain heart infusion agar (Carl Roth GmbH & Co. KG, Karlsruhe, Germany) using sterile glass beads. After incubating the plates aerobically at 30 °C for 3 days, the numbers of colony forming units on the plates were counted and the units per gram of sample (CFU/g) were calculated. Minced beef was analyzed on day 0, 2, 5 and 7, type "Lyoner" sausage and beef steaks on day 0, 2, 5, 7, 9 and 12.

2.6.3. Color measurement

For the color measurement, the CIE L*a*b* - values were measured on day 0, 2, 5, 7, 9 and 12 using a non-contact digital color imaging system DigiEye (DigiEye V2.62, VeriVide, Leicester England). The measurement was performed non-destructively on the unopened samples through the packaging. Five measurements of each sample on different locations were taken, so the average values were calculated out of 15 color measurements (since each sample was stored in triplicate). The measurements were taken in an enclosed DigiEye Cube and sample illumination was done with a diffuse illuminant D65, which was part of the DigiEye Cube. The images were taken with a Nikon D90 digital camera (objective: AF Nikkor 35mm1:2D, Nikon Europe BV, Amsterdam, Netherlands) at a distance of 0.5 m to the sample, placed on a blue chart. The system was calibrated with the DigiEye Digitizer Chart prior to the measurement, as already described in (Nadine Böhner & Rieblinger, 2016).

2.6.4. Destructive determination of O_2 and CO_2 gas concentrations

The MAP packaging of the minced beef was additionally monitored with a destructive measurement device on day 0, 2, 5 and 7. For this purpose, a gas analyzer (MAT1500, A.KRÜSS Optronic GmbH, Hamburg, Germany) with a Zirconium dioxide sensor for O_2 detection and a non-dispersive infrared sensor for CO_2 detection was used. To extract small aliquots (7 ml) of the gas atmosphere, a hollow needle belonging to the measuring device was inserted into the headspace of the packaging via a septum attached to the lid film. The destructive measurement of the vacuum packaging was unfortunately not possible, as the gas flow was too low.

2.6.5. Non-destructive determination of O_2 gas concentration

The samples with the integrated sensor material were monitored during the storage with the non-destructive measurement device. MAP-packed minced beef was measured non-destructively on day 0, 1, 2, 5, 6 and 7. The vacuum packed samples were monitored over a storage period of 13 days on day 0, 1, 2, 5, 6, 7, 8, 9, 12 and 13. For the measurement, the respective calibration data, the temperature and the daily ambient pressure were set on the device.

2.7. Statistical analysis

The drawings and statistical analysis were performed using MS Excel and MATLAB (R2019b, MathWorks Inc.). All data are presented as the arithmetic mean ± standard deviation. For the calculation of the statistical significance, two-sample t-tests (two-tailed) were performed at an alpha level of 0.05. An analysis of variance was performed to test for equal variances prior to t-test analysis. For the evaluation of the results obtained in 2.2.2 (Comparison of different polymer films), an univariate, one-way analysis of variance (ANOVA) was used to determine the influence of the films on the measurement accuracy. In addition, the corresponding values were compared with each other by means of a multiple comparison of means (Tukey HSD test).

3. Results and discussion

3.1. Validation of the measuring accuracy

3.1.1. Calibration of the sensor spots

The measuring range between 40% and 70% (approx. 400–700 hPa) O_2 was chosen, because in the later application a modified atmosphere at higher O_2 levels between 50% and 80% are common.

As expected, the calibration at higher O_2 amounts (576 hPa or 672 hPa O_2) resulted in much better measuring qualities between 384 and 672 hPa O_2, compared to the calibration at ambient air (see Fig. 6).

Overall, K60 had the highest measuring quality, with a maximum volume deviation of 2.02 ± 3.74 hPa at 384 hPa O_2. The calibration at ambient air (K20) results in the lowest precisions with absolute deviations up to 35.42 ± 6.72 hPa O_2 for 672 hPa. Therefore, all trials - excepted of 2.2.2 and partly 2.2.3 - were carried out with previous two-point-calibrations at 100% N_2 and 60%O_2/40%CO_2 (K60).

3.1.2. Comparison of O_2 partial pressure measurements through different polymer films

The results of the measured O_2 contents are shown in Table 4. The values determined through the film samples vary around the mean value of 193.4 hPa, with the highest deviation at 4.25 hPa in absolute and relative terms by 0.98% respectively. The result of the measurement through the quartz glass also deviates by 0.09% absolute from the mean value of the entire film samples.

No significant difference was found between the mean values obtained through the quartz glass and through all the film samples ($p \leq 0.05$). In addition, although a significant difference was found between the measured mean oxygen content through the individual films, no mean values differed from each other in the post hoc test. This could be due to individual outliers in the measurements, to which the analysis of variance is more sensitive than the Tukey HSD test. Since there was homogeneity of variance, it can be assumed that the type of film has no significant influence on the measurement results - at least if they are completely transparent in the visible spectral area. However, it is noticeable that all results deviate significantly from the real oxygen content and show significantly lower measured O_2 partial pressure, compared to K60 and K70 in 3.1.1. This seems to be therefore a systematic deviation, maybe induced by inaccuracies in calibration. The results clearly show that a recalibration of the spots is not necessary for the integration, regardless of the type of film used. The only
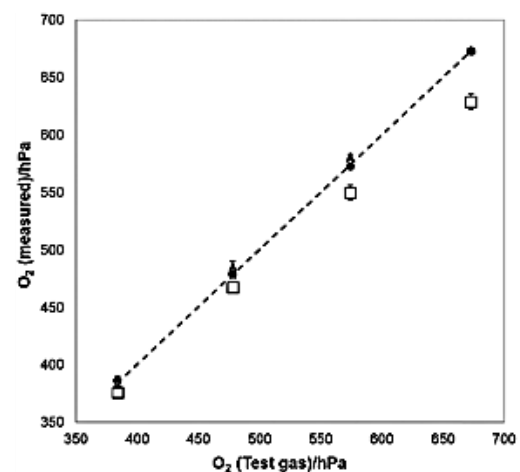

Fig. 6. Measured oxygen concentrations at 384.0, 480.0, 576.0 and 672.0 hPa O_2 (test gas: dotted line) using three different calibration standards: K20: □, K60: ● and K70: ▲. Ambient air pressure: 960hPa.

Table 4

Mean atmospheric oxygen content through quartz glass (n = 20) and through different polymer films (n = 10 each) compared to the calculated reference value of 199.4 hPa. The ambient air pressure was 967 hPa.

Polymer	Oxygen [hPa]
Reference value	199.40
Quartz glass	194.27 ± 2.80
Mean value of all films	193.40 ± 2.22
Cellulose hydrate	195.04 ± 1.45
EVOH	193.88 ± 1.35
PA/PE	193.40 ± 1.64
PA/PP/PA/PP	194.85 ± 2.13
PE-LD	193.11 ± 1.45
PE/PA/EVOH/PA/PP$_{peel}$	189.15 ± 1.64
PP	193.30 ± 1.45
PS	193.98 ± 1.64
PVC	193.50 ± 1.84

characteristic that a film must have is that it is transparent in the visible area.

3.1.3. Influence of storage conditions to long-term stability of the calibration values

The long-term stability of the calibration values showed clear trends depending on their storage conditions, which can be seen in Fig. 7. All sensor spots stored at room temperature or higher showed a clear increase in measurement inaccuracy within 112 days of storage. The sensor spots stored at 6 °C, however, were still in an acceptable accuracy after 1 year of storage.

At room temperature or higher, the embedded fluorophores seem to undergo an altering process, leading to a change of the luminescence lifetime and therefore the calibration values. The chilled storing of the sensor material seems to prevent these effects. The relative humidity seems not to have a great influence, as both samples stored at 23 °C had a similar trend.

For the application, these experiments allow two conclusions to be drawn: either the sensor material must be applied to the film immediately before the integration into the lid film, or prepared films must be stored refrigerated until application. In that latter case, some trials to ensure the film-stability should be made. It is not possible to do a

previous application from the packaging specific point of view, as the film would probably be wound properly any more.

3.2. Integration into a packaging system via heat-sealing

3.2.1. Heat-sealing with annular sealing seam

During the variation of sealing temperature and time with the heat-sealing tool, visually good sealings for each tested polymer combination were obtained.

The following Table 5 shows the best results. As expected, the best results for the sealings were around the melting points, shown in Table 1.

3.2.2. Dye penetration testing of the integrity of the seal of the cover film

To make sure that no leaks are present as a sealing result, the already described Rhodamine test was done subsequently. The results can be seen in Table 6.

Fortunately, only the reference and the obviously too hot sealed PP-PP sample at 170 °C showed a coloration of the blotting paper. All the other sealings seemed to be tight within the detection limit, as no dye penetrated into the packaging. Some of the samples appear colored (e.g. the PE-LD$_{50\ \mu m}$ – PE-LD$_{50\ \mu m}$ sample), however, this was the coloration of the film itself, on its outer side. That makes it very likely, that the sealings went well, and the spot material as well as the packed good are protected against each other, which is very important for the application, as already described in the introduction. However, leakage channels narrower than 10–20 μm, depending on the surface energy of the films, cannot be detected by this method (Arndt, 1995; Hurme & Ahvenainen, 1998). The measurement of the migration behavior (see 3.3) can make a better statement in this respect.

3.2.3. Influence of the heat-sealing process to the measuring quality

As mentioned earlier, the heat-sealing steps are potentially threatening to measurement quality because the fluorophores could be altered by heat exposure (Lakowicz, 2006). The measurement results for the tested films are shown in Table 7. Surprisingly, the majority of the measurements did not show significant changes in measurement precision. The film combination PA/PE – PE-LD$_{15\ \mu m}$ showed for example for both heat-sealing steps significant deviations from the mean value after calibration, but with mean values between 566.38 and 570.32 hPa these
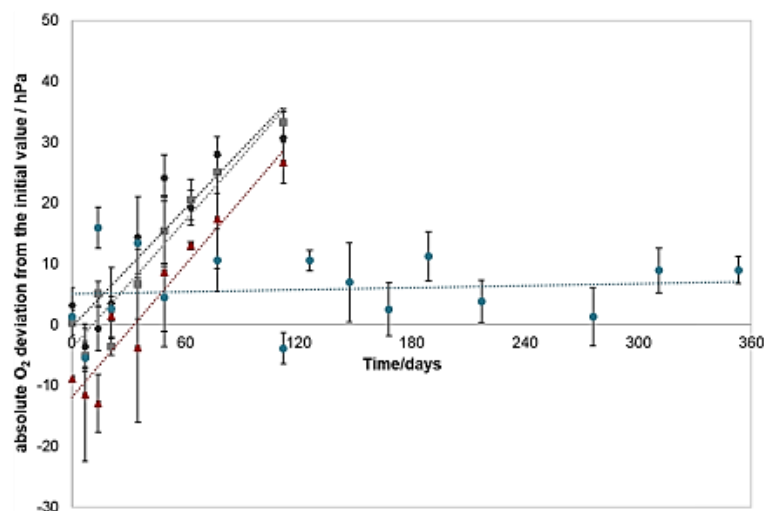
Fig. 7. Oxygen partial pressure: deviation from the initial value of 576 hPa O$_2$ measured with sensor spots stored over a period of 112 or 353 days at different storage conditions: ●: θ= 6 °C/φ = 70%; ■: θ= 23 °C/φ = 27%; ◆: θ= 23 °C/φ = 50% and ▲: θ= 40 °C/φ = 50 (n = 3 for each storage condition). The dotted lines are trend lines. The deviation refers absolutely to the value determined on day 0 immediately after calibration.

8

Table 5
Sealed-in sensor spots between different polymers at defined sealing temperature and time, and a constant pressure of 0.5 bar. The images were done with the DigiEye.

Table 6
Rhodamine penetration test of the polymer sealings with sealed-in blotter sheets and unpacked blotter sheets, after penetration test.
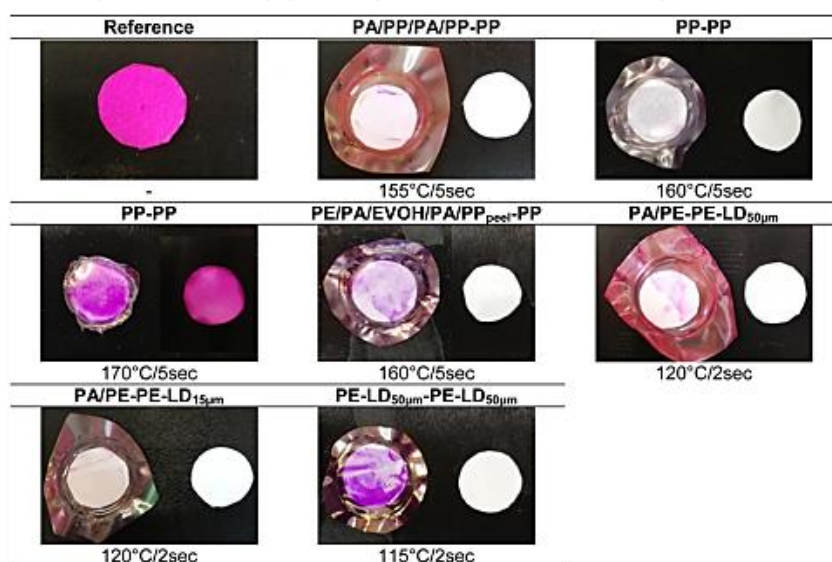
results are still in range of the measurement variations specified by the manufacturer, which also applies to the other deviations. If the fluorophore would have been affected, higher statistical significance for the samples sealed at higher temperatures would be the logical consequence, which was not present in our trials.

The results are well in common with the current literature. Kelly et. al also sandwich-laminated fluorophore based material between PE-based films in 2020 and analyzed the luminescence lifetime before and after the laminating process at zero percentage O_2 and at ambient air. As conclusion, no significant change of the luminescence lifetime occurred (C. Kelly et al., 2020). However, it was not noted at which temperature the sealing process was done, but as PE was the sealed polymer, temperatures around 120 °C are very probable.

3.3. Screening analyses of a sensor spot for migration of organic and inorganic components

The results of the organic screening of the PA/PE – PE-LD$_{50 \mu m}$ sealed-in spots (two approaches: a) and b)) and the reference gave a signal at a retention time of 9.5 min, which is known to be caprolactam from the PA in the PA/PE film. In the retention range from 14 to 25 min, a larger number of potentially migratable components were detectable

in the samples with sealed-in sensor spots, as well as in the reference. For approach a) of the sealed in sensor spot sample, the peaks were more visible than for the second approach b). In the comparison of approach b) with the two references, no significant differences could be detected, in particular no additional signals indicating any contribution from the sensor spot material. No organic components could be detected in the extracts of the uncovered separate sensor spots, which were examined following the one-sided extraction.

For the inorganic compound analysis, only iron and zinc were present in comparable concentrations, in both, the reference and the samples with sealed-in spots. Compared to the reference, no additional metals could be determined in the migrates of the sealed sensor spots at the corresponding limits of quantification, not even metals (Pt, Pd) possibly originating from the sensor dye.

However, the significance of the analyses performed is subject to limitations. The differences in approach a) and b) are therefore unclear, however, as no organic component was found for the uncovered sensor spots, we assume that an external contamination (e.g. vacuum grease) led to a higher increase of the peaks between 14 and 25 min for approach a). The analysis of the film combination "PA/PE film" and "PE-LD$_{50 \mu m}$ monofilm" as reference samples showed also a large number of migratable components in the retention time range from 14 to 25 min,

Table 7

Mean measured phase angles and oxygen amounts before and after different heat sealing steps (previous calibration with 60%O_2/40%CO_2). Significant deviations from the calibration values are marked ($p \leq 0.05$ *; $p \leq 0.01$ **; $p \leq 0.001$ ***). (n = 3 for each film combination, n = 12 for the calculation of "All").

	Phase Angle Φ/°		
	Calibration	Sealing Tool	Traysealer
PA/PE–PE-LD$_{50\,\mu m}$ 115 °C	17.52 ± 0.28	17.29 ± 0.38	17.07 ± 0.14 *
PA/PE–PE-LD$_{15\,\mu m}$ 120 °C	17.24 ± 0.40	17.23 ± 0.43	16.96 ± 0.21
PA/PP/PA/PP–PP 155 °C	16.66 ± 0.26	17.11 ± 0.45	16.78 ± 0.39
PP–PP 160 °C	16.51 ± 0.50	17.52 ± 0.62	16.58 ± 0.57
All	16.98 ± 0.53	17.29 ± 0.44	16.85 ± 0.37
	Oxygen /hPa		
	Calibration	Sealing Tool	Traysealer
PA/PE–PE-LD$_{50\,\mu m}$ 115 °C	581.68 ± 5.34	556.37 ± 15.37	582.22 ± 10.14
PA/PE–PE-LD$_{15\,\mu m}$ 120 °C	586.85 ± 1.94	566.38 ± 4.62 *	570.32 ± 2.55 **
PA/PP/PA/PP–PP 155 °C	585.56 ± 2.80	562.99 ± 11.18	597.66 ± 2.95 **
PP–PP 160 °C	584.26 ± 3.41	570.74 ± 8.61	584.15 ± 8.43
All	584.59 ± 3.66	564.12 ± 10.64 ***	583.58 ± 11.70

Table 8

90% response-time and the measured and theoretical *permeation coefficients* P for different film combinations. The response-time refers to the respective test-gases at 965 mbar air pressure. The results of the permeation coefficients are mean values of the stationary O_2 increase or decrease, after flooding the measuring cell with different gas compositions (n = 3).

Film combination	90% response-time/h			P cm^3 (STP)/ (m^2*d*bar) * 100 μm	Theoretical P
	772 hPa	579 hPa	193 hPa		
PE-LD$_{50\,\mu m}$–PE-LD$_{50\,\mu m}$	3.58	0.47	4.61	2055 ± 224	2000
PA/PE–PE-LD$_{15\,\mu m}$	2.58	0.67	4.75	2015 ± 295	
PA/PE–PE-LD$_{50\,\mu m}$	5.68	0.81	4.68	1923 ± 410	1729
PP–PP	13.60	1.92	15.83	793 ± 183	300–800
PA/PP/PA/PP–PP	18.11	4.17	29.06	453 ± 101	178–461
PE/PA/EVOH/PA/PP$_{peel}$–PP	28.80	6.38	37.51	477 ± 147	241–640

which could overlay possible mass transfers from the sensor spots. It should be noted that these analyses do not represent a comprehensive compliance test to show conformity with the applicable legal requirements for food contact materials (including Plastics Regulation (EU) No. 10/2011 and Framework Regulation (EC) No. 1935/2004). However, they can give a first impression that the application as described in this publication may be promising in terms of compliance.

3.4. Real-time determination of oxygen gas concentration with sealed-in sensor spots

3.4.1. Determination of O_2 response-time in a closed system

Fig. 8 shows the O_2 gas concentration development measured with the sealed in sensor spots in the spot area for six different film combinations (Table 8). The sensor material covered with PE-LD$_{50\,\mu m}$ monofilm, having a PE-LD$_{50\,\mu m}$ lid film shows the fastest increase and decrease of O_2, after flooding the measuring cell with the test-gases. For the film combinations with the higher O_2 barrier (e.g. PE/PA/EVOH/PA/PPpeel-PP), results in real-time are more unlikely.

The defined 90% response-time (Table 8) further underlines the results shown in Fig. 8. The samples covered with PE-LD material showed
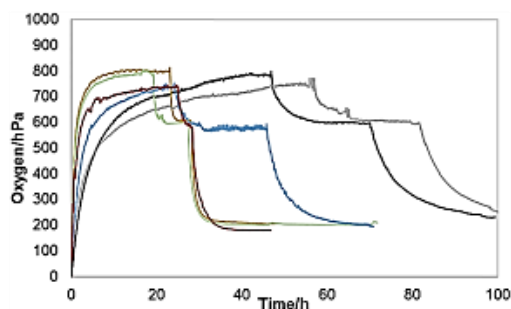
Fig. 8. Development of the O_2 partial pressure over the time measured in the spot area for different film combinations at 21 °C and an ambient air pressure of 965 mbar: PE-LD$_{50\,\mu m}$-PE-LD$_{50\,\mu m}$ (green), PA/PE-PE-LD$_{15\,\mu m}$ (brown), PA/PE-PE-LD$_{50\,\mu m}$ (red), PP-PP (blue), PA/PP/PA/PP-PP (black) and PE/PA/EVOH/PA/PP$_{peel}$-PP (grey). (n = 3).

the relatively best response time, especially for the decrease after flooding the measuring cell with 60% O_2/40% CO_2. The spots sealed-in with PP and PA based lid-films and PP-monofilm covering were hardly able to detect the O_2 change in real-time. The measured permeation coefficients were well in common with the theoretical values. Nevertheless, these kinetics can only be compared with limited extent to real packaging systems, since we have permeation processes on the downside as well as on the upper side of the film when using the measuring chamber. For this reason, tests were carried out in real packaging systems in the following.

3.4.2. Determination of O_2 gas concentration in real-packaging systems

The first set-up served for the simulation of a packaging defect, the second set-up served for the simulation of a microbiological O_2 respiration during spoilage, which can be seen in Fig. 5.

Fig. 9 shows the results for a simulated packaging defect, which means that the gas diffusing into the packaging is ambient air and thus consists mainly of N_2. For both polymer-covering types, a significant difference between the non-destructive and destructive O_2 detection was noticeable at some points. Precise real-time measurement results were obtained after 48 h for the packaging with the PE-LD$_{50\,\mu m}$ covered sensor-material and after 72 h for the first time for the packaging with the PP covered sensor-material. It is also noticeable, that the N_2 amount increases, while the CO_2 amount decreases as well. At the end of the storage, the gas atmosphere in the packages reached almost the ambient air levels.

The simulation of a O_2 respiration process can be seen in Fig. 10. The O_2 respiration due to microorganisms is characterized by a simultaneous release of CO_2 (Höll et al., 2016). For this reason, high CO_2 and low O_2 as gas diffusing into the packaging was chosen as it can be seen in Fig. 5. The obtained results significantly differed to those in Fig. 9, for both, the PE-LD$_{50\,\mu m}$ and the PP covering. The non-destructive and destructive evaluation of O_2 was well in common, only having a statistical significance for the PE-LD$_{50\,\mu m}$ covering after 48 h and for the PP covering on point 0 h, however, that seems to be a random error. The CO_2 increased, while the O_2 decreased over the time, while the N_2 amounts did not change in a significant way, which proves that the created tray-system was tight. The values for N_2 have the greatest inaccuracy, because the N_2 value is obtained only by taking the difference between total pressure and the values for O_2 and CO_2.

A possible explanation for the different development in case of atmospheric air diffusion is as follows: The gas composition in the headspace of the perforated packing is changed quickly, since N_2 and O_2 diffusion occurs at approximately the same rate. However, permeation process of N_2 into the spot area is 4 times slower than O_2 permeation out
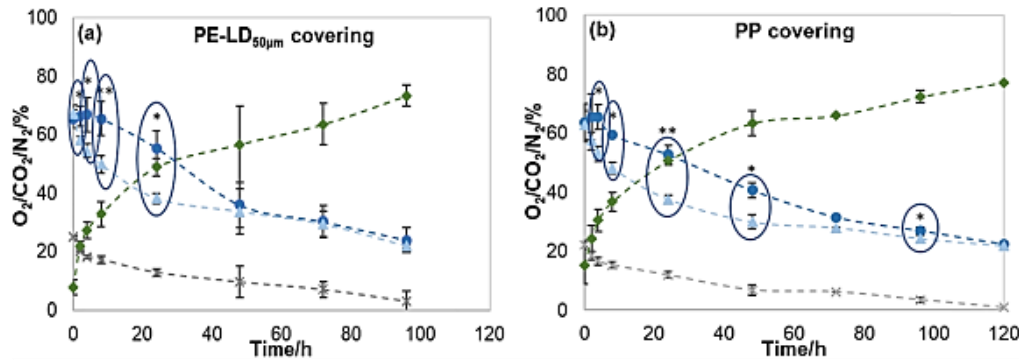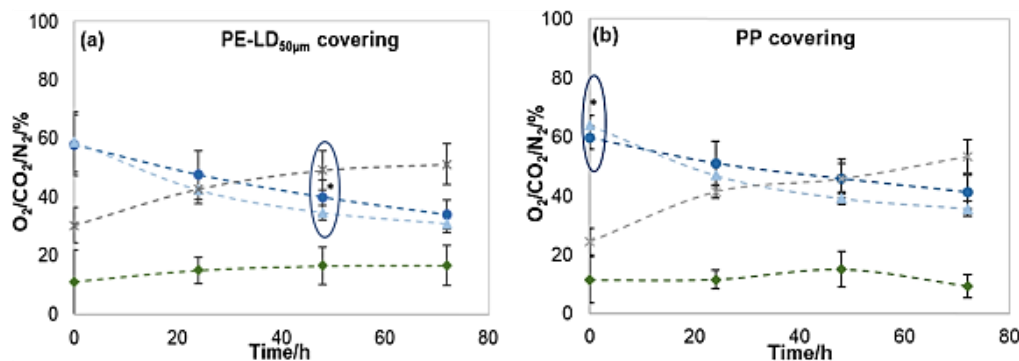
10

Fig. 9. Development of the gas composition in perforated (n = 1), modified atmosphere - filled (70% O_2/25% CO_2/5% N_2) food trays with integrated fluorescence material covered with polyethylene (PE-LD$_{50\,\mu m}$) **(a)** and polypropylene **(b)** and stored at 4 °C in ambient air (n = 4). Gas detection occurred non-destructively (O_2: ●) and destructively (O_2: ▲, CO_2: x, N_2: ◆) over a period of 96 h **(a)** and 120 h **(b)**. Indices and blue circles indicate a significant difference between the O_2 curves measured with destructive and non-destructive measurement devices:* $p \leq 0.05$, **$p \leq 0.01$, and ***$p \leq 0.001$.

Fig. 10. Development of the gas composition in perforated (n = 1) modified atmosphere - filled (60% O_2/25% CO_2/15% N_2) food trays with integrated fluorescence material covered with polyethylene (a) and polypropylene (PE-LD$_{50\,\mu m}$) (b) and stored at 4 °C in a 80% CO_2/20% O_2 atmosphere (n = 4). Gas detection occurred non-destructively (O_2: ●) and destructively (O_2: ▲, CO_2: x, N_2: ◆) over a period of 72 h. Indices and blue circles indicate a significant difference between the O_2 curves measured with destructive and non-destructive measurement devices: *$p < 0.05$, **$p \leq 0.01$, and ***$p \leq 0.001$.

of spot area, therefore an underpressure is created in the spot area. The O_2 partial pressure difference decreases, slowing down the permeation process. After a partial pressure balance is set, gas change in the spot space occurs in real time. However, this assumption cannot be explicitly proven, since nitrogen and CO_2 measurements in the spot space, as well as partial pressure determinations, would be necessary for this.

However, these results strongly indicate that the integration of fluorescence material in the way described in this publication are highly useful for the detection of gas changes within a closed system, however, packaging defects are not detectable in real-time within the first 48–72 h, which is a huge gap for cases where the system should be used for at-line outgoing goods inspection at the producer or incoming goods inspection at the distributor. To enhance this, further trials with optimized material with very high O_2 permeability for the covering of the sensor material has to be done.

3.5. Application in various food packaging

3.5.1. Microbiological analysis

The results for the determination of the TVC are shown in Fig. 11. It is very striking, that the initial bacteria count was very high, compared to those mentioned in the literature (Hilgarth, Lehner, Behr, & Vogel, 2019; Kameník, Saláková, Hulánková, & Borilova, 2015; Taylor, Down, & Shaw, 1990). However, for our research, the high initial CFU was
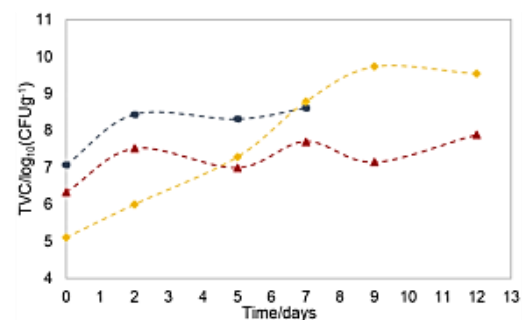
Fig. 11. Total viable count of minced beef (●) under high oxygen atmosphere, and vacuum packed type "Lyoner" sausage (◆) and beef steak (▲) stored at 4 °C for 7 (minced beef) and 12 ("Lyoner" and steak) days.

more advantageous, as changes would be visible more faster. Minced beef already reached the critical value for fresh beef of 10^7 CFU/g (Baumgart et al., 2016) on day 0, beef steak on day 2. For the type "Lyoner" sausage, that value was reached on day 5, however, for sliced boiled sausage, the guideline values of "The German Society for Hygiene and Microbiology" are 5×10^6 CFU/g, but no critical values are

11

available (The German Society for Hygiene and Microbiology, 2018). Nevertheless, the TVC for the sausage was the highest at the end of storage with 3.5×10^9 CFU/g, the beef steak showed a slower increase with values around 7.5×10^7 CFU/g after 12 days of storage. Minced beef was only stored for 7 days, finally reaching 4×10^8 CFU/g.

3.5.2. Development of gas composition

For all stored samples, changes from the initial O_2 gas concentration were detectable. Fig. 12 shows the results for minced beef. It can be seen clearly that the non-destructive and destructive measurements agreed well except for day 0, which again can be explained by the previously discussed permeation of O_2 into the spot-area. There were slightly significant deviations on day 5 and 7 between the two measurement principles, however, the decrease of O_2 was good visible for both measurements. Since the initial bacterial count for minced beef of 1.16×10^7 CFU/g was already very high, it is very likely that the change of O_2 in the headspace was due to microbial respiration. As we previously demonstrated in Dold et al. (2022), the change in O_2 headspace gas concentration was hardly detectable in poultry stored at 4 °C, even when the critical value of 10^7 CFU/g was reached. However, Kolbeck et al. (2019) have already shown the dependence of microbial respiratory activity on the presence of heme, which could be an explanation for the improved O_2 respiration in the experiments with minced beef compared to those with poultry. Therefore, the dominant bacterial species is therefore probably *Brochothrix thermosphacta*, as this bacterium is known to grow on minced beef at chilled temperatures, with simultaneous ability to respire O_2 to CO_2 (Hilgarth et al., 2019; Kolbeck et al., 2021).

Fig. 13 shows the development of O_2 gas concentration in empty and filled vacuum packed samples with integrated sensor material. In these experiments, the "Lyoner" type sausage was packed by setting the packaging machine to 100 hPa, whereas for the beef steak samples, the chamber vacuum was set to the minimum possible nominal value of 1 hPa. However, it was noticed for empty bags that the mean values of O2 gas concentration for both settings were in a similar range (~10–15%). This can have various reasons. For example, the samples and the packaging material still release absorbed water vapor and O_2, which is why lower O_2 partial pressures were apparently not achievable. However, this circumstance was advantageous for the evaluation of the product effect to the development of the O_2 gas concentration. The packed sausage showed a slow decrease in O_2 gas concentration within the first 5 days of storage. Then, a fast decrease occurred, with a significant deviation between the empty and the filled bags from day 7 on, with O_2
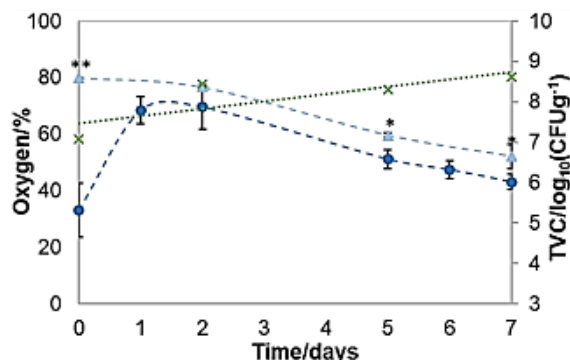
Fig. 12. Development of O_2 gas concentration in the headspace of packaged minced beef (80% O_2/20% CO_2) (n = 3) during 7 days of storage at 4 °C in PP trays, measured with a non-destructive (●) and a destructive (▲) device, with additional determination of the total viable count (x). Indices indicate a significant difference between the curve measured with destructive and non-destructive measurement devices: *$p < 0.05$, **$p < 0.01$.

values reaching almost zero. The steak samples showed an earlier and faster decrease in O_2 concentration, reaching the first significant deviation on day 2 and values around zero on day 5. The decrease of O_2 correlated very well with reaching a TVC of 10^7 CFU/g for both products.

The main spoilers for cooked vacuum packed sausages are lactic acid bacteria (LAB) (Kameník et al., 2015; Samelis et al., 2000), which are also able to respirate O_2 during growth (Kolbeck et al., 2019). According to (Jääskeläinen et al., 2016; Kameník et al., 2014; Sakala et al., 2002), the predominant species for vacuum packed beef steak samples are also LAB's, which makes the microbiologically induced O_2 consumption for this samples also very likely. *Brochothrix thermosphacta* and *Pseudomonas* seems to be suppressed by the presence of LAB's in vacuum packed samples (Blixt & Borch, 2002; Kameník et al., 2014). However, not only the presence of microorganisms are possible factors for O_2 decrease, also the absorption to the product itself might have an effect, but this effect probably occurs within the first 48 h (Chaix et al., 2015). The high standard deviations on day 5 and 6 for the type "Lyoner" sausage, and on day 1 and 2 for the beef steak indicate a difference in O_2 consumption, which underlines that this effect is individual for each sample and its microbiota (Dold et al., 2022; Kolbeck et al., 2021). For the evaluation of the shelf-life quality of vacuum packed meat and meat products, however, these results can only be applied to a limited extent, since the quantification of gas concentration in vacuum packaging is difficult. However, the decrease of O_2 was visible in our trials and was in a temporal context with reaching the critical value of 10^7 CFU/g.

3.5.3. Color measurement

The color measurement through the closed package could be an additional tool to evaluate the quality of food, as microbiological activities or chemical processes lead to oxidation, which could affect the color of the meat and meat products. As far as we know, this simple measurement has not been widely used for non-destructive quality evaluation of already packaged food, since in most studies the samples were unpacked before measurement (Dold & Langowski, 2022).

Fig. 14 shows the results for the L*a*b* color measurement during the storage period of 7 days of the high O_2 packed minced beef. It is clearly noticeable that the redness a* as well as the yellowness b* decreased significantly during storage. As we know from the gas determination (see Fig. 13), the O_2 concentration decreased also significantly during storage. Therefore it is not surprising that the red color of the minced beef decreased, and became greyish-brownish, as it can also be seen in the image below. The oxidation of oxymyoglobin (MbFe(II)) to metmyoglobin (MbFe(III)) by the absence of O_2 leads to a color change from red to brown in red muscle beef (Hood & Riordan, 1973). For high O_2 packed beef products, the non-destructive evaluation of the surface color might therefore be also an opportunity to evaluate the microbiological quality. However, further trials with lower initial bacteria counts would be useful for this purpose.

For the vacuum packaged samples (see Fig. 15) the results are not that clear. The type "Lyoner" sausage showed no trend in the change of L*a*b* color measurement. Only the brightness on day 7 and 12 deviated statistically significant, however, these are more probably random errors. This observation agrees well with the known literature, also no changes in the sausage color were observed (Kameník et al., 2015; Wenjiao et al., 2014). This is caused by the stability of nitrosylmyoglobin (pink coloration of type "Lyoner" sausage), as long as the samples are stored in the dark. A discoloration into brown generally occurs due to photooxidation (N. Böhner et al., 2014).

The steak samples showed significant changes in L* values compared to day 0, however, no trend was visible. These values – especially the redness a*- is in good agreement with the literature (Avilés et al., 2014; Lagerstedt et al., 2011). The lower a* values compared to the high O_2 packed samples are due to the lack of O_2, and the transition from oxymyoglobin to myoglobin (Boles & Pegg, 2010).

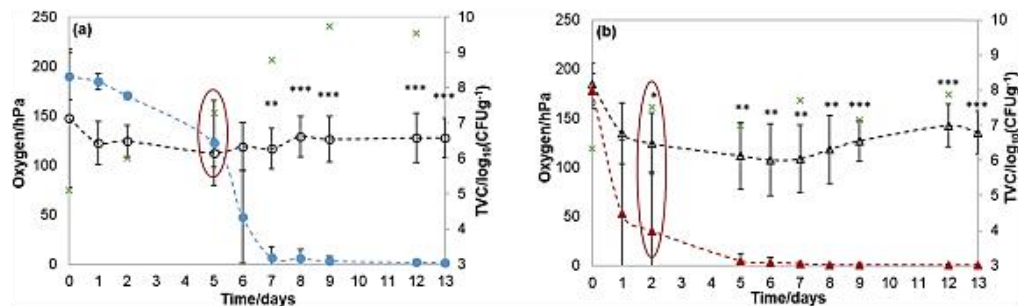The color measurements showed that for high O_2 packed red meat, a

12

Fig. 13. Development of O_2 gas concentration in empty (o/△) and filled (●/▲) vacuum bags over a storage period of 13 days at 4 °C: (a) type "Lyoner" sausage and (b) beef steak measured with a non-destructive device, with additional determination of the total viable count (x) (n = 3 for each sample). Indices indicate a significant difference between the oxygen curves with and without product: *$p < 0.05$, **$p < 0.01$, and ***$p < 0.001$. The red circle marks the point when the critical value of 10^7 CFU/g was reached.
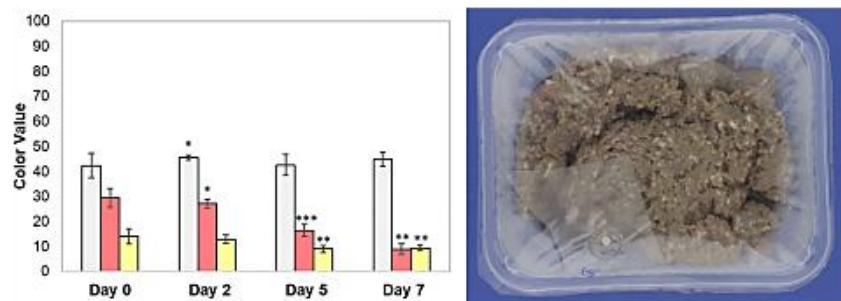
Fig. 14. Surface color measurement of minced beef during 7 days of storage (4 °C). Grey: L*- lightness, Red: a*- redness, Yellow: b*- yellowness. Indices indicate a significant difference between the L*, a* or b* values compared to day 0:* $P < 0.05$, ** $P < 0.01$, and *** $P < 0.001$ (left) and packaged minced beef with integrated sensor spot on day 7 (right).

simple, non-destructive measurement can give an evidence to the microbiological quality. For the vacuum packed samples, the color measurement gave no informative value.

4. Conclusion

This work was able to demonstrate that the integration of fluorophore-based sensor spots into food packaging systems for the non-destructive real-time determination of oxygen gas concentration is possible, with some limitations:

We showed that the usage of common food packaging materials as e. g. PP, PE-LD, PA and EVOH has no influence to the measurement quality, even if the sensor-material is heat-treated at different heat-sealing steps for the integration of the fluorophores into the lid-film of packages. The covering of the sensor-material with an additional lid-film was chosen for the following reasons: We wanted to assess predominantly the composition of the gas atmosphere during storage for shelf life monitoring. Here, not only the protection of the food against migration of substances from the sensor-materials has to be ensured, but the sensor material has also to be protected against contamination by the food in order to guarantee the required measurement precision.

We also demonstrated that the fluorophores appear to be most stable when the integrated sensor spots are stored at 6 °C. Covering the sensor material with a highly gas-permeable monofilm by heat sealing resulted in tight seam seals. This configuration does not lead to any critical migration of components of the sensor spot, so that food law conformity can be expected. The latter has to be further evaluated by conformity tests in future. The sealing of the sensor spots onto the intact lidding film, however, would create bumps that would hinder proper winding of the film. Therefore, we propose integration directly in the packaging.

The device for this and its practical application would still have to be developed and verified.

The response-time of the oxygen partial pressure measured in the closed system, as well as the "real-time determination" after the integration process led to different results and pointed out some difficulties:

It is also clear that - due to the response time of the sealed-in sensor of 2–3 days - checking the gas composition in the headspace at the exit of the packaging machine, e.g. for leak testing, would lead to erroneous results. The concept is thus particularly suitable for monitoring relatively slow spoilage processes, such as those that occur during microbial growth.

As final application test, we were able to demonstrate the usability of the set-up for the determination of microbiologically induced quality changes: Minced beef stored at high oxygen concentrations clearly reduced the head-space oxygen gas concentration when a critical microbiologic value of 10^7 CFU/g was reached. The decrease of the oxygen gas-concentration in the headspace was measurable with the non-destructive fluorescence based method with the integrated sensor material, as well as with the destructive reference method.

In addition, we also successfully demonstrated that a simple color measurement through the intact package can also be used for non-destructive quality evaluation of minced beef in a transparent, high oxygen MAP packaging.

The integration of sensor spots for vacuum packed meat and meat-products were also possible, however, the measurement is more complex in this case, as remaining water vapor or solved oxygen in the product and packaging material increases the partial pressure afterwards. However, we were also able to show a temporal correlation between the decrease of O_2 partial pressure and the reaching of the microbiological critical value for vacuum packed beef steak and type
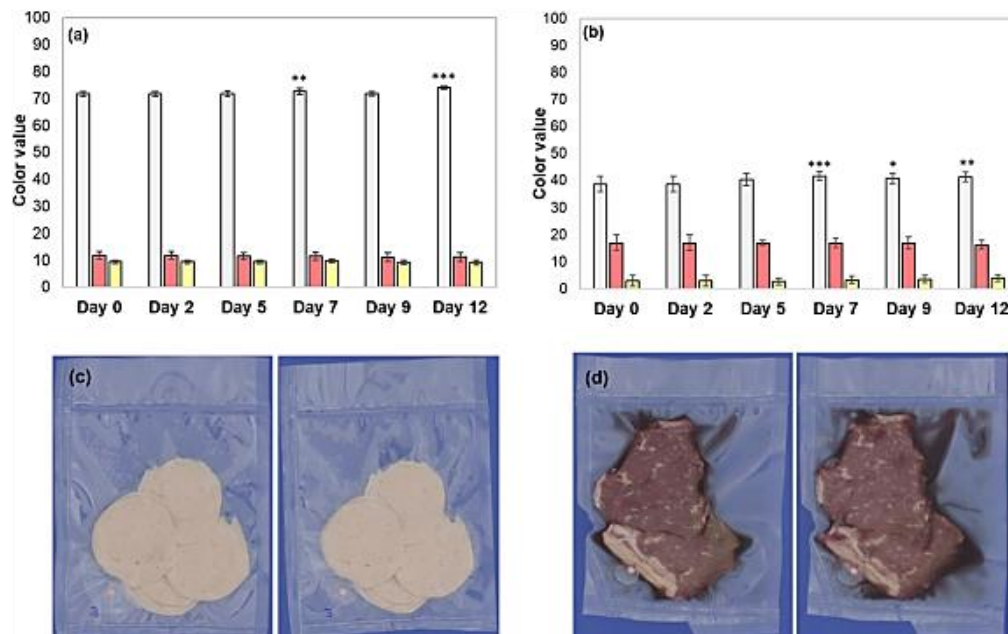
13

Fig. 15. (a)+(b) Surface color measurement of a) type "Lyoner" sausage and b) beef steak during 12 days of storage (4 °C). Grey: L* - lightness, Red: a* - redness, Yellow: b*- yellowness. Indices indicate a significant difference between the L*, a* or b* values compared to day 0:*$p < 0.05$, **$p < 0.01$, and ***$p < 0.001$. (c) + (d) packaged samples with integrated senor spot on day 0 (left) and day 12 (right).

"Lyoner" sausage, as well. A correlation with the color-change was, however, not detectable for these samples. In summary, we can say that the developed packaging-system is mainly suitable for the determination of headspace oxygen gas concentration during the storage of a product and here, to detect a change in the gas atmosphere caused by microbiological or chemical processes. Covering the sensor-spot in this application also has the advantage that the measurement might not be disturbed by possible contamination from the food product e.g. meat juice.

Funding

CRediT authorship contribution statement

Jasmin Dold: Conceptualization, Methodology, Validation, Formal analysis, Investigation, Data curation, Writing – original draft, Visualization, Project administration. **Melanie Eichin**: Methodology, Validation, Formal analysis, Investigation. **Horst-Christian Langowski**: Conceptualization, Methodology, Writing – review & editing, Supervision, Funding acquisition.

Declaration of Competing Interest

The authors declare that they have no known competing financial interests or personal relationships that could have appeared to influence the work reported in this paper.

Data availability

Data will be made available on request.

Acknowledgments

References

American Society for Testing and Materials, 2004, Standard Test Method for Detecting Seal Leaks in Porous Medical Packaging by Dye Penetration (F1929 - 98(2004)).

Arndt, G.W., 1995, Examination of Flexible and Semirigid Food Containers for Integrity: Gaithersburg: AOAC International. Bacteriological Analytical Manual, 2.35–22.74.

Avilés, C., Juárez, M., Larsen, I. L., Rodas-González, A., & Aalhus, J. L. (2014). Effect of multiple vacuum packs on colour development and stability in beef steaks. *Canadian Journal of Animal Science, 94*(1), 63–69. https://doi.org/10.4141/CJAS2013-037

Banerjee, S., Kelly, C., Kerry, J. P., Joseph, P., & Papkovsky, D. B. (2016). High throughput non-destructive assessment of quality and safety of packaged food products using phosphorescent oxygen sensors. *Trends in Food Science & Technology, 50*, 85–102. https://doi.org/10.1016/j.tifs.2016.01.021

Baumgart, J. , Becker, B. , & Stephan, R. (Eds.), 2016, Mikrobiologische Untersuchung von Lebensmitteln: Ein Leitfaden für das Studium (6th ed.). B.Behr's Verlag GmbH & Co. KG.

Blixt, Y., & Borch, E. (2002). Comparison of shelf life of vacuum-packed pork and beef. *Meat Science, 60*(4), 371–378. https://doi.org/10.1016/S0309-1740(01)00145-0

Böhner, N., Hösl, F., Rieblinger, K., & Danzl, W. (2014). Effect of retail display illumination and headspace oxygen concentration on cured boiled sausages. *Food Packaging and Shelf Life, 1*(2), 131–139. https://doi.org/10.1016/j.fpsl.2014.04.003

Böhner, N., & Rieblinger, K. (2016). Impact of different visible light spectra on oxygen absorption and surface discoloration of bologna sausage. *Meat Science, 121*, 207–209. https://doi.org/10.1016/j.meatsci.2016.06.019

Boles, J., & Pegg, R. (2010). Meat color. Montana State University and Saskatchewan Food Product Innovation.

Chaix, E., Couvert, O., Guillaume, C., Gontard, N., & Guillard, V. (2015). Predictive Microbiology Coupled with Gas (O 2 /CO 2) Transfer in Food/Packaging Systems: How to Develop an Efficient Decision Support Tool for Food Packaging Dimensioning. *Comprehensive Reviews in Food Science and Food Safety, 14*(1), 1–21. https://doi.org/10.1111/1541-4337.12117

Church, I. J., & Parsons, A. L. (1995). Modified atmosphere packaging technology: a review. *Journal of the Science of Food and Agriculture, 67*, 143–152.

14

87

DIN Standards Committee Packaging, 2014, DIN 53380–5: Testing of plastics - Determination of gas transmission rate - Part 5: Optical method for plastic films and moulded plastic parts. Beuth Verlag GmbH.

Dold, J., Kehr, C., Hollmann, C., & Langowski, H.-C. (2022). Non-destructive measuring systems for the evaluation of high oxygen stored poultry: development of headspace gas composition, sensory and microbiological spoilage. Foods, 11(4), 592. https://doi.org/10.3390/foods11040592

Dold, J., & Langowski, H.-C. (2022). Optical measurement systems in the food packaging sector and research for the non-destructive evaluation of product quality. Food Packaging and Shelf Life, 31, Article 100814. https://doi.org/10.1016/j.fpsl.2022.100814

Escobedo Araque, P., Perez de Vargas Sansalvador, I. M., Lopez Ruiz, N., Erenas, M. M., Carvajal Rodriguez, M. A., & Martinez Olmos, A. (2018). Non-invasive oxygen determination in intelligent packaging using a smartphone. IEEE Sensors Journal, 18 (11), 4351–4357. https://doi.org/10.1109/JSEN.2018.2824404

Franz, R., Gmeiner, M., Gruner, A., Kemmer, D., & Welle, F. (2016). Diffusion behaviour of the acetaldehyde scavenger 2-aminobenzamide in polyethylene terephthalate for beverage bottles. Food Additives & Contaminants Part A, Chemistry, Analysis, Control, Exposure & Risk Assessment, 33(2), 364–372. https://doi.org/10.1080/19440049.2015.1128566

German Institute for Standardization, 2004, Materials and articles in contact with foodstuffs – Plastics substances subject to limitation - Part 1: Guide to test methods for the specific migration of substances from plastics to foods and food simulants and the determination of substances in plastics and the selection of conditions of exposure to food simulants; (DIN EN 13130–1). Berlin. Beuth Verlag GmbH.

German Institute for Standardization, 2017, Water quality - Application of inductively coupled plasma mass spectroscopy (ICP-MS) - Part 2: Determination of selected elements including uranium isotopes (DIN EN ISO 17294–2). Berlin. Beuth Verlag GmbH.

The German Society for Hygiene and Microbiology, 2018, Mikrobiologische Richt- und Warnwerte zur Beurteilung von Lebensmitteln: Richt- und Warnwerte für Brühwurst, Kochwurst, Kochpökelwaren sowie Sülzen und Aspikwaren auf Handelsebene. ⟨https://www.dghm.org/wp-content/uploads/2018/10/Entw%C3%BCrfe_03.18_Ver%C3%B6ff._NEU.pdf⟩.

Haar, L., Gallagher, J. S., & Kell, G. S. (1988). In U. Grigull (Ed.), NBS/NRC Wasserdampftafeln: Thermodynamische und Transportgrößen mit Computerprogrammen für Dampf und Wasser in SI-Einheiten. Springer Berlin Heidelberg. https://doi.org/10.1007/978-3-642-52087-7.

Havens, M.R., Austin, D.C., & Paul, D.J. (2007). Method and Apparatus for Measuring Oxygen Concentration(WO2007/106776 A1).

Herbert, U., Albrecht, A., & Kreyenschmidt, J. (2015). Definition of predictor variables for MAP poultry filets stored under different temperature conditions. Poultry Science, 94(3), 424–432. https://doi.org/10.3382/ps/peu002

Hilgarth, M., Lehner, E. M., Behr, J., & Vogel, R. F. (2019). Diversity and anaerobic growth of Pseudomonas spp. Isolated from modified atmosphere packaged minced beef. Journal of Applied Microbiology, 127(1), 159–174. https://doi.org/10.1111/jam.14249

Höll, L., Behr, J., & Vogel, R. F. (2016). Identification and growth dynamics of meat spoilage microorganisms in modified atmosphere packaged poultry meat by MALDI-TOF MS. Food Microbiology, 60, 84–91.

Hood, D. E., & Riordan, E. B. (1973). Discolouration in pre-packaged beef: measurement by reflectance spectrophotometry and shopper discrimination. International Journal of Food Science and Technology, 8, 333–343.

Huber, C. (2008). Wie viel kommt durch? Ermittlung der Sauerstoffdurchlässigkeit von PET-Flaschen. Getränkeindustrie, 11, 48–57.

Hurme, E. U., & Ahvenainen, R. (1998). A nondestructive leak detection method for flexible food packages using hydrogen as a tracer gas. Journal of Food Protection, 61 (9), 1165–1169. https://doi.org/10.4315/0362-028X-61.9.1165

Jääskeläinen, E., Hultman, J., Parshintsev, J., Riekkola, M.-L., & Björkroth, J. (2016). Development of spoilage bacterial community and volatile compounds in chilled beef under vacuum or high oxygen atmospheres. International Journal of Food Microbiology, 223, 25–32. https://doi.org/10.1016/j.ijfoodmicro.2016.01.022

Kameník, J., Saláková, A., Hulánková, R., & Borilova, G. (2015). The effect of high pressure on the microbiological quality and other characteristics of cooked sausages packed in a modified atmosphere or vacuum. Food Control, 57, 232–237. https://doi.org/10.1016/j.foodcont.2015.04.010

Kameník, J., Saláková, A., Pavlík, Z., Bořilová, G., Hulanková, R., & Steinhauserová, I. (2014). Vacuum skin packaging and its effect on selected properties of beef and pork meat. European Food Research and Technology, 239(3), 395–402. https://doi.org/10.1007/s00217-014-2233-9

Kelly, C., Yusufu, D., Okkelman, I., Banerjee, S., Kerry, J. P., Joe, P., Mills, A., & Papkovsky, D. B. (2020). Extruded phosphorescence based oxygen sensors for large-scale packaging applications. Sensors and Actuators B: Chemical, 304, Article 127357. https://doi.org/10.1016/j.snb.2019.127357

Kolbeck, S., Hilgarth, M., & Vogel, R. F. (2021). Proof of concept: Predicting the onset of meat spoilage by an integrated oxygen sensor spot in MAP packages. Letters in Applied Microbiology, 73(1), 39–45. https://doi.org/10.1111/lam.13473

Kolbeck, S., Reetz, L., Hilgarth, M., & Vogel, R. F. (2019). Quantitative oxygen consumption and respiratory activity of meat spoiling bacteria upon high oxygen modified atmosphere. Frontiers in Microbiology, 10, 2398.

Krottmaier, J., & Ribitsch, V. (2015). Measurement of the Fluorescence of an Idicator in a Gas-Tight Packaging, which Contains Products Having Limited Storage Time (WO2015/172166 A1).

Lagerstedt, Å., Ahnström, M. L., & Lundström, K. (2011). Vacuum skin pack of beef–a consumer friendly alternative. Meat Science, 88(3), 391–396. https://doi.org/10.1016/j.meatsci.2011.01.015

Lakowicz, J.R. (2006). Principles of Flourescence Spectroscopy (3rd ed.). Springer Science+Business Media, LLC.

Lee, K., Park, H., Baek, S., Han, S., Kim, D., Chung, S., Yoon, J.-Y., & Seo, J. (2019). Colorimetric array freshness indicator and digital color processing for monitoring the freshness of packaged chicken breast. Food Packaging and Shelf Life, 22, Article 100408 (Article).

Mortimer, C.E., & Müller, U. (2020). Chemie: Das Basiswissen der Chemie (13., vollständig überarbeitete Auflage). Georg Thieme Verlag.

O' Callaghan, K. A. M., Papkovsky, D. B., & Kerry, J. P. (2016). An Assessment of the Influence of the Industry Distribution Chain on the Oxygen Levels in Commercial Modified Atmosphere Packaged Cheddar Cheese Using Non-Destructive Oxygen Sensor Technology. Sensors (Basel, Switzerland), 16(6). https://doi.org/10.3390/s16060916

Robertson, G.L., 1993, Food packaging: Principles and practice. Packaging and converting technology: Vol. 6. Dekker. ⟨http://www.loc.gov/catdir/enhancements/fy0745/92025591-d.html⟩.

Sakala, R., Hayashidani, H., Kato, Y., Hirata, T., Makino, Y., Fukushima, A., Yamada, T., Kaneuchi, C., & Ogawa, M. (2002). Change in the composition of the microflora on vacuum-packaged beef during chiller storage. International Journal of Food Microbiology, 74(1–2), 87–99. https://doi.org/10.1016/S0168-1605(01)00732-2

Samelis, J., Kakouri, A., & Rementzis, J. (2000). Selective effect of the product type and the packaging conditions on the species of lactic acid bacteria dominating the spoilage microbial association of cooked meats at 4°C. Food Microbiology, 17(3), 329–340. https://doi.org/10.1006/fmic.1999.0316

Santovito, E., Elisseeva, S., Cruz-Romero, M. C., Duffy, G., Kerry, J. P., Joseph, P., & Papkovsky, D. B. (2021). A Simple Sensor System for Onsite Monitoring of O2 in Vacuum-Packed Meats during the Shelf Life. Sensors (Basel, Switzerland), 21(13). https://doi.org/10.3390/s21134256

Steffen, A., Jaindl, R., & Krottmaier, J. (2018). Gas Concentration Measurement with Temperature Compensation(WO2018/202784 A1).

Taylor, A. A., Down, N. F., & Shaw, B. G. (1990). A comparison of modified atmosphere and vacuum skin packing for the storage of red meats. International Journal of Food Science & Technology, 25(1), 98–109. https://doi.org/10.1111/j.1365-2621.1990.tb01064.x

Wenjiao, F., Yunchuan, C., Junxiu, S., & Yongkui, Z. (2014). Effects of tea polyphenol on quality and shelf life of pork sausages. Journal of Food Science and Technology, 51(1), 191–195. https://doi.org/10.1007/s13197-013-1076-x

7.3 Publication III

A non-destructive measuring device in the mid-infrared range for measuring the CO_2 concentration in the headspace of food packaging

Jasmin Dold [a,b,*], Lukas Götzendörfer [c], Clarissa Hollmann [a,d], Horst-Christian Langowski [e,f]

[a] Chair of Brewing and Beverage Technology, Technical University of Munich, Weihenstephaner Steig 20, 85354, Freising, Germany
[b] BayWa AG, Arabellastraße 4, 81925, Munich, Germany
[c] KNESTEL Technologie & Elektronik GmbH, Osterwalder Straße 12, 87496, Hopferbach, Germany
[d] Roche Diagnostics GmbH, Nonnenwald 2, 82377, Penzberg, Germany
[e] TUM School of Life Sciences, Technical University of Munich, Weihenstephaner Steig 22, 85354, Freising, Germany
[f] Fraunhofer Institute for Process Engineering and Packaging, Giggenhauser Str. 35, 85354, Freising, Germany

ABSTRACT

Carbon dioxide (CO_2) is the most common gas used in modified atmosphere packaging (MAP) to protect packaged foods from spoilage and pathogenic microorganisms and thus extend the shelf life of food products. Non-destructive measurement of CO_2 concentration of the packaging headspace is of great interest as it could be used at various stages of the value chain, from outgoing goods inspection to storage tests and possible monitoring of the modified atmosphere at retail. Therefore, the aim of this work was to develop a measuring device operating non-destructively on closed MAP trays. Absorption measurement in the mid-infrared range at four different wavelengths proved to be a suitable principle for determining the CO_2 gas concentration in a closed packaging system: 4.26 µm (2347 cm^{-1}) and 4.27 µm (2342 cm^{-1}) in the range of the antisymmetric stretching vibration, as well as 4.45 µm (2247 cm^{-1}) at the edge of the antisymmetric stretching vibration, and 3.95 µm (2532 cm^{-1}) as a reference measurement outside the absorption band with a thermal infrared source. Measurement principle and setup - the measurement in the absorbing and non-absorbing range and the guiding of the thermal infrared (IR) emitter at a 45° angle through the corner of the tray - allows a measurement largely independent of tray shape, height, and packaged product. The measurement can also be used for pigmented and printed trays - except for carbon black pigments. Optical impairments of the packaging and labeled areas of the lidding film appeared to have the greatest influence on the measurement accuracy. The applicability of the measurement system was evaluated and successfully demonstrated using commercially available food packaging from a local supermarket by comparing the CO_2 gas concentrations yielded with those obtained using a destructive measurement device.

1. Introduction

In terms of food quality, packaging food in polymer-based packaging is one of the most important processing steps. The packaging is among others responsible for the protection of food against mechanical and atmospheric influences, exogenous water, light and aroma loss, and chemical, physical or biological contaminations ((Piringer and Baner, 2008; Singh et al., 2017).To retain the quality during storage for longer periods, many food products are packed under a protective gas atmosphere, a technique called modified atmosphere packaging (MAP). As gases potentially acting against spoilage, nitrogen (N_2), carbon dioxide (CO_2) and oxygen (O_2) are used most often. The special function of CO_2 consists in inhibiting microorganisms, as it has a toxic effect on

organisms at concentrations of 20% (v/v) and higher (Gill and Tan, 1980; Mortazavi et al., 2023).

However, the gas concentration changes during storage of the packaged product for various reasons. The difference in partial pressure inside and outside of the packaging leads to permeation processes through the polymer (Langowski, 2017; Piringer and Baner, 2008), which can lead to a decrease or increase in the concentration of the respective gas inside the packaging. In case of CO_2, the gas will always permeate from the inside of the packaging to the outside, as its atmospheric concentration relative to the inside of the package is virtually zero (0.042 %) (Boetcher et al., 2023). Other reasons for changes in headspace gas composition are absorption and desorption processes of the product and the packaging material, as well as chemical and

microbiological processes (Chaix et al., 2015; Chmiel et al., 2018; Kolbeck et al., 2019; Tofteskov et al., 2019). In summary, the CO_2 concentration in a package is the result of the adjusted modified atmosphere, the film permeability and the CO_2 respiration and sorption processes of the product and the packaging material, which influences the shelf life.

Beside these "natural factors", also packaging defects or perforations induced by improper transport can lead to unwanted gas concentration changes and therefore quality loss.

CO_2 can be detected via infrared (IR) spectroscopy. The gas has weaker and stronger absorption bands in the near infrared, the mid infrared as well as in the far infrared spectra (Atkins et al., 2022; BERNSTEIN et al., 2005; Wordsworth et al., 2010). In the near infrared (NIR: 0.8–2.5 μm or 12500–4000 cm^{-1}) and the mid infrared (MIR: 2.5 μm–50 μm or 4000–200 cm^{-1}), the absorption is created by the excitation of molecular vibrations, and in the far infrared (FIR: 50 μm–500 μm or 200–20 cm^{-1}) due to rotations of the molecules (Atkins et al., 2022). The strongest absorption band of CO_2 is located at 4.26 μm (2349 cm^{-1}) in the MIR (G. Zhang and Wu, 2004), which is known as normal mode ν_3, an antisymmetric stretch vibration (Atkins et al., 2022).

Thermoformed polymer trays are common packaging types, often consisting of polypropylene (PP), polyethylene terephthalate (PET) and polyethylene (PE) as monomaterials or multilayer thermoplasts having an additional barrier such as thylene vinyl alcohol copolymer (EVOH). To shape the polymers into the desired packaging form, films are heated and formed into a tray with the use of pressure and molds. This tray in turn can be sealed with a lid film by a heat-sealing process after the food has been inserted (e.g. under protective gas) (Piringer and Baner, 2008). In the course of this heating and cooling process, the amorphous-to-crystalline ratio of the polymer is affected. The degree of crystallinity depends on the cooling rate, additives and the number of branches, with slower cooling and a lower number of branches resulting in a higher crystalline content. Generally, the higher the crystalline fraction of a thermoplast is, the lower is the (visual) light transmittance due to light scattering by the crystallites (Lee et al., 2008; Lin et al., 2020).

Using IR light sources for the non-destructive determination of the quality of already packaged food is a topic of broad interest in the industry and food science, and therefore, a lot of research has already been carried out. For the first time in 1992, NIR reflectance spectroscopy and NIR transmission spectroscopy were used to analyze fat, protein and water content of beef through a multi-layer film (Isaksson et al., 1992). In this case, the light source was guided directly on the product surface, which is why this measurement can be categorized as *direct* measurement of product quality parameters. The *direct* measurement has also been used for the determination of adulteration or authenticity (Parastar et al., 2020; Schmutzler et al., 2016) or spoilage (Arias et al., 2022; Girón et al., 2014; Grau et al., 2011; W. Zhang et al., 2023) of food products. However, the *direct* measurement has a disadvantage that changes in the absorption spectra may have different causes, or that several absorption bands overlap. This always leads to the fact that the results are to be interpreted with a certain uncertainty. When using an *indirect* measurement method, in this case the measurement of the concentration of a specific gas is carried out at a specified wavelength in the headspace of the packaging to quantify a change in quality, overlapping bands of the product itself can be neglected. This was for example done by analyzing CO_2 in milk or milk beverages via Tunable Diode Laser Absorption Spectroscopy (TDLAS) and to correlate the CO_2 development with the microbiological spoilage, as it is known that the growth of microorganisms leads to the increase of the CO_2 concentration in the headspace (Danilovic et al., 2016; Danilović et al., 2018; T. Li et al., 2017). The quantification of CO_2 concentration using TDLAS has also been successfully used to monitor microbiological spoilage, e.g. by spore formers such as *Bacillus fengqiuensis* in aseptically packaged food (Myintzaw et al., 2023). TDLAS is a good application for the non-destructive detection of CO_2 in the IR range. However, TDLAS has

the disadvantage that the measurement set-up is considerably more expensive than a thermal IR emitter, which is why the latter is more suitable for inexpensive production of practical hand-held devices for use in retail for incoming goods inspection, for example.

Existing commercial handheld devices on the market for the detection of CO_2 gas concentration in protective gas packaging are either invasive (i.e. the packaging is perforated with a fine needle, which is used to extract gas from the packaging), or they calculate the CO_2 gas concentration based on the measured O_2 gas concentration. The O_2 content is measured at a wavelength of 760 nm, which limits the usability of these devices to transparent packaging only (Czerwiński et al., 2021). In addition, they work with a beam path that passes vertically through the lidding film from above, which means that the positioning of the food in the packaging is always a disruptive factor. This factor will become even more relevant in the future, as the packaging levy set out in the Single-Use Plastics Directive (European Union, 2019) will have to be borne directly by food manufacturers in Germany from 2024 and will therefore lead to savings in packaging material, meaning that packaging will tend to be smaller.

No study on the non-destructive optical detection of gases in MAP packaging has so far dealt with all packaging-relevant influencing factors such as shape, polymer type, polymer composition, pigmentation and the influence of food residues on measurement precision (Dold and Langowski, 2022). Although the individual transmission values in the corresponding IR range of specific polymers can be found in the literature, practical correlations such as influence of the polymer structure after the thermoforming process have not been the focus of the literature to date. There is also no known study on the transmission behavior of differently pigmented food polymer packaging. Other practical influencing factors such as condensate or food residues are also a gap in the literature, as most approaches take place under optimized laboratory conditions. The developed construction presented in the following article must intentionally address practice-relevant influencing factors, as the developed prototype is intended for a convenient application in industry and food retail.

To close these gaps, we built a novel, non-destructive measurement device, using four different wavelengths in the mid-infrared for the determination of the CO_2 concentration in the packaging headspace through a polymer tray, using a thermal infrared source: 4.26 μm (2347 cm^{-1}) and 4.27 μm (2342 cm^{-1}) in the range of the antisymmetric stretching vibration of CO_2 as well as 4.45 μm (2247 cm^{-1}) which is located at the side edge of the band (Atkins et al., 2022; NIST, 2023) and 3.95 μm (2532 cm^{-1}) as a reference measurement outside the absorption band. The thermal IR emitter is guided at a 45° angle through the corner of a tray, which leads to several advantages such as independency of the tray shape, height and filling good, as well as a constant length of the measurement path. We further evaluated different factors influencing the measurement quality, such as packaging shape, color (pigments and printings), polymer defects and optical polymer irregularities, as well as food and water residues inside the packaging. To make a statement about the applicability and limitations of the device e.g. for the quality control in logistics and retail, we analyzed the headspace composition of commercial MAP packed products in trays of different colors, shapes, materials and designs with the developed non-destructive measurement device and compared the results using an invasive CO_2 gas analyzer, which extracts small aliquots of the gas atmosphere by inserting a needle through the lid film of the packaging.

2. Materials and methods

2.1. Non-destructive measurement device

For the non-destructive detection of CO_2, a novel measurement device ("Demonstrator") was constructed. The principle for the CO_2 detection is the use of MIR spectroscopy.

The non-destructive measurement device was constructed in such a

2

way that a conventional packaging tray – such as it is used for the packaging of MAP products – can be measured. Therefore, a rail system was integrated, which served as holder, so the packaging could be easily placed into the device (compare Fig. 1) without having to hold it manually during measurement. That is also an advantage when it comes to standardization of the measurement, as the measured trays are fixed in a standardized position.

A miniaturized thermal mid infrared source (MIR-source), which can be modulated in frequencies up to 6 Hz, was used for the investigations presented here. The emission characteristic is close to that of a black-body emitter, whose significant part of its spectral power density lies within the MIR at the operating temperature of the source of 600 °C (Hlavatsch and Mizaikoff, 2022; Schossig et al., 2015). Detection of the transmitted radiation was performed using a 4-channel pyroelectric detector with optical bandpass filters with different transmission ranges positioned in front of its four detector segments. Of the four channels, three are sensitive to CO_2 because they have a spectral overlap with the main CO_2 absorption bands mentioned in the introduction. One channel has a filter that is far from any CO_2 absorption, thus acting as a reference channel that only responds to the total radiation intensity (compare Table 1 and Fig. 3).

The MIR-source (HIS550R–0WC TO-39/TO-5 Thermal Infrared Emitter, Infrasolid GmbH, Dresden, Germany) and the detector (LIM-054-#, Pyromid® multi channel pyroelectric detector, InfraTec GmbH, Dresden, Germany) were placed in such a way that the thermal IR emitter beam is guided at a 45° angle through the corner of the tray. This has the advantage that no packaged food product could disrupt the measurement and a constant measurement path – independent of the tray size – can always be guaranteed. Fig. 2 shows the path of the thermal IR emitter in a technical drawing (side view, without the electronical components). The technical data of the thermal IR emitter and the detector are shown in Table 1.

Due to the simultaneous reference measurement at 3.95 μm, it is probably possible to compensate to a large extent for different transmission characteristics of the packaging, e.g. due to optical inhomogeneities or impurities, in relation to the measurement in the absorption ranges of the CO_2, as long as the packaging material has a certain residual transmission in the wavelength range between 3.9 μm and 4.6 μm.

Fig. 3 illustrates the measurement ranges of the different channels in accordance with the infrared transmittance spectra of CO_2 in the region of the asymmetric stretching vibration (Atkins et al., 2022; NIST, 2023). The figure shows that channels 1 and 3 measure directly on the CO_2 absorption band, channel 2 at the edge of the absorption band and the reference channel 4 uses the range where no CO_2 absorption is present.

The sensor temperature was set to 40 °C, as the detection was most

Table 1
Technical data of the IR emitter and the detector. NBP=Narrow Bandpass Filter with bandwidth (full width at half maximum); AOI = angle of incidence.

| Light Source		Detector and Measuring Ranges	
Thermal IR Emitter		Multi Channel Detector (manufacturer designation)	
Wavelength range	2–20 μm	Channel 1 ("CO_2 standard")	4.26 μm (NBP: 180 nm)
Modulation frequency	6 Hz	Channel 2 ("CO_2 long path")	4.45 μm (NBP: 60 nm)
Optical output power	max. 215 mW	Channel 3 ("CO_2 high AOI")	4.27 μm (NBP: 170 nm)
Electrical power	max. 700 mW	Channel 4 ("Reference")	3,95 μm (NBP:90 nm)
Radiating element temperature	600 °C at 650 mW		
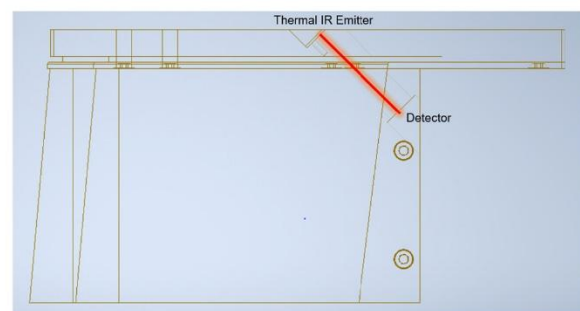
Fig. 2. Technical drawing (side view) to show the measuring path (without electronics) of the Demonstrator.

stable at this temperature and especially condensation effects at high air humidity could be avoided. For the measurement, a microcomputer (Raspberry Pi 2 Modell B v1.1, Raspberry Pi Ltd, Cambridge, United Kingdom) is connected to the laptop or computer, and the IP address specified for it must be connected. After successful connection, a web interface can be opened, through which the measurement can be monitored.

2.2. Calibration

Calibration can be performed with zero gas (in this work we used ambient air) as well as with a defined CO_2 concentration (="End-calibration").
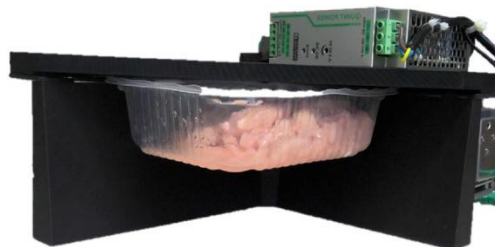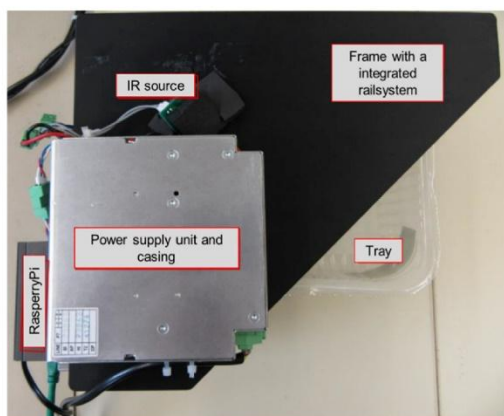
Fig. 1. Non-destructive measurement device ("Demonstrator"): top view (left) and side view with a MAP tray filled with poultry (right).
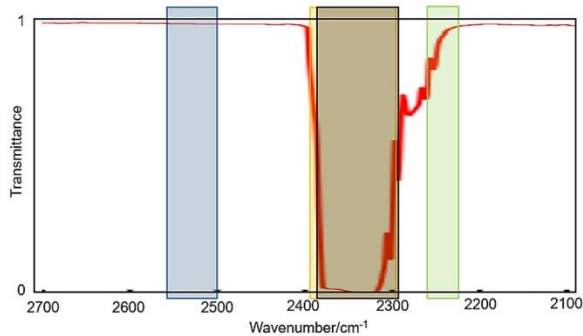
Fig. 3. CO_2 infrared spectra (adapted to NIST, 2023) with the plotted channels/bandpass filters used in the detector: channel 1 (yellow), channel 2 (green), channel 3 (black) and channel 4 (blue). The area of the markings shows the measurement area of the band pass filters.

Zero gas calibration is performed to set a value for transmittance when no sample gas is present. For this, a tray with the desired tray-shape was purged and filled with a mixture of 80 % (v/v) N_2 and 20 % (v/v) O_2 and closed by heat sealing of the lid film.

As second calibration point, a defined CO_2 gas concentration was used. Therefore, the tray was flooded with a test gas (40% (v/v) CO_2/ 60% (v/v) O_2 or 20% (v/v) CO_2/80% (v/v) O_2, both Linde GmbH, Pullach, Germany), by perforating the tray on two opposite sides with a needle and flooding the gas mixture in a flow mode trough the tray (10 min). The holes were sealed with a septum afterwards, to ensure a stable gas concentration during the calibration. The calibration as well as the measurement can only start after the device reached its operating temperature of 40 °C. To ensure a stable value of the measured CO_2 gas concentration, a waiting period of 45 s is needed for a stable value for all channels.

2.2.1. Measurement

After successful calibration, the measurement can be done as follows: As soon as the operating temperature of 40 °C is reached, the status displayed in the web interface changes from "heating" to "empty". Then the tray to be measured should be placed carefully into the rail system (compare Fig. 1), which leads to the change of the status "empty" to "ready". After 45 s, the measurement can occur.

2.3. Influence of different packaging properties to the measuring quality

2.3.1. Packaging shape

One question was whether the measurement accuracy would benefit from a special tray geometry in form of a straight "test corner". Therefore, trays in two different shapes were tested and the results were compared to those obtained with the standard tray with the roundish corner. The first test corner consisted of two straight surfaces integrated into the tray surface, one of which was parallel to the top and the other connected to it perpendicularly at the edge of the tray. Therefore, the radiation of the thermal IR emitter entered the tray at an angle of 45° and exited at the same angle. The second standard corner was integrated into the packaging at an angle so that a 90° angle to the IR beam was achieved (see Fig. 4).

To prepare these corners, transparent, flat polypropylene (PP) pieces were cut out of transparent PP trays, shaped accordingly, inserted into a corner of a transparent PP tray (205x160 × 50mm, ES-Plastic GmbH, Hutthurm, Germany) and fixed (instant adhesive "Plastix", Pattex, Henkel AG & Co. KgaA, Düsseldorf, Germany). Afterwards, the trays were filled with the relevant gas mixtures and closed using a semi-automatic Traysealer (T250, Multivac GmbH & Co. KG, Wolfertschwenden, Germany), operating at 160 °C for 4 s, and a PP/PA/PP/PA lid-film (100 µm, allvac Folien GmbH, Waltenhofen, Germany). Following, the demonstrator was zero-calibrated (ambient air) and end-calibrated (compare chapter 4) to the respective test corner to be examined.

For the determination of the measurement precision at 40% (v/v) CO_2, the test gas with 20% (v/v) CO_2/80% (v/v) O_2 was taken for the end-calibration and for the determination of the measurement precision at 20% (v/v) CO_2, the 40% (v/v) CO_2/60% (v/v) O_2) test-gas was taken for the end-calibration. This combination was chosen because the results of calibrating and measuring at the same CO_2 gas concentration would not be representative of the measurement accuracy.

For the measurement, the trays were flooded with the respective gas to be tested (for the measurement precision at 40% (v/v) CO_2, the 40% (v/v) CO_2/60% (v/v) O_2 test gas was used, and for the measurement precision at 20% (v/v) CO_2, the 20% (v/v) CO_2/80% (v/v) O_2 test gas was used) again for a duration of t = 5 min. The measurement occurred in a quadruple determination.

2.3.2. Packaging pigmentation and printings

Pigmentation of packaging materials may be responsible for a reduced transmission for the radiation of the thermal IR emitter, which can lead to higher inaccuracy. Since a wide range of packaging types should be measurable for a successful application of a non-destructive
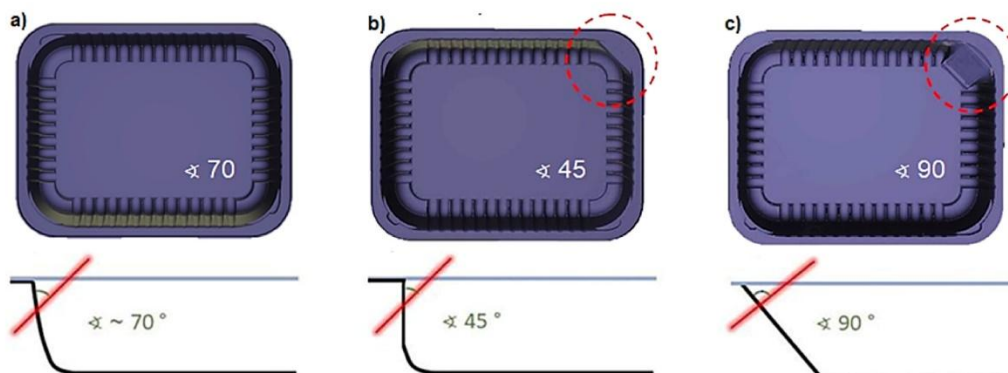

Fig. 4. Different tray shapes to determine the influence on the measurement accuracy: **a)** unmodified standard tray **b)** tray with integrated vertical surface **c)** tray with integrated inclined surface. The numbers indicate the angle at which the thermal IR emitter enters the tray. Transparent trays were used for this series of experiments.

4

instrument, further tests were carried out on the influence of tray pigmentation and lid film printings. Therefore, pigmented polymer trays as well as a printed lid-film were evaluated regarding measuring accuracy and transmission in the mid-infrared. As pigmented polymer trays, the following types were chosen: black (PP, 227x178 × 60mm, PM000784), green (PP, 227x178 × 50mm, PM002354), red (PP/EVOH/PP, 227x178 × 50mm, PM001839), yellow (PP/EVOH/PP, 227x178 × 60mm, PM000869) and white (PP/EVOH/PE value, 205x160 × 37mm), all obtained from ES-Plastic GmbH, Hutthurm, Germany. The trays were heat-sealed with a transparent PP/PA/PP/PA lid film, as already described in 5. The demonstrator was first zero calibrated with the pigmented tray in each case. For the end-calibration, pigmented trays in the first run were flooded with 40% (v/v) CO_2/60% (v/v) O_2 test gas. Following this, the trays were filled with the 20% (v/v) CO_2/80% (v/v) O_2 test gas and analyzed. For the second run, the end-calibration was done with the 20% (v/v) CO_2/80% (v/v) O_2 test gas and after flooding again with 40% (v/v) CO_2/60% (v/v) O_2, they were analyzed using the demonstrator. The samples were compared to a transparent standard tray as described in 5.

The printed lid film (PE/PA/EVOH/PA/PPpeel, 56 µm, SÜDPACK Verpackungen GmbH & Co. KG, Ochsenhausen, Germany) included a partial multi-colored printing. The lid-film was heat-sealed onto a transparent PP tray, using the same sealing conditions already mentioned. In the first run, the zero and end-calibrations were performed with a printed area of the film. The calibration and measurement were done in the same way then for the pigmented trays. After flooding the tray with the test gas, both the corners with printed and with transparent lid film was then examined non-destructively. In the second run, however, the zero and end-calibration was performed with a transparent area of the film. The gassed packages were examined analogously to the first run using the demonstrator. The mean values of the measurement through different printings (n = 8) were compared to those obtained on the transparent area (n = 8) of the film. Film and tray samples were also investigated regarding their transmission spectra in the mid-infrared region as described in 7.

2.3.3. Optical polymer irregularities

To investigate the influence of optical polymer irregularities, such as surface defects or a stronger scattering optical structure inside the polymer, trials were carried out as follows: For the simulation of packaging defects, grid-shaped damages on the polymer surface of transparent PP trays and the PP/PA/PP/PA lid-film were carried out in the area where the thermal IR emitter passes the packaging, using a scissor. For investigation of the influence of another, even stronger scattering optical structure, PP trays with such kind of visual irregularities were used and sealed with an intact PP/PA/PP/PA lid-film. The calibration of the demonstrator occurred with an intact reference. All samples were investigated afterwards using the 40% (v/v) CO_2/60% (v/v) O_2 and 20% (v/v) CO_2/80% (v/v) O_2 test gas and compared to the results of the reference (n = 8, respectively).

We assumed that the stronger scattering optical structure could be a result of a higher crystallization degree (Lee et al., 2008; Lin et al., 2020). However, the truth in this assumption is to be proven by also generating quantitative values. For a *qualitative* visualization of the "crystallinity" of the packaging, a ring-shaped LED light source (6″ Ring Light, UBeesize, City of Industry, California, United States) was placed under the determined area. For a *quantification* of the crystallinity, a differential scanning calorimetry (DSC) measurement was conducted. Therefore, a differential scanning calorimeter of the type DSC25 (TA Instruments, New Castle, USA) was used, and the measurement was carried out as follows: Polymer sheets with a diameter of 5 mm were punched out and placed in a 40 µl aluminum, hermetic sealable pan and sealed with the sealing press. The initial weight was between 5 mg and 12mg. Two heating runs with a temperature profile of 25 °C–200 °C at 10 K/min and an isotherm at 25 °C between the first and second heating run of 10 min under nitrogen atmosphere were run through. For the

evaluation, the difference of peak area (enthalpy) and the peak shape between the reference and the "crystalline" sample was considered.

2.3.4. Influence of food residues

During the transport and storage of food, a contamination with food residues and the formation of water condensation on the inner packaging surface can often be observed. Therefore, it is necessary to check the influence of these contaminations on the measurement accuracy of the demonstrator.

For the simulation of product residues, fresh poultry was packed with 20% (v/v) CO_2/80% (v/v) O_2 and 40% (v/v) CO_2/60% (v/v) O_2 test gas and turned over to bring the meat into contact with the corner of the packaging for a few seconds, leaving a residue of product on the inner polymer surface. A two-point calibration with zero and 20% (v/v) CO_2/80% (v/v) O_2 or 40% (v/v) CO_2/60% (v/v) O_2 test gas was performed using an untreated transparent PP tray as a reference.

To test the influence of H_2O condensation, a relative humidity of 100% was imitated in the tray by sealing wet fleeces into transparent PP trays that were afterwards filled with the 20% (v/v) CO_2/80% (v/v) O_2 and 40% (v/v) CO_2/60% (v/v) O_2 test gas, respectively (see Fig. 5). During subsequent storage in the refrigerator, a finely distributed film of water was formed on the polymer surface, which is similar to the condensation that occurs when products with a high water-activity as e. g. poultry meat is packaged. All samples were compared to the results of the reference (n = 8, respectively).

2.4. Screening of real packaging systems

For an application e.g., in the in-line control or incoming goods inspection, the applicability of the demonstrator to different commercially available packaging types and shapes had to be assessed. For this purpose, a selection of different MAP packages was purchased at local supermarkets (see Table 2).

In Fig. 6, the process of calibration (I + II) and the measurement of "fresh", unopened products after the calibration with the associated calibration standard (III) is shown, and further described hereafter.

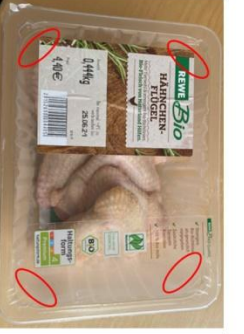### 2.4.1. Preparing and calibration of standards (I + II)

The different "calibration standards" were created out of the purchased samples shown in Table 2 as follows: After the food was removed from the trays while partially opening the lid films, the trays were cleaned, flooded with atmospheres of defined composition and then the lid films were reclosed, using the instant adhesive "Plastix" (I). These standards were now used for the two-point calibration of the demonstrator. First, the zero-calibration with the ambient air as filling gas was used, and then the tray was flooded as described in 4 with 40% (v/v) CO_2/60% (v/v) O_2 test gas in the flow-through mode. The perforations were closed afterwards using a septum (II). For the packaging without

Fig. 5. Packaging with adjusted relative humidity of 100% to evaluate the influence of H_2O condensation within a package on the measurement accuracy of the demonstrator.

Table 2
Different MAP food products for the screening of real packaging systems, purchased at a local supermarket. The product packaging differed in coloration, polymer composition, shape, size and printing or labelling. The red ellipse marks the measuring range in which the IR emitter passes through the packing *polymer composition not clearly mentioned (resin identification number 7).

1	2	3	4
„Garden Gourmet", Sensational Bratwurst Tivall Deutschland GmbH, Frankfurt, Germany	„Garden Gourmet" Vegetarian fillet strips Tivall Deutschland GmbH, Frankfurt, Germany	"ja!" pork cutlets E. Schiller Fleisch GmbH, Hof/Saale, Germany	"REWE Bio" Chicken wings Hubers Landhendl GmbH, Pfaffstätt, Germany
translucent PP/EVOH/PP 187137/40	dark green PP/EVOH/PP 187/137/40	transparent/printed PP 190/144/50	transparent/labeled PP 187/137/76

5	6	7	8
"The vegetarian butcher", Sieht Chick aus Burger Unilever Deutschland GmbH, Hamburg, Germany	"Rügenwalder Mühle", vegan minced beef Carl Müller GmbH und Co. KG, Bad Zwischenahn, Germany	"Zuarina" Mortadella sausage, ZUARINA S.p.A, Langhirano, Italy	"Fair&Gut" chicken breast fillet, LOHMANN & CO. AG, Bogen, Germany
transparent with grooves PET 175/135/40	transparent with round corners/labeled other resins* 192/130/37	transparent with straight corners other resins* 194/124/40	bright green/labeled PP 190/144/50

clearly indicated polymer composition mentioned, an additional DSC analysis was carried out.

2.4.2. Non-destructive detection of CO_2 gas concentration in "fresh products" (III)

For the validation of the applicability, an unopened equivalent of each calibration standard 1–8 (compare Table 2) was measured (n = 4) with the demonstrator after calibration with the associated calibration standard. The measurement was thus made through the transparent part of the lid-film, but for some samples also through the printed or labeled area.

2.4.3. Invasive detection of CO_2 gas concentration in "fresh products" (III)

The CO_2 gas concentration in the purchased samples was further evaluated by using an invasive method. For this purpose, a gas analyzer (MAT1500, A. KRÜSS Optronic GmbH, Hamburg, Germany) with a Zirconium dioxide sensor for O_2 detection and a non-dispersive infrared sensor for CO_2 detection was used. To extract small aliquots (7 ml) of the gas atmosphere, a hollow needle belonging to the measuring device was inserted into the headspace of the packaging via a septum attached to the lid film.
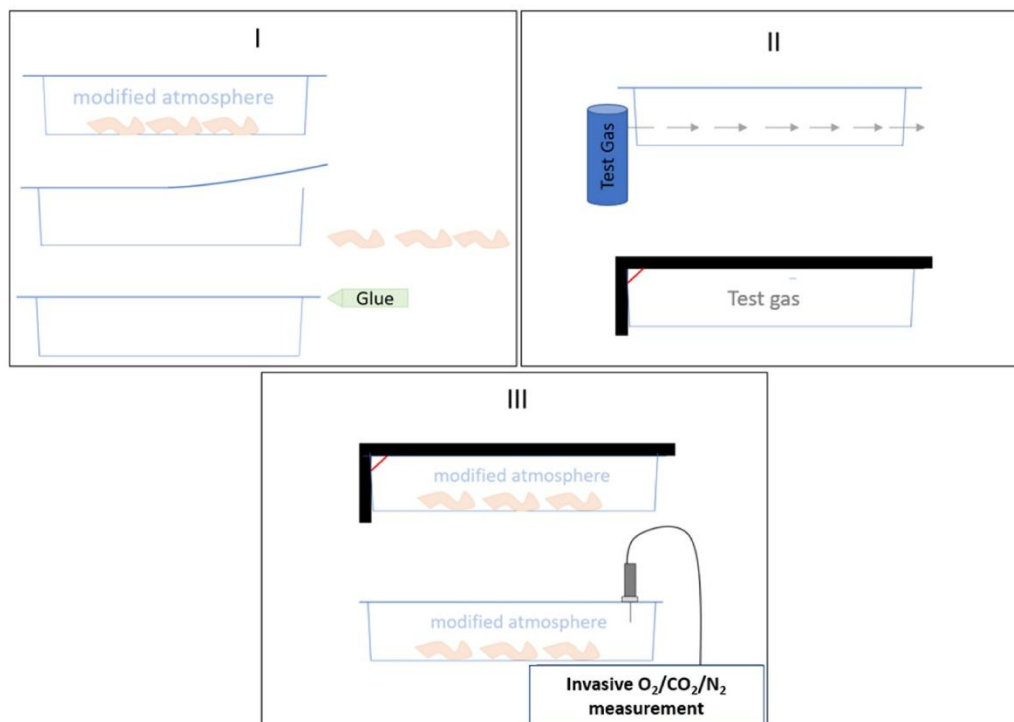
6

94

Fig. 6. Schematic illustration of the methods **(I)** to prepare calibration standards, **(II)** to calibrate the Demonstrator with the standard and **(III)** to measure the CO_2 gas atmosphere of the associated "fresh products" with the Demonstrator and an invasive device.

2.4.4. Transmission spectra of the commercial packaging's

To further understand the gained results, the samples (tray material, transparent lid film and printed or labeled lid film) were analyzed regarding their transmission in the mid-infrared range, using a FT-IR Spectrometer (Spotlight 400, Frontier, PerkinElmer Inc., Waltham, United States). The transmission was evaluated within a spectral range of 4000-1600 cm^{-1}.

2.5. Statistical analysis

The drawings and statistical analysis were performed using MS Excel and Origin version 2021 (Origin Lab., Hampton, VA, USA). All data are presented as the arithmetic mean ± standard deviation. For the calculation of the statistical significance, two-sample t-tests (two-tailed) were performed (alpha level 0.05). A univariate, one-way analysis of variance (ANOVA) was used to determine the influence of the tray shape to the measurement accuracy (alpha level 0.05). In addition, the values were compared with each other by means of a multiple comparison of means (Tukey HSD test).

3. Results and discussion

3.1. Influence of different packaging properties to the measuring quality

3.1.1. Packaging shape

The samples measured with channel 2–4.45 μm/60 nm – is not suitable for gaining useful measurement results, as it can be seen in Fig. 7 **b)**. The specific deviations of this channel span almost the entire measuring range. This is due to the fact, that the spectral filter lies at the edge of the CO_2 absorption band (compare Fig. 3) and thus only a small change of the transmission occurs, compared to channel 1 and 3. This small change is extrapolated and thereby creates an increased measurement error. Because of the low informative value of channel 2, the statistical analysis was not done for those results and in the following chapters, the results for channel 2 are excluded.

The ANOVA and the Tukey test gave no significant difference in comparison to the test gas and between the different tray shapes (alpha level 0.05). That means that the device works for all commercial tray shapes investigated with a sufficient accuracy. The integration of a modified "test corner" is therefore not necessary for the application.

3.1.2. Packaging pigmentation and printings

As it can be seen in Table 3, the packaging pigmentation or printings of the trays and the lid-film did not have a significant influence on the measurement precision in most cases. The black tray showed the strongest statistical significance, as it absorbs virtually the whole light in the mid-infrared. This can also be seen in the results of the spectral transmission measurement, which is shown in Fig. 8. The tray with the white coloration showed a significant deviation ($p < 0.05$) for the test with 40% (v/v) CO_2/60% (v/v) O_2. However, as the measurement at 20% (v/v) CO_2/80% (v/v) O_2 and showed no statistical significance, it is more likely that external influencing factors caused the deviation.

The transmission spectra in the mid-infrared of the different colored samples are shown in Fig. 8. The PP based trays showed – with exception of the black sample – typical transmission characteristics for this polymer, with its big absorption band between 3000 and 2800 cm^{-1} (Tsilingiris, 2003). The lid film showed an additional absorption band at 3000 and around 3300 cm^{-1} (see red-circled area Fig. 8 (c)), which is probably assigned to the polyamide (PA) layer of the lid film, as PA is known to have absorption bands at 3300 cm^{-1} (N–H stretch) and 3081 cm^{-1} (overtone N–H band) (R. Li et al., 2012; Smith, 2023). However, this could also overlap with the broad EVOH absorption band, also located between 3000 and 3500cm-1 (Xu et al., 2018).

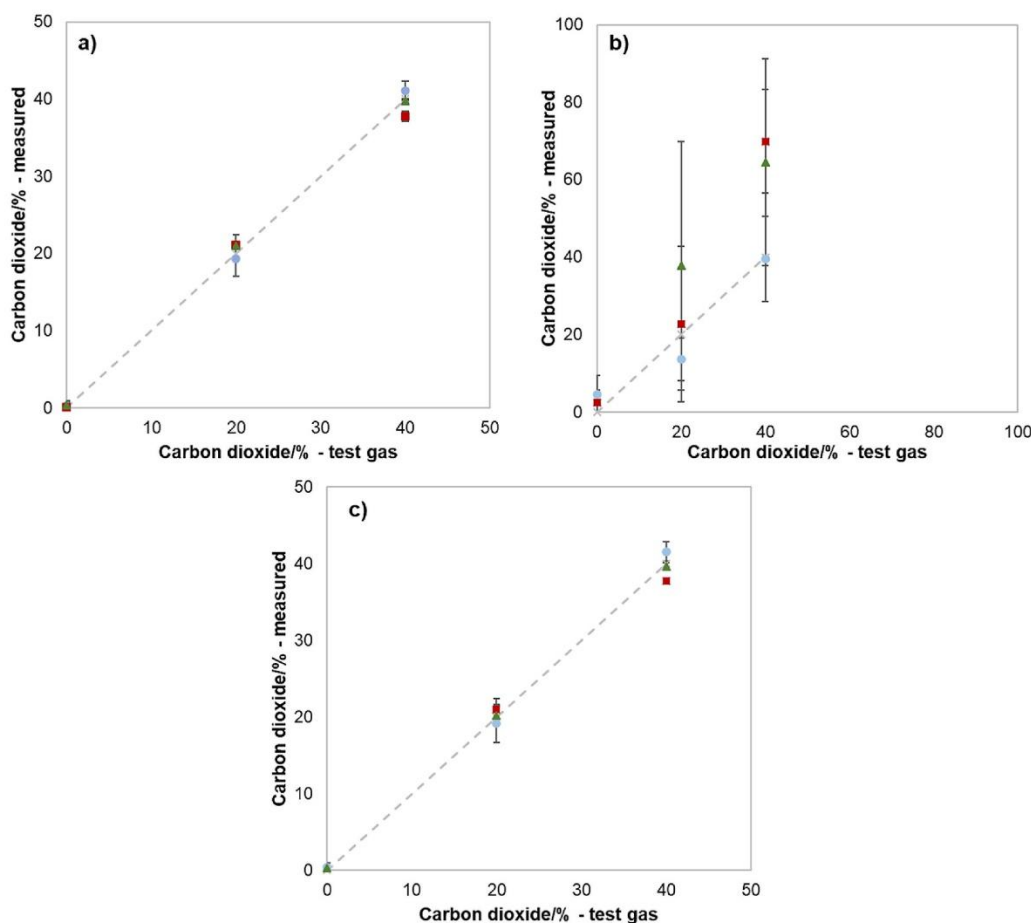Fig. 9 (b) shows the absorbance and the transmission of the black PP

Fig. 7. Measuring precision of: ● unmodified standard tray, ■ tray with integrated vertical surface and ▲ tray with integrated inclined surface (compare Fig. 4) at headspace CO_2 gas concentrations of 0, 20 and 40% (v/v) measured with the non-destructive device at **a)** 4.26μm/180 nm **b)** 4.45μm/60 nm and **c)** 4.27μm/170 nm (n = 4).

Table 3

Mean CO_2 gas concentrations (4.26μm/180 nm and 4.27μm/170 nm) as measured in diverse pigmented trays with printed lid films at headspace CO_2 gas concentrations of 20 and 40% (v/v) CO_2 in comparison to transparent trays and lid film: [a] calibrated with a transparent polymer [b] calibrated with a printed polymer. Indices indicate a significant difference between the results measured for the pigmented and the transparent trays.*$p < 0.05$,**$p < 0.01$, and ***$p < 0.001$.

Tray						Lid film	
Black	Green	Red	Yellow	White	Transparent	Printing	Transparent
-0.09 ± 0.05[a,***]	21.47 ± 0.72[a]	20.74 ± 1.45[a]	20.65 ± 2.5[a]	19.96 ± 2.75[a]	20.22 ± 2.24[a]	18.59 ± 2.19[a]	20.12 ± 1.51[a]
						20.43 ± 2.32[b]	20.87 ± 1.34[b]
-0.04 ± 0.06[a,***]	41.31 ± 4.23[a]	40.12 ± 2.69[a]	41.61 ± 1.55[a]	38.25 ± 1.0[a,*]	40.63 ± 2.1[a]	39.28 ± 3.08[a]	40.45 ± 1.95[a]
						40.54 ± 2.87[b]	40.33 ± 3.14[b]

tray multiplied with 100, according to a study of O'Reilly & Mosher which was published already in 1983. The results highly indicate the use of carbon black as filler material, as carbon black is known to lead to a high absorbance (O'Reilly and Mosher, 1983) and is mainly used in food packaging as filling pigment.

In most cases, organic colorations – or mostly pigments – are used for the coloration of packaging materials, however, sometimes they are combined with inorganic inks e.g. for printings (Hunger and Schmidt, 2018).

3.1.3. Optical polymer irregularities

Several different optical polymer irregularities could be a reason on impacting the measurement accuracy, such as surface defects like scratches, but also irregularities inside the polymer resulting in an irregular structure -e.g., due to a different degree on crystallization – might influence the measurement results.

Table 4 shows the results for the CO_2 gas concentrations measured in the headspace of the packages with different surface polymer defects and an optical irregular structure, after flooding the trays with 20% (v/v) CO_2/80% (v/v) O_2 and 40% (v/v) CO_2/60% (v/v) O_2 test gas, respectively, compared to the reference. It can be clearly seen that all
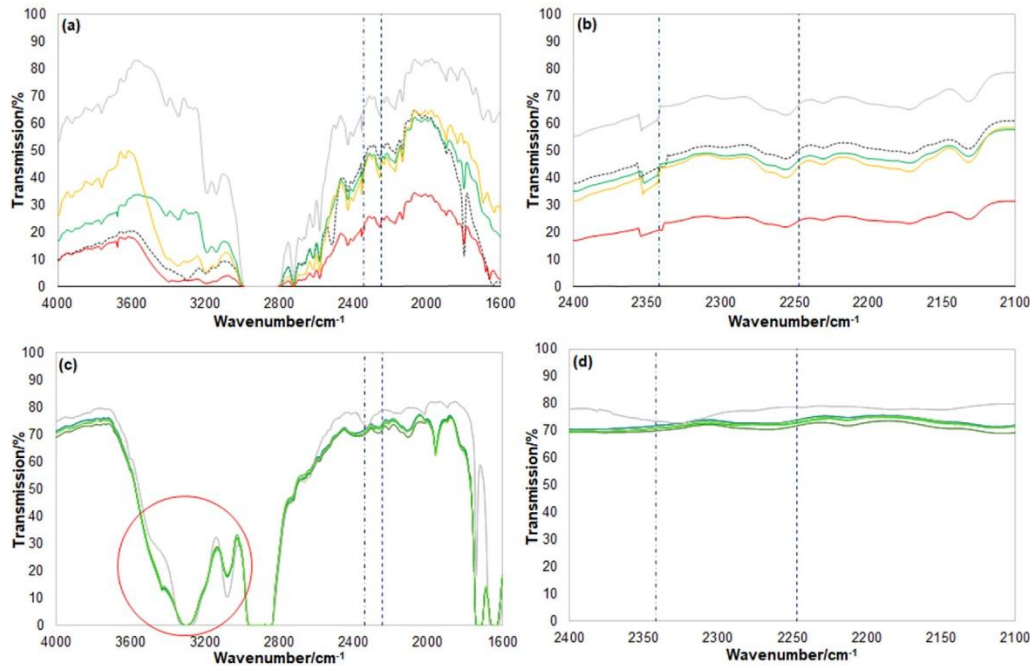
8

Fig. 8. Transmission spectra in the mid-infrared of **(a)/(b)** colored trays and **(c)/(d)** the lid-film between 4000 and 1600 cm^{-1} **(a)/(c)** and 2400 and 2100 cm^{-1} **(b)/(d)**. The grey curves represent the transparent samples, the black dashed curve represents the white tray. The red circle marks the PA/EVOH induced absorption band between 3000 and 3300 cm^{-1}. The other spectra are colored according to their tested polymer color. The vertical lines mark the location of channel 1/3 at 2342 cm^{-1} (dash-dot) and channel 2 at 2247 cm^{-1} (dashed).
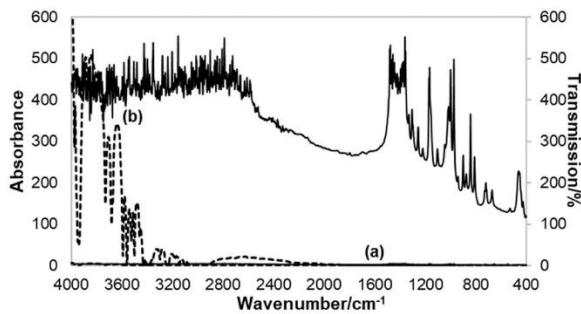
Fig. 9. Absorbance (black line) and Transmission (dashed line) at **(a)** normal scaling **(b)** absorbance/transmission x 100 of the black polypropylene tray.

Table 4
Mean measured CO_2 gas concentrations (4.26μm/180 nm and 4.27μm/170 nm) of damaged packaging components and optical irregular structured trays at a headspace CO_2 gas concentrations of 20 and 40% (v/v) CO_2 in comparison to intact transparent trays and lid film (reference). Indices indicate a significant difference between the reference and impaired samples: $p < 0.05$, $**p < 0.01$, and $***p < 0.001$.

Defect simulation (scratches)			Optical Irregular Structure	Reference
Lid-film	Tray	Both		
17.39 ± 1.37***	17.95 ± 1.42***	18.74 ± 2.65	25.41 ± 1.57***	20.33 ± 1.08
39.15 ± 3.93**	37.09 ± 2.55	41.38 ± 1.80	55.71 ± 4.28***	40.13 ± 1.69

irregularities are potentially responsible for significant measurement deviations. Especially the sample with the optical irregular structure – which was clearly an inhomogeneous inner polymer structure (compare Fig. 10) seems to have a high impact. However, the higher signal for the sample with the optical irregular structure speaks rather against a higher degree of crystallinity, since crystalline structures have a higher scattering effect than amorphous ones and consequently the signal would have to decrease in this case. The lower signal for the defect simulation could be a results of light scattering due to the defect surface (Frick and Stern, 2011; Lin et al., 2020).

Fig. 10 shows a visual *qualitative* comparison between two transparent PP trays used for the trial. Sample (a) was used as a standard tray, sample (b) was a tray which had a stronger scattering optical structure, which we assumed could be a higher degree of crystallization. However, the results of the non-destructive measurement of the CO_2 gas concentration as just described do not indicate a higher degree of crystallization.

To check for a different degree of the crystallization, the DSC measurement of both – the reference (a) and the polymer with a stronger scattering optical structure (b) was done:

The DSC measurement indeed showed a difference in peak shape between both samples (see Fig. 11). However, comparing the peak area, no significant deviation (alpha level 0.05) was measurable ($\Delta H_{Ref} = 85.87 \pm 2.44$ J/g and $\Delta H_{Anisotropic} = 86.79 \pm 1.61$ J/g). That confirms that the difference in optical appearance and the difference in measurability with the Demonstrator was not due to a different degree of crystallization, as a higher degree in crystallization would lead into a higher peak area, as the part of amorphous structures would be lower. However, the shape difference of the peak – and the difference of the optical structure – could be explained as follows: The sample with the optical irregular structure is much more unsymmetrical in melting, comparing to the reference. It also shows a shoulder at 155 °C and has a shifted peak-maximum to 167 °C (165 °C for the reference). During the

9

Fig. 10. Visual comparison of a transparent polypropylene tray under a ring-shaped light: **(a)** regular reference and **(b)** polymer with a stronger scattering optical structure.
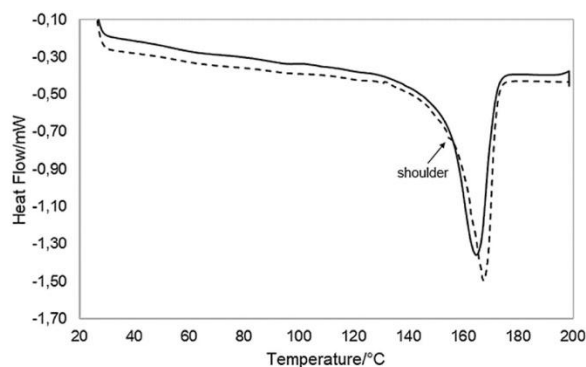

Fig. 11. Mean values of DSC curves of reference trays (line) and trays with an anisotropic appearance (dotted) (n = 3).

thermoforming process, it can happen that the cooling rate of the PP is not evenly, which can result in an unclean crystal structure after the cooling process – leading to those optical irregularities as seen in Fig. 10. The shoulder and the shifted peak position in the thermogram is a sign for a rearrangement (Cho et al., 1999).

Both packaging impairments can lead to statistically significant differences using the non-destructive MIR device.

3.1.4. Influence of food residues

The meat juice of poultry on the inner side of the tray did not show a great effect, only the measurement with 40% (v/v) CO_2/60% (v/v) O_2 showed a slightly significant deviation ($p < 0.05$). The formation of H_2O condensate on the inner side of the polymer tray led to a high statistically significant deviation ($p < 0.001$) for the measurement results with 20% (v/v) CO_2/80% (v/v) O_2 and with 40% (v/v) CO_2/60% (v/v) O_2,

Table 5
Mean measured CO_2 gas concentrations (4.26μm/180 nm and 4.27μm/170 nm) of trays with H_2O condensate or poultry meat juice residues on the inner side of the polymer surface at headspace CO_2 gas concentrations of 20 and 40% (v/v) CO_2 in comparison to transparent trays and lid film (reference). Indices indicate a significant difference between the reference and impaired samples: $p < 0.05$, **$p < 0.01$, and ***$p < 0.001$.

H_2O condensate	Food residue (Meat juice)	Reference
16.78 ± 0.48***	18.81 ± 1.08	19.86 ± 1.79
32.72 ± 3.01***	41.80 ± 2.63*	39.96 ± 0.94

compared to the reference (see Table 5).

The main absorption bands of H_2O are located at 3756 cm^{-1}, 3652 cm^{-1} and 1595 cm^{-1} and do therefore not overlap with the thermal IR emitter located between 2342 cm^{-1} and 2247 cm^{-1} on the CO_2 absorption band (Atkins et al., 2022). Nevertheless, there was a strong inaccuracy due to the formation of condensate, which is probably mainly caused by scattering effects on the many small water droplets. The measurement with the demonstrator with a simultaneous presence of condensate in the measuring field must therefore be avoided. The impairment of the tray with meat juice occurred with fresh meat – mainly consisting of water, what might be an explanation for the less influence of this residue. When it comes to higher amounts of bacterial growth such as meat spoilage *Pseudomonas* and therefore the formation of a biofilm matrix containing e.g. bacterial exopolysaccharides or proteins, an influence cannot be ruled out (Charles et al., 2006; Wickramasinghe et al., 2020). The influence of marinades are also a potential source for imprecise measurement results, however, common plant-based oils have also no absorption band in the measuring range (Tarhan et al., 2017; Valenzuela et al., 2013; Yuzhen et al., 2014).

3.2. Screening of real packaging systems

The results of the screening seen in Fig. 12 and Table 6 show clearly that using the original tray for calibration for each respective sample can lead to very precise results within the defined statistical significance. For
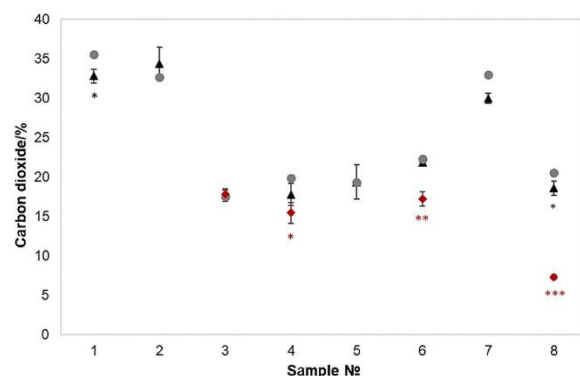

Fig. 12. CO_2 gas concentration of the measured samples (1–8) with the invasive measurement device (●) and the non-destructive measurement device through the transparent (▲) and printed or labeled (♦) parts of the lid film (Level of significance: $p < 0.05$, **$p < 0.01$, and ***$p < 0.001$).

Table 6

CO$_2$ gas concentrations (% (v/v)) of different MAP food products, measured with the non-destructive device through the transparent part of the lid-film and labeled or printed part of the lid film in comparison to the CO$_2$ gas concentration measured with the invasive device. (Level of significance: a: $p < 0.05$, b: $p < 0.01$, and c $p < 0.001$). *polymer composition not clearly mentioned (resin identification number 7).

	1	2	3	4	5	6	7	8
	translucent PP/EVOH/PP 187 137/40	dark green PP/EVOH/PP 187/137/40	transparent/printed PP 190/144/50	transparent/ labeled PP 187/137/76	transparent with grooves PET 175/135/40	transparent with round corners/labeled other resins* 192/130/37	transparent with straight corners other resins* 194/124/40	bright green/labeled PP 190/144/50
Non-destructive (n.-d.)	32.81 ± 0.85[a]	34.38 ± 2.06	17.74 ± 0.81	17.78 ± 1.42	19.38 ± 2.16	21.87 ± 0.00	29.97 ± 0.65	18.58 ± 0.92
n.-d. labeled/printed	opaque (cardboard)	opaque (cardboard)	17.80 ± 0.58	15.48 ± 1.33[a]	opaque (cardboard)	17.21 ± 0.92[b]	no printed area in measurement range	7.30 ± 0.33[c]
Invasive	35.53 ± 0.21	32.70 ± 0.14	17.53 ± 0.06	19.90 ± 0.10	19.37 ± 0.06	22.27 ± 0.12	32.97 ± 0.12	20.53 ± 0.06

the comparison of the precision, the non-destructive measurement was compared to an invasive method. The best results are in case the non-destructive measurement occurred through the transparent parts of the lid film. However, for some measurement conditions, significant deviations compared to the invasive CO_2 gas concentration measurement were noticeable. Sample 1 and sample 8 showed a significant deviation ($p \leq 0.05$) for the measurement through the transparent lid film and the pigmented trays. When comparing the transmission data (see Fig. 13), the pigmented trays indeed have a much lower transmission compared to the lid film, but as the calibration was done with the pigmented trays as well it is more likely that there is a random error, as we demonstrated in 8 that a tray pigmentation has no influence to the measuring quality, even at lower transmission degrees.

When the measurement occurred through a printed or labeled area of the lid film, we observed larger deviations (comp. sample 4, 6 and 8). As it can be seen in Fig. 13, these areas exhibit a much lower transmission compared to the transparent parts of the lid film. Especially the samples with a sticker (sample 6 and 8) have a significantly lower transmission at

4.27 μm with values of 14.5% or 0.21%, respectively. In case of outgoing or incoming goods inspection, it would therefore make sense to avoid these areas in the measuring field.

The transmission data shown in Fig. 13 in combination with the interpretation of the DSC measurement in Fig. 14 allows also some additional information about the composition of the polymers – especially for those that haven't been mentioned clearly by the manufacturers and the lid film combinations.

The trays of samples 5 (black dotted) and 7 (light blue) show the same transmission curve – with a big absorption peak around 2000 cm^{-1}, which indicates a high PET composition (red circle in Fig. 13), as the aromatic ester C≡O stretch absorbs at this area (Smith, 2022). The DSC measurement of sample 7 with a melting peak at 250 °C further underlines this assumption. The trays of samples 1 and 6 also have a simultaneous absorption curve, which in combination with the DSC data obtained indicates a PP/EVOH/PP composite.

The PET related absorption peaks are also visible for the lid-films of sample 4 (pink), 3 (dark blue), 7 (light blue) and 8 (light green) (red
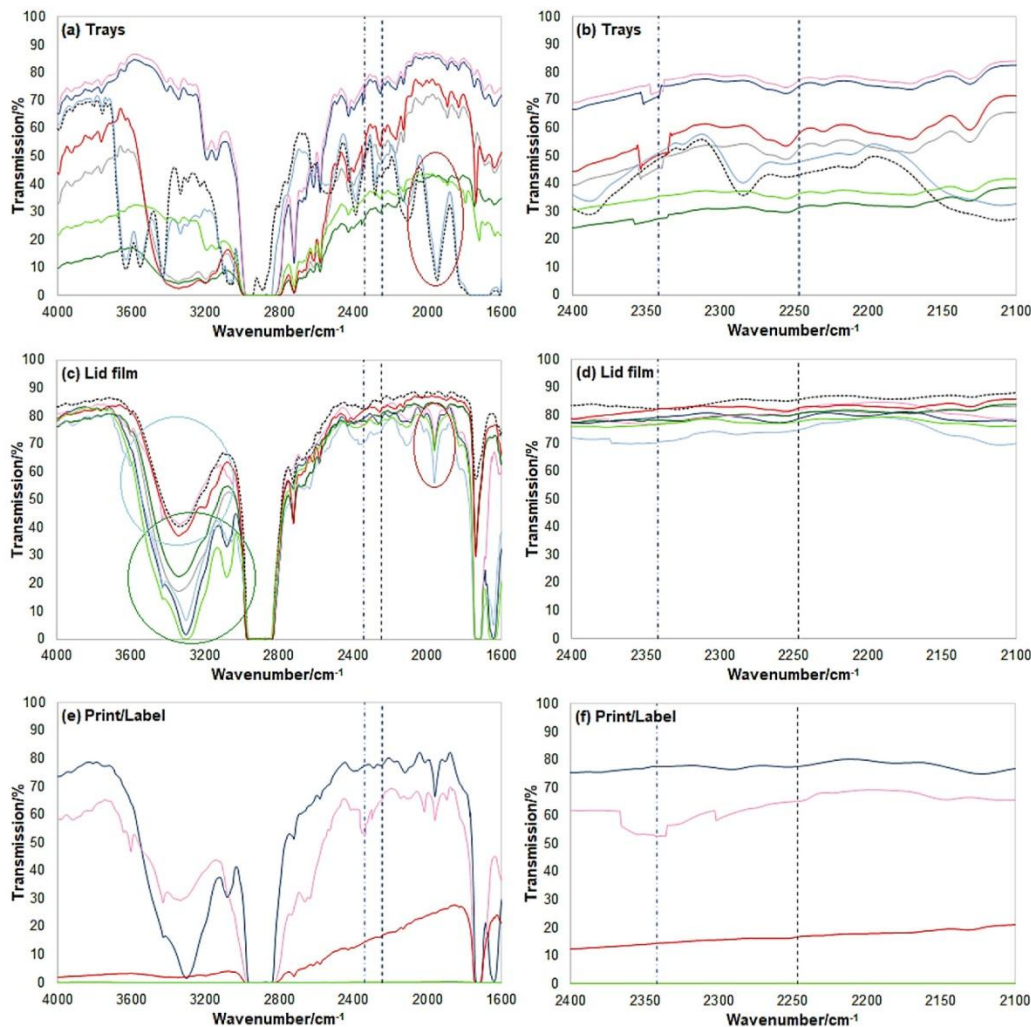

Fig. 13. Transmission spectra in the mid-infrared of the screened supermarket samples (1–8) **(a)/(b)** trays, **(c)/(d)** lid film and **(e)/(f)** printed parts or labeled parts of the lid film, between 4000 and 1600 cm^{-1} **(a)/(c)/(e)** and 2400 and 2100 cm^{-1} **(b)/(d)/(f)**. The color assignment of the samples is as follows: 1: grey, 2: dark green, 3: dark blue, 4: pink, 5: black (dotted), 6: red, 7: light-blue, 8: light green. The vertical lines mark the location of channel 1/3 at 2342 cm^{-1} (dash-dot) and channel 2 at 2247 cm^{-1} (dashed). The red circle marks the PET, the blue circle the EVOH and the green circle the PA related band.

12

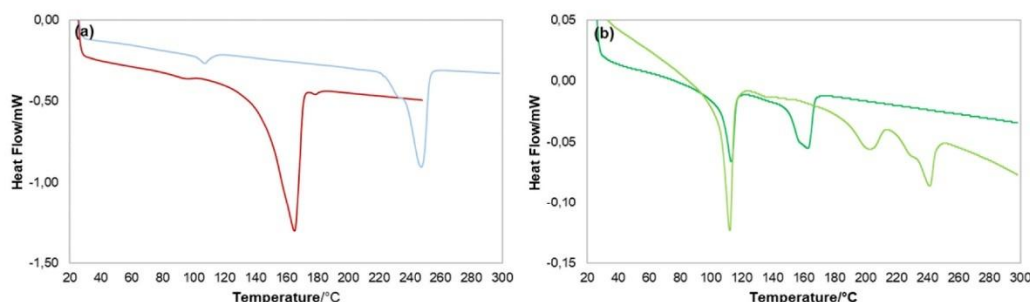

Fig. 14. DSC measurement of **(a)** trays **(b)** lid-films from the retail samples with unknown resin combination. red: sample 6, light-blue: sample 7, dark-green: sample 2, light-green: sample 8.

circled area, Fig. 13 (c)). The DSC measurement of sample 8 further underlines this, having a melting peak at 250 °C (Fig. 14 (b)). This lid film seems to be a multi-layer film, with PE and a PA combination, which can also be seen in the absorption data, as absorption bands at 3300 cm^{-1} (N–H stretch) and 3081 cm^{-1} (overtone N–H band) are visible (Smith, 2023). The same absorption peaks are also visible for sample 3, 4 and 7 (compare green circled area in Fig. 13 (c)).

The broad absorption peak between 3000 and 3500 cm^{-1} (compare blue circled area Fig. 13 (c)) is probably related to an EVOH layer, which is also visible for sample 2 in the DSC measurement (double peak with PP between 160 and 180 °C) (Lagaron et al., 2001; Xu et al., 2018).

The results confirm that the constructed measurement device is suitable for different tray colors, shapes, sizes, and polymer compositions, provided that one avoids particularly unsuitable configurations. To the best of our knowledge, it is also currently the only portable measuring device that can carry out measurements of the headspace gas atmosphere on such a broad product variety without the risk of the filling good interrupting the measuring path or - if it is working in the reflectance mode - differences in the surface properties can lead to measurement inaccuracies. This distinguishes the developed construction decisively from the gas analyzers already available on the market (Czerwiński et al., 2021).

Other approaches for determining the quality of packaged food in retail such as the state of spoilage are based on so-called food freshness indicators (FFIs), which react to the formation of volatile substances such as ammonia (NH_3) (Luo et al., 2022). An indicator paper or print integrated into the packaging reacts to the change in pH value due to the formation of the volatiles, resulting in a color change. As a result, either the consumer himself or an employee in the retail could sort out the product. In 2022, for example, Cai et al. for example developed a curcumin-based fluorescent ink system that shows a color change at a wavelength of 365 nm when NH_3 was formed by shrimp (Cai et al., 2022). However, these processes are dependent on the formation of various volatile compounds induced by different possible biological processes. They are therefore less reliable in detecting microbiological activity and they are not suitable for detecting other impairments such as leakages caused by transportation. They also have the disadvantage that the packaging has to be modified, which in turn represents a higher cost factor for the food producer.

4. Conclusion

We demonstrated that the combined use of a thermal MIR emitter which is guided at a 45° angle through the corner of the packaging and a pyroelectric detector operating simultaneously around the CO_2 absorption maximum and outside the absorption band exhibits many advantages.

The measurement allows very precise results within the defined statistical range, independent of the shape of the tray corner, as well as

for pigmented trays and printed lid-films, with some limitations (carbon black pigments).

An optical Irregular polymer structure seems to have a high effect to the measurement accuracy – both in case of surface defects like scratches, or also different polymer structures probably due to cooling effects during tray thermoforming.

The influence of food residues cannot be excluded in total. However, the residue of meat juice showed no statistically relevant influence on the measuring accuracy. Contrary, the presence of H_2O condensate had a significant influence, even though water showed a good transmission at 4.26 and 4.27 µm. To prevent this in future applications, the integration of a punctual heating element would be useful to evaporate water droplets in the measuring area.

A screening of diverse packaging with modified atmosphere purchased from a local supermarket further underlined the usability of the device for different tray shapes, colors, polymer types and sizes. When the calibration of the system was done with the associated tray ("calibration standards"), precise results in comparison to the invasive CO_2 gas concentration measurement were gained, if the measurement occurred not through a labeled part of the lid-film.

The results show that the developed device can cover a wide range of applications and at the same time is convenient to use. For example, the device can be used to detect changes in the gas atmosphere when premature microbiological spoilage occurs due to improper storage. But the developed device would also be very well suited for an application at the beginning of the food value chain, namely for monitoring the modified gas atmosphere after the packaging process at the food producer (outgoing goods inspection) or for incoming goods inspection in retail.

This wide range of applications clearly sets the measuring device apart from existing approaches to non-destructive gas detection.

In order to broaden the field of application even further, the next step would be to design a device that covers other packaging forms (e.g. tubular bags) and wavelengths (for the detection of different gases). For example, the installation of an oxygen sensor could be useful for quality analysis. Oxygen has its main absorption band at 760 nm which, however, has comparatively weak absorption properties. The use of a TDLAS-based system, for example, would be suitable here. However, the O_2 absorption measurement has the disadvantage that it is located directly at the transition between visible light and the near-infrared range, which can severely limit the transmission of printed or pigmented packaging.

Funding

CRediT authorship contribution statement

Jasmin Dold: Writing – original draft, Visualization, Validation, Project administration, Methodology, Investigation, Formal analysis, Data curation, Conceptualization. **Lukas Götzendörfer:** Writing – review & editing, Validation, Methodology. **Clarissa Hollmann:** Visualization, Validation, Methodology, Formal analysis. **Horst-Christian Langowski:** Writing – review & editing, Supervision, Methodology, Funding acquisition, Conceptualization.

Declaration of competing interest

The authors declare that they have no known competing financial interests or personal relationships that could have appeared to influence the work reported in this paper.

Data availability

Data will be made available on request.

Acknowledgments

References

Arias, E., Sierra, V., Prado, N., González, P., Fiorentini, G., Díaz, J., Oliván, M., 2022. Development of a portable near-infrared spectroscopy tool for detecting freshness of commercial packaged pork. Foods 11 (23). https://doi.org/10.3390/foods11233808.

Atkins, P., Paula, J. de, Keeler, J., 2022. Atkins' Physical Chemistry, twelfth ed. Oxford University Press.

Bernstein, M., Cruikshank, D., Sandford, S., 2005. Near-infrared laboratory spectra of solid HO/CO and CHOH/CO ice mixtures. Icarus 179 (2), 527–534. https://doi.org/10.1016/j.icarus.2005.07.009.

Boetcher, S.K., Perskin, J.B., Maidenberg, Y., Traum, M.J., Hippel, T. von, 2023. Direct atmospheric cryogenic carbon capture in cold climates. Carbon Capture Sci. Technol. 8, 100127 https://doi.org/10.1016/j.ccst.2023.100127.

Cai, S., Song, G., Zhang, G Guofan, Wang, L., Jian, T., Xu, J., Su, F., Tian, Y., 2022. A multicolor fluorescent sensor array based on curcumin and its analogs as a shrimp freshness indicator. Sensor. Actuator. B Chem. 367, 132153 https://doi.org/10.1016/j.snb.2022.132153.

Chaix, E., Couvert, O., Guillaume, C., Gontard, N., Guillard, V., 2015. Predictive microbiology coupled with gas (O 2/CO 2) transfer in food/packaging systems: how to develop an efficient decision support tool for food packaging dimensioning. Compr. Rev. Food Sci. Food Saf. 14 (1), 1–21. https://doi.org/10.1111/1541-4337.12117.

Charles, N., Williams, S.K., Rodrick, G.E., 2006. Effects of packaging systems on the natural microflora and acceptability of chicken breast meat. Poultry Sci. 85 (10), 1798–1801. https://doi.org/10.1093/ps/85.10.1798.

Chmiel, M., Hać-Szymańczuk, E., Adamczak, L., Pietrzak, D., Florowski, T., Cegiełka, A., 2018. Quality changes of chicken breast meat packaged in a normal and in a modified atmosphere. J. Appl. Poultry Res. 27 (3), 349–362. https://doi.org/10.3382/japr/pfy004.

Cho, K., Li, F., Choi, J., 1999. Crystallization and melting behavior of polypropylene and maleated polypropylene blends. Polymer 40 (7), 1719–1729. https://doi.org/10.1016/S0032-3861(98)00404-2.

Czerwiński, K., Rydzkowski, T., Wróblewska-Krepsztul, J., Thakur, V.K., 2021. Towards impact of modified atmosphere packaging (MAP) on shelf-life of polymer-film-packed food products: challenges and sustainable developments. Coatings 11 (12), 1504. https://doi.org/10.3390/coatings11121504.

Danilovic, B., Cocola, L., Fedel, M., Poletto, L.L., Savic, D., 2016. Formation and cumulation of CO2 in the bottles of the fermented milk drinks. IPCBEE 95, 26–31.

Danilović, B., Savić, D., Cocola, Lorenzo, Fedel, M., Poletto, L., 2018. Determination of CO 2 content in the headspace of spoiled yogurt packages. J. Food Qual. 2018, 1–6. https://doi.org/10.1155/2018/8121606.

Dold, J., Langowski, H.-C., 2022. Optical measurement systems in the food packaging sector and research for the non-destructive evaluation of product quality. Food Packag. Shelf Life 31, 100814. https://doi.org/10.1016/j.fpsl.2022.100814.

European Union, 2019. Directive (EU) 2019/904 of the European Parliament and of the COUNCIL: of 5 June 2019 on the reduction of the impact of certain plastic products on the environment. https://eur-lex.europa.eu/eli/dir/2019/904/oj.

Frick, A., Stern, C., 2011. Praktische Kunststoffprüfung. Hanser.

Gill, C.O., Tan, K.H., 1980. Effect of carbon dioxide on growth of meat spoilage bacteria. Appl. Environ. Microbiol. 39 (2), 317–319. https://doi.org/10.1128/aem.39.2.317-319.1980.

Girón, J., Ivorra, I., Sánchez, A.J., Fernández-Segovia, I., Barat, J.M., Grau, R., 2014. Preliminary study using visible and SW-NIR analysis for evaluating the loss of freshness in commercially packaged cooked ham and Turkey ham. Czech J. Food Sci. 32 (4), 376–383. https://doi.org/10.17221/370/2013-CJFS.

Grau, R., Sánchez, A.J., Girón, J., Iborra, E., Fuentes, A., Barat, J.M., 2011. Nondestructive assessment of freshness in packaged sliced chicken breasts using SW-NIR spectroscopy. Food Res. Int. 44 (1), 331–337. https://doi.org/10.1016/j.foodres.2010.10.011.

Hlavatsch, M., Mizaikoff, B., 2022. Advanced mid-infrared lightsources above and beyond lasers and their analytical utility. Anal. Sci. : The International Journal of the Japan Society for Analytical Chemistry 38 (9), 1125–1139. https://doi.org/10.1007/s44211-022-00133-3.

Hunger, K., Schmidt, M.U., 2018. Industrial Organic Pigments: Production, Crystal Structures, Properties, Applications (Fourth, Completely Revised Edition). WILEY-VCH Verlag GmbH & Co. KGaA.

Isaksson, T., Miller, C.E., Næs, T., 1992. Nondestructive NIR and NIT determination of protein, fat, and water in plastic-wrapped, homogenized meat. Appl. Spectrosc. 46 (11), 1685–1694. https://doi.org/10.1366/0003702924926745.

Kolbeck, S., Reetz, L., Hilgarth, M., Vogel, R.F., 2019. Quantitative oxygen consumption and respiratory activity of meat spoiling bacteria upon high oxygen modified atmosphere. Front. Microbiol. 10, 2398.

Lagaron, J.M., Giménez, E., Saura, J.J., 2001. Degradation of high barrier ethylene-vinyl alcohol copolymer under mild thermal-oxidative conditions studied by thermal analysis and infrared spectroscopy. Polym. Int. 50 (6), 635–642. https://doi.org/10.1002/pi.674.

Langowski, H.-C., 2017. Shelf life of packed food and packaging functionality. In: Singh, P., Wani, A.A., Langowski, H.-C. (Eds.), Food Packaging Materials. CRC Press, pp. 11–66. https://doi.org/10.4324/9781315374390-2.

Lee, D.S., Yam, K.L., Piergiovanni, L., 2008. Food Packaging Science and Technology. CRC Press. https://doi.org/10.1201/9781439894071.

Li, R., Pei, J.Z., Li, Y.W., Shi, X., Le Du, Q., 2012. Preparation, morphology and dielectric properties of polyamide-6/poly(vinylidene fluoride) blends. Adv. Mater. Res. 496, 263–267. https://doi.org/10.4028/www.scientific.net/AMR.496.263.

Li, T., Lin, H., Zhang, H., Svanberg, S., Svanberg, S., 2017. Application of tunable Diode laser spectroscopy for the assessment of food quality. Appl. Spectrosc. 71 (5), 929–938. https://doi.org/10.1177/0003702816667515.

Lin, Y., Bilotti, E., Bastiaansen, C.W., Peijs, T., 2020. Transparent semi-crystalline polymeric materials and their nanocomposites: a review. Polym. Eng. Sci. 60 (10), 2351–2376. https://doi.org/10.1002/pen.25489.

Luo, X., Zaitoon, A., Lim, L.-T., 2022. A review on colorimetric indicators for monitoring product freshness in intelligent food packaging: indicator dyes, preparation methods, and applications. Compr. Rev. Food Sci. Food Saf. 21 (3), 2489–2519. https://doi.org/10.1111/1541-4337.12942.

Mortazavi, S.M.H., Kaur, M., Farahnaky, A., Torley, P.J., Osborn, A.M., 2023. The pathogenic and spoilage bacteria associated with red meat and application of different approaches of high CO2 packaging to extend product shelf-life. Crit. Rev. Food Sci. Nutr. 63 (12), 1733–1754. https://doi.org/10.1080/10408398.2021.1968336.

Myintzaw, P., Johnson, N.B., Begley, M., Callanan, M., 2023. Detection of microbial growth in aseptic food products using non-invasive Tunable Diode Laser Absorption Spectroscopy (TDLAS). Food Control 145, 109452. https://doi.org/10.1016/j.foodcont.2022.109452.

NIST, 2023. NIST Chemistry WebBook, SRD69. National Institute of Standards and Technology. https://webbook.nist.gov/cgi/cbook.cgi?ID=C124389&Type=IR-SPEC&Index=1#IR-SPEC.

O'Reilly, J.M., Mosher, R.A., 1983. Functional groups in carbon black by FTIR spectroscopy. Carbon 21 (1), 47–51. https://doi.org/10.1016/0008-6223(83)90155-0.

Parastar, H., van Kollenburg, G., Weesepoel, Y., van den Doel, A., Buydens, L., Jansen, J., 2020. Integration of handheld NIR and machine learning to "Measure & Monitor" chicken meat authenticity. Food Control 112, 107149. https://doi.org/10.1016/j.foodcont.2020.107149.

Piringer, O.G., Baner, A.L. (Eds.), 2008. Plastic Packaging: Interactions with Food and Pharmaceuticals, second ed. WILEY-VCH Verlag GmbH & Co. KGaA.

Schmutzler, M., Beganovic, A., Böhler, G., Huck, C.W., 2016. Modern safety control for meat products: near infrared spectroscopy utilised for detection of contaminations and adulterations of premium veal products. NIR News 27 (4), 11–13. https://doi.org/10.1255/nirn.1610.

Schossig, M., Ott, T., Hüller, S., Norkus, V., Gerlach, G., 2015. 3.4 - efficient thermal infrared emitter with high radiant power. In: Proceedings IRS² 2015. AMA Service GmbH, Von-Münchhausen-Str, pp. 934–937. https://doi.org/10.5162/irs2015/3.4, 49, 31515 Wunstorf, Germany.

Singh, P., Wani, A.A., Langowski, H.-C. (Eds.), 2017. Food Packaging Materials. CRC Press. https://doi.org/10.1201/9781315374390.

Smith, B.C., 2022. Infrared spectroscopy of polymers, VIII: polyesters and the rule of three. Spectroscopy 25–28. https://doi.org/10.56530/spectroscopy.ta9383e3.

Smith, B.C., 2023. Infrared spectroscopy of polymers, XI: introduction to organic nitrogen polymers. Spectroscopy 14–18. https://doi.org/10.56530/spectroscopy.vd3180b5.

Tarhan, İ., Ismail, A.A., Kara, H., 2017. Quantitative determination of free fatty acids in extra virgin olive oils by multivariate methods and Fourier transform infrared spectroscopy considering different absorption modes. Int. J. Food Prop. 20 (Suppl. 1), S790–S797. https://doi.org/10.1080/10942912.2017.1312437.

14

Tofteskov, J., Tørngren, M.A., Bailey, N.P., Hansen, J.S., 2019. Modelling headspace dynamics in modified atmosphere packaged meat. J. Food Eng. 248, 46–52. https://doi.org/10.1016/j.jfoodeng.2018.12.013.

Tsilingiris, P.T., 2003. Comparative evaluation of the infrared transmission of polymer films. Energy Convers. Manag. 44 (18), 2839–2856. https://doi.org/10.1016/S0196-8904(03)00066-9.

Valenzuela, C., Abugoch, L., Tapia, C., 2013. Quinoa protein–chitosan–sunflower oil edible film: mechanical, barrier and structural properties. LWT - Food Sci. Technol. (Lebensmittel-Wissenschaft -Technol.) 50 (2), 531–537. https://doi.org/10.1016/j.lwt.2012.08.010.

Wickramasinghe, N.N., Hlaing, M.M., Ravensdale, J.T., Coorey, R., Chandry, P.S., Dykes, G.A., 2020. Characterization of the biofilm matrix composition of psychrotrophic, meat spoilage pseudomonads. Sci. Rep. 10 (1), 16457 https://doi.org/10.1038/s41598-020-73612-0.

Wordsworth, R., Forget, F., Eymet, V., 2010. Infrared collision-induced and far-line absorption in dense CO2 atmospheres. Icarus 210 (2), 992–997. https://doi.org/10.1016/j.icarus.2010.06.010.

Xu, D., Lu, J., Yan, S., Xiao, R., 2018. Aminated EVOH nanofiber membranes for Cr(vi) adsorption from aqueous solution. RSC Adv. 8 (2), 742–751. https://doi.org/10.1039/C7RA11940B.

Yuzhen, L., Du, Changwen, Yanqiu, S., Jianmin, Z., 2014. Characterization of rapeseed oil using FTIR-ATR spectroscopy. Journal of Food Science and Engineering (4), 244–249. https://doi.org/10.17265/2159-5828/2014.05.004.

Zhang, G Guangjun, Wu, X., 2004. A novel CO2 gas analyzer based on IR absorption. Opt Laser. Eng. 42 (2), 219–231. https://doi.org/10.1016/j.optlaseng.2003.08.001.

Zhang, W., Pan, L., Lu, L., 2023. Prediction of TVB-N content in beef with packaging films using visible-near infrared hyperspectral imaging. Food Control 147, 109562. https://doi.org/10.1016/j.foodcont.2022.109562.

103

7.4 Publication IV

Article

Non-Destructive Measuring Systems for the Evaluation of High Oxygen Stored Poultry: Development of Headspace Gas Composition, Sensory and Microbiological Spoilage

Jasmin Dold [1,*], Caroline Kehr [1], Clarissa Hollmann [1] and Horst-Christian Langowski [2,3]

[1] Chair of Brewing and Beverage Technology, Technical University of Munich, Weihenstephaner Steig 20, D-85354 Freising, Germany; caroline.kehr@tum.de (C.K.); clarissahollmann@gmail.com (C.H.)
[2] TUM School of Life Sciences, Technical University of Munich, Weihenstephaner Steig 22, D-85354 Freising, Germany; h-c.langowski@tum.de
[3] Fraunhofer Institute for Process Engineering and Packaging, Giggenhauser Straße 35, D-85354 Freising, Germany
* Correspondence: jasmin.dold@tum.de; Tel.: +49-8161-71-5633

Abstract: As poultry is known to be a perishable food, the use-by date is set in such a way that food safety is guaranteed even with a higher initial bacterial count. This means, however, that some products are wasted, even if they are still safe to eat. Therefore, non-destructive measurement devices might be a good opportunity for individual shelf-life prediction, e.g., in retail. The aim of this study was therefore to use non-destructive measurement devices based on fluorescence quenching (oxygen detection) and mid-infrared laser spectroscopy (carbon dioxide detection) for the monitoring of high-oxygen-packed poultry in different storage conditions. During 15 days of storage, the gas composition of the headspace was assessed (non-destructively and destructively), while total plate count was monitored and a comprehensive sensory evaluation was performed by a trained panel. We were able to demonstrate that in most cases, non-destructive devices have comparable precision to destructive devices. For both storage conditions, the sensory attribute *slime* was correlated with reaching the critical microbiological value of 10^7 CFU/g; the attribute *buttery* was also useful for the prediction of regularly stored poultry. The change in the gas atmosphere as a sign of premature spoilage, however, was only possible for samples stored in irregular conditions.

Keywords: modified atmosphere packaging; non-destructive; shelf-life prediction; sensory evaluation; fluorescence quenching; infrared spectroscopy; meat quality

1. Introduction

Food waste is a global issue, estimated by the FAO (Food and Agriculture Organization of the United Nations) to be about 1.3 billion tons per year worldwide [1]. In the wealthier industrialized countries, more than 50% of food waste happens during distribution in the retail sector or at the consumer's home, often due to an expired "best before" or "use by" date [1,2]. The individual quality evaluation of an already packed foodstuff represents a major research topic of our time for different reasons. First of all, the quality standards and consumer expectations of foodstuffs are constantly increasing. To integrate an intelligent sensor, e.g., a colorimetric dye, into a packaging system can serve as both a safeguard for the manufacturer to ensure quality and at the same time to give the consumer the feeling that they are in charge of quality control. The latter, however, brings the disadvantage that consumers are often insecure in estimating the information in the right way, which can cause unnecessary food waste [3]. In addition, the risk remains that the indicator is false negative due to the lack of the relevant metabolites, for example, something that could have very negative consequences if pathogens (e.g., *Campylobacter jejuni*) are present [3,4]. Contrary to the earlier assumption that chicken meat is best packed in a low-oxygen (O_2)

atmosphere [5], nowadays, a modified atmosphere packaging (MAP) with a high O_2 and a low carbon dioxide (CO_2) content is often chosen, as the high O_2 amount is known to inhibit the growth of the anaerobic pathogen *C. jejuni* [6]. Therefore, some studies focusing on the growth of microorganisms on fresh poultry under high O_2 atmosphere were conducted. By identifying different types of microorganisms as being part of the spoilage—such as *Brochothrix thermosphacta* or *Carnobacteria*—they also noticed a decrease in O_2 and an increase in CO_2 in the headspace of the packaging during the storage time, measured via destructive gas detection devices [7,8]. Further studies confirmed the connection of O_2 consumption in the headspace of packed meat products with the growth of different types of microorganisms [9,10]. However, the authors were not in full agreement whether the change in gas composition was really correlated with the critical value of spoilage or not. The critical value is defined as 10^7 colony-forming units per gram of sample (CFU/g) [11].

The quality determination of food by optical measurement methods has some advantages that cannot be denied. First of all, most of the methods are very fast and easy to handle. In addition, a lot of successful research that provides a good basis for the comparability and interpretation of results was conducted in the past. Another big advantage is that the measurements are non-destructive in most cases and can therefore be used for the quality evaluation of already packed foodstuffs. There are systems available over a wide range of the optical spectrum, with several advantages and disadvantages, as we already discussed in Dold and Langowski (2022) [12]. In our work shown here, we used measurement systems based on fluorescence quenching and infrared (IR) spectroscopy. Fluorescence quenching—or more precisely, dynamic quenching—can be used for determining O_2 concentrations, as these molecules are able to absorb the energy of a fluorophore excited by visible light which leads to a shorter luminescence lifetime as a consequence. This effect can be described with the Stern–Volmer equation [13]. It is therefore a useful tool for the detection of packaging integrity for modified atmosphere packed products [14] but may also be useful for a statement on microbiological spoilage [15], by successful integration into a suitable packaging system. Measurement systems based on IR are also well studied for the quality determination of food and already packaged foodstuffs. Schmutzler et al., for example, studied the adulteration of veal sausage with pork products, using different near-infrared (NIR) devices in 2016 [16]. When light is used in the NIR and mid-infrared (MIR) range, vibrational states of the molecules are excited; in the far-infrared (FIR), IR radiation leads to the excitation of rotational states [17]. The resulting absorption peaks are characteristic for many different properties, such as gas concentration [18] or moisture content [19]. In this work, we used a device working in the MIR range for the detection of CO_2.

At the 2nd International Electronic Conference on Foods—"Future Foods and Food Technologies for a Sustainable World", we already showed some of our results, showing that non-destructive measurement devices are able to monitor the gas atmosphere in the headspace of transparent packages. Therefore, high-O_2-packed poultry was stored over a period of 15 days at two different temperatures. We showed the development of the headspace concentrations of O_2 and CO_2 during storage via the non-destructive devices and the development of the microbiological spoilage in comparison to sensory acceptability. These results are also presented in the following publication. We concluded that the systems cannot be used for the shelf-life prediction of regularly stored poultry with only these parameters. We decided that a correlation with volatile emissions (volatile organic compounds (VOCs)) might be useful, which had to be part of an extensive sensory evaluation. In this publication, we show a more extensive sensory panel evaluation of the samples during storage, as well as the results of the previous training of the panelists. These results were further correlated in detail with the gas change and microbiological spoilage. In addition, the formed VOCs were theoretically assigned to typical meat spoilers. We also studied the influence of the headspace to meat ratio for best possible measurement accuracy. To further demonstrate the suitability of the non-destructive devices, their measurement precision was compared to that of the destructive devices.

2. Materials and Methods

2.1. Panel Training for the Sensory Evaluation

For the sensory evaluation of the samples, a panel ($n = 15$) consisting of 5 female and 10 male participants with an average age of 29 years was selected.

First, a descriptive analysis was carried out. Therefore, the panelists had to describe two poultry strips in their own words. The first sample was fresh slaughtered poultry and the second a forced-aged sample (4 days stored at 23 °C). A distinction was thereby made between visual and olfactory impression.

Based on the descriptive analysis, fitting references for further training (olfactory references) and for the sensory evaluation (olfactory and visual references) were selected and prepared, respectively. As olfactory references, common odor substances (e.g., diacetyl for *buttery*) were used. For the visual evaluation, a color chart for fresh and forced-aged poultry was designed. For this purpose, the RGB values of the meat samples were measured and transferred for both fresh and forced-aged poultry to a color chart, which was available to the panelists during the evaluation. In addition, images of fresh and forced-aged poultry were printed as image reference.

Subsequently, the named attributes were collected, and the most frequently described attributes were selected for the second part of the training, consisting of an odor identification test. For this purpose, the participants were given standardized flavors (references) corresponding to the attributes selected above, which they had to match to the correct attributes. In addition, they had to evaluate the odor intensity for each sample with the help of a line scale, ranging from weak (0) to strong (100). This was used to determine how sensitive each panelist was to the flavors.

2.2. Determination of the Headspace Gas Atmosphere

2.2.1. Non-Destructive Determination of O_2 Concentration

For the non-destructive determination of O_2 gas concentration, a fluorescence-based measurement system and associated sensor spots containing a fluorescent dye (PreSens Precision Sensing GmbH, Regensburg, Germany) were used. The measurement device works via fiber optics, exciting the embedded fluorophores at a wavelength of 505 nm. The excited fluorophores emit fluorescent light at a wavelength of 650 nm, when returning back to the ground state. Fiber optics has an integrated photodiode (which measures the luminescence lifetime of the emitting fluorophores) that is directly linked with the O_2 concentration, as already described in the Introduction section. To integrate the sensor spots into the lid film, a sensor spot was placed on the inside of the lid film, (PP/PA/PP/PA, 100 μm, allvac Folien GmbH, Waltenhofen, Germany) covered with a PP film (56 μm, Huhtamaki Flexible Packaging Germany GmbH & Co. KG, Ronsberg, Germany) and sealed with a ring-shaped sealing tool at 155 °C. Before sealing, a two-point calibration of the sensor spots in the relevant measuring range (0 and 60% O_2 % (v/v)) was carried out. All O_2 gas concentrations mentioned in the text are to be understood as percent by volume (v/v).

2.2.2. Non-Destructive Determination of CO_2 Concentration

The non-destructive measurement of CO_2 was carried out with a measurement system based on MIR spectroscopy (KNESTEL Technologie und Elektronik GmbH; Hopferbach, Germany). Three different wavelengths in the region of the CO_2 vibrational mode were used: $\lambda 1 = 4.26$ μm, $\lambda 2 = 4.45$ μm, and $\lambda 3 = 4.27$ μm. The beam of a tunable diode laser was directed at 45° through the corner of the transparent packaging. A two-point calibration with 0% (v/v) and 40% (v/v) CO_2 was carried out on the empty reference trays. All CO_2 gas concentrations mentioned in the text are to be understood as percent by volume (v/v).

2.2.3. Destructive Determination of O_2 and CO_2 Concentration

To estimate the measuring accuracy of the non-destructive devices, a comparison with a destructive measurement system was made. Therefore, a gas analyzer (MAT1500,

106

A.KRÜSS Optronic GmbH, Hamburg, Germany) with a zirconium dioxide sensor for determining O_2 and a non-dispersive infrared sensor for determining CO_2 gas concentration were used. To extract small aliquots (7 mL) of the gas atmosphere, a hollow needle belonging to the measuring device was inserted into the headspace of the packaging via a septum attached to the lid film.

2.3. Microbiological Analysis

Samples were prepared for microbiological analysis as already described in Höll et al., 2016 [7], with slight modifications: In a typical analysis, a total of 70 g of chicken strips were weighed in a sample bag (VWR International, Darmstadt, Germany) and homogenized for 120 s with 50 mL Ringer's solution (Merck KGaA, Darmstadt, Germany) in a stomacher (LabBlender400, Gemini BV, Apeldoorn, Netherlands). A tenfold dilution series of chicken homogenate was prepared with Ringer's solution. An amount of 100 µL of each dilution was later spread onto the brain heart infusion agar (Carl Roth GmbH & Co. KG, Karlsruhe, Germany) using sterile glass beads. After incubating the plates aerobically at 30 °C for 3 days, the number of colony-forming units on the plates were counted and the units per gram sample (CFU/g) were calculated.

2.4. Influence of the Headspace-to Product Ratio

For the selection of an appropriate headspace:meat ratio, a pre-trial was carried out, with two different headspace:meat ratios—6:1 and 3:1. For this purpose, 200 g fresh chicken strips (Donautal Geflügelspezialitäten, Bogen, Germany) for the 6:1 and 400 g fresh chicken strips for the 3:1 ratio were weighed in transparent polypropylene trays (ES-Plastic GmbH, Hutthurm, Germany) and sealed with a semiautomatic tray sealer (T250, MULTIVAC Sepp Haggenmüller SE & Co. KG, Wolfertschwenden, Germany) under a modified gas atmosphere of 70% O_2/30% CO_2. Afterwards, the samples were stored at 10 °C for 11 days, as a greater change in the gas atmosphere was expected at this temperature. The O_2 and CO_2 concentrations were measured with a destructive measuring device (see Section 2.2.3) during storage.

2.5. Storage at Different High-Oxygen Atmospheres
2.5.1. Sample Preparation

For the main trials, a total of 400 g of fresh chicken strips were weighed into transparent polypropylene trays and sealed with the semiautomatic tray sealer at two modified gas atmosphere compositions: 70% O_2/30% CO_2 or 80% O_2/20% CO_2. For each atmosphere, six packages were prepared using lid films with integrated sensor spots as described above. In addition, 44 samples were prepared for each gas atmosphere without integrated sensor materials for the destructive gas concentration measurement as well as for the sensory and microbiological evaluation. Samples were stored at 4 °C and 10 °C. Furthermore, three empty trays were prepared for each temperature and gas combination with sealed-in sensor spots to monitor the concentrations of O_2 and CO_2 without product influence during storage. For destructive monitoring, two empty trays were prepared for each day of measurement and each gas concentration or storage temperature ($n = 64$).

2.5.2. Determination of O_2 and CO_2 Gas Concentration

The gas atmosphere of the prepared trays was monitored for 15 days (except for day 3 for the filled trays and days 3, 5, 6, 12, and 13 for the empty trays) via the non-destructive measurement devices for O_2 and CO_2 detection. In addition, measurements with the destructive measuring device for O_2 and CO_2 detection were carried out on days 0, 1, 4, 6, 8, 11, 13 and 15 to validate the measuring precision of the non-destructive devices for this purpose.

2.5.3. Determination of the Total Viable Count

The total viable count (TVC) was determined for each temperature and gas composition on days 0, 1, 4, 6, 8, 11, 13, and 15 in duplicate.

2.5.4. Sensory Evaluation during Storage

During the storage trial, the samples were investigated by the panelists on days 0, 1, 4, 6, and 8 (4 °C and 10 °C), and on days 11 and 14 for the samples stored at 4 °C. The intensity of the previously specified and trained attributes was evaluated visually and olfactorily on a line scale ranging from 0 to 100 (0 = not perceptible; 100 = strongly perceptible). In addition, it was asked whether the sample was perceived as visually and olfactorily fresh or rotten. This was also classified by a line scale ranging from 0 (fresh) to 100 (rotten). For the evaluation, a sample was defined as no longer acceptable when the average value of the olfactory or visual impression was ≥ 50.

2.6. Statistical Analysis

The drawings and statistical analysis were performed using MS Excel and Origin version 2021 (Origin Lab., Hampton, VA, USA). All data are presented as the arithmetic mean $\pm$ standard deviation. For the calculation of the statistical significance, two-sample t-tests (two-tailed) were performed (alpha level 0.05). An analysis of variance was performed to test for equal variances prior to t-test analysis.

3. Results and Discussion

3.1. Panel Training

The first part of the panel training consisted of a descriptive analysis. The summed attributes of the panel are shown in Table 1 for both the visual and olfactory impressions. For the forced-aged sample, many more attributes were found. This is to be expected, as fresh poultry is rather odorless and characterized by a neutral pink coloration [20]. The named attributes for the forced-aged samples were also mostly described in the literature [20–23]. The two odors, *buttery* (diacetyl) and *pungent* (acetic acid), which are also linked with the spoilage of poultry [22,23], were not mentioned by the panel. Nevertheless, they were added to the descriptors and were part of the second part of the training. One possible reason for the missing perception of these attributes during the descriptive analysis might be the forcing at room temperature. In this case, the sulfurous impression became very intense, which probably overlapped with the presence of the diacetyl and pungent odor. For the second part of the training, the references showed in Table 2 were chosen for the odor identification test. All panelists were able to correctly match the flavors to their fitting attributes.

Table 1. Results of the descriptive analysis for the visual and olfactory attributes named by the panel for a fresh and forced-aged (4 days at 23 °C) poultry sample.

Visual Impression				Olfactory Impression			
Fresh Poultry		**Forced-Aged Poultry**		**Fresh Poultry**		**Forced-Aged Poultry**	
Fresh	11	Grey	11	Fresh	10	Rotten egg/sulfurous	15
Pink	10	Green	8	Neutral	8	Rotten	9
Salmon-colored	3	Slime	6	Poultry typical	2	Rancid	7
Solid shape	2	Glossy	6	Weak	1	Fishy	6
Skin-colored	1	Weeping/wet	5			Cheesy	5
Appealing	1	Rotten	3			Sweet	3
		Brown	2			Fruity	2
		Yellowish	1			Acidic	2
		Mushy	1			Ammonia	1
						Flowery	1
						Lemony	1
						Drain-like	1

108

Table 2. Chosen descriptors for the sensory evaluation, based on the descriptive analysis of the panel training. The references and scale for the olfactory impression were also used for the second part of the training—the odor identification test.

Descriptor	Scale	Reference
Visual Impression		
Overall impression	0 (fresh)–100 (rotten)	Images fresh and forced-aged sample
Color	0 (pink)–100 (grey)	Color chart
Green discoloration	0 (none)–100 (clear)	Color chart
Slime	0 (not present)–100 (present)	-
Gloss	0 (weak)–100 (strong)	Images fresh and forced-aged sample
Olfactory Impression		
Overall impression	0 (fresh)–100 (rotten)	-
Odor	0 (neutral)–100 (intense)	Water
Buttery	0 (not perceptible)–100 (clearly perceptible)	Diacetyl
Fruity/peach	0 (not perceptible)–100 (clearly perceptible)	Gamma-decalactone
Rotten egg	0 (not perceptible)–100 (clearly perceptible)	Sodium sulfide
Fishy	0 (not perceptible)–100 (clearly perceptible)	Cis-4-heptenal
Cheesy/rancid	0 (not perceptible)–100 (clearly perceptible)	Butanoic acid
Pungent	0 (not perceptible)–100 (clearly perceptible)	Acetic acid

3.2. Influence of the Headspace to Product Ratio

The measurement of O_2 and CO_2 over a storage period of 11 days at 10 °C with two different headspace:meat volume ratios showed very clearly that the headspace volume is decisive for the effect of O_2 respiration, which was previously described. In Figure 1, it can be seen that the samples with a headspace:meat volume of 3:1 experienced a considerable change in headspace atmosphere, as both O_2 and CO_2 reached a concentration between 45 and 50% on day 11. This means that the O_2 amount decreased and the CO_2 amount increased, as the starting concentration was 70% O_2 and 30% CO_2.
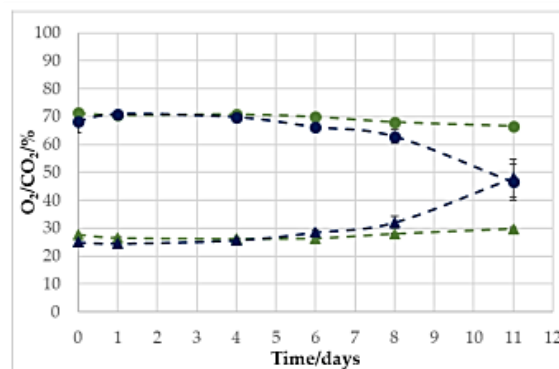

Figure 1. Development of the relative volume concentration of O_2 (•/•) and CO_2 (▲/▲) for a headspace:meat ratio of 6:1 (•/▲) and 3:1 (•/▲) at a storage temperature of 10 °C for 11 days ($n = 2$ for each measuring point).

However, the samples with a 6:1 ratio showed hardly any change, with end-concentrations on day 11 of 66.6 ± 0.2% O_2 and 29.8 ± 0.37% CO_2. For this reason, the following trials were carried out with a headspace:meat volume ratio of 3:1.

3.3. Non-Destructive vs. Destructive Determination of O_2 and CO_2 Concentration

To estimate the measuring precision and the suitability of the tested application, a comparison of the non-destructive and destructive measurement systems was carried out and can be seen in Figure 2. Clearly, the measuring points on day 0 and 1 for O_2 were not in agreement with the destructive measurement. That is due to the fact that the sensor spots were integrated into the packaging lid under atmospheric oxygen partial pressure, and therefore the higher O_2 concentration of the MAP had to permeate first into the spot area. For the CO_2 measurement, the values could be recorded directly in real time.

From day 4, the measured values of the non-destructive methods of both O_2 and CO_2 were mostly in agreement with the destructive measurements, with individual exceptions, which are explainable by measurement inaccuracies. However, it is also noticeable that a very high standard of deviations were partially present. Presumably, two effects must be distinguished here. If we look at the measuring point on day 11 of graph d, it becomes clear that this must be an effect in which the gas development in different packages was different, since both the O_2 and the CO_2 content have a similarly large deviation. Here, the individual development of the gas atmosphere by spoilage—which builds the basis of this research—is again clarified.
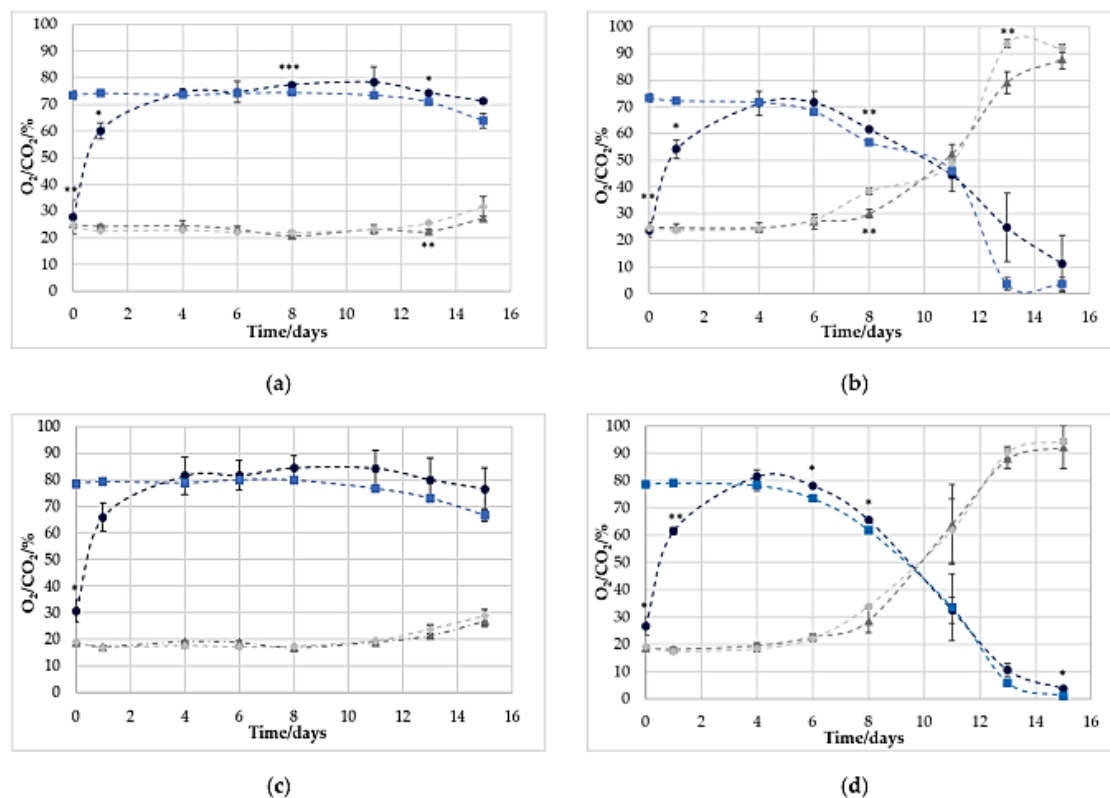

Figure 2. Comparison between the destructive (■/◆) and non-destructive (●/▲) measurement devices for the investigation of O_2 (■/●) and CO_2 (◆/▲) during the storage of poultry over 15 days under different storage conditions: (a) 70% O_2/30% CO_2 4 °C (b) 70% O_2/30% CO_2 10 °C (c) 80% O_2/20% CO_2 4 °C (d) 80% O_2/20% CO_2 10 °C. Indices indicate a significant difference between the curves measured with the destructive and non-destructive measurement devices: * $p < 0.05$, ** $p < 0.01$, and *** $p < 0.001$.

3.4. Development of the Gas Concentration in Empty and Filled Trays

Since the non-destructive measuring systems had similar accuracies compared to the destructive systems, the following results were obtained using only the non-destructive devices. The results are shown in Figure 3.

For the empty trays, almost no changes in the gas content were detected. The amount of O_2 and CO_2 increased and decreased slightly, respectively. In addition, the optical measurement method for O_2 deviated from the real values at the first two to three measurement points. This was because the sensor spots were sealed into the lid film under atmospheric conditions and the higher O_2 concentration in the MAP had to permeate into the spot area first, which was previously discussed in Section 3.3.
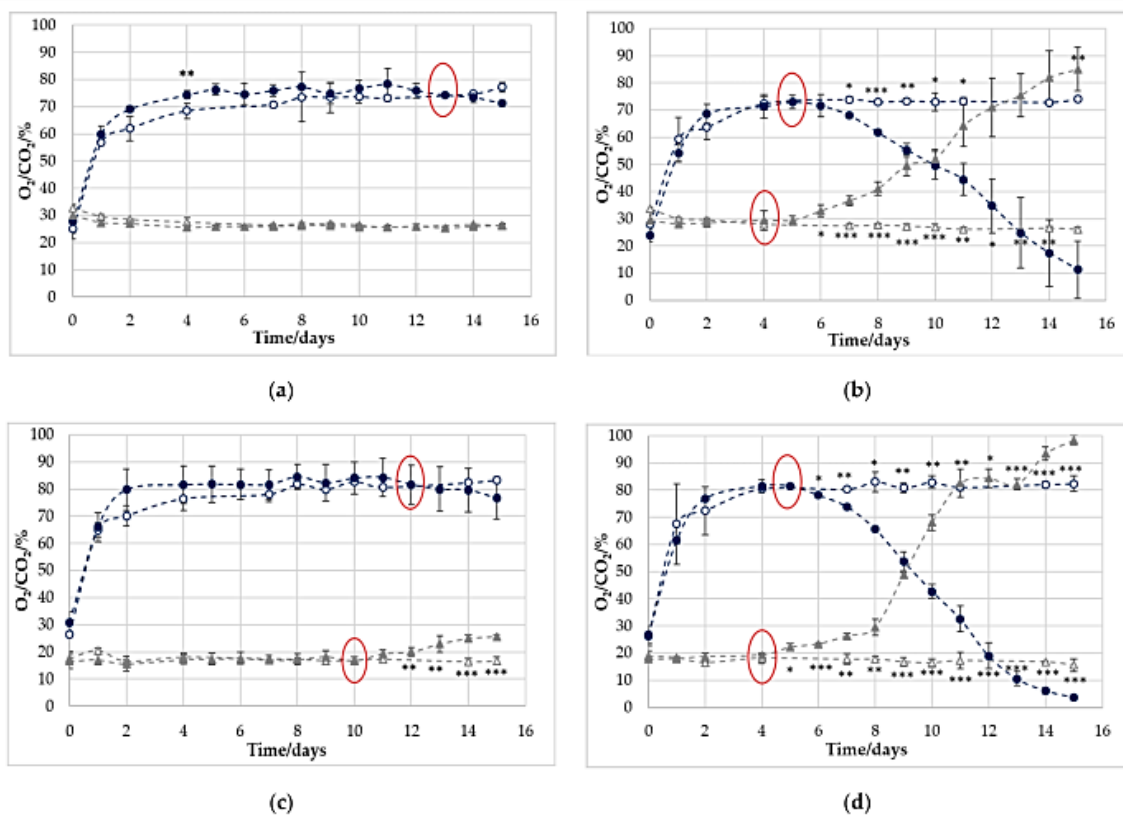
Figure 3. Development of O_2 ($\bigcirc$/$\bullet$) and CO_2 ($\triangle$/$\blacktriangle$) under different storage conditions over 15 days in trays with ($\bullet$/$\blacktriangle$) and without poultry ($\bigcirc$/$\triangle$): (**a**) 70% O_2/30% CO_2 4 °C (**b**) 70% O_2/30% CO_2 10 °C (**c**) 80% O_2/20% CO_2 4 °C (**d**) 80% O_2/20% CO_2 10 °C. Indices indicate a significant difference between the curves with and without poultry: * $p < 0.05$, ** $p < 0.01$, and *** $p < 0.001$. The red circles mark the point when the curve of the respective gas concentration in the filled trays intersects that for the empty trays (cross-over), which indicates a microbiologically induced change in the headspace atmosphere.

By comparing the empty and filled trays, the influence of the product was determined. The samples stored at 4 °C and flushed with 70% O_2 and 30% CO_2 (Figure 3a) showed the least change, only having a noticeable cross-over on day 13 for O_2. A "cross-over" was defined as the day when the curve of the respective gas concentration in the filled trays intersects that of the empty trays. This is an indication of a microbiologically induced change

111

in the headspace atmosphere. For CO_2 content, however, no change in the headspace atmosphere was observed for the filled and empty trays.

The sample stored at 10 °C (Figure 3b) showed significant greater effects. For these samples, a cross-over for O_2 was detected on day 5, and for CO_2 was detected one day earlier. For both gases, the first significant deviation between empty and filled trays was present two days after having the cross-over (O_2: day 7; CO_2: day 6). Afterwards, a rapid decrease in the O_2 and a similar increase in the CO_2 concentration were visible. For both, the O_2 and the CO_2 measurements of the filled trays, high standard deviations were visible from day 11 on. As already described in the prior chapter, this was an effect induced by the individual development of the microbiota.

For the 80% O_2/20% CO_2 MAP samples stored at 4 °C (Figure 3c), a significant deviation was noted between the filled and empty trays for the CO_2 measurement from days 12 to 15. However, O_2 did not show a statistically significant deviation. The cross-over was on day 12 and then the O_2 content of the filled package decreased steadily until day 15. Samples stored at 10 °C showed the earliest deviation from the empty trays, with a significant change at day 5 for CO_2 and day 6 for O_2. The cross-over was on day 4 (CO_2) and 5 (O_2), similar to the samples packed at lower oxygen amounts. The O_2 decrease and CO_2 increase was even faster, with values almost reaching 100% CO_2, and totally respired O_2 on day 15.

The results clearly indicate that a difference in microbiological spoilage was present. However, the fact that the samples stored at 4 °C showed such a low change in gas concentration stands in contrast to the underlying study of Höll et al., 2016 [7]. Herbert et al. showed more similar results in their study, published in 2015. In that study, the O_2 decrease and CO_2 increase were comparable for the 4 °C samples, packed under 70% O_2/30% CO_2 MAP. The chicken stored at 10 °C had already reached its cross-over at day 2, and the O_2 decreased to a value of 20%, while the CO_2 increased to 60% on day 5 [8]. These results raise the question of whether the overall degree of microbiological spoilage has a lesser impact, and the composition of the microbiome may play a much greater role. To further answer this, the next chapter shows the determined TVCs.

3.5. Microbiological Growth

All samples had a similar starting value of the total viable count of approximately 10^4 CFU/g (see Table 3 and Figure 4). The samples that were stored at 10 °C showed a faster and more immediate growth and reached the defined critical value of 10^7 CFU/g [11] after about 3 (80/20) or 4 days (70/30). The samples that were stored at 4 °C grew significantly slower and reached this value after about 6 (80/20) or 7 (70/30) days. At the end of storage, all the samples were well above the critical limit. The highest value of >10^{10} CFU/g was reached by the sample packed with 80% O_2 and 20% CO_2, which was stored at 10 °C. However, the samples stored at 4 °C also reached final values of >10^9 CFU/g.

Comparing these results with the literature, only partially similar results are evident. Höll et al., for example, observed a different growth of the TVC during their 2016 study, although they chose the same storage conditions (80% O_2/20% CO_2 at 4 and 10 °C) and had similar starting values of TVC. For the samples stored at 4 °C, they reached the critical value for the first time at day 10; for the samples stored at 10 °C, it was reached on day 6 [7]. Rossaint et al. also showed a lower increase in their TVC at 4 °C [20]. However, other studies showed results more similar to ours, reaching critical values between day 4 and 6 [8,21,22] for the samples stored at 4 °C, and on day 2 for the samples stored at 10 °C [8].

These results show very clearly that the type of microorganisms is decisive for O_2 consumption and CO_2 generation, not necessarily the absolute number of microorganisms. This fact may present difficulties for the prediction of shelf life.

(a) (b)
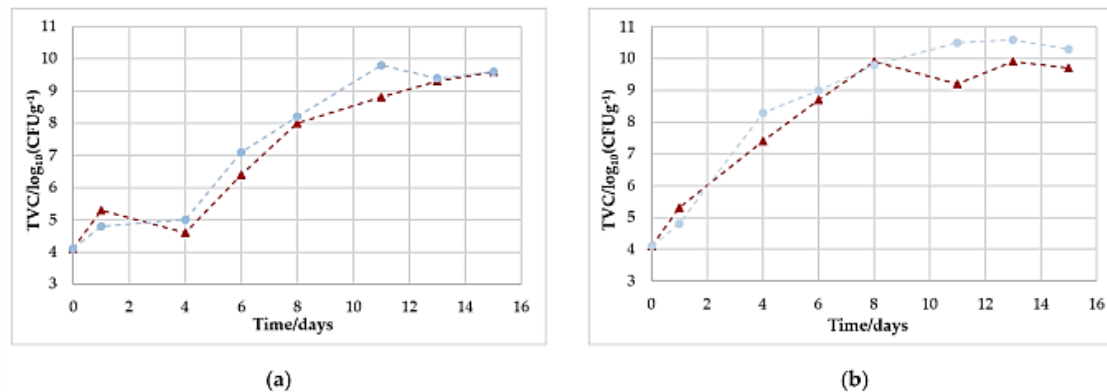
Figure 4. Development of the total viable count (TVC) for poultry stored under different storage conditions over 15 days in trays with initial gas concentrations of 70% O_2/30% CO_2 (▲) and 80% O_2/20% CO_2 (●) at (a) 4 °C and (b) 10 °C.

Table 3. Total viable count (TVC) for the poultry on days 0 and 15 for each storage condition ($n = 4$) and the day the critical limit of 10^7 CFUg^{-1} was reached (end of shelf life).

	Day 0	Day 15	Shelf Life Expired
80/20 4 °C	1.36×10^4 CFUg^{-1}	4.00×10^9 CFUg^{-1}	Day 6
70/30 4 °C	1.27×10^4 CFUg^{-1}	4.29×10^9 CFUg^{-1}	Day 7
80/20 10 °C	1.36×10^4 CFUg^{-1}	2.19×10^{10} CFUg^{-1}	Day 3
70/30 10 °C	1.27×10^4 CFUg^{-1}	4.47×10^9 CFUg^{-1}	Day 4

3.6. Sensory Evaluation

The sensory panel was able to determine changes for the visual and olfactory attributes that were defined in Table 2. In Figure 5, the sensory evaluation of the samples stored at 4 °C are shown for both gas concentrations. Aside from the visual descriptor, *gloss*, all attributes increased during the storage time. For the visual evaluation, the *overall impression* (fresh/rotten), *slime* (not present/present) and *color* (pink/grey) increased the most, all signs of spoilage. For the orthonasal evaluation, the *overall impression* and the intensity of the *odor* showed the highest change. The descriptor *buttery* also noticeably increased. Except for the descriptor *gloss*, all attributes were still below 50 scores, prior to the end of the shelf life. This becomes even clearer when looking at Figure 5c,d.

For both gas concentrations, the overall olfactory impression reached the limit of 50 scores clearly after the critical value of 10^7 CFU/g was achieved. More specifically, the sample packed with a MAP of 70% O_2/30% CO_2 was classified as rotten only on the last day of evaluation; for the sample packed with 80% O_2/20% CO_2, olfactory spoilage was reached on day 11. Poultry stored at 10 °C (see Figure 6) showed a very similar progression to the 4 °C stored sample but at a much faster rate. However, some attributes were even more evident than those in the samples stored at 4 °C. For the visual evaluation, the samples were classified as more *greyish* and *greenish* on day 8. For the olfactory evaluation, the descriptors *buttery* and *cheesy/rancid* were slightly higher than the 4 °C samples on day 14. However, again, by reaching the critical microbiological limit value, the impressions were below the 50 scores value and therefore, visual and olfactory were rated as still *fresh*.

(a)

(b)

(c)

(d)
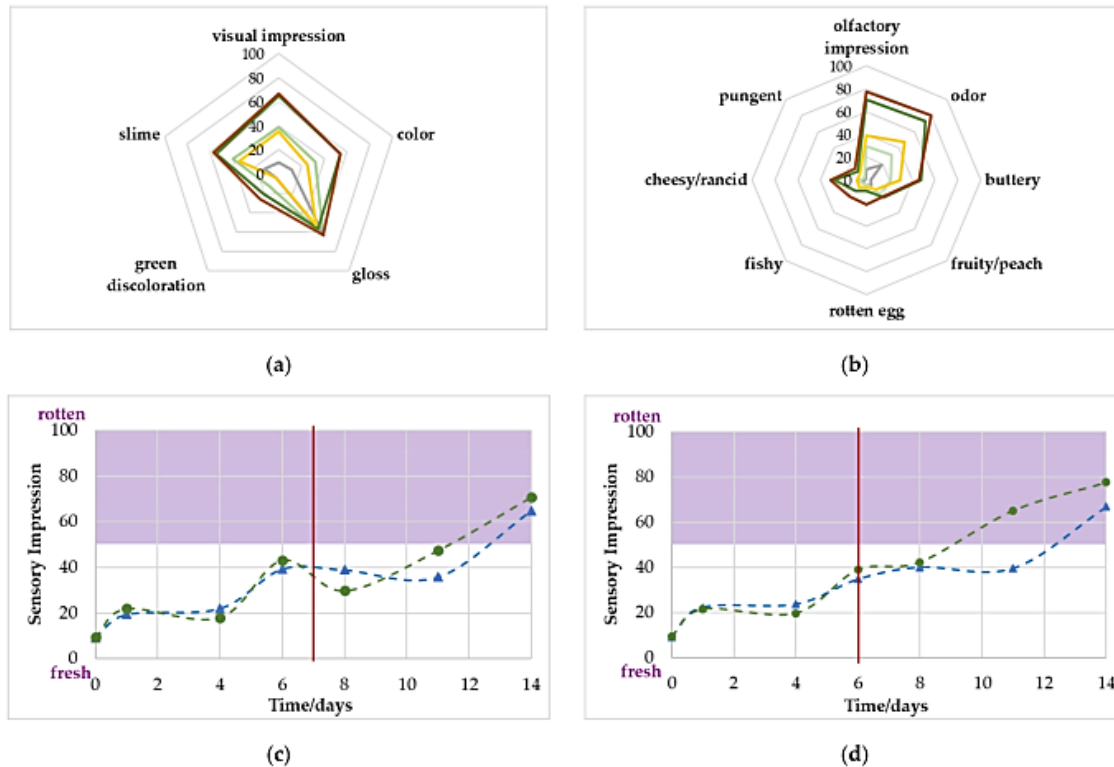
Figure 5. (**a,b**): Sensory evaluation of the poultry stored at 4 °C by the panel with the chosen descriptors for (**a**) visual and (**b**) olfactory attributes on day 0 (grey line), after reaching the critical value of 10^7 CFU/g (70% O_2/30% CO_2: light green; 80% O_2/20% CO_2: yellow) and on day 14 (70% O_2/30% CO_2: dark green; 80% O_2/20% CO_2: brown). (**c,d**): Change in the overall visual (▲) and olfactory (•) impression during the storage time: (**c**) 70% O_2/30% CO_2 4 °C and (**d**) 80% O_2/20% CO_2 4 °C. The red line marks the point when the microbiological limit value was achieved. The purple area indicates the previously defined sensory limit of 50 scores.

Table 4 compares the evaluation of the sensory attributes more precisely. It is also shown which VOC is dominant or typical for the descriptor on high-oxygen-stored poultry and which microorganisms are often responsible for the emitted substances. With respect to this, it should be said that almost all meat spoilage organisms can form the typical spoilage aroma and it is assumed, that the formation of VOCs can be a result of the interactions between different spoilage bacteria, which makes it difficult to assign specific odors to a single species [24]. However, we focused on the involvement of *Brochothrix thermosphacta*, lactic acid bacteria (LAB) (e.g., *Carnobacterium* ssp., *Leuconostoc* ssp., *Lactobacillus* ssp.) and *Pseudomonas* ssp. because, based on previous studies, we assumed that these were the main spoilage bacteria in our chicken samples [7,22,25,26].

All samples showed a noticeable change in meat *color*, changing from *pink* to *grey*. For beef, this effect is related to low oxygen levels, as red oxymyoglobin turns into metmyoglobin, which is known to appear as grey–brown [27]. However, this mechanism cannot be the cause for the color change observed in poultry, as several studies have shown that lower levels of oxygen actually result in a more stable color in fresh poultry [28]. In 2017, Franke et al. also showed that storing poultry in two different oxygen-rich atmospheres resulted in similar greying effects, which is consistent with our experiments [22]. From our point of view, the greying must be an oxidation effect initiated by several microorganisms.
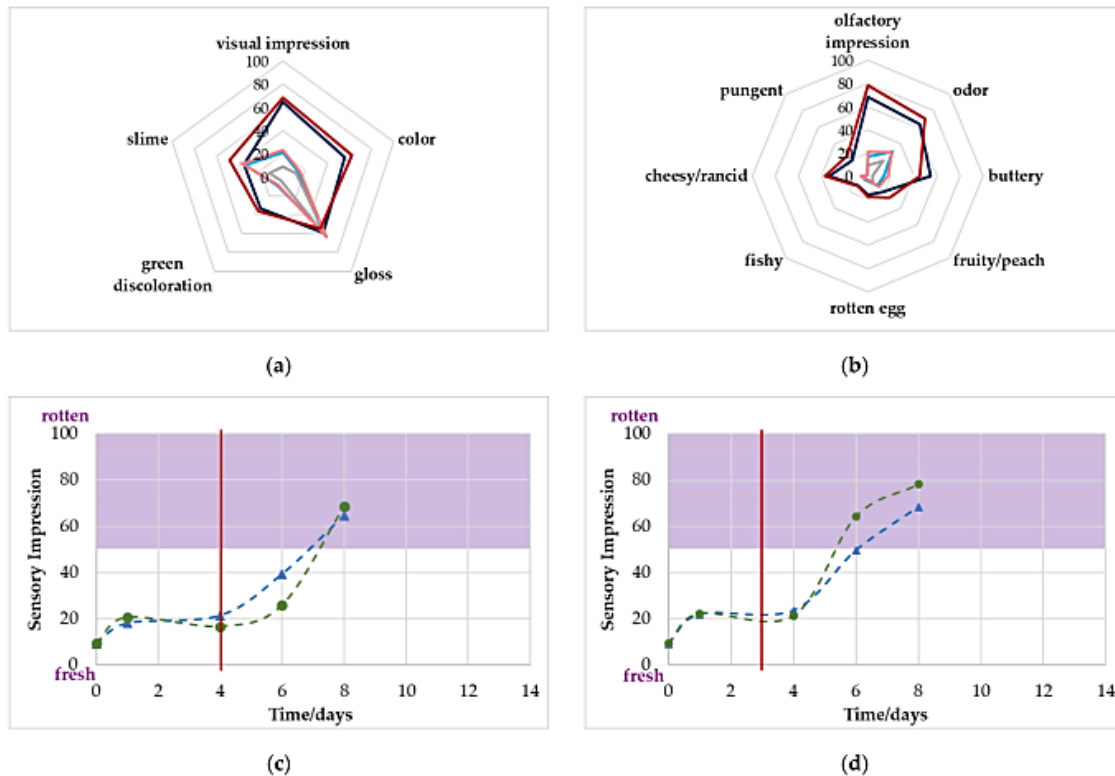
Figure 6. (**a**,**b**): Sensory evaluation of poultry stored at 10 °C by the panel with the chosen descriptors for (**a**) visual and (**b**) olfactory attributes on day 0 (grey line), after reaching the critical value of 10^7 CFU/g (70% O_2/30% CO_2: light blue; 80% O_2/20% CO_2: pink) and on day 8 (70% O_2/30% CO_2: dark blue; 80% O_2/20% CO_2: red). (**c**,**d**): Change in the overall visual (▲) and olfactory (●) impression during the storage time: (**c**) 70% O_2/30% CO_2 10 °C and (**d**) 80% O_2/20% CO_2 10 °C. The red line marks the point when the microbiological limit value was achieved. The purple area indicates the previously defined sensory limit of 50 scores.

Gloss seems not to be an attribute that can be linked with the poultry quality, as no change was observed by the panel.

The *green discoloration* was more present for the samples stored at 10 °C at the end of the storage, compared to the samples stored at 4 °C. However, both samples showed a significant increase during this observation. The greening of food of animal origin is known to be induced by several microorganisms [29,30]; however, several studies were able to connect *Pseudomonas* with this phenomenon as a result of the formation of sulfur compounds [23,31–33]. Since the *green discoloration* was clearly increased in the descriptive analysis (see Section 3.1) and a connection with the *rotten egg* attribute was also seen here, this assumption is supported once again.

In general, *slime* formation is not a question of which microorganisms dominate, but how large the microbial count is, as the breakdown of the tissue begins at 10^8 CFUg^{-1}, in other words, after the sample is microbiologically spoiled [34]. This is also consistent with the panel's perception at the time that the critical limit was reached for most of the samples, as the slime formation clearly already increased in this regard.

Table 4. Sensory evaluation of the visual and olfactory descriptors under different storage conditions from day 0 to the last day of sensory evaluation (4 °C: Day 14, 10 °C: Day 8). Each + stands for an increase of 10 scores on the line scale, each − stands for a decrease of 10 scores, 0 stands for a change <10 scores. * Responsible VOCs and spoilage bacteria regarding the literature-based assumptions for the tested descriptors, e.g., lactic acid bacteria (LAB).

Descriptor	Development by Storage at				VOCs *	Spoilage Bacteria *
	4 °C		10 °C			
	70/30	80/20	70/30	80/20		
Color	++++	++++	++++	+++++	Not known	Unclear
Gloss	-	0	0	-	Not known	Not known
Green discoloration	++	++	+++	+++	Sulfur compounds [33]	*Pseudomonas* ssp., *LAB* [23,30–32]
Slime	++++	++++	++	++++	-	Diverse [29,34]
Buttery	++++	++++	+++++	++++	2,3-butanedione (diacetyl) [35]	*LAB* [25,32] *B. thermosphacta* [29]
Fruity	+	+	+	++	Ethyl esters [23,35,36], 1-Hexanol [25]	*Pseudomonas* ssp. [36]
Rotten egg	+	++	+	+	Sulphur compounds [33]	*Pseudomonas* ssp. [23,31]
Fishy	+	++	+	+	Trimethylamine [37]	*Pseudomonas* ssp. [22]
Cheesy/Rancid	++	+++	+++	+++	Isovaleric acid; (2- and 3-methyl) butanoic acid [38,39]	*LAB* [25] *B. thermosphacta* [32,39]
Pungent	+	+	++	++	Lactic acid [40], acetic acid [41], propanoic acid [25]	*LAB* [25] *B. thermosphacta* [32,35,41]

The descriptor with the strongest increase—aside from the *overall visual* and *olfactory impression*—was *buttery*, which is linked with the VOC diacetyl (2,3-butanedione). Diacetyl is synthesized by LABs as *Carnobacterium divergens* or *B. thermosphacta* [25,42], but it can be also present for *Pseudomonas* inoculated samples [35]. With the exception of the 70/30 sample stored at 10 °C, the increase in the attribute *buttery* was rated by the panel as equivalent (++++). Therefore, it is very likely that a mixture of LAB and *B. thermosphacta* was responsible for this VOC formation.

Typical VOCs, which are perceived as *fruity*, are ethyl esters—such as ethyl acetate, ethyl butanoate, ethyl 2-hexenoate, etc.—and are very often produced by *Pseudomonas* [23]. As this aroma was more present for the 10 °C stored samples packed at 80% O_2/20% CO_2, we assume that these microorganisms were highly present, especially at the end of storage. This also agrees well with the *greening* previously described. However, the evaluation of the attributes *rotten egg* and *fishy* do not totally fit that presumption, as a highest increase was present here for the 4 °C 80/20 samples.

Volatile fatty acids are responsible for a *cheesy* or *rancid* odor. These are often formed by *B. thermosphacta*, but can also be formed during spoilage where high amounts of LABs are present [25,32,39]. This fits very well with our results, as the samples stored at 10 °C, and the 80/20 sample stored at 4 °C showed an increase in these attributes. These samples also showed a decrease in the concentration of O_2 in the headspace. This is in line with the respiration abilities of these microorganisms, especially with those of *B. thermosphacta* and *Leuconostoc gelidum* [10].

The oxygen consumption by *B. thermosphacta* and LABs for the samples stored at 10 °C can be further underlined by the higher increase in the attribute *pungent* for these samples, as the formation of acetic and lactic acid is linked with these meat spoilers [32,35,40,41].

3.7. Correlation of the Results

Table 5 gives an overview of the tested parameters and indicates some observed correlations. "Correlations" are understood as mutual, temporal relationships. The correlations refer to effects (e.g., the change in gas content and microbiological spoilage) that occurred at the same or a similar point in time. Yellow describes a possible association between

the cross-over and microbiological spoilage. Orange indicates a correlation between the cross-over and sensory changes. Green indicates a correlation between the change in gas concentrations in the headspace and sensory changes. Grey stands for a correlation of microbiological spoilage and sensory changes.

Table 5. Observed correlations between the tested parameters. $p \leq 0.05$ represents the first day where the difference between empty and filled trays was significant with $p \leq 0.05$, after the cross-over was reached. "Microbiologically spoiled" indicates a TVC of 10^7 CFUg^{-1} and "sensory changes" shows the panel classification of the sensory panel with: >50 scores for the overall olfactory impression ("olfactory spoiled") and an increase of >20 scores in the descriptors *slime*, *color*, *buttery* and *cheesy*. A description of the color marking of the correlations can be found in the previous text.

		4 °C		10 °C	
		80/20	70/30	80/20	70/30
	Cross-over O_2	12	13	5	5
	Cross-over CO_2	10	-	4	4
	$p \leq 0.05$ O_2	-	-	6	7
	$p \leq 0.05$ CO_2	12	-	5	6
	Microbiologically spoiled	6	7	3	4
Sensory Changes	Overall olfactory impression	11	14	6	8
	Slime	6	6	4	4
	Color	8	8	6	8
	Buttery	6	6	6	8
	Cheesy/rancid	11	14	6	8

3.7.1. Correlation of Change in Gas Concentrations with Microbiological Spoilage

As described previously, some studies were carried out that also indicate a correlation between O_2 respiration and microbiological spoilage for chicken meat [7,9]. However, this study could not completely confirm these findings. For all samples, no significant change in the gas concentration of the headspace was noted when the limit of 10^7 CFU/g was reached. Microbial spoilage might be visible with the help of the previously described cross-over point for CO_2 detection; however, this is only valid for the samples that were stored at 10 °C. This point was reached either on the day (70/30) or 1 day after (80/20) the critical value of 10^7 CFU/g was reached. The suggestion that the cross-over could be an indication of premature spoilage, e.g., due to improper storage, is further underlined in the literature, where chicken samples were also stored at 70% O_2 and 30% CO_2 at 10 and 15 °C, and the cross-over of the reference and the packed sample for O_2 and CO_2 measured with a destructive device (=empty tray) were consistent in reaching their critical value [8].

A significant change in the headspace gas atmosphere occurred in the samples stored at 10 °C, and also for CO_2 detection in the 80/20 4 °C samples; however, the TVC was already $\geq 10^9$ CFU/g in these cases. For the samples stored at 10 °C, a very strong change occurred for both gases in the gas atmosphere after 5 or 6 days. At the end of the storage period, the gas atmosphere completely changed in the headspace. Nevertheless, the total microbiological growth was not very different compared with the 4 °C samples after 15 days. This is a strong indication that the type of microorganisms, and not necessarily the quantity, was crucial for O_2 consumption. This was confirmed in a study wherein beef was inoculated with different meat-spoiling bacteria. Samples contaminated with *Brochothrix thermospacta* showed significant O_2 consumption, while samples contaminated with *Carnobacterium divergens* and *Carnobacterium maltaromaticum* showed no consumption

at all, even at microbial populations of $\geq 10^8/cm^2$ [10]. This shows that it is mainly the individual microbiota that determines O_2 consumption and CO_2 production, which makes a shelf-life prediction on this basis difficult. However, the cross-over seems to be a useful tool for identifying inappropriately stored samples, e.g., in case of cold-chain interruption.

3.7.2. Correlation of Change in Gas Concentrations with Sensory Evaluation

There appeared to be a correlation between the gas development and sensory acceptance or descriptors in some cases. For the poultry that was stored at 4 °C at initial gas concentrations of 80% O_2 and 20% CO_2, a significant change in CO_2 was observed on day 12, and the cross-over happened on day 10. This agreed with the *overall olfactory impression* on day 11 when the panel classified the sample as *not acceptable* for the first time. The 4 °C 70/30 sample had its cross-over with O_2 on day 13 and the first classification as *olfactory spoiled* on day 14. However, the classification on day 11 was slightly below the 50 scores limit, which is why a prediction of shelf life via a determination of the composition of the headspace gases is rather unlikely. The *overall olfactory impression* was probably mostly induced by the descriptor *cheesy/rancid* in this case, as both attributes were rated by the panel with an increase of >20 scores compared to day 0 on the same days for each gas composition (80/20: day 11; 70/30: day 14). For the samples stored at 10 °C, however, a very good fit between the gas concentration and the sensory changes was observed. The 80/20 samples experienced their significant change in CO_2 on day 5 and for O_2 on day 6. At this time, the *overall olfactory impression* was scored as spoiled by the panel and the *greyish color*, and the descriptors *buttery* and *cheesy/rancid* increased by >20 scores. For the 70/30 sample, the gas change occurred one day later; for both gases and the sensory changes, the defined levels were reached on day 8, except for *slime*.

3.7.3. Correlation of Sensory Evaluation with Microbiological Spoilage

Several sensory attributes show a correlation with microbiological spoilage. For the samples stored at 4 °C, the descriptors *slime* and *buttery* increased by >20 scores on day 6 (80/20) or day 7 (70/30), while the critical value of 10^7 $CFUg^{-1}$ was reached on day 6 for both initial gas compositions. Inappropriately stored samples at 10 °C also showed the *slime* formation when the critical TVC was reached. This fact demonstrates the need for other detection methods, especially for the samples stored at 4 °C, as the non-destructive gas evaluation seems not to be suitable here. The identification of *slime* could be possible using other spectroscopic analysis methods such as absorption spectroscopy in the infrared or Raman spectroscopy on the surface of the sample. Another possibility would be the use of hyperspectral imaging. All of these are useable as non-destructive methods for already packed products as well [12].

3.8. Influence of the Microbiome

These results allow some conclusions to be drawn about the type of spoilage microorganisms, with some limitations. Franke et al. (2017) showed that chicken breasts packed at high O_2 and stored at 4 °C were mainly populated with *B. thermospacta*, and developed *Carnobacteria* sp. and *Pseudomonas* sp., mainly under MAP with lower CO_2 concentrations ($\leq$15%) [22]. Because *Pseudomonas* sp. are responsible for the formation of VOCs [20], this agreed well with the earlier sensory spoilage of the 80/20 sample, compared with that of the 70/30 sample. However, O_2 was hardly respired at this point, which could be because of the small population of *B. thermospacta;* the lack of heme, compared to beef; or because of the low temperature [9,10]. The influence of storage temperature was visible, especially with respect to sensory evaluation and gas development. In addition, this was also observed by Höll et al. (2016). They had a mixed microbiota at the beginning of storage. Later, at 4 °C, a mixture of *B. thermospacta*, *Pseudomonas* sp., and *Carnobacteria* sp. grew, and at 10 °C, the microbiota mainly consisted of *Pseudomonas* sp. and *Serratia* sp. at the end of storage period. After 4–8 days, *B. thermospacta* was present, which likely favored O_2

consumption. Then, VOC-forming *Pseudomonas* sp. could grow [7]. This effect was likely the same as that observed in this study.

In conclusion, the composition of the microbiome in this work can only be estimated based on the gas change in the headspace and the VOCs produced. So, a reliable statement can be made and the clarification of the species would have to be carried out in the future, e.g., using MALDI-TOF MS.

4. Conclusions

This study showed that the presented non-destructive measurement systems can monitor the O_2 and CO_2 concentrations in the headspace of a package in real time and showed little to no deviations to the destructive methods in which gas samples were extracted from the headspace. The measurement of the CO_2 with the infrared-based systems showed no problems. The observed variations in headspace gas composition could be attributed to individual compositions of the microbiota on the samples. The systems, however, cannot be used to predict the shelf life of high-O_2-packed poultry stored under regular conditions and the resulting regular decay mechanisms. For the detection of premature microbial spoilage, however, e.g., due to contamination or an interruption in the cold chain, CO_2 detection might be especially useful because a significant change in the CO_2 fraction of the headspace could be observed before sensory spoilage, and the defined cross-over was correlated with reaching the critical value of 10^7 CFU/g. The predominant sensory changes identified by the successfully trained panel were *overall olfactory* and *visual impression*, the formation of *slime*, *color* change from *pink* to *grey*, and the formation of the odors *buttery* and *cheesy/rancid*. However, a correlation with the microbiological shelf life (10^7 CFU/g) was only possible with the formation of *slime* (4 °C and 10 °C) and *buttery* (4 °C). As the formation of VOCs also strongly depends on the microbiome, the detection of diacetyl (=*buttery*) is not a recommendable approach in our view. This is particularly true because the detection of individual substances using simple indicators can be disturbed by the presence of other substances. The optical detection of *slime* could instead be more promising. In addition, the influence of the heme concentration should be clarified by experiments with beef in the future, as this seems to have a main role in O_2 consumption. Another possible application for the technologies might be the detection of leakages in packages or process control for MAP production lines. For this purpose, further investigations should be carried out on the measurement accuracy of the two non-destructive methods.

Author Contributions: Conceptualization, J.D., C.H., C.K. and H.-C.L.; methodology, J.D., C.H., C.K. and H.-C.L.; validation, J.D., C.H. and C.K.; formal analysis, J.D. and H.-C.L.; investigation, J.D., C.H. and C.K.; data curation, J.D., C.H. and C.K.; writing—original draft preparation, J.D.; writing—review and editing, H.-C.L.; visualization, J.D. and C.K.; supervision, H.-C.L.; project administration, J.D. and H.-C.L. All authors have read and agreed to the published version of the manuscript.

Institutional Review Board Statement: The study was conducted according to the guidelines of the Declaration of Helsinki and the TUM ethic committee.

Informed Consent Statement: Informed consent was obtained from all subjects involved in the study.

Data Availability Statement: Not applicable.

Conflicts of Interest: The authors declare no conflict of interest.

References

1. FAO. *Global Food Losses and Food Waste—Extent, Causes and Prevention*; Food and Agriculture Organization: Rome, Italy, 2011.
2. Lipinski, B.; Hanson, C.; Lomax, J.; Kitinoja, L.; Waite, R.; Searchinger, T. *Reducing Food Loss and Waste*; World Resources Institute: Washington, DC, USA, 2013; pp. 1–40.
3. Kerry, J.P.; O'Grady, M.N.; Hogan, S.A. Past, current and potential utilisation of active and intelligent packaging systems for meat and muscle-based products: A review. *Meat Sci.* **2006**, *74*, 113–130. [CrossRef] [PubMed]
4. Heiss, R.; Eichner, K. *Haltbarmachen von Lebensmitteln: Chemische, Physikalische und Mikrobiologische Grundlagen der Qualitätserhaltung*, 4th ed.; Springer: Berlin/Heidelberg, Germany, 2002; ISBN 3-540-43137-3.
5. Buchner, N. *Verpackung von Lebensmitteln: Lebensmitteltechnologische, Verpackungstechnische und Mikrobiologische Grundlagen*; Springer: Berlin/Heidelberg, Germany, 1999; ISBN 978-3-642-63658-5.
6. Meredith, H.; Valdramidis, V.; Rotabakk, B.T.; Sivertsvik, M.; McDowell, D.; Bolton, D.J. Effect of different modified atmospheric packaging (MAP) gaseous combinations on Campylobacter and the shelf-life of chilled poultry fillets. *Food Microbiol.* **2014**, *44*, 196–203. [CrossRef] [PubMed]
7. Höll, L.; Behr, J.; Vogel, R.F. Identification and growth dynamics of meat spoilage microorganisms in modified atmosphere packaged poultry meat by MALDI-TOF MS. *Food Microbiol.* **2016**, *60*, 84–91. [CrossRef] [PubMed]
8. Herbert, U.; Albrecht, A.; Kreyenschmidt, J. Definition of predictor variables for MAP poultry filets stored under different temperature conditions. *Poult. Sci.* **2015**, *94*, 424–432. [CrossRef]
9. Kolbeck, S.; Reetz, L.; Hilgarth, M.; Vogel, R.F. Quantitative Oxygen Consumption and Respiratory Activity of Meat Spoiling Bacteria Upon High Oxygen Modified Atmosphere. *Front. Microbiol.* **2019**, *10*, 2398. [CrossRef]
10. Kolbeck, S.; Hilgarth, M.; Vogel, R.F. Proof of concept: Predicting the onset of meat spoilage by an integrated oxygen sensor spot in MAP packages. *Lett. Appl. Microbiol.* **2021**, *73*, 39–45. [CrossRef]
11. Baumgart, J.; Becker, B.; Stephan, R. *Mikrobiologische Untersuchung von Lebensmitteln: Ein Leitfaden für das Studium*, 6th ed.; Behr's GmbH: Hamburg, Germany, 2015; ISBN 978-3-95468-333-8.
12. Dold, J.; Langowski, H.-C. Optical measurement systems in the food packaging sector and research for the non-destructive evaluation of product quality. *Food Packag. Shelf Life* **2022**, *31*, 100814. [CrossRef]
13. Lakowicz, J.R. *Principles of Fluorescence Spectroscopy*, 3rd ed.; Springer Science + Business Media, LLC: New York, NY, USA, 2006; ISBN 978-0-387-31278-1.
14. O'Callaghan, K.A.M.; Papkovsky, D.B.; Kerry, J.P. An Assessment of the Influence of the Industry Distribution Chain on the Oxygen Levels in Commercial Modified Atmosphere Packaged Cheddar Cheese Using Non-Destructive Oxygen Sensor Technology. *Sensors* **2016**, *16*, 916. [CrossRef]
15. Araque, P.E.; Sansalvador, I.M.P.D.V.; Ruiz, N.L.; Erenas, M.M.; Rodriguez, M.A.C.; Olmos, A.M. Non-Invasive Oxygen Determination in Intelligent Packaging Using a Smartphone. *IEEE Sens. J.* **2018**, *18*, 4351–4357. [CrossRef]
16. Schmutzler, M.; Beganovic, A.; Böhler, G.; Huck, C.W. Modern Safety Control for Meat Products: Near Infrared Spectroscopy Utilised for Detection of Contaminations and Adulterations of Premium Veal Products. *NIR News* **2016**, *27*, 11–13. [CrossRef]
17. Böcker, J. *Spektroskopie: Instrumentelle Analytik mit Atom-und Molekülspektrometrie*, 1st ed.; Vogel Communications Group GmbH & Co.KG: Vilzburg, Germany, 1997; ISBN 3-8023-1581-2.
18. Dong, M.; Zheng, C.; Miao, S.; Zhang, Y.; Du, Q.; Wang, Y.; Tittel, F.K. Development and Measurements of a Mid-Infrared Multi-Gas Sensor System for CO, CO_2 and CH_4 Detection. *Sensors* **2017**, *17*, 2221. [CrossRef] [PubMed]
19. Novo, J.M.; Iriel, A.; Lagorio, M.G. Rapid spectroscopic method to assess moisture content in free and packaged oregano (*Origanum vulgare* L.). *J. Appl. Res. Med. Aromat. Plants* **2016**, *3*, 211–214. [CrossRef]
20. Rossaint, S.; Klausmann, S.; Kreyenschmidt, J. Effect of high-oxygen and oxygen-free modified atmosphere packaging on the spoilage process of poultry breast fillets. *Poult. Sci.* **2015**, *94*, 96–103. [CrossRef] [PubMed]
21. Katiyo, W.; de Kock, H.L.; Coorey, R.; Buys, E.M. Sensory implications of chicken meat spoilage in relation to microbial and physicochemical characteristics during refrigerated storage. *LWT* **2020**, *128*, 109468. [CrossRef]
22. Franke, C.; Höll, L.; Langowski, H.-C.; Petermeier, J.; Vogel, R.F. Sensory evaluation of chicken breast packed in two different modified atmospheres. *Food Packag. Shelf Life* **2017**, *13*, 66–75. [CrossRef]
23. Casaburi, A.; Piombino, P.; Nychas, G.-J.; Villani, F.; Ercolini, D. Bacterial populations and the volatilome associated to meat spoilage. *Food Microbiol.* **2015**, *45*, 83–102. [CrossRef]
24. Gram, L.; Dalgaard, P. Fish spoilage bacteria—Problems and solutions. *Curr. Opin. Biotechnol.* **2002**, *13*, 262–266. [CrossRef]
25. Alessandroni, L.; Caprioli, G.; Faiella, F.; Fiorini, D.; Galli, R.; Huang, X.; Marinelli, G.; Nzekoue, F.; Ricciutelli, M.; Scortichini, S.; et al. A shelf-life study for the evaluation of a new biopackaging to preserve the quality of organic chicken meat. *Food Chem.* **2022**, *371*, 131134. [CrossRef]
26. Borch, E.; Kant-Muermans, M.-L.; Blixt, Y. Bacterial spoilage of meat products and cured meat. *Int. J. Food Microbiol.* **1996**, *33*, 103–120. [CrossRef]
27. Hood, D.E.; Riordan, E.B. Discolouration in pre-packaged beef: Measurement by reflectance spectrophotometry and shopper discrimination. *Int. J. Food Sci. Technol.* **1973**, *8*, 333–343. [CrossRef]
28. Sante, V.; Renerre, M.; Lacourt, A. Effect of modified atmosphere packaging on color stability and on microbiology of turkey breast meat. *J. Food Qual.* **1994**, *17*, 177–195. [CrossRef]

29. Nychas, G.-J.; Skandamis, P.N.; Tassou, C.C.; Koutsoumanis, K.P. Meat spoilage during distribution. *Meat Sci.* **2008**, *78*, 77–89. [CrossRef] [PubMed]
30. Lee, B.H.; Simard, R.E. Evaluation of Methods for Detecting the Production of H₂S, Volatile Sulfides, and Greening by Lactobacilli. *J. Food Sci.* **1984**, *49*, 981–983. [CrossRef]
31. McMeekin, T.A.; Patterson, J.T. Characterization of hydrogen sulfide-producing bacteria isolated from meat and poultry plants. *Appl. Microbiol.* **1975**, *29*, 165–169. [CrossRef] [PubMed]
32. Mead, G. *Microbiological Analysis of Red Meat, Poultry and Eggs*; Elsevier: Burlington, NJ, USA, 2006; ISBN 978-1-84569-059-5.
33. Kadota, H.; Ishida, Y. Production of volatile sulfur compounds by microorganisms. *Annu. Rev. Microbiol.* **1972**, *26*, 127–138. [CrossRef]
34. Charles, N.; Williams, S.K.; Rodrick, G.E. Effects of packaging systems on the natural microflora and acceptability of chicken breast meat. *Poult. Sci.* **2006**, *85*, 1798–1801. [CrossRef]
35. Keupp, C.; Höll, L.; Beauchamp, J.; Langowski, H.-C. Online monitoring of volatile freshness indicators from modified atmosphere packaged chicken meat using PTR-MS. In Proceedings of the 27th IAPRI Symposium on Packaging 2015, Valencia, Spain, 8–11 June 2015.
36. Freeman, L.R.; Silverman, G.J.; Angelini, P.; Merritt, C.; Esselen, W.B. Volatiles produced by microorganisms isolated from refrigerated chicken at spoilage. *Appl. Environ. Microbiol.* **1976**, *32*, 222–231. [CrossRef]
37. Balamatsia, C.; Patsias, A.; Kontominas, M.; Savvaidis, I. Possible role of volatile amines as quality-indicating metabolites in modified atmosphere-packaged chicken fillets: Correlation with microbiological and sensory attributes. *Food Chem.* **2007**, *104*, 1622–1628. [CrossRef]
38. Mikš-Krajnik, M.; Yoon, Y.-J.; Yuk, H.-G. Detection of volatile organic compounds as markers of chicken breast spoilage using HS-SPME-GC/MS-FASST. *Food Sci. Biotechnol.* **2015**, *24*, 361–372. [CrossRef]
39. Dainty, R.H.; Hibbard, C.M. Precursors of the major end products of aerobic metabolism of Brochothrix thermosphacta. *J. Appl. Bacteriol.* **1983**, *55*, 127–133. [CrossRef]
40. Nassos, P.S.; King, A.D.; Stafford, A.E. Relationship between lactic acid concentration and bacterial spoilage in ground beef. *Appl. Environ. Microbiol.* **1983**, *46*, 894–900. [CrossRef] [PubMed]
41. Kakouri, A.; Nychas, G.J. Storage of poultry meat under modified atmospheres or vacuum packs: Possible role of microbial metabolites as indicator of spoilage. *J. Appl. Bacteriol.* **1994**, *76*, 163–172. [CrossRef] [PubMed]
42. Höll, L.; Hilgarth, M.; Geissler, A.J.; Behr, J.; Vogel, R.F. Metatranscriptomic analysis of modified atmosphere packaged poultry meat enables prediction of Brochothrix thermosphacta and Carnobacterium divergens in situ metabolism. *Arch. Microbiol.* **2020**, *202*, 1945–1955. [CrossRef] [PubMed]